Westinghouse Energy Systems

WCAP-12392

WESTINGHOUSE BOILING WATER REACTOR

EMERGENCY CORE COOLING SYSTEM EVALUATION MODEL:

CODE SENSITIVITY

By

D. B. Ebeling-Koning
M. E. Nissley
R. M. Jakub

October 1989

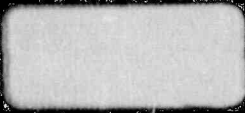2044v:1D/111689

Westinghouse Energy Systems

WESTINGHOUSE BOILING WATER REACTOR

EMERGENCY CORE COOLING SYSTEM EVALUATION MODEL:

CODE SENSITIVITY

By

D. B. Ebeling-Koning
M. E. Nissley
R. M. Jakub

October 1989

WESTINGHOUSE ELECTRIC CORPORATION
Nuclear Energy Systems
P.O. Box 355
Pittsburgh, Pennsylvania 15230

UNITED STATES
NUCLEAR REGULATORY COMMISSION
WASHINGTON, D. C. 20555

August 22, 1989

Mr. W. J. Johnson, Manager
Nuclear Safety Department
Westinghouse Electric Corporation
Nuclear Energy Systems
P. O. Box 355
Pittsburgh, Pennsylvania 15230

Dear Mr. Johnson:

SUBJECT: ACCEPTANCE FOR REFERENCING OF LICENSING TOPICAL
REPORTS WCAP-11284 AND WCAP-11427 REGARDING THE
WESTINGHOUSE BOILING WATER REACTOR EMERGENCY
CORE COOLING SYSTEM EVALUATION MODEL

We have completed our review of the subject topical reports. We find these
reports acceptable for referencing in license applications to the extent
specified and under the limitations delineated in the reports and the
associated NRC evaluation which is enclosed. The evaluation defines the basis
for acceptance of the reports.

We do not intend to repeat our review of the matters described in the reports
and found acceptable when the reports appear as references in license
applications except to assure that the material presented is applicable to the
specified plant involved. Our acceptance applies only to the matters
described in the reports.

In accordance with procedures established in NUREG-0390, it is requested that
Westinghouse publish accepted versions of WCAP-11284 and WCAP-11427,
proprietary and non-proprietary, within 3 months of receipt of this letter.
The accepted versions should incorporate this letter and the enclosed
evaluation between the title page and the abstract. The accepted versions
shall include an -A (designating accepted) following the report identification
symbol.

Should our criteria or regulations change such that our conclusions as to the
acceptability of the reports are invalidated, Westinghouse and/or the
licensees referencing the topical reports will be expected to revise and

UNITED STATES
NUCLEAR REGULATORY COMMISSION
WASHINGTON, D. C. 20555

August 22, 1989

Mr. W. J. Johnson, Manager
Nuclear Safety Department
Westinghouse Electric Corporation
Nuclear Energy Systems
P. O. Box 355
Pittsburgh, Pennsylvania 15230

Dear Mr. Johnson:

SUBJECT: ACCEPTANCE FOR REFERENCING OF LICENSING TOPICAL
REPORTS WCAP-11284 AND WCAP-11427 REGARDING THE
WESTINGHOUSE BOILING WATER REACTOR EMERGENCY
CORE COOLING SYSTEM EVALUATION MODEL

We have completed our review of the subject topical reports. We find these
reports acceptable for referencing in license applications to the extent
specified and under the limitations delineated in the reports and the
associated NRC evaluation which is enclosed. The evaluation defines the basis
for acceptance of the reports.

We do not intend to repeat our review of the matters described in the reports
and found acceptable when the reports appear as references in license
applications except to assure that the material presented is applicable to the
specified plant involved. Our acceptance applies only to the matters
described in the reports.

In accordance with procedures established in NUREG-0390, it is requested that
Westinghouse publish accepted versions of WCAP-11284 and WCAP-11427,
proprietary and non-proprietary, within 3 months of receipt of this letter.
The accepted versions should incorporate this letter and the enclosed
evaluation between the title page and the abstract. The accepted versions
shall include an -A (designating accepted) following the report identification
symbol.

Should our criteria or regulations change such that our conclusions as to the
acceptability of the reports are invalidated, Westinghouse and/or the
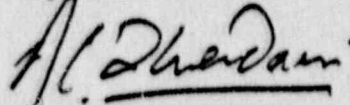licensees referencing the topical reports will be expected to revise and

resubmit their respective documentation, or submit justification for the continued effective applicability of the topical reports without revision of their respective documentation.

Sincerely,

Ashok C. Thadani, Assistant Director
   for Systems
Division of Engineering & Systems Technology
Office of Nuclear Reactor Regulation

Enclosure:
Evaluation Report

SAFETY EVALUATION BY THE OFFICE OF NUCLEAR REACTOR REGULATION
RELATING TO THE WESTINGHOUSE ELECTRIC CORPORATION
BOILING WATER REACTOR EMERGENCY CORE COOLING SYSTEM EVALUATION MODEL

1.0 INTRODUCTION

By letter dated September 30, 1986, Westinghouse Electric Corporation submitted
for review licensing topical report WCAP-11284 entitled "Westinghouse Boiling
Water Reactor Emergency Core Cooling System Evaluation Model: Code Description
and Qualification" (Ref. 1). By letter dated June 30, 1987, Westinghouse
submitted WCAP-11427 entitled "Westinghouse Boiling Water Reactor Emergency
Core Cooling System Evaluation Model: Code Sensitivity" (Ref. 2) which was
reviewed by the NRC concurrently with WCAP-11284. The staff requested
assistance in the review from Los Alamos National Laboratory (LANL). LANL
identified additional information needs to which Westinghouse responded in an
amendment document, WCAP-11284-Amendment 1/WCAP-11427-Amendment 1, "Westinghouse
Boiling Water Reactor Emergency Core Cooling System Evaluation Model: Response
to Request for Additional Information and Errata" (Ref. 3).

The Office of Nuclear Reactor Regulation (NRR) is responsible for the review
and evaluation of licensing analyses and methodology. The review was conducted
to provide a technical assessment of conformance of the Westinghouse emergency
core cooling system (ECCS) model to Appendix K of 10 CFR Part 50 (Code of
Federal Regulations - Energy). The ECCS model will be part of the safety
analysis methodology applicable to boiling water reactor (BWR) fuel manufactured
and marketed by Westinghouse Electric Corporation. The ECCS loss-of-coolant
accident (LOCA) methodology was developed by ASEA-ATOM, Sweden, and has been in
use in Europe in the study of boiling water reactor performance.

This safety evaluation (SE) documents the review of Westinghouse large-break
and small-break LOCA analysis methods applicable to BWR types 2 through 6
plants. The SE is divided into eight sections. Section 2 presents a summary

of the topical reports and Section 3 provides a code description summary and assessment (WCAP-11284). Section 4 discusses the code sensitivity studies and assessment (WCAP-11427). Section 5 describes the integral system qualifications. and Section 6 discusses compliance with Appendix K requirements. Section 7 provides the staff conclusions resulting from this review, and Section 8 contains the references applicable to the review.

2.0 SUMMARY OF TOPICAL REPORTS

Westinghouse uses the GOBLIN system of computer codes (Ref. 1) to evaluate ECCS performance during postulated LOCAs in BWRs. The system codes calculate the BWR transient responses to both large-break and small-break LOCAs. The system is composed of three major computer codes (GOBLIN, DRAGON, and CHACHA-3C), an auxiliary code (BILBO), and several input/output data processors (HOBIT, FRODO, CHINE, PLOAUX, and SUPERB). A brief description of the more important codes follows.

GOBLIN - Analyzes the LOCA blowdown and reflood thermal-hydraulic transient for the entire reactor, including the interactions with various control and safety systems. GOBLIN calculates the pressure and enthalpy at the core inlet and outlet, using the core power generation, system geometry, ECCS performance, and the break type.

DRAGON - Performs the hot fuel channel, thermal-hydraulic transient calculations. DRAGON is virtually identical to GOBLIN except several calculation models are bypassed. Using channel power, geometry, and boundary conditions from the GOBLIN calculations, DRAGON calculates the coolant temperature and pressure, the void fraction, and the heat-transfer coefficients.

CHACHA-3C - Performs detailed temperature calculations at a specified axial level within the fuel assembly previously analyzed by the DRAGON code. All necessary fluid boundary conditions are obtained from the DRAGON calculation. CHACHA-3C calculates the time-dependent, pellet-to-clad gap, heat-transfer coefficients, as well as clad swelling and potential burst. It determines the temperature distribution of each rod throughout the transient and ultimately

determines the peak clad temperature (PCT) and cladding oxidation at the axial plane under investigation. It also provides input for the calculation of total hydrogen generation by supplying the local oxidation at a number of axial and radial locations in the core.

Westinghouse has performed integral system qualification analyses to compare the code simulation with the two-loop test apparatus (TLTA) test data. The objective of this verification program is to demonstrate the code's ability to predict plant responses to a design-basis LOCA correctly. To support the LOCA evaluation methodology to be used in the licensing calculations for a BWR/5, Westinghouse also has performed sensitivity studies (Ref. 2) that consider hydraulic models, plant parameters, numerical convergence, and nodalization.

3.0 CODE DESCRIPTION AND ASSESSMENT

3.1 Thermal-Hydraulic Analysis Codes: GOBLIN/DRAGON

The GOBLIN code performs one-dimensional, thermal-hydraulic calculations for the entire reactor during a postulated LOCA. The system response from blowdown through reflood is calculated for both small- and large-break events. GOBLIN is divided into four main sections.

The power generation model calculates the heat generation resulting from fission, decay heat, and metal-water reactions. Fission power is determined by a point kinetics model that allows for up to six delayed neutron groups. Reactivity feedback is included for void fraction, moderator (coolant) temperature, fuel temperature, and reactor control rods. The decay power generation is calculated by the sum of 11 fission product decay groups and the actinide decay of U-239 and Np-239. The Baker-Just model is used to determine the heat generation from the metal-water reactions.

The hydraulic model solves the mass, energy, and momentum conservation equations together with the equation of state for each control volume. This model includes empirical constitutive correlations for the calculation of

pressure drops, two-phase energy flow (drift flux), two-phase level tracing, spray-fluid interaction, and critical flow rate.

The system models contain detailed models of the various reactor components and the safety systems that are activated after a LOCA. They include the ECCS; the steam separators and dryers; the reactor level measurement, trip, and depressurization systems; and the recirculation and jet pumps.

The thermal model calculates the heat conduction and heat transfer from the fuel rods, pressure vessel, and internals (plates) to the coolant. The model solves the material heat conduction equation and calculates the heat transfer from the fuel and structures to the coolant. The heat-transfer coefficients couple the hydraulic solution to the thermal conduction solution through the coolant state and surface temperature. Empirical heat-transfer coefficient correlations are modeled for single-phase liquid-heat transfer, two-phase non-dryout transition boiling, post-dryout heat transfer and single-phase vapor, and surface-to-surface radiation heat transfer.

DRAGON is used to simulate the hot fuel channel by specifying the inlet and outlet plenum pressures and enthalpies from the GOBLIN simulation. DRAGON incorporates the channel power and geometry and inlet/outlet hydraulic properties to produce coolant temperature and pressure, void fraction, and heat-transfer coefficients. The following subsections describe the key models in the GOBLIN/DRAGON code.

3.1.1 Decay of Actinides and Fission Products

Three actinide decay groups are modeled. The decay time constants and effective energy fractions are taken from a Westinghouse fuel design code, PHOENIX, that has received NRC approval. The fission product decay model uses decay constants and effective energy fractions that best fit the 1971 American Nuclear Society (ANS) decay power guideline. An uncertainty of 20 percent is added to the resultant fission product power generation. Westinghouse assumes that the total gamma energy deposition fraction outside of the fuel rod is 2

percent of the total power generation. Westinghouse has performed sensitivity studies and identified that the effect on the PCT is negligible by delaying the time to increase the power generation fraction from 96 percent to 98 percent of the total power generation (see Reference 3, response to Question 2). The sensitivity studies performed by Westinghouse are in response to an Appendix K, Section I.A.4 requirement to justify a gamma energy deposition fraction outside the fuel rod that is less than 1.0. Westinghouse also has partitioned pellet and cladding power distribution and found that the no-partition case would be more conservative, that is, would produce a higher PCT. The differences in PCT as reported in the Reference 3 sensitivity studies confirmed that the effect of the assumption of a 2-percent energy deposition fraction outside the fuel rod is small.

3.1.2 Two-Phase Energy Flow Model

The enthalpy flow rate for the two-phase flow is determined using a drift-flux correlation developed from the work of J.A. Holmes (Ref. 4) and includes a counter-current flow limitation (CCFL) correlation of the form defined by H.B. Wallis (Ref. 5). The constants used in the CCFL correlations originally were derived from formulations and data developed by R.V. Bailey (Ref. 6) and S.O. Eriksson (Ref. 7). Westinghouse has performed a series of experiments to test the conservatism of the CCFL correlation. The results indicate that the CCFL correlation used in the GOBLIN/DRAGON is 25 percent more restrictive in the liquid drain flow rate than was observed in the experiment.

3.1.3 Two-Phase Level Tracking

GOBLIN can specify a series of control volumes in which a two-phase level is to be calculated and tracked with time. The level tracking model replaces a fixed control volume boundary with a moving boundary located at the two-phase level. The flow rate through the boundary is determined by maintaining continuity of the phasic flow rates through the two-phase level for a given level velocity. The phasic flow rates are calculated for the volume above and below the level by the drift-flux correlation. With level tracking, the control volume boundaries continuously change with time. Hence, the boundaries

of the level-tracking region become a significant nodalization parameter. The use of moving boundaries at the two phase level is consistent with other ECCS evaluation models which have been approved by the staff.

3.1.4 Frictional and Local Form Pressure Drop Correlations

The original two-phase multipliers in WCAP-11284 for the frictional and local form pressure drop were modified for the QUAD+ fuel design modelled for the sensitivity studies reported in WCAP-11427. Other modifications will be required when the methodology is applied to an accepted fuel design.

3.1.5 Injection-Flow/Vessel-Fluid Interaction

The external water is added to a control volume as a mass and energy source item. If the water level falls below the injection point, the injection water is added to the liquid in the uppermost liquid control volume, together with the steam that has condensed from the upper control volume. A falling distance of 0.3 meter assumed in the GOBLIN analysis is based on experimental data (Ref. 8) that demonstrates that the injection water has essentially reached saturation in that distance.

3.1.6 Critical Flow Model

The GOBLIN code uses the Moody critical flow model for the two-phase break flow and a modified Bernoulli model that assumes zero flow resistance from stagnation point to the exits for the subcooled critical flow. Both models are typical of those used in approved ECCS evaluation models.

3.1.7 Heat-Transfer Regimes

The heat-transfer regimes modeled in GOBLIN are identified in Sections 2 and 3 of WCAP-11284. The regimes are characterized by dryout conditions, single- and two-phase fluid conditions, and Reynolds' Number. Void fraction limits denote transition to dispersed flow conditions and transition from inverted annular flow to dispersed flow.

During its review, the staff noted that a maximum differential of 2.5 percent in voids could result in an oscillatory solution instability. However, Westinghouse responded that no oscillatory solutions have been observed before core reflood.

3.1.8 Dryout Correlation

The boiling transition between non-dryout heat transfer and post-dryout heat transfer is determined from a critical heat flux (CHF) correlation. The CHF used is the maximum between a flow-boiling and a pool-boiling correlation. Westinghouse has conducted steady-state and transient CHF tests using a simulated QUAD+ mini-bundle. The resulting test data were used to develop and verify the WB-1 correlation (for QUAD+ fuel), which uses the critical quality boiling length formulation. This correlation was intended to replace the AA-74 correlation for use in the QUAD+ fuel analysis. The staff has not reviewed the WB-1 correlation; a staff-approved correlation must be used when the subject ECCS methodology is used in a licensing analysis.

3.2 Rod Heatup Analysis Codes: CHACHA-3C/BILBO

Detailed fuel rod heatup calculations are performed with the CHACHA-3C code using boundary conditions of the coolant pressure and temperature supplied by DRAGON. The prime use of CHACHA-3C is to determine the PCT at the hottest axial plane in the peak power bundle. It also is used to determine the total hydrogen generation by evaluating local cladding oxidation at a number of axial and radial locations in the core.

The major components of the CHACHA-3C code include (1) a fuel rod conduction model; (2) a channel temperature model; (3) a heat generation model; (4) a metal-water reaction model; (5) a gas plenum temperature and pressure model; (6) a pellet/cladding-gap, heat-transfer model; (7) a cladding strain-and-rupture model; (8) a thermal radiation model; and (9) a spray heat-transfer model. The first two models use a conventional finite-difference method to

treat heat conduction in the fuel rod and channel. The heat generation model in CHACHA-3C is identical to that in GOBLIN/DRAGON. The gas plenum temperature-and-pressure model and the pellet/cladding-gap, heat-transfer model use the analytical models in the NRC-approved PAD code. The cladding strain-and-rupture model uses the NRC-approved materials properties data from MATPRO Version II and General Electric (GE) stress/strain correlations, including cladding strain versus temperature before perforation, circumferential strain versus cladding differential pressure, and a lower bound curve for the data for strain versus temperature taken from NEDO-20566 (Ref. 9). The following subsections describe the thermal radiation and channel rewet models.

3.2.1 Thermal Radiation Model

The thermal radiation model was formulated using the following assumptions:

(1) All surfaces in the rod bundle are gray, diffuse, and nontransparent.

(2) The emission of radiation takes place isotropically.

(3) Reflection of radiation is divided into isotropic and anisotropic components.

(4) The anisotropic reflection reverts back to the origin of radiation.

(5) Absorption, emission, and dispersion in coolant are omitted.

(6) All surfaces are in thermal quasi-equilibrium during each time step.

The gray-body factors are calculated by the auxiliary code BILBO, which evaluates geometric view factors for two geometries: (1) all rods at normal dimensions, and (2) all rods fully strained. The emissivities of dry and wet surfaces are taken as 0.67 and 0.96, respectively.

• The thermal radiation model is considered conservative and adequate because of (1) the derivation of the dry emissivities taking into consideration oxide buildup as a function of local burnup, and (2) the omission of coolant absorption.

3.2.2 Spray Heat-Transfer Model

ASEA-ATOM (A-A) has performed experiments using the A-A 8x8 design and demonstrated that the Appendix K coefficients acceptable for the 7x7 fuel are applicable to the A-A 8x8 design, when an isotropic radiation model was used. A-A also developed the convective heat-transfer coefficients that when applied with an anisotropic model would match the 8x8 temperature distributions calculated with the Appendix K coefficients and the isotropic model. This new set of coefficients then was reduced by 15 percent for the QUAD+ fuel bundle design.

The Westinghouse ECCS evaluation model compliance with Appendix K, Sections I.D.6 and I.D.7, use convective heat transfer coefficients derived from the Appendix K-recommended values. The experimental data used to verify the values should be justified as applicable to the particular fuel design for which the overall methodology is to be applied.

4.0 CODE SENSITIVITY STUDIES AND ASSESSMENT

4.1 Nodalization

Westinghouse has performed sensitivity studies for the nominal (six volumes), coarse (five volumes), and fine (eight volumes) cases near the break location. The pressure and void at the break indicate that the coarse noding is nonconservative because of a lower break flow. However, the fine and nominal cases compare well throughout the transient.

Westinghouse also performed sensitivity studies in the bypass and upper plenum to demonstrate adequate noding at injection locations of the ECCS. Five cases were studied, and the results show that the mid-plane reflood times compare

well when the level tracking scheme was used. The sensitivity to the location of the bottom of level trackings is negligible. A coarser noding case results in a slightly different time of refilling guide tubes and bypasses. However, the final reflooding time of the mid-plane (a parameter in determining the PCT) remains within a time period of one second of the standard noding case.

The standard CHACHA-3C fuel rod noding consists of seven pellet nodes of equal volume and three cladding nodes of equal thickness. The sensitivity of the PCT to fuel-rod noding was evaluated by comparing results obtained from the standard case to those obtained with 5-pellet/2-cladding nodes and 10-pellet/4-cladding nodes. The results indicate negligible difference in the PCT calculated from three cases. As a result, it is concluded that standard fuel noding is appropriate for CHACHA-3C. CHACHA-3C uses the watercross thickness to calculate channel temperature. The sensitivity to the thickness of channel and watercross was evaluated, and results show that the PCT is relatively insensitive to the channel noding and is overestimated by 16°F using the watercross thickness.

4.2 Plant Parameter Studies

The sensitivity of the nuclear peaking factors, including the axial peaking factor, bundle relative power, and peaking location, was evaluated. Five cases were studied, and the results show that the cases with a higher bundle relative power dried out and uncovered faster than the cases with a lower bundle relative power. The PCT for the peak-to-top power is slightly higher than that for the cosine power (by 25°F). However, the peak-to-top power would correspond to an operation with the control rods inserted approximately halfway into the core, which is inconsistent with the full-power operation. Because of the relative insensitivity to the power distribution and the inherent tendency of BWRs operating with slightly peak-to-bottom power shapes, the 1.5 cosine shape has been used in the DRAGON model. Axial peaking factors were considered as part of the power distribution sensitivity studies by Westinghouse. The sensitivity study for axial peaking factors in the range 1.5 to 1.6 covers the upper bound normally expected for a BWR/5. It is

concluded that adequate consideration has been given to the sensitivity of the nuclear peaking factors.

Westinghouse has performed studies varying the plant initial conditions and transient conditions (scram time, time of main steam isolation valve (MSIV) closure, initial water level, pressure form-loss coefficients, and feedwater and recirculation pump coastdown rates) to determine their effect on the time of mid-plane dryout. The results show that the largest change in mid-plane dryout time as a consequence of any of these sensitivities was about 1 second. As a result, the plant variables used in the Westinghouse evaluation models are considered adequate.

A reduced core flow sensitivity was performed for 68 percent of rated core flow and 104.3 percent rated power. Because of the initial lower enthalpy in the lower plenum, the reduced core flow case would delay the lower plenum flashing by 1 second and extend the midplane dryout by 2.5 seconds. As a result, the reference LOCA would result in a higher PCT and is more conservative.

4.3 Numerical Convergence

Westinghouse has varied convergence criteria and time steps to show that the calculated solution is unique and within acceptable limits of the ideal asymptotic solution. Three convergence criteria were involved: thermal-hydraulic, fuel rod temperature, and surface heat transfer. A range of convergence criteria (by three orders of magnitude), time-step size (by one order of magnitude), and surface heat transfer (by one order of magnitude) were studied.

Three key system parameters, steamdome pressure, rod surface temperature, and core void fraction calculated from GOBLIN/DRAGON, demonstrated an asymptotic solution as the time-step size was reduced. The calculation of pressure shows the sensitivity of hydraulic models; the surface temperature calculation demonstrates the sensitivity of the heat transfer models; and the void fraction calculation warrants the adequacy of core flow rate, heat rate, and pressure. Varying the convergence criteria has negligible effect on the GOBLIN/DRAGON solutions.

Convergence criteria in CHACHA-3C also have been changed by an order of magnitude: the relative change in both rod surface heat flux and rod surface temperature, the absolute change in nodal temperature, and the relative change in channel temperature were the parameters identified in Reference 2, Section 7. The results show identical PCTs in the two runs. In order to evaluate the sensitivity of time-step sizes, values of time-step sizes were reduced by 80 percent for different phases: blowdown, dryout, dryout to uncovering, uncovering to reflood. The results show a difference of approximately 2°F in PCT.

It is concluded that the time-step/convergence criteria study conducted by Westinghouse demonstrates convergence of the GOBLIN/DRAGON and CHACHA-3C codes to a unique asymptotic solution.

4.4 Break Spectrum

The limiting break is a combination of break size, location, and single failure that yields the highest PCT. The break spectrum studied by Westinghouse included:

Case I: A full guillotine break in a recirculation suction line with failure of the low-pressure core spray (LPCS) diesel generator.

Case II: A full guillotine break in a recirculation suction line with failure of the high-pressure core spray (HPCS) system.

Case III: A 0.0084-m² (0.09-ft²) split break in a recirculation suction line with failure of the HPCS system.

Case IV: A full break in a spray line with failure of the LPCS diesel generator (Division I).

For Case I, additional break sizes of 80 percent, 60 percent, and 40 percent of the full break were analyzed. Based on the results from Case I (four break sizes) and Case II, the full-size break in Case I would result in a higher PCT

of 1897°F. This was mainly because of a larger break size (compared with fractional break sizes) and smaller ECC flow (loss of LPCS versus HPCS flow). Cases III and IV are considered to be small breaks. Both cases result in a substantially lower PCT than that from the Case I full break by about 800°-900°F. The Westinghouse results were compared with those from the GE 8x8 safety analysis for the reference BWR. The Westinghouse-calculated PCTs are relatively consistent with the GE results. The differences in the PCTs can be attributed to a different maximum linear heat generation rate used (Westinghouse 14.5 kW/ft versus GE 13.4 kW/ft) and an earlier calculated low level 1 signal in the Westinghouse analysis. An earlier low level 1 signal would result in an earlier MSIV closure, an earlier automatic depressurization system actuation, and an earlier subsequent ECC injection. Regardless, in either analysis, the result is the same; namely, that the small LOCA is significantly less limiting than the 100 percent, double-ended guillotine recirculation pipe break.

4.5 Transition Core

Reload analyses have been performed by Westinghouse using GOBLIN for a full QUAD+ core, a mixed core of GE 8x8 fuel and QUAD+ fuel core, and a full core of GE 8x8 fuel. The key phenomena compared include the core inlet flow rate during blowdown, the vessel depressurization rate, and the time of core reflood. The core inlet flow dictates the time of boiling transition and uncovering. The vessel depressurization rate determines the time at which spray flow is initiated. The reflood time determines the time at which the fuel rod heatup is terminated.

A full core of GE 8x8 fuel was modeled by GOBLIN with necessary modifications of the noding set for the QUAD+ fuel. The general system responses are similar for the GE 8x8 fuel core and the QUAD+ fuel core. The QUAD+ active core flow is slightly higher before lower plenum flashing as a result of draining of the watercross. The mid-plane dryout times are almost the same (by a 0.7 second difference). The vessel depressurization rate is almost identical. The mid-plane reflood times differ by 7 seconds because the watercross helps refill

the lower plenum slightly faster in the QUAD+ core. Therefore, similar system responses for the two fuel designs were concluded for the limiting LOCA.

Westinghouse also did a mixed-core LOCA system response analysis to demonstrate that each fuel design does not have an adverse effect on the other fuel design. A GOBLIN calculation was made with one third 8x8 fuel and two thirds QUAD+ fuel. The results of times for the initial blowdown phenomena, depressurization, and core flood closely follow that for a full core of QUAD+ fuel. The active core inlet flow and flow rate at the top of each fuel type are similar, and both assemblies receive comparable ECC flow rates. The potential of an uneven flow distribution of ECC water into different fuel assemblies during the refill/reflood phase was studied and excluded.

In summary, results from the analyses for the 8x8 fuel, QUAD+ fuel, and a mixed core fuel showed very minor changes in the timing of the key phenomena. As a result, introducing the QUAD+ fuel in a transition core of GE 8x8 fuel will not adversely affect the fuel-type-specific LOCA maximum average planar linear heat generation rate limits determined on the basis of a full core of the respective fuel type.

The use of a different fuel design other than QUAD+ fuel in a transition core should be addressed in a generic Reference Safety Report.

5.0 INTEGRAL SYSTEM QUALIFICATIONS

The system codes were assessed against several tests. These tests provided information on the integral system behavior under the influence of many interacting thermal-hydraulic phenomena. Westinghouse provided comparisons using the experimental data from TLTA Test 6425/2 (average power and average ECC), TLTA Test 6423/3 (high power and low ECC), TLTA Tests 6007/26 and 6006/3 (blowdown heat transfer), TLTA-5B and -5C small-break LOCA tests, and the FIX-II break spectrum tests. The results from a preliminary assessment indicated that the comparison of the Westinghouse simulations and these tests was unsatisfactory, particularly in the areas of time-zero offsets, system pressure, bundle mass, break flow rate, and fuel rod temperature. Other issues

needing clarification included code versions (the Westinghouse version versus the A-A version) and supporting plot data.

Westinghouse responded to our request for additional information by performing additional analyses using TLTA 6423/3, which involves a large-break LOCA with high power and low ECC. Major improvements made in these analyses included a much better match of the initial and boundary conditions with the tests, particularly for the initial downcomer mass inventory, lower plenum enthalpy, and steamline flow rate. The downcomer mass affects the initial depressurization through the recirculation line uncovering; the lower plenum enthalpy affects the time of lower plenum flashing; and modeling of the steamline valve closure improves the early pressure transient.

The GOBLIN simulation of TLTA Test 6423/3 excluded several Appendix K evaluation model requirements in order to best simulate the test phenomena. The differences between the simulation assumption/modeling and the Appendix K requirements are as follows:

°   Rewetting of the fuel rods was allowed.

°   The best-estimate homogeneous equilibrium critical flow model with subcooled flow multipliers on TLTA orifice critical flow data was used, replacing the Appendix K-required Moody model.

°   The actual test power history was used instead of the Appendix K-required ANS 1971 decay heat curve plus a 20 percent conservatism.

The calculated system pressure and mass flow were compared with measured data. The calculated pressure before the MSIV closure compares well with the measured data. The bundle inlet flow for the initial phase of the transient agrees with the experiment. The good agreement of the total mass inventory and system pressure confirms the accurate calculation of the break flow through the transient. Westinghouse also provided data on the mass inventory in the components of the system. The mass inventory distribution, including downcomer, bypass, guide tube, upper plenum, and lower plenum, was provided and

compared fairly well with the test results. Comparisons of the test thermo-couple measurements at various elevations with GOBLIN predictions show general agreement in trends and timing (Ref. 3); the selection of nodes for the rod dryout, heatup, and rewet comparisons is acceptable.

To demonstrate the conservative margin, Westinghouse performed more rod temperature analyses incorporating portions of the Appendix K requirement (no rewetting of the rods, zero heat-transfer coefficient following uncovering, and Appendix K-prescribed heat-transfer coefficients during spray cooling and after reflood). The resulting rod temperature shows about a 380°F margin. An additional PCT margin is inherent in the evaluation model because of other conservative Appendix K requirements excluded from the simulation (that is, the Moody break flow model and decay heat curve plus 20 percent conservatism).

6.0 COMPLIANCE WITH APPENDIX K REQUIREMENTS

Appendix K to 10 CFR Part 50 sets forth certain required and acceptable features of evaluation models for calculating ECCS performance to demonstrate that the acceptance criteria of 10 CFR 50.46 are met. These required and acceptable features involve both individual calculational models and inputs to the licensing model.

The staff, with assistance from LANL, has conducted a review of the Westinghouse boiling water reactor ECCS evaluation model (BWR ECCS EM) to verify compliance of the model with 10 CFR Part 50 Appendix K, requirements and to ensure that the methodology provides an acceptable calculational frame-work for evaluating the behavior of a BWR reactor system during a postulated loss-of-coolant accident in the classes of boiling water reactors presently licensed for operation. The review included those aspects of the methodology relevant to the calculation of peak cladding temperature (PCT) and hydrogen generation for a spectrum of break sizes.

Conformance of the Westinghouse BWR ECCS EM to each applicable item of the requirements established in 10 CFR Part 50, Appendix K, concerning ECCS evaluation models is addressed in the following.

I. Required and Acceptable Features of the Evaluation Models

I.A. Sources of Heat During the LOCA

All licensing basis LOCA calculations will be performed for a power level 1.02 times the licensed power level as required by Appendix K.

I.A.1. The Initial Stored Energy in the Fuel -- Fuel rod conditions at the initiation of the postulated LOCA are generated using an approved methodology (the PAD code). An evaluation was performed to determine a conservative burnup for the reference fuel design. These considerations result in acceptable compliance with Appendix K.

I.A.2. Fission Heat -- Fission power and point kinetics parameters are developed using an NRC-approved methodology (the PHOENIX code).

I.A.3. Decay of Actinides -- The actinide decay power is determined using a model described in American Nuclear Society Standard 5.1 "Decay Energy Release Rates Following Shutdown of Uranium-Fueled Thermal Reactors." This model is used for the calculations at the time in the fuel cycle that yields the highest calculated fuel temperature during the LOCA, as required by Appendix K.

I.A.4. Fission Product Decay -- The acceptable model ANS Standard 5.1 is used with a 1.2 multiplier as prescribed in Appendix K.

I.A.5. Metal-Water Reaction Rate -- The rate of energy release, hydrogen generation, and cladding oxidation is determined from the Baker-Just equation which is acceptable as specified in Appendix K.

I.A.6.   Reactor Internals Heat Transfer -- Heat transfer from non-fuel reactor components have been considered, as required by Appendix K.

I.B. Swelling and Rupture of the Cladding and Fuel Rod Thermal Parameters

As discussed in Section 3.2 of this Safety Evaluation, the cladding burst model employed in the Westinghouse BWR ECCS EM is a model developed for CHACHA-3C and which uses NRC-approved materials properties data. Cladding stress/strain functions are taken from a previously approved methodology.

I.C. Blowdown Phenomena

I.C.1.   Break Characteristics and Flow -- The sensitivity study provided by Westinghouse included the results of a break spectrum analysis for a BWR/5. Plant-specific applications should include or reference a sensitivity study applicable to the facility BWR class. The discharge model used in BWR ECCS EM is the Moody model as specified in Appendix K and is acceptable.

I.C.2.   Frictional Pressure Drops -- The frictional losses are calculated with commonly accepted relationships of friction factor and Reynolds number and two-phase friction multipliers as required by Appendix K.

I.C.3.   Momentum Equation -- The momentum equation used in the GOBLIN series of codes includes all terms specified in Appendix K.

I.C.4.   Critical Heat Flux -- A staff-approved correlation must be used when the subject methodology is used in a licensing analysis.

I.C.5.   Post-Critical Heat Flux Heat Transfer Correlations -- The heat transfer correlations used in GOBLIN are the Groeneveld 5.7 correlation specified in Appendix K or other NRC-approved correlations.

I.C.6.   Pump Modeling -- The recirculation pump model used in GOBLIN is developed from a basic conservation of angular momentum equation. Single-phase and degraded two-phase pump performance are modeled through performance curves which are addressed in a plant-specific application. The jet pump model in GOBLIN accounts for momentum and resistance effects as required by this rule item.

Section I.C.7 is not applicable to BWRs.

I.D. Post-Blowdown Phenomena; Heat Removal by the ECCS

I.D.1.   Single Failure Criterion -- The sensitivity studies provided by Westinghouse included relevant single failure considerations and comparisons with previous evaluations by the nuclear steam supply system vendor. This is acceptable.

I.D.2.   Containment Pressure -- GOBLIN analyses will conservatively assume atmospheric pressure in the containment volume throughout the LOCA transient. This assumption adequately addresses the requirements for this feature of Appendix K.

Sections I.D.3 through I.D.5 are not applicable to BWRs.

I.D.6.   Convective Heat Transfer Coefficients for BWR Fuel Rods Under Spray Cooling -- The Westinghouse CHACHA-3C code will use the rod surface heat transfer coefficients calculated by DRAGON before the end of lower plenum flashing. After this period, the convective coefficients will be derived from Appendix K recommendations. Heat transfer coefficients developed from experimental data should be justified as applicable to the particular fuel design for which the overall methodology is to be used.

I.D.7.   The Boiling Water Reactor Channel Box Under Spray Cooling -- The Westinghouse CHACHA-3C code will use the convective heat transfer coefficients calculated by DRAGON prior to the end of lower

plenum flashing. After this period but prior to core spray reaching rated flow, the channel convective heat transfer coefficient will be set to zero. Experimental data used to verify the applicability of heat transfer coefficients derived from Appendix K recommended values should be justified as applicable to the particular fuel design for which the overall methodology is to be used. The channel wetting time will be determined based on the modified Yamanouchi correlation plus 60 seconds, as prescribed by Appendix K.

II. Required Documentation

The documentation provided in References 1 through 3 was in sufficient detail which (1) allowed technical review of the analytical approach, (2) provided sensitivity studies of pertinent variables, system and fuel noding, and calculational time step, (3) provided adequate comparisons with experimental data, and (4) demonstrated an acceptable margin of safety comparable to other acceptable evaluation models.

The staff has confirmed that Westinghouse has addressed those features of Appendix K applicable to BWRs.

7.0 CONCLUSIONS

The Westinghouse BWR ECCS evaluation model (WCAP-11284) and sensitivity studies (WCAP-11427) were reviewed in reference to the Appendix K requirements. We conclude that Westinghouse/ASEA-ATOM has developed and documented an adequate information data base to address and meet the Appendix K requirements. Westinghouse also has performed an integral system qualification analysis to compare the ECCS model calculations against applicable groups of test data.

From our present evaluation of the adequacy of the models used in the Westinghouse BWR ECCS EM and the conformance of the calculations to Appendix K requirements, it is concluded that the model described in Reference 1 will provide adequately representative and conservative predictions for large-break

and small-break LOCAs in boiling water reactors. Because the analysis predictions were based on data and characteristics of a fuel design (QUAD+) not presently scheduled for production and commercial use, this conclusion is subject to certain conditions before use of the methodology for licensing actions. These conditions are specified in the following Regulatory Position.

Regulatory Position

(1) The staff concludes that the Westinghouse BWR ECCS EM provides an acceptable evaluation model of loss-of-coolant accidents for use in calculations of peak clad temperature (PCT) and hydrogen generation made in accordance with Appendix K licensing calculations for large-break and small-break LOCAs in boiling water reactor BWR/2 through BWR/6 plants. The basis for this position is the staff review of licensing topical reports WCAP-11284 (Ref. 1) and WCAP-11427 (Ref. 2) and the evaluation summarized in this safety evaluation. This conclusion is subject to the conditions described in paragraphs 2 and 3 below.

(2) The staff concludes that the Westinghouse BWR ECCS EM has provisions and options to conform with the required modelling features of Appendix K. Conformance to plant-specific requirements of Appendix K (e.g., I.C.6, Pump Modeling) for use in licensing calculations must be specified in the license application reload safety analysis report. This report should include or reference a sensitivity study for the BWR type identified in the license application.

(3) Certain specific model areas of the Westinghouse BWR ECCS EM discussed in WCAP-11284 are specific to a fuel design (QUAD+). These areas are the critical heat flux (CHF) and fuel design characteristics for the QUAD+ fuel assemblies. A staff-approved CHF correlation must be used when the subject ECCS methodology is used in a licensing analysis (Section 3.1.8). The experimental data used to verify the convective spray heat transfer coefficients should be justified as applicable to the particular fuel design for which the overall methodology is to be applied (Section 3.2.2). The use of a fuel design other than QUAD+ fuel in a transition core should also be addressed.

8.0 REFERENCES

1. D. B. Ebeling-Konig, M. E. Nissley, J. T. Dederer, A. G. Gagnon, and J. M. Brennan, "Westinghouse Boiling Water Reactor Emergency Core Cooling System Evaluation Model: Code Description and Qualification," Westinghouse report WCAP-11284 (September 30, 1986).

2. D. B. Ebeling-Konig, M. E. Nissley, and R. M. Jakub, "Westinghouse Boiling Water Reactor Emergency Core Cooling System Evaluation Model: Code Sensitivity," Westinghouse report WCAP-11427 (June 30, 1987).

3. "Westinghouse Boiling Water Reactor Emergency Core Cooling System Evaluation Model: Response for Additional Information and Errata," WCAP-11284-Amendment 1/WCAP-11427-Amendment 1 (July 18, 1988).

4. J. A. Holmes, "Description of the Drift Flux Model in the LOCA Code RELAP-UK," Conference on Heat and Fluid Flow in Water Reactor Safety, I. Mech. E. Manchester, 1977.

5. G. B. Wallis, One-Dimensional Two-Phase Flow (New York: McGraw-Hill, Inc., 1969).

6. R. V. Bailey et al., "Transport of Gases Through Liquid-Gas Mixtures," AICHE New Orleans Meeting (1956).

7. S. O. Eriksson et al., "Experiment Med Motriktade Angfloden I Strilkylningskretsen," GOTA Studsvik report, AES-15 (1977).

8. P. W. Ianni, "Effectiveness of Core Standby Cooling Systems for General Electric Boiling Water Reactors," APED-5458, March 1968.

9. NEDO-20566, "General Electric Company Analytical Model for Loss-of-Coolant Accident Analysis in Accordance with 10 CFR Part 50, Appendix K," January 1976.

ABSTRACT

This report describes the Westinghouse approach to performing Loss of Coolant Accident (LOCA) sensitivity studies and defining the 10CFR50 Appendix K evaluation methodology for boiling water reactors. The evaluation model for BWR/5 plant designs is defined and justified using this methodology. A break spectrum calculation is performed using this model. Peak cladding temperatures from the break spectrum are presented for Westinghouse QUAD+ fuel operating at a maximum linear heat generation rate limit of 14.5 kW/ft.

The Westinghouse method for assessing the LOCA impact of using multiple fuel designs in a reload core is also described in this report. A sample calculation is presented for a BWR/5.

TABLE OF CONTENTS

TABLE OF CONTENTS (CONTINUED)

ACKNOWLEDGEMENTS

LIST OF TABLES

LIST OF FIGURES

LIST OF FIGURES (CONTINUED)

LIST OF FIGURES (CONTINUED)

LIST OF FIGURES (CONTINUED)

1.0 INTRODUCTION

The GOBLIN system of computer codes is used by Westinghouse to evaluate Emergency Core Cooling (ECC) system performance in boiling water reactors (BWR). These codes have previously been described in detail (Reference 1). This report presents the results of the Loss of Coolant Accident (LOCA) sensitivity studies which have been performed by Westinghouse in order to define the LOCA evaluation methodology to be used in licensing calculations for a BWR/5.

The method used to perform the sensitivity studies is based on a systematic assessment of the impact of LOCA modeling on calculational results for the plant design in question. The results of these sensitivity studies are used to define the LOCA evaluation methodology which conforms to the acceptance criteria of 10CFR50.46 and Appendix K (Reference 2). A flowchart of this strategy is shown in Figure 1.1. Examples of "models based on test data" from Figure 1.1 include correlations for heat transfer coefficients, countercurrent flow limitation, dryout and pressure drop. Examples of "generic sensitivity studies" include time step, convergence criteria and some noding sensitivity studies (e.g. core, rod, and channel noding). The approach in Figure 1.1 is applicable to any BWR plant type, and is described in detail in this report.

Section 2 of this report provides a brief overview of the GOBLIN series of computer codes used in Westinghouse BWR LOCA analyses. Section 3 describes in detail the code results for the limiting break in a BWR/5, as determined using the final evaluation methodology. This transient serves as the reference case for the remainder of the report. Sections 4 through 7 provide justification for the evaluation methodology by examining the sensitivity of the LOCA results to key modeling assumptions and code inputs. The break spectrum results which verify the limiting break are given in Section 8. Finally, the method used to evaluate the impact of mixed fuel designs on BWR LOCA transients is presented in Section 9. Sample results are presented for the case of a BWR/5 core comprised of Westinghouse QUAD+ fuel and General Electric 8x8R fuel. It should be noted that since Westinghouse BWR reload fuel assemblies are designed to be compatible with the resident fuel design, no significant impact is expected for the mixed fuel cycles.
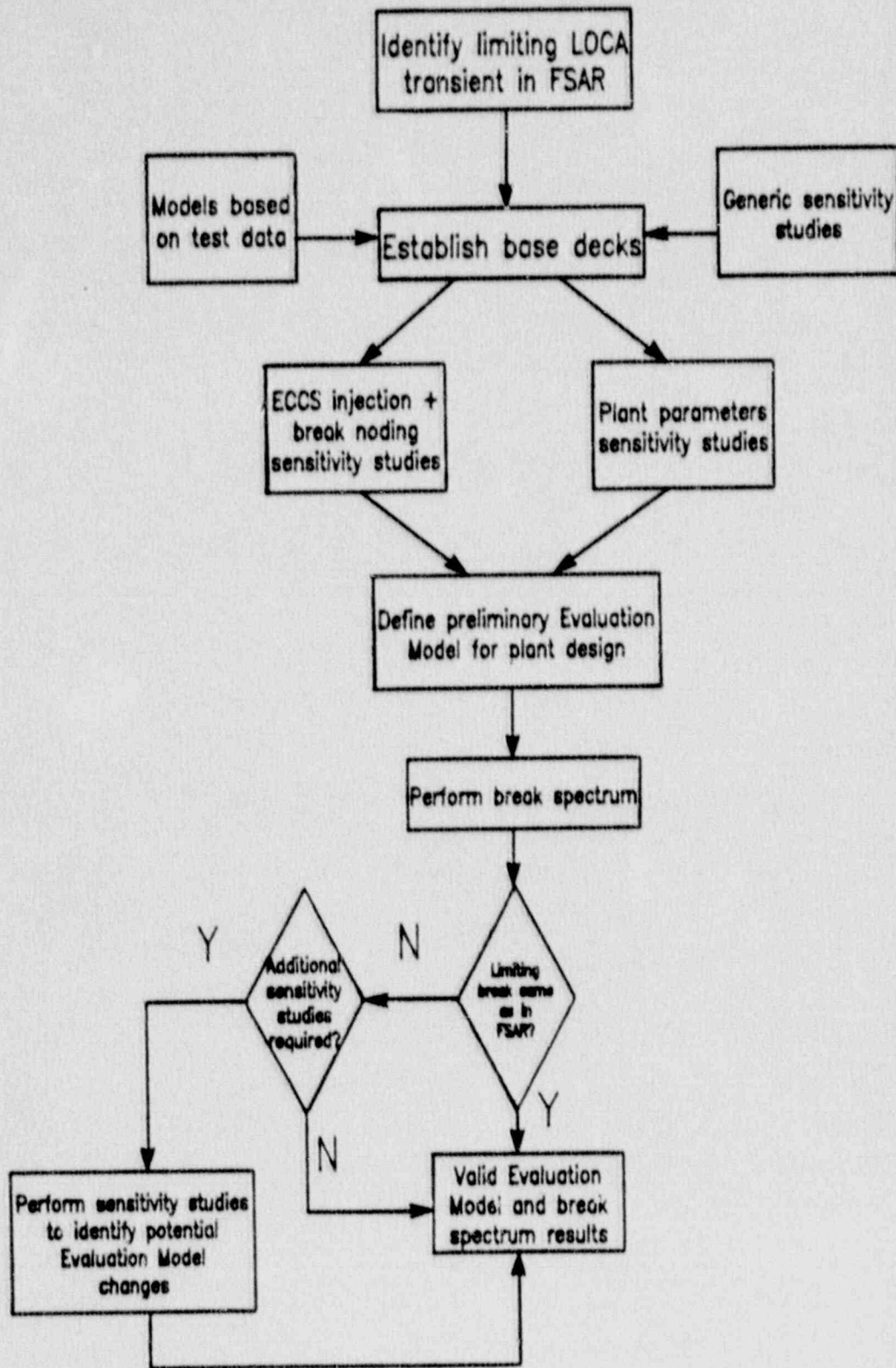
Figure 1.1 - Method Used to Define LOCA Evaluation Model

2.0 OVERVIEW OF COMPUTER CODES

The GOBLIN series of computer codes uses one-dimensional assumptions and solution techniques to calculate the BWR transient response to both large and small break LOCAs. The series is composed of three major computer codes-- GOBLIN, DRAGON and CHACHA-3C. The function of the individual codes are:

GOBLIN - Performs the analysis of the LOCA blowdown and reflood thermal hydraulic transient for the entire reactor, including the interaction with various control and safety systems.

DRAGON - Performs the hot fuel assembly thermal hydraulic transient calculations using boundary conditions from the GOBLIN calculation. (DRAGON is virtually identical to GOBLIN, the only difference is that several calculation models are bypassed in DRAGON.)

CHACHA-3C - Performs detailed fuel rod mechanical and thermal response calculations at a specified axial level within the fuel assembly previously analyzed by the DRAGON code. All necessary fluid boundary conditions are obtained from the DRAGON calculation. CHACHA-3C determines the temperature distribution of each rod throughout the transient and ultimately the peak clad temperature (PCT) and cladding oxidation at the axial plane under investigation. It also provides input for the calculation of total hydrogen generation.

The flow of information between these codes is shown in Figure 2.1. Detailed code descriptions may be found in Reference 1.
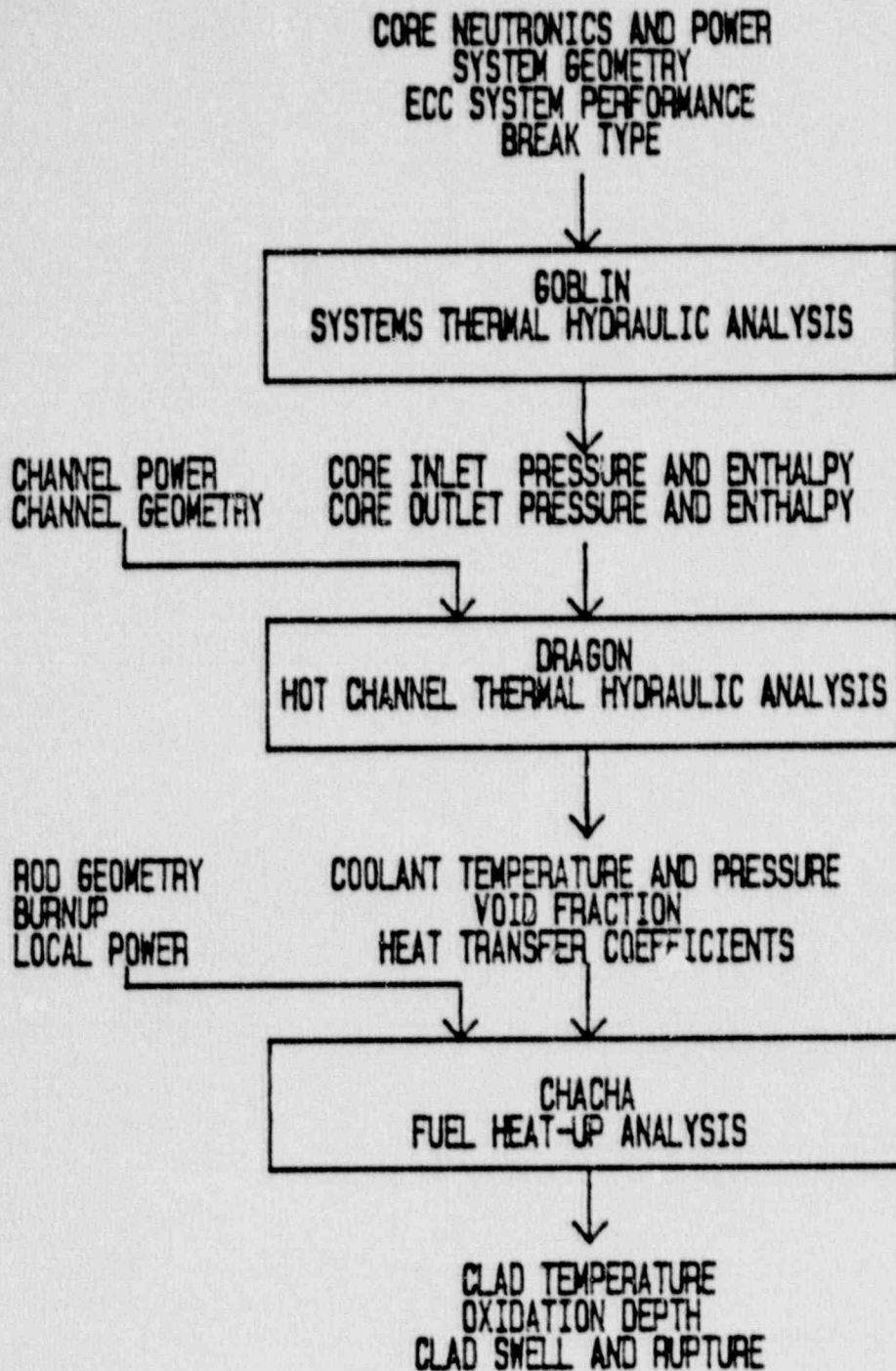
Figure 2.1 - Flow of Information Between Computer Codes

3.0 REFERENCE LOCA

In this section the reference LOCA transient response is described in detail. The reference plant type analyzed is a General Electric BWR/5 design. Figure 3.1 shows a schematic diagram of the BWR/5 vessel, internals and recirculation system. Table 3.1 summarizes the key features of the reference plant.

A brief description of the emergency core cooling systems is first presented, then the reference LOCA is described.

3.1 BWR Emergency Core Cooling Systems

The BWR ECC system is a plant standby safeguard system designed to maintain reactor core cooling in the event of a loss of reactor coolant. The ECC system consists of a number of diverse, automatically actuated, and redundant safety systems whose primary function is to replenish the reactor vessel coolant.

The ECC system designs vary between the BWR/2 through BWR/6 designs. A specific plant ECC system includes several of the following subsystems.

Low Pressure Core Spray (LPCS)

The low pressure core spray system supplies coolant to a ring spray sparger above the reactor core. The LPCS system includes large capacity low pressure pumps (shutoff head of typically 300 psia) that can spray water across the entire core via nozzles in the ring sparger. This system is employed in all BWR designs.

High Pressure Core Spray (HPCS)

The high pressure core spray system supplies water above the core via a separate ring sparger. Lower capacity pumps with a shutoff head above the reactor operating pressure are used to spray water into the vessel. This system is used in the BWR/5 and BWR/6 designs.

High Pressure Coolant Injection (HPCI)

In the BWR/2 through BWR/4 designs a high pressure coolant injection system (or in a few plants feedwater coolant injection) is used to supply auxiliary reactor coolant at high pressures. The HPCI is introduced into the vessel via the feedwater sparger in the reactor downcomer.

Low Pressure Coolant Injection (LPCI)

The low pressure coolant injection system is used to refill the reactor vessel from below the reactor core. Like the LPCS system it uses low pressure high capacity pumps. The injection location varies between plant design. In the BWR/3 and BWR/4 the LPCI is injected in the jet pump drive line. In the BWR/5 and BWR/6 the LPCI is injected in the core bypass region between the fuel channels and the inner shroud.

Automatic Depressurization System (ADS)

The automatic depressurization system consists of a set of safety/relief valves which may be automatically actuated to depressurize the reactor vessel. The ADS is designed to reduce the vessel pressure below the shutoff pressure of the large capacity LPCS and LPCI systems, allowing a more rapid replenishing of the coolant inventory and refilling of the core.

The ECC subsystems are automatically actuated on signals from the reactor vessel level, reactor pressure, and/or containment drywell pressure measurement systems.

The BWR/5 plant design presented in this report includes one LPCS subsystem, three LPCI subsystems, one HPCS subsystem and an ADS. Figure 3.2 shows the ECC pump systems and their individual power sources, designated Division I, II, and III.

3.2 Accident Description

The reference LOCA transient is a full guillotine break of a recirculation suction line in a BWR/5 plant. This reference transient assumes failure of the low pressure core spray diesel generator (Division I) which results in the limiting break for a BWR/5 plant. The transient response is described in three sections. The system response calculated with the GOBLIN code is described first. Next the hot fuel assembly response calculated with the DRAGON code is described. Then the hot axial plane fuel rod heatup response calculated with the CHACHA-3C code is presented.

3.2.1 Reactor System Response

The GOBLIN code is used to calculate the reactor vessel system response to a postulated LOCA in a BWR. The GOBLIN nodalization used for the reference analysis is shown in Figure 3.3. The LOCA analysis is initiated from 104.3 percent of rated full power, a pressure of 70.7 bar (1055 psia), and 100 percent of rated core flow. The LOCA is initiated at time zero by an instantaneous 100 percent guillotine break in a recirculation suction line. Also at time zero, offsite power is assumed lost, which causes tripping of the two main recirculation pumps. Reactor scram and MSIV closure occur in the first second of the transient.

Figure 3.4 shows the initial vessel pressure response and subsequent depressurization. The initial pressure response is governed by the time of reactor scram, MSIV closure and jet pump suction uncovery. In the reference transient the pressure initially drops due to the inventory loss out the break and steamlines. When the MSIV are closed, the vessel pressure recovers and starts to pressurize until the jet pump suction uncovers. Once the downcomer level falls below the top of the jet pumps a steam vent path is created out the break, increasing the volumetric inventory loss. This stops the short-lived vessel repressurization. About two seconds after jet pump uncovery, the recirculation line uncovers, significantly increasing the volumetric flow out the break. The recirculation line uncovery causes a subsequent rapid depressurization to near atmospheric pressure in about 50 seconds.

Figure 3.5 shows the total break mass flow rate. Note that although the break mass flow rate decreases after the downcomer empties (at about 8 seconds), the break volumetric flow rate increases due to steam venting out the break. Hence the pressure vessel depressurizes faster.

Figure 3.6 shows the active core inlet flow rate during the initial phase of the transient. Several key phenomena are visible in this plot. They include jet pump uncovery, jet pump flashing and lower plenum flashing. The core inlet flow drops off rapidly in the initial seconds due to the loss of the broken recirculation line drive flow and initial coastdown of the intact recirculation loop. At about 6 seconds the jet pump suctions uncover, further degrading the intact jet pump performance. Less than a second later the vessel pressure has dropped to the point where the jet pump fluid saturates and flashes, causing a surge in core inlet flow. At about nine seconds the lower plenum fluid flashes, causing a larger surge in core inlet flow rate. The lower plenum continues to flash at a slower rate for the next 10 seconds. This is evident by the slow decay in the core inlet flow rate.

Figure 3.7 shows the total core side entry orifice inlet flow rate. The results show the initial flow rate decrease, periods of fluid flashing, and the subsequent draining of the core through the lower plenum and out the break.

The vessel draining, ECC system actuation, and subsequent refilling and reflooding of the vessel regions can be seen in Figures 3.8 and 3.9. Figure 3.8 shows the total system mass inventory. As can be seen in the figure, HPCS actuation does not compensate for the inventory loss out the break. However, once the LPCI is actuated the vessel inventory starts to be replenished. The mass inventory distribution in the reactor vessel can be seen in Figure 3.9. The guide tubes refill first, followed by the lower plenum and bypass region. The core and upper plenum are last to refill.

Figure 3.10 shows the mixture levels in the downcomer, upper plenum and lower plenum. The mixture levels clearly show the downcomer and lower plenum draining and subsequent refill processes. Two periods of liquid stacking in the upper plenum are visible. The first is just after LPCI actuation and before sufficient liquid can penetrate the bypass region. The second stacking

is caused by flashing of the ECC fluid which is heated to saturation temperature by the hot guide tube and bypass structures. This flashing steam holds up further penetration of ECC fluid into the bypass region. Following these initial hold up periods the ECC fluid steadily drains and refills the guide tubes, bypass and lower plenum. This is shown in the lower plenum mixture level. Following reflooding of the core, the upper plenum level returns as the vessel is refilled.

The timing of the key events in the system response analysis are summarized in Table 3.2. A detailed description of the hot assembly thermal-hydraulic response is given in the next section.

3.2.2 Hot Assembly Response

The DRAGON code is used to calculate the thermal and hydraulic response of the hot assembly in a BWR during a postulated LOCA. Boundary conditions (e.g., pressure and enthalpy for the upper plenum and lower plenum and the bypass regions), and the core relative power as a function of time from the GOBLIN calculation are used in the hot assembly analysis. The upper plenum and lower plenum enthalpy boundary conditions from the GOBLIN reference transient are shown in Figures 3.11 and 3.12. The core pressure drop boundary condition is shown in Figure 3.13.

The core noding used for the DRAGON analysis in the Westinghouse evaluation model is shown in Figure 3.14. The fuel rod conduction model considers 4 rod groups in the assembly (Figure 3.15). The choice of DRAGON rod grouping has no impact on an Appendix K analysis, since all rods are assumed to dry out at the same time as the lead rod. However, this rod grouping does provide a preliminary look at the bundle radial temperature profile.

The reference DRAGON transient used a 1.5 cosine axial power distribution with a planar linear heat generation rate of 12.5 kw/ft at the midplane. Each rod group was specified to have a local peaking factor of 1.16, corresponding to a maximum linear heat generation rate of 14.5 kw/ft. The planar linear heat generation rate is used in the energy conservation equation, and the local

peaking factor is included in the pool boiling critical heat flux calculation. Assembly power was increased by 2 percent to account for potential uncertainties in initial core power measurement, as required by 10CFR50 Appendix K.

The key results from the reference DRAGON transient are shown in Table 3.3 and Figures 3.16 through 3.19. The timing of events is very similar to the GOBLIN results (Table 3.3 vs. Table 3.2), with midplane dryout occurring about one second earlier in the hot assembly. The hot assembly active channel inlet flow also follows the GOBLIN results very closely (Figure 3.16 vs. Figure 3.6). The void fraction at the bundle midplane is shown in Figure 3.17. Cladding temperature turnaround at the midplane is seen to occur at the same time as in the GOBLIN transient (Table 3.2). Bundle mass inventory throughout the transient is shown in Figure 3.18. Again, the same trends are seen as in the GOBLIN transient (Figure 3.9).

The DRAGON results which are passed to CHACHA-3C for use in the rod heatup calculations are coolant pressure, rod heat transfer coefficients prior to uncovery, and reflood time. The coolant pressure and rod heat transfer coefficients for the midplane are shown in Figures 3.19 and 3.20. The uncovery time is defined as the time at which the transition from the film boiling heat transfer regime to steam cooling begins. The reflood time is defined as the time at which the DRAGON temperature transient is mitigated by the transition from steam cooling to the low flow film boiling heat transfer regime. Therefore, the reflood time is the same as the DRAGON cladding temperature turnaround time.

3.2.3 CHACHA-3C Reference Transient

The CHACHA-3C code is used to perform the detailed fuel rod heatup calculations at a specified elevation from the hot assembly analysis. The reference CHACHA-3C calculation has been performed using boundary conditions from the midplane of the reference DRAGON transient (Figures 3.19 and 3.20). A typical fuel design for a BWR/5 operating with 24 month cycles was considered as the reference design (Figure 3.21).

Nuclear and fuel rod performance data corresponding to an average planar burnup of 22 GWD/MTU were used in the reference CHACHA-3C transient. This burnup is conservative for the reference fuel design for several reasons:

1. The gadolinium has been depleted to the point where the interior rods are operating at or near their highest local peaking factors throughout life. Higher interior rod peaking factors yield higher peak cladding temperatures for a given planar linear heat generation rate.

2. The maximum local peaking factor for the assembly is very close to unity (see Figure 3.22). Therefore the planar linear heat generation rate is very close to the maximum linear heat generation rate (assumed to be 14.5 kw/ft).

3. Rod internal pressure is higher than at lower burnups, increasing the likelihood of burst.

4. Beyond this burnup (approximately) the fuel can no longer achieve limiting power levels.

The cladding temperature transient for the rod with the peak cladding temperature is shown in Figure 3.23. This rod was calculated to burst 98 seconds into the transient. At that time, metal-water reaction begins on the cladding inner surface, and the gray body factors used in the radiation heat transfer calculation are modified to account for strained cladding dimensions. (See Reference 1 for a detailed discussion of the prediction and consequences of burst in the Westinghouse BWR LOCA evaluation model.)

The temperature transient was turned around by reflood at 142 seconds, prior to rewet of the channel and watercross by top down quenching. The calculated peak cladding temperature was 1036°C (1897°F), well below the acceptance criterion of 1204°C (2200°F). The calculated maximum oxidation fraction was 0.031, also well below the acceptance criterion of 0.17.

TABLE 3.1
REFERENCE PLANT DESIGN FEATURES

Plant Type   GE BWR/5
Number of Fuel Assemblies   764
Fuel Design   W QUAD+
Recirculation Lines   2
Number of Jet Pumps   20

Rated Power   3323 MWt
Rated Steam Flow 14.3×10^6 lbm/hr
Rated Core Flow 108.5×10^6 lbm/hr
Steam Dome Pressure   1020 psia
Feedwater Temperature   420°F

TABLE 3.2
TIMING OF SYSTEM RESPONSE KEY EVENTS

	Time (sec)
Break Initiates	0.0
Reactor Scram/MSIVs Begin to Close	1
MSIVs Closed	4
Jet Pumps Uncover	5
Jet Pump Flashing	6
Downcomer Level Below Break Elevation	8
Lower Plenum Flashing	10
Avg. Channel Midplane Dryout	22
HPCS Initiation	27
Initiation of Spray Cooling	48
LPCI Initiation	53
Guide Tubes Full	113
Bypass Full	125
LP Full	135
Midplane Reflood	142

TABLE 3.3
TIMING OF HOT ASSEMBLY KEY EVENTS

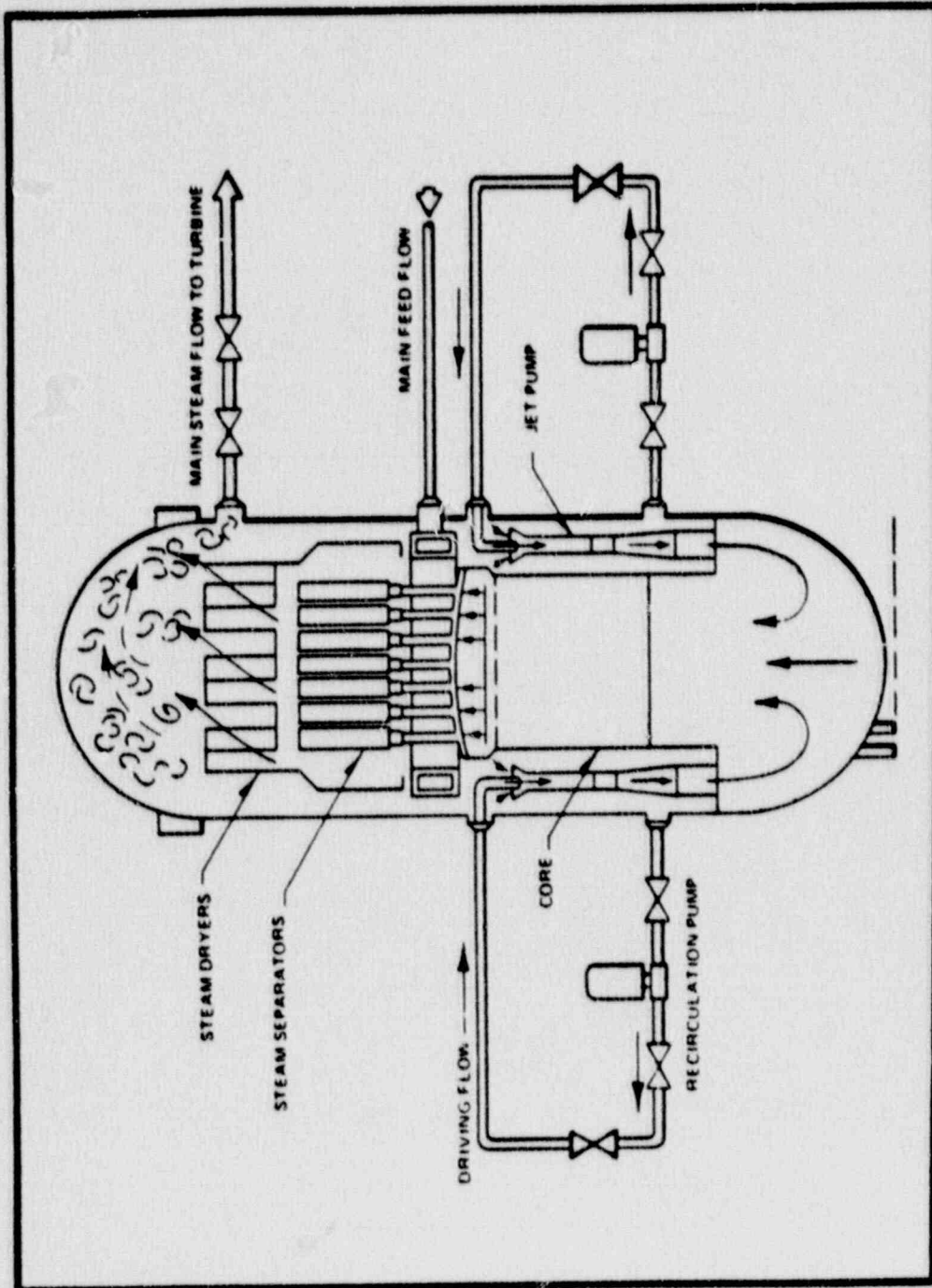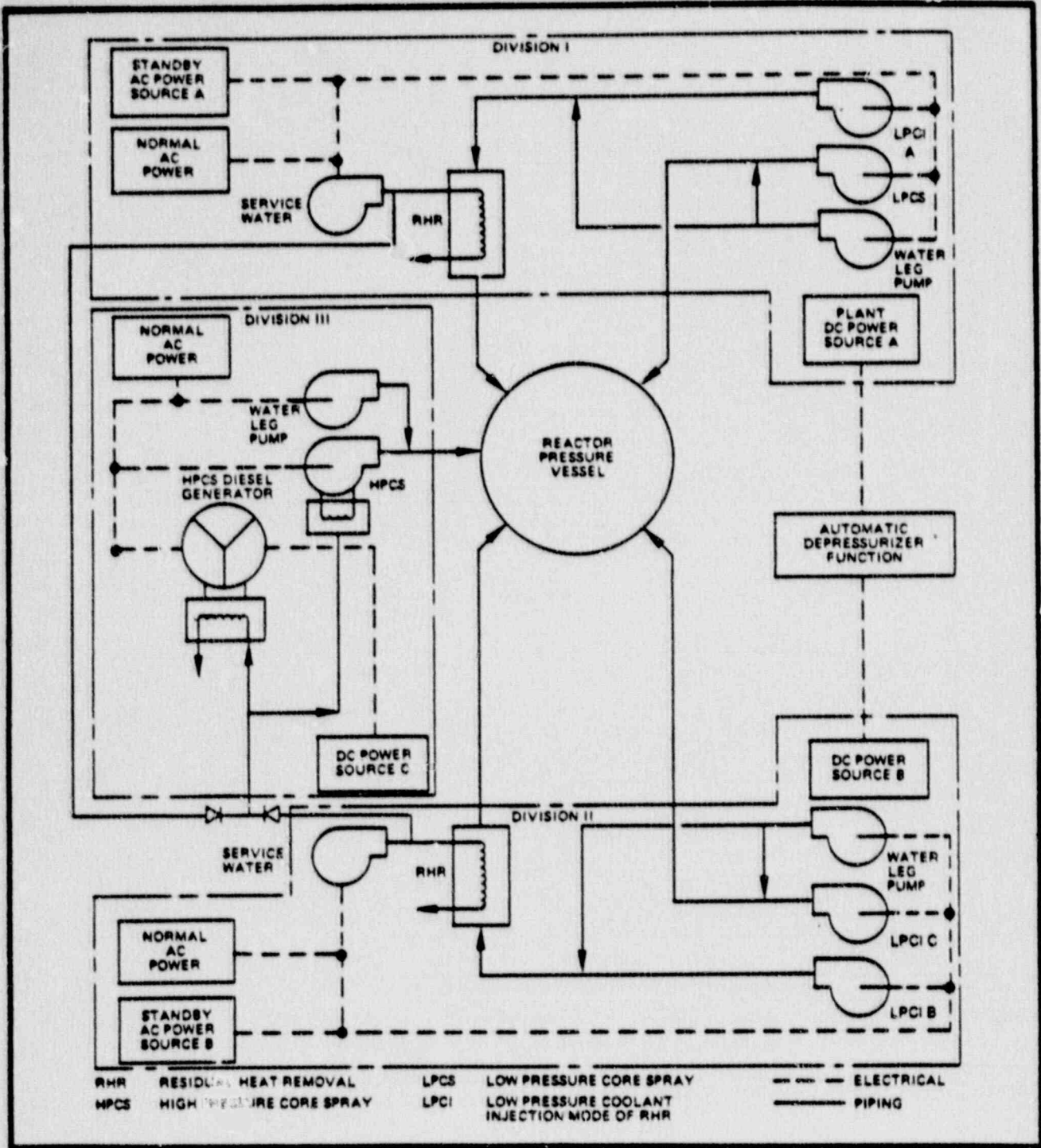|	Time (sec)
First Dryout	1.2
Midplane Dryout	21.5
Midplane Uncovery	28.7
Midplane Reflood	142

Figure 3.1 - Jet Pump Boiling Water Reactor

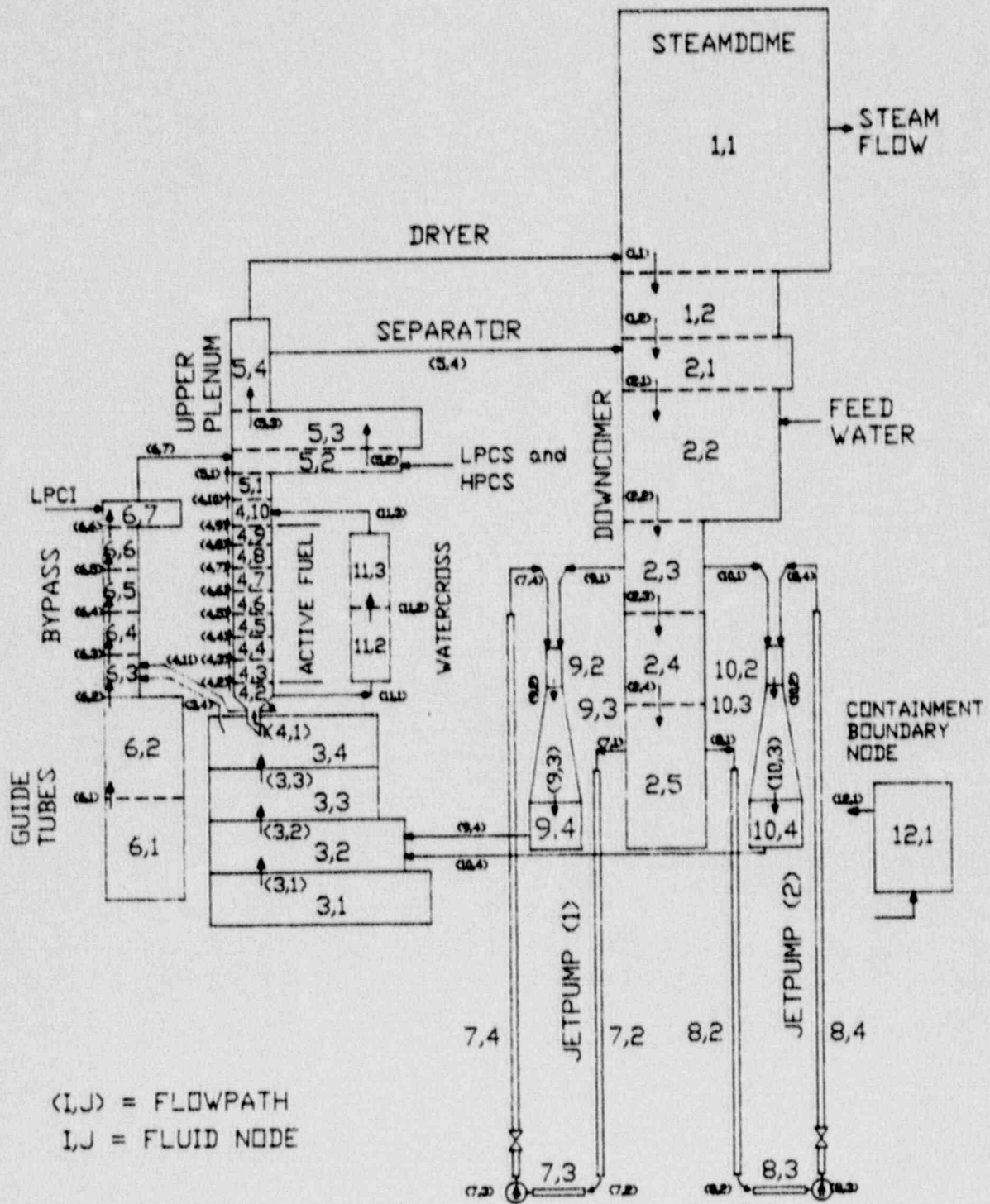Figure 3.2 - Emergency Cooling System Network for BWR/5

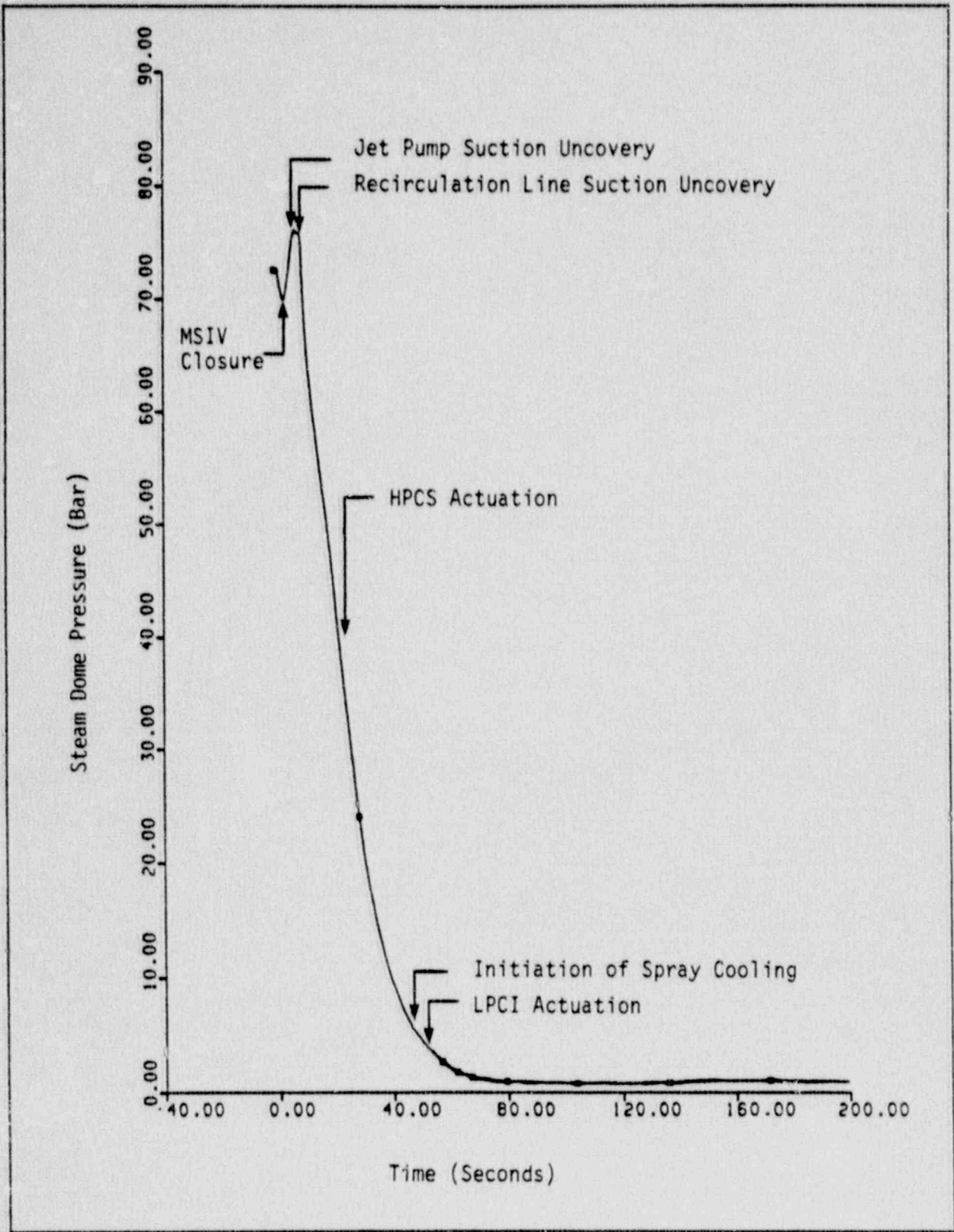Figure 3.3 - GOBLIN Nodalization for a BWR/5 with QUAD+ Fuel

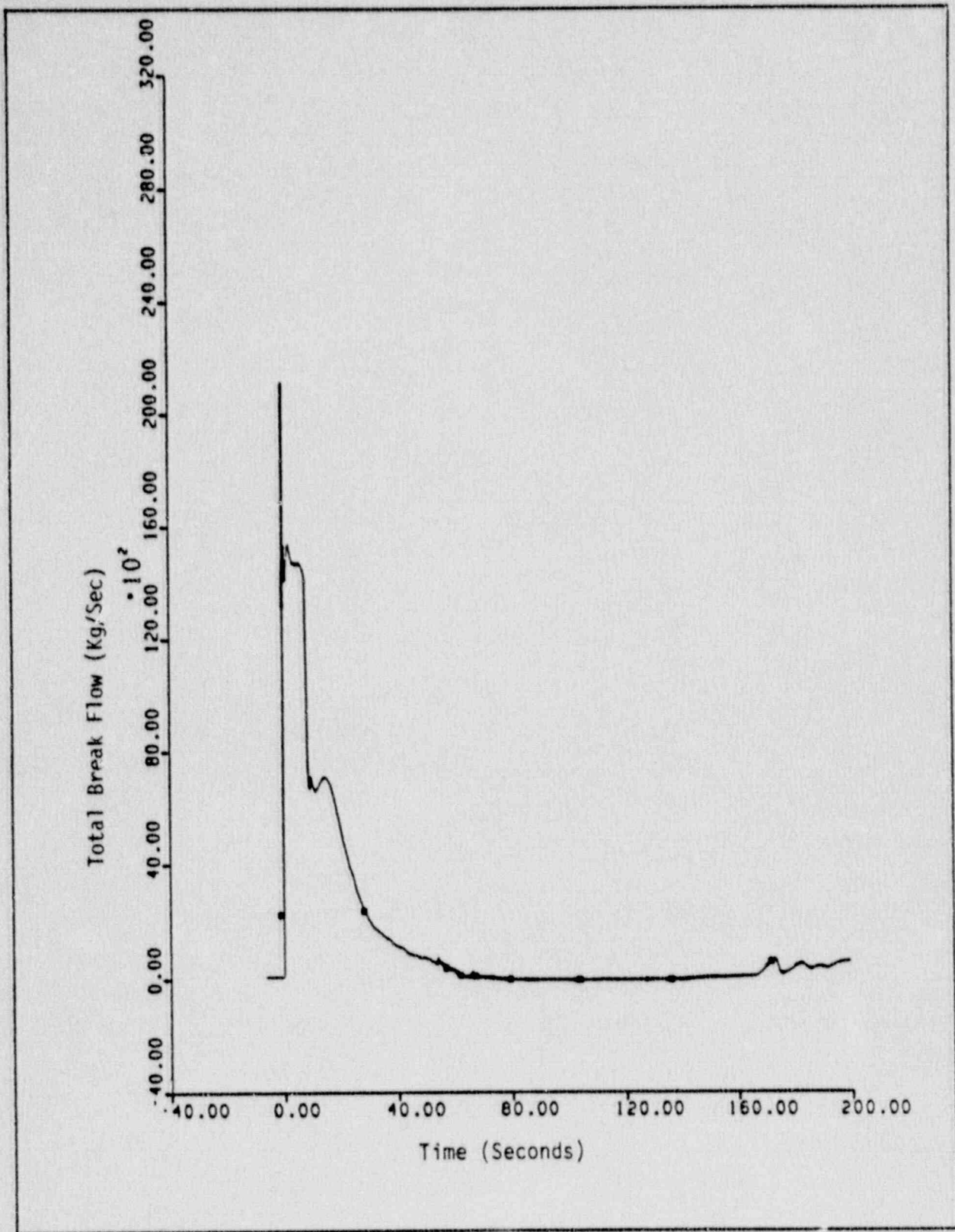Figure 3.4 - Vessel Steam Dome Pressure
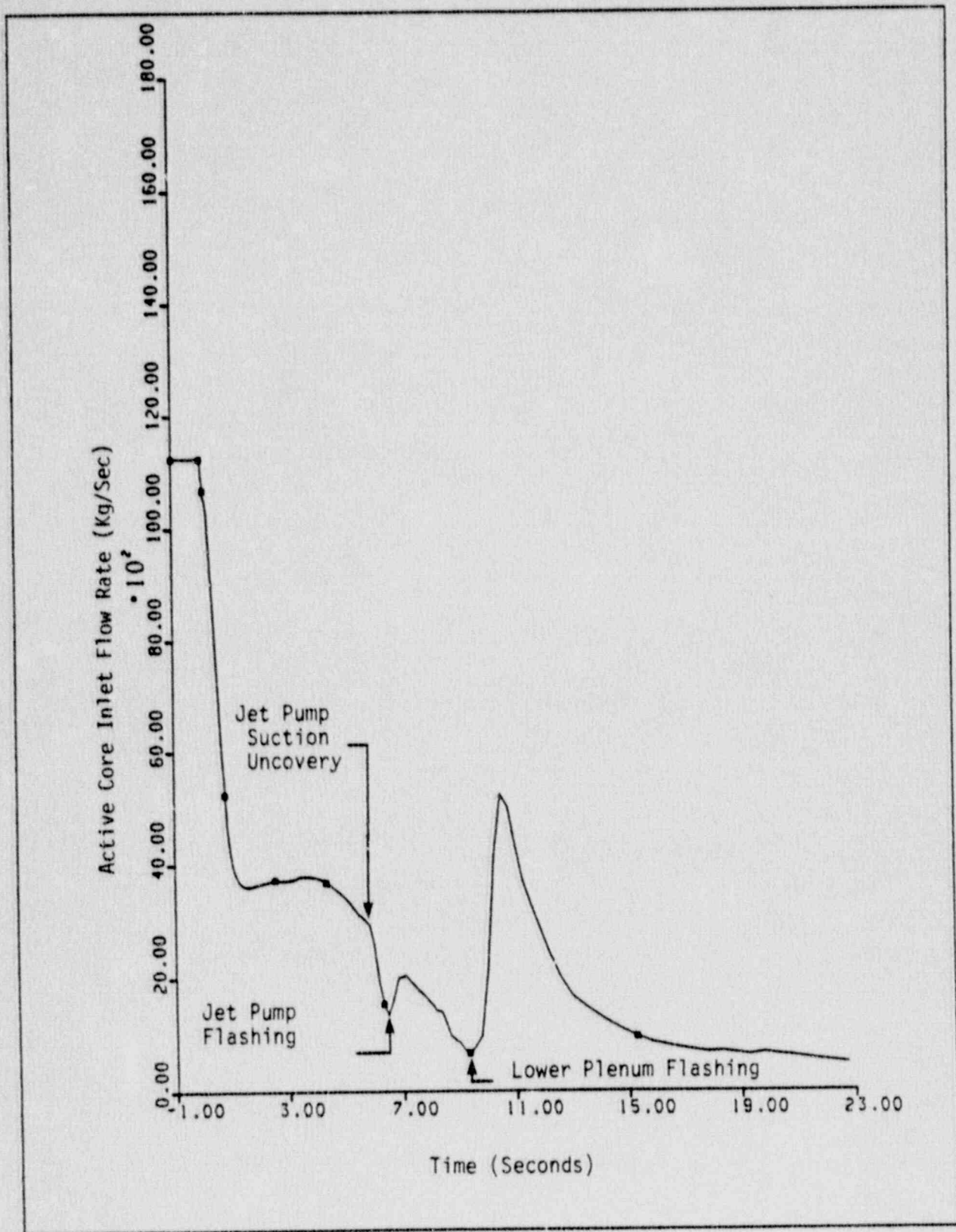
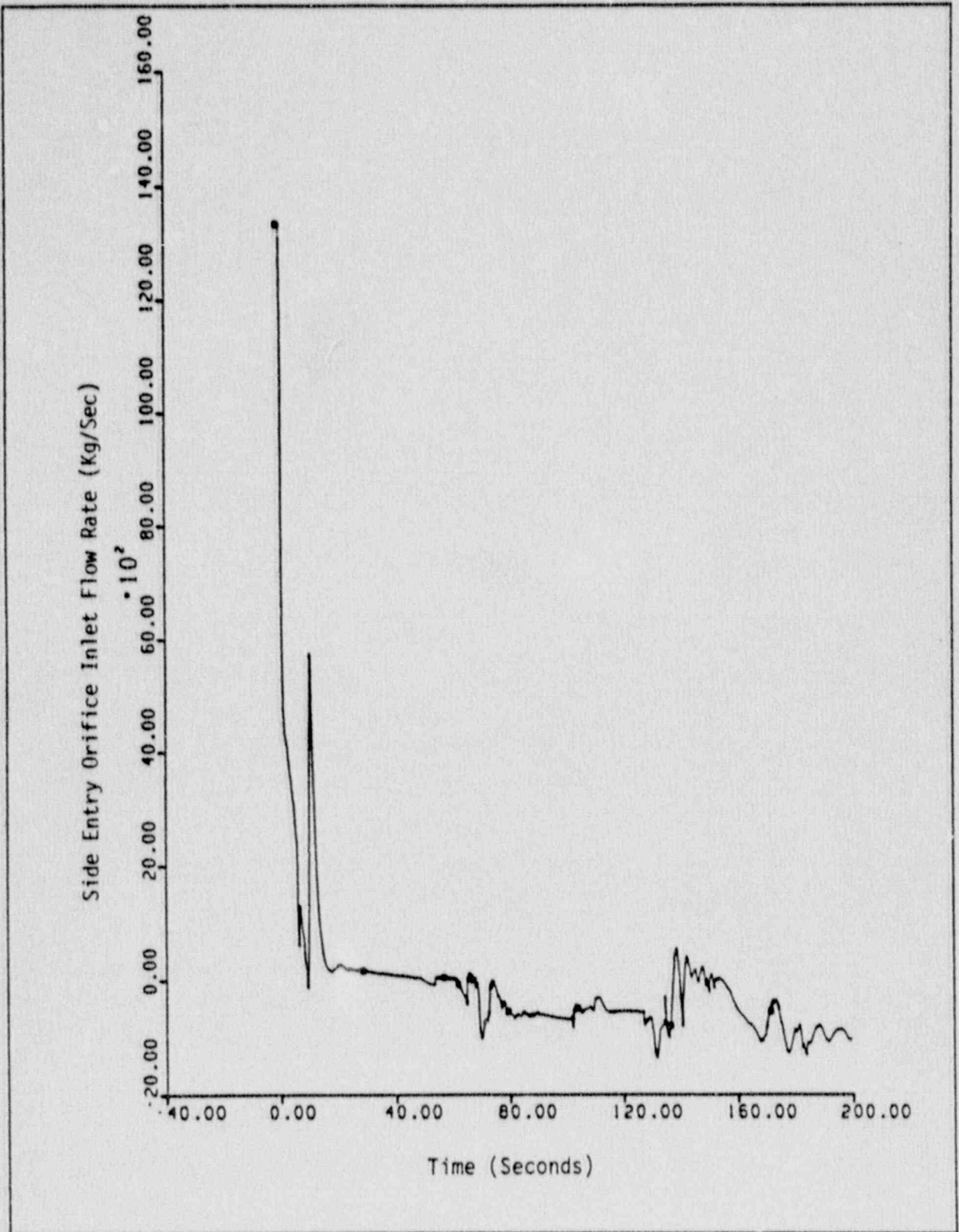Figure 3.5 - Total Break Flow Rate

Figure 3.6 - Active Core Inlet Flow Rate

Figure 3.7 - Total Side Entry Orifice Inlet Flow Rate
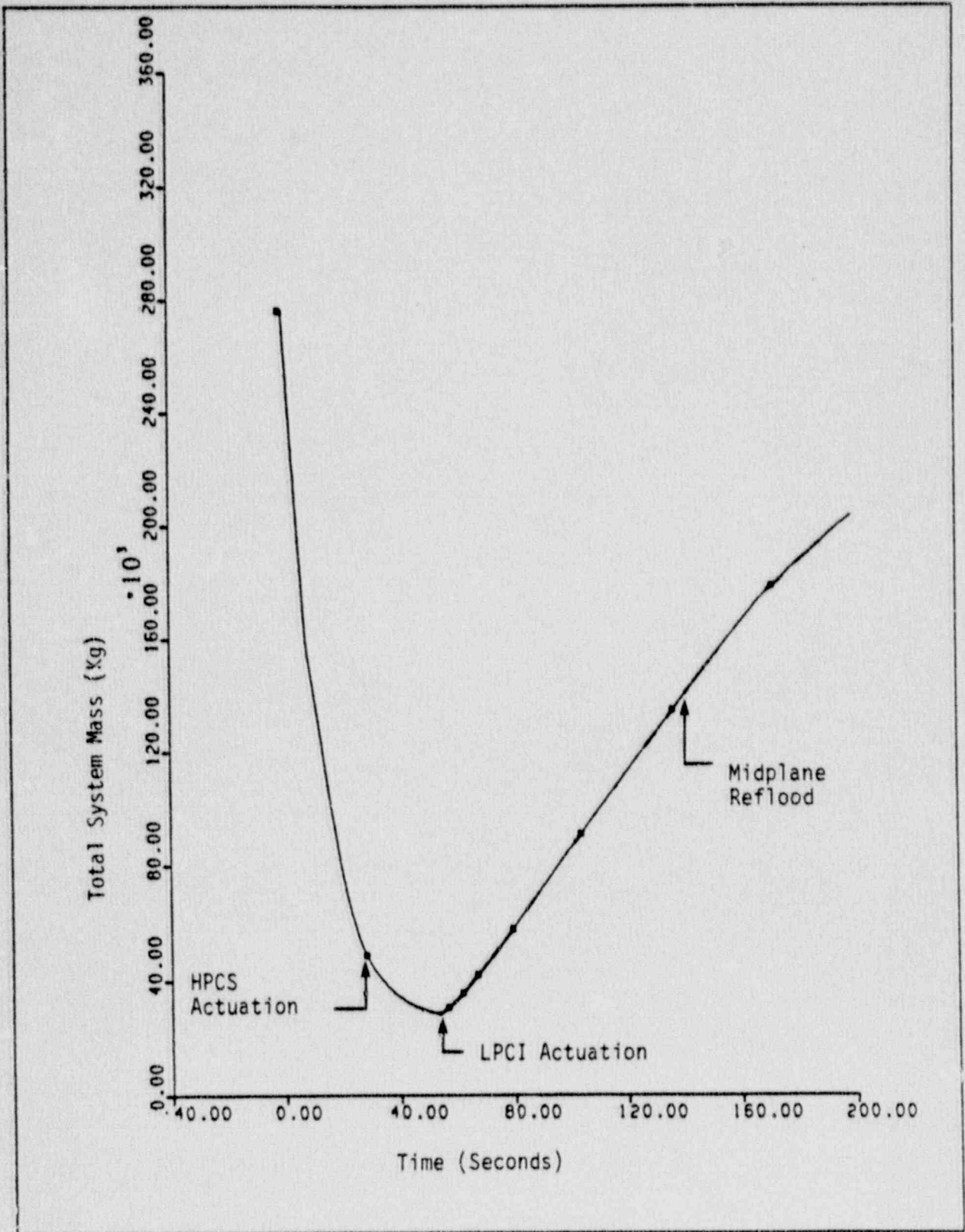
Figure 3.8 - Total Vessel and Recirculation Line Mass Inventory

Upper Plenum Mass (Kg)

Downcomer Mass (Kg)

Core Mass (Kg)

Bypass Mass (Kg)

Lower Plenum Mass (Kg)

Guidetube Mass (Kg)
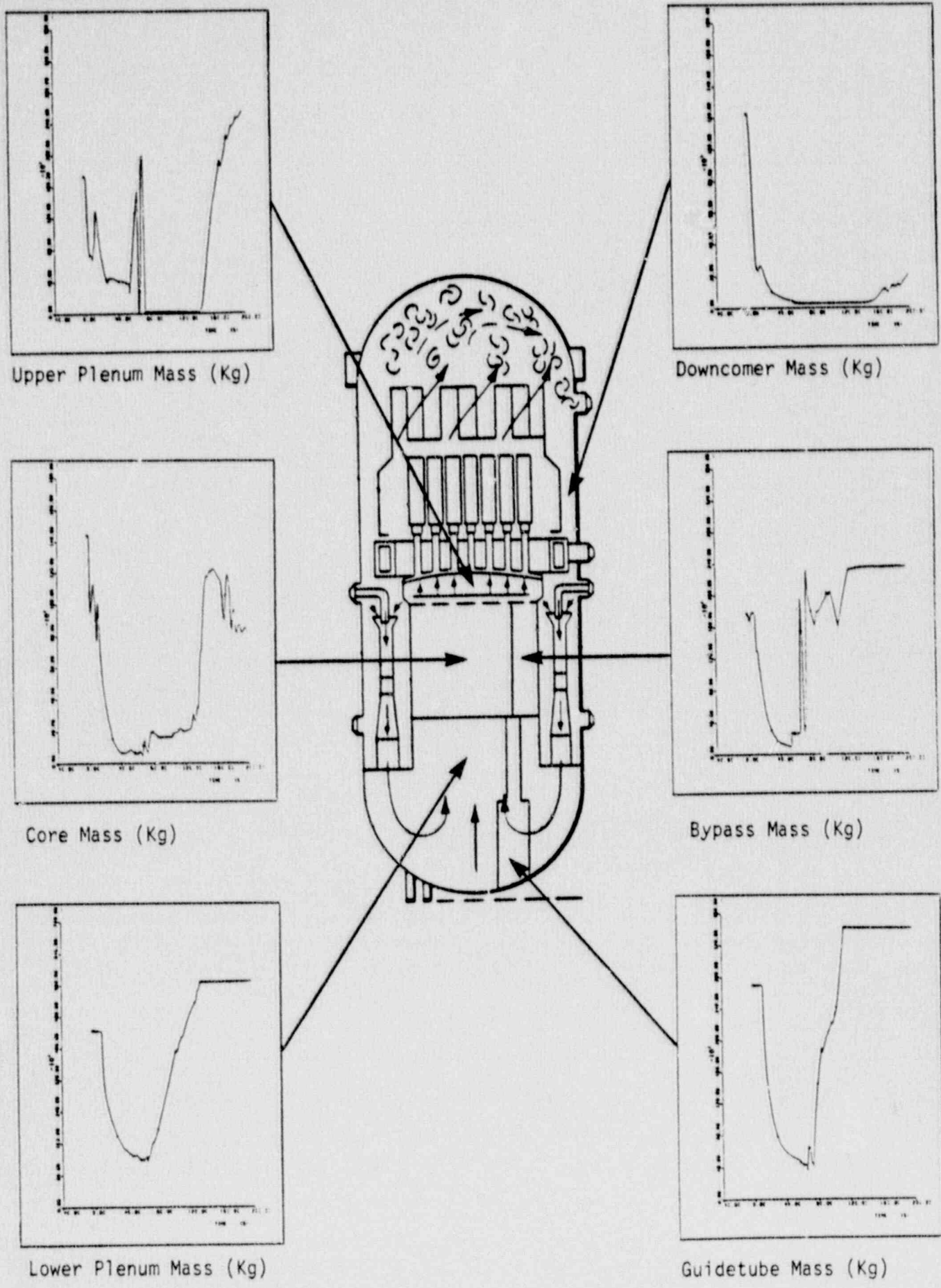
Figure 3.9 - Reactor Vessel Mass Distribution
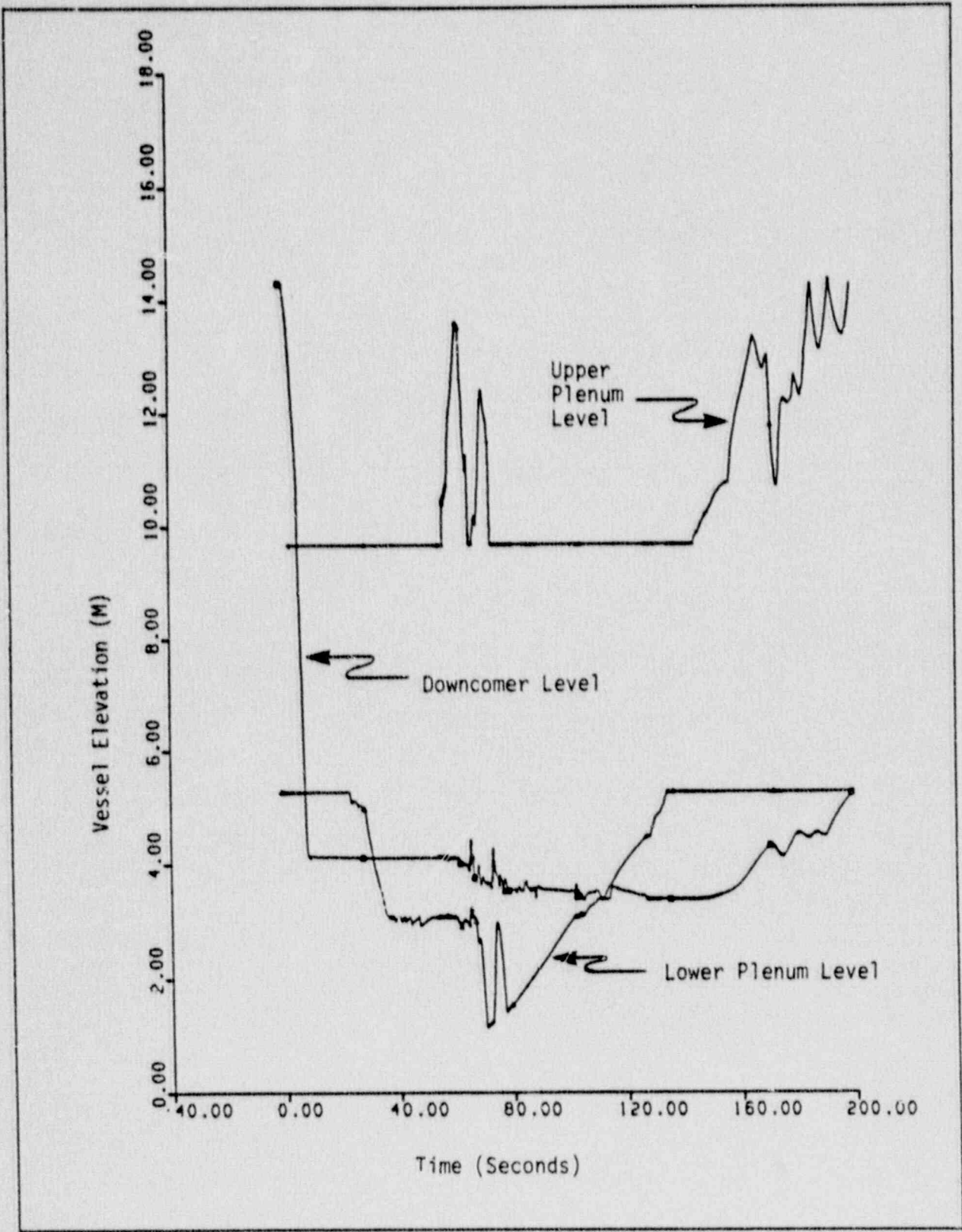
Figure 3.10 - Vessel Mixture Levels
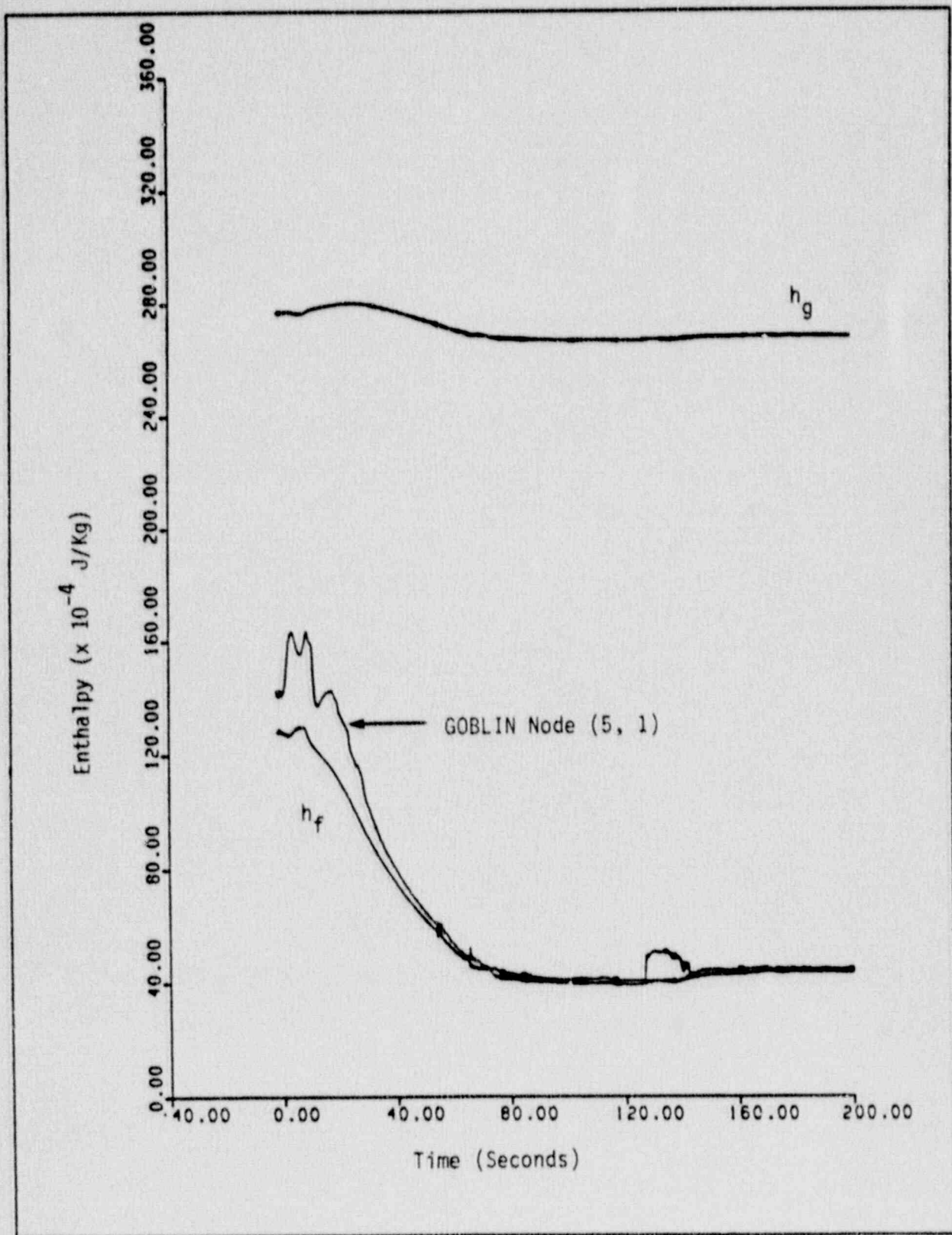
Figure 3.11 - Upper Plenum Enthalpy Boundary Condition
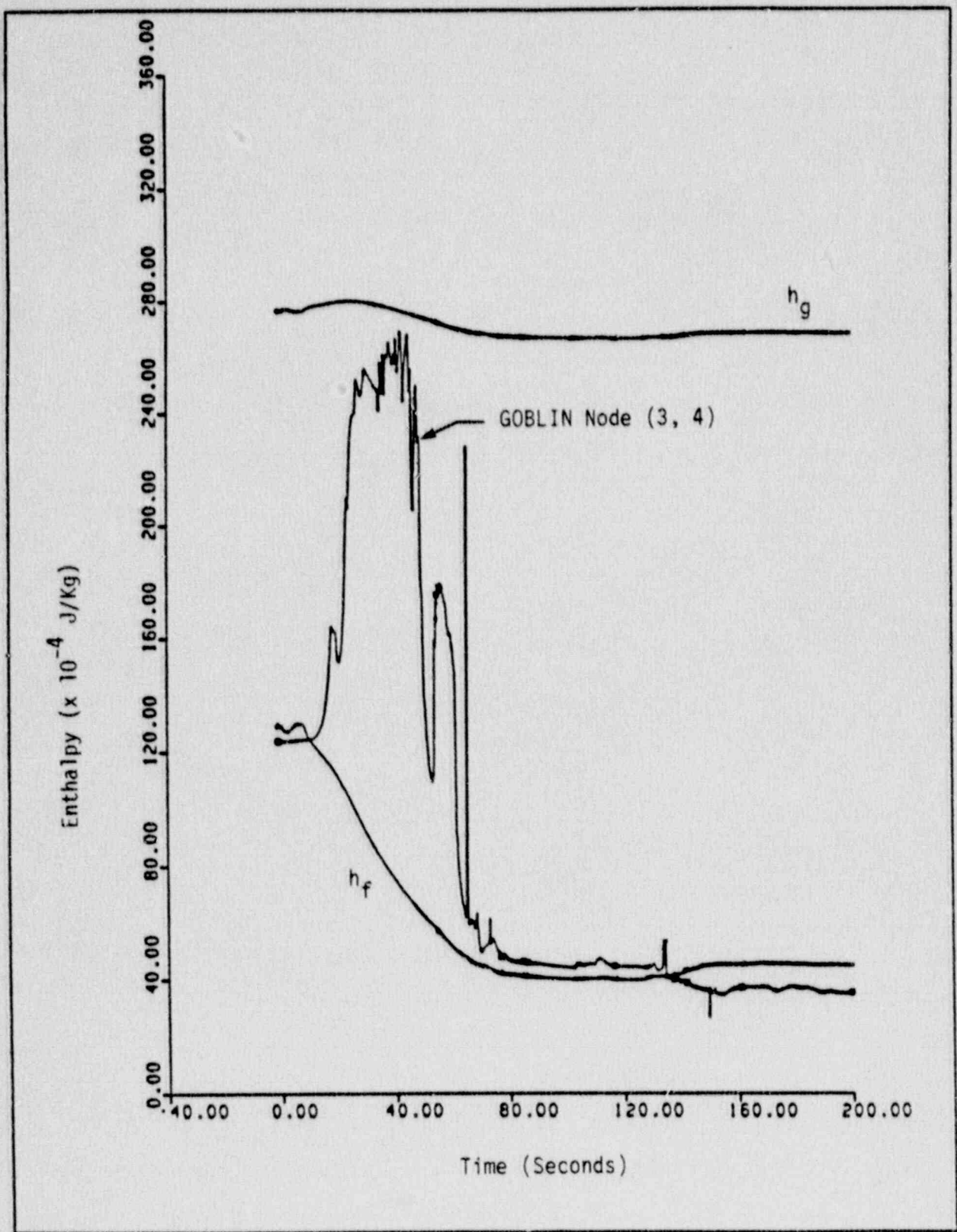
Figure 3.12 - Lower Plenum Enthalpy Boundary Condition
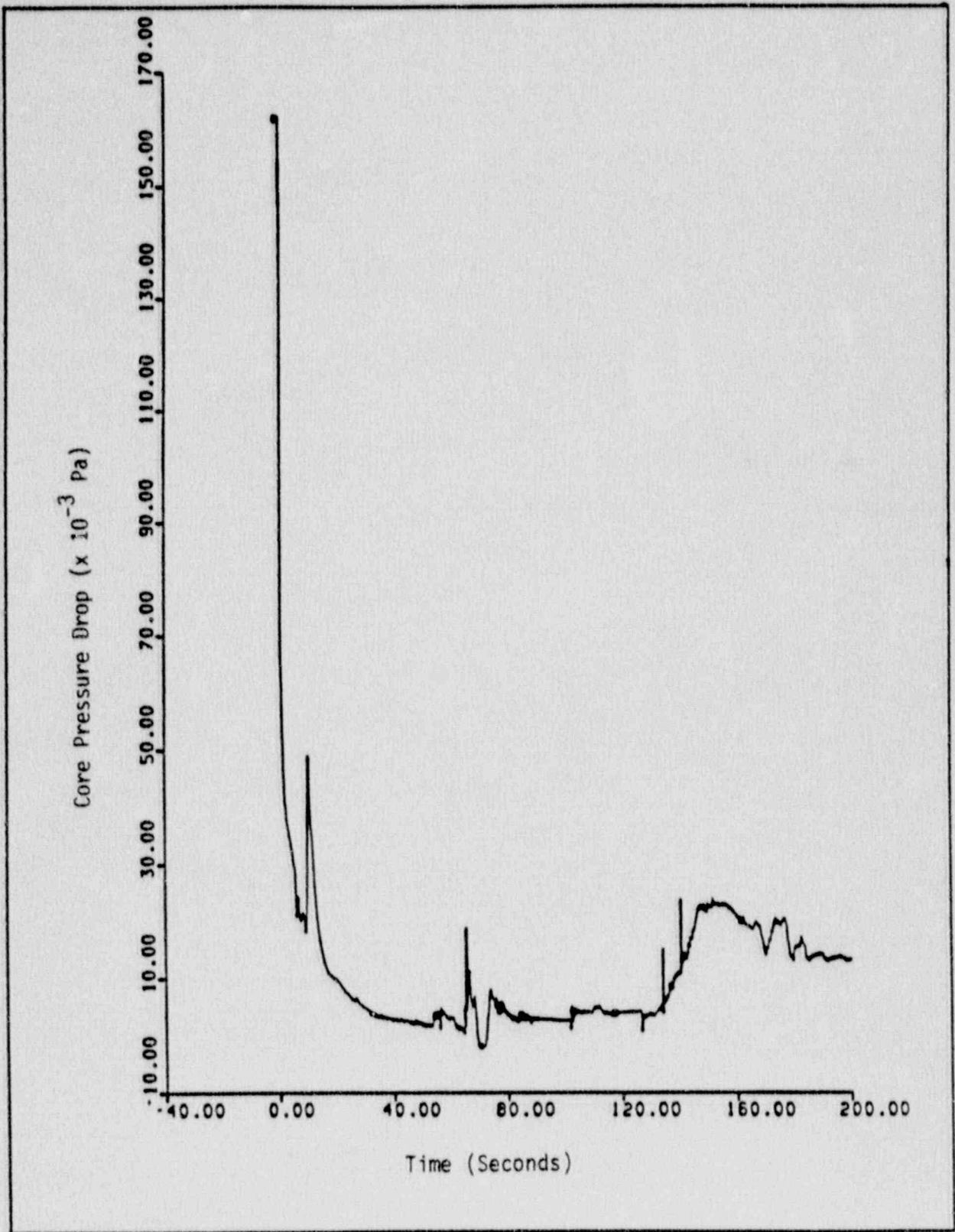
Figure 3.13 - Core Pressure Drop Boundary Condition
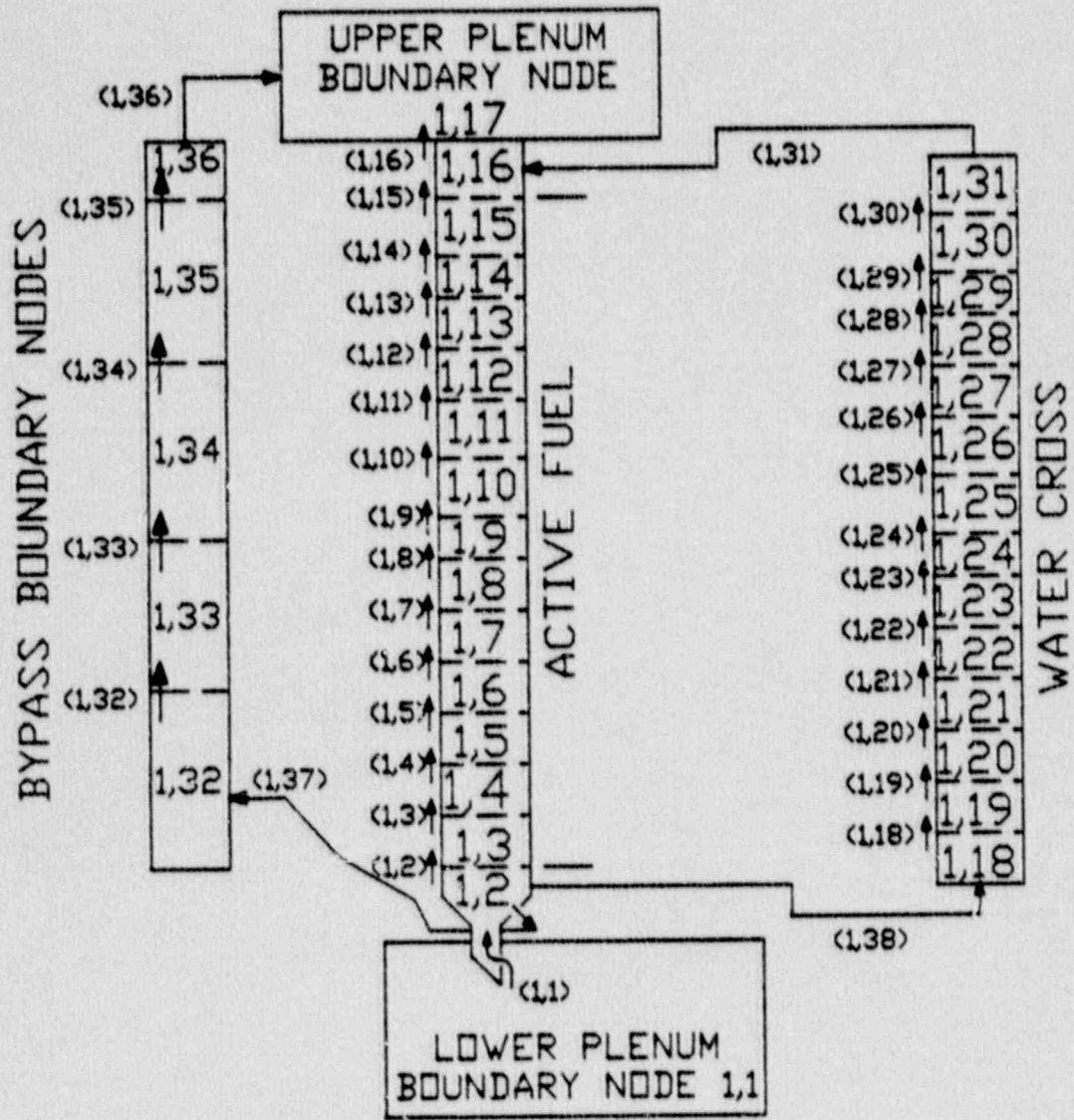
(I,J) = FLOWPATH

I,J = FLUID NODE

Figure 3.14 - DRAGON Nodalization for a QUAD+ Fuel Assembly
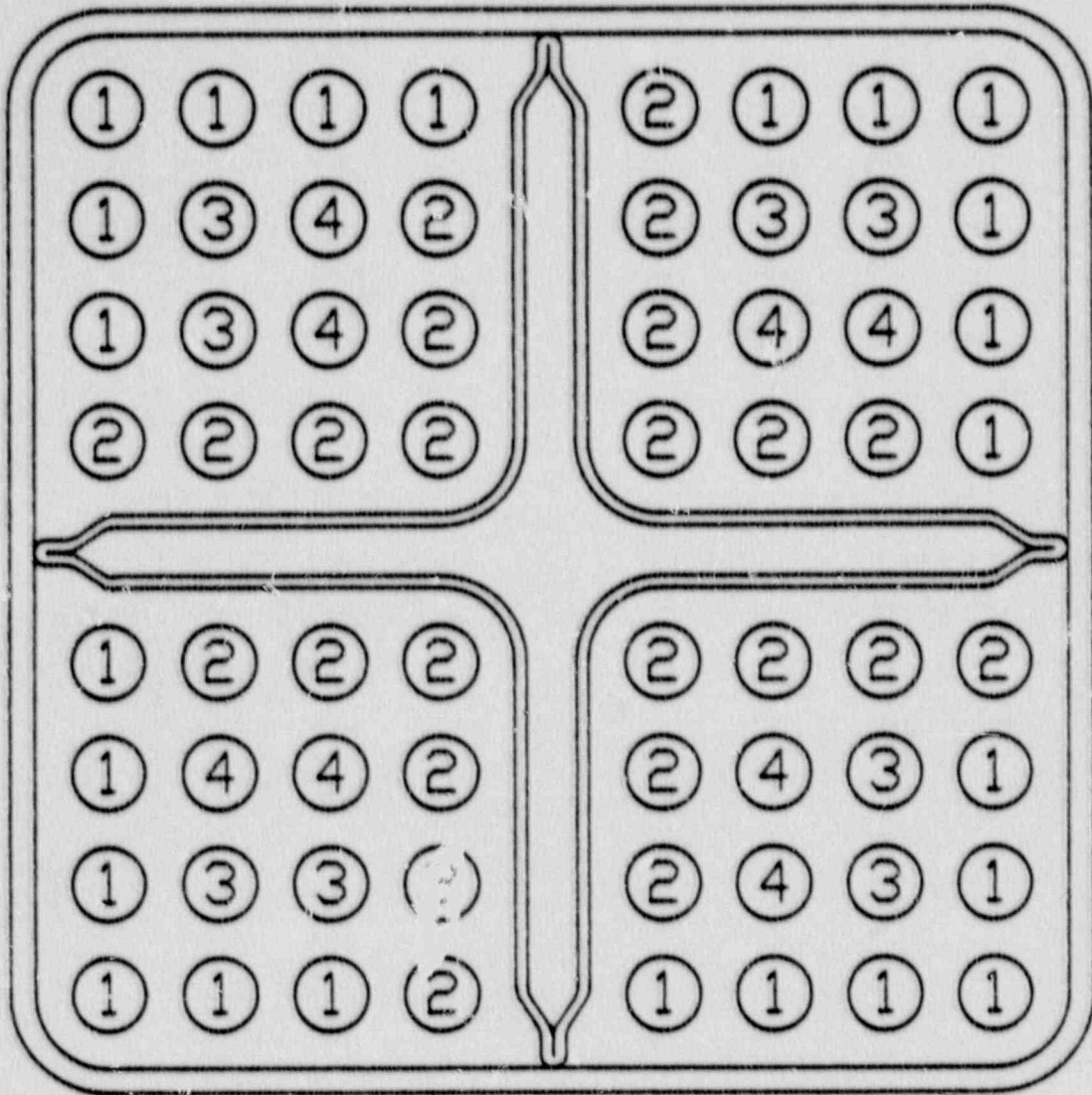
Figure 3.15 - DRAGON Rod Groups for a QUAD+ Fuel Assembly
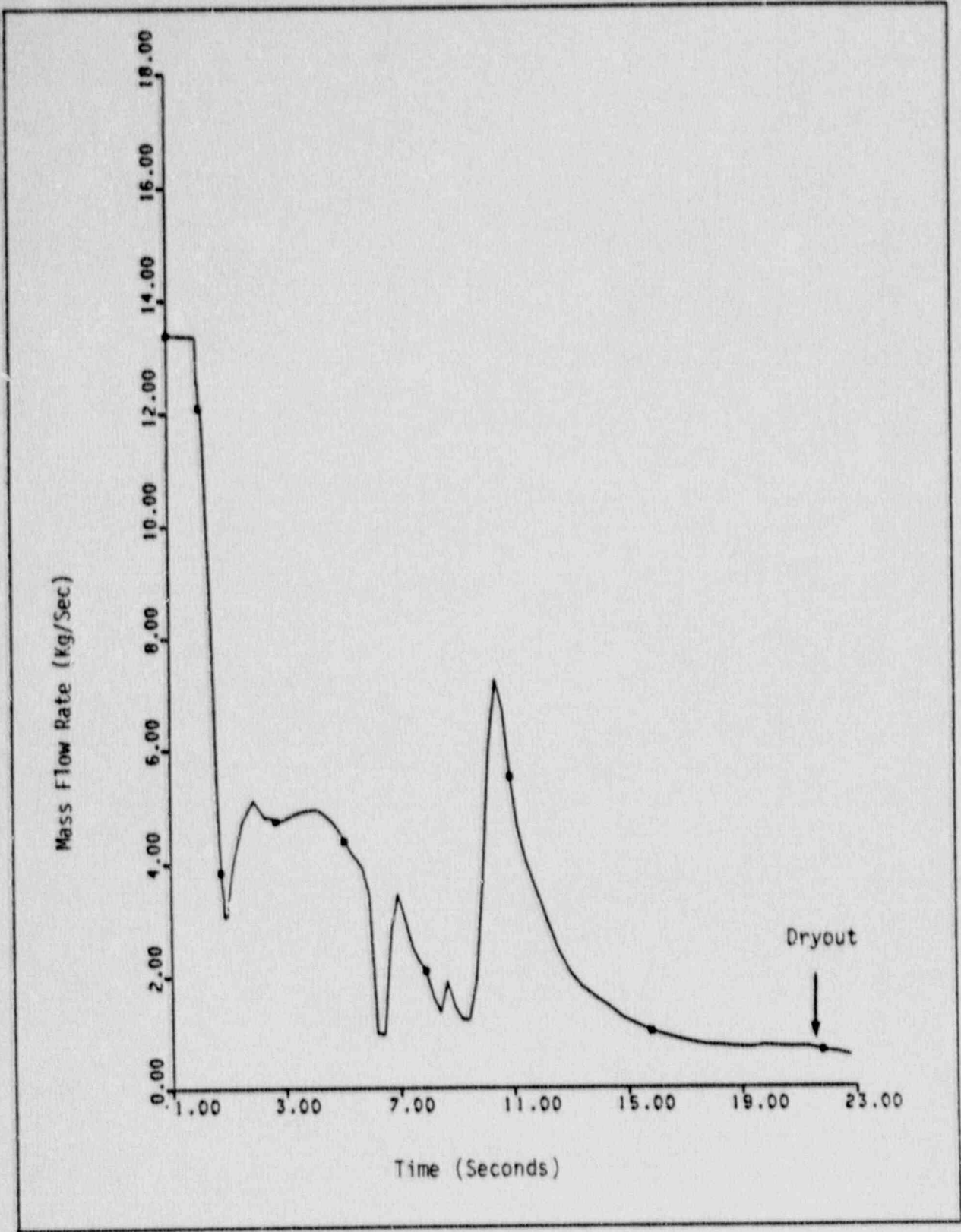
Figure 3.16 - Hot Assembly Active Channel Inlet Flow
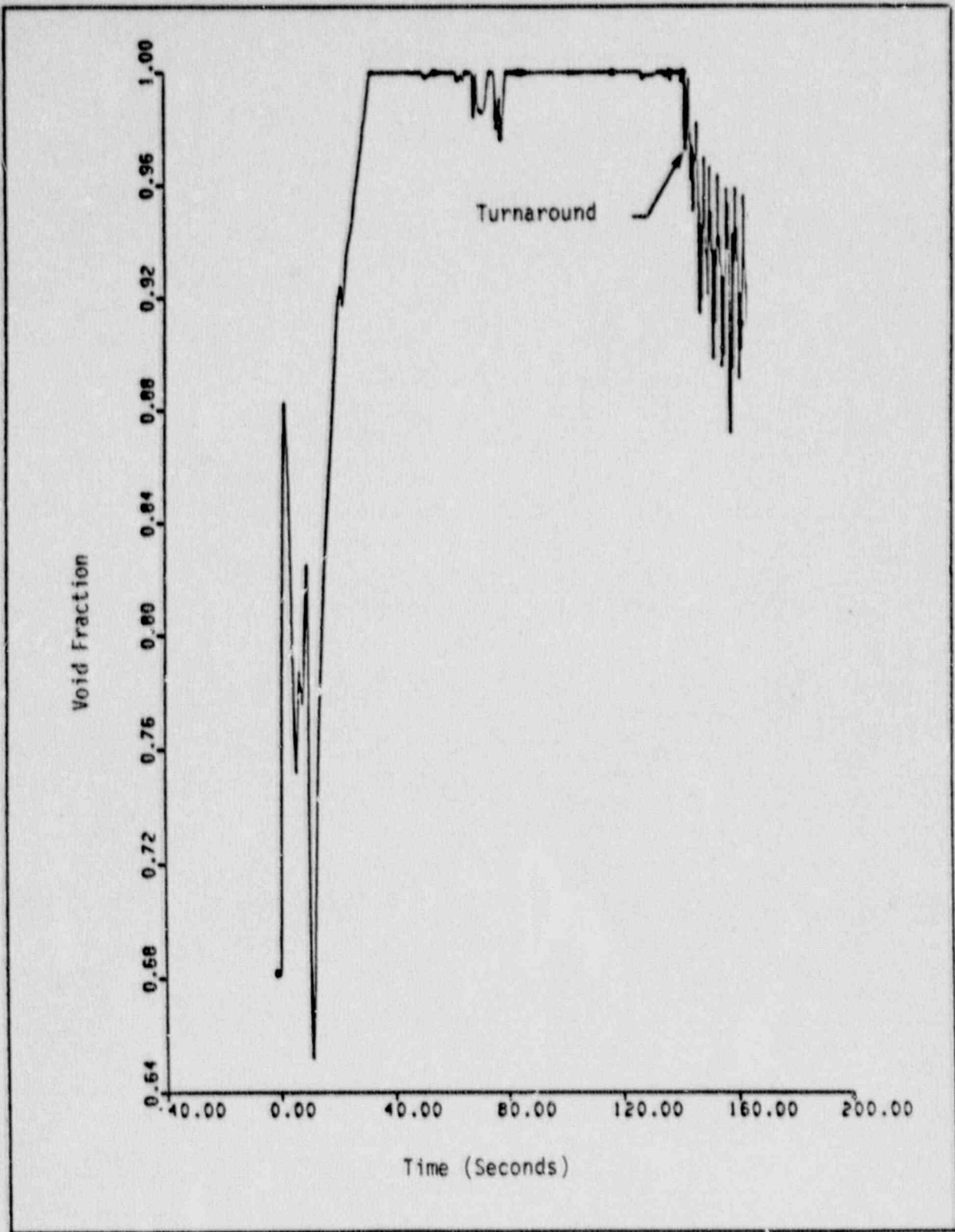
Figure 3.17 - Hot Assembly Midplane Void Fraction
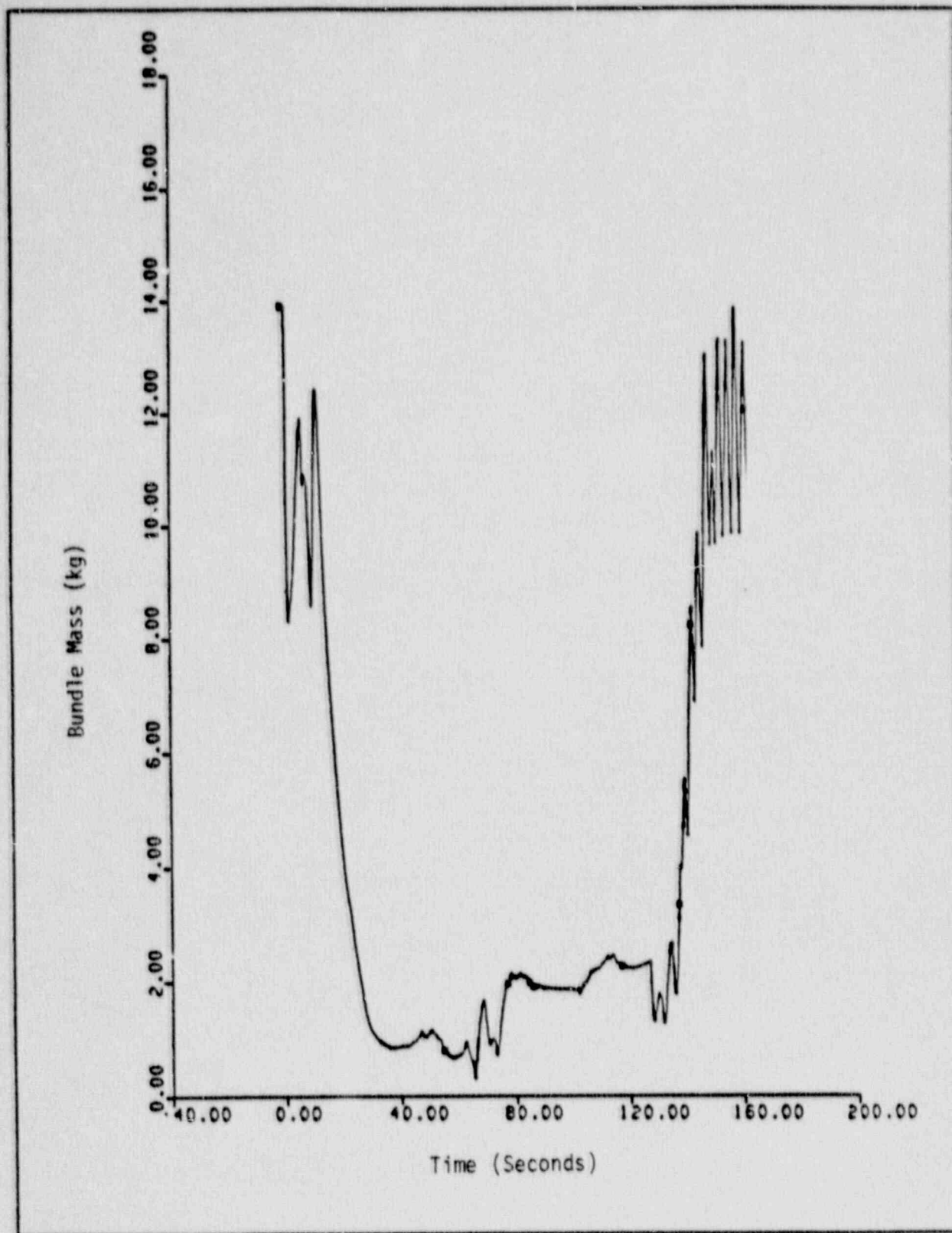
Figure 3.18 - Hot Assembly Mass Inventory
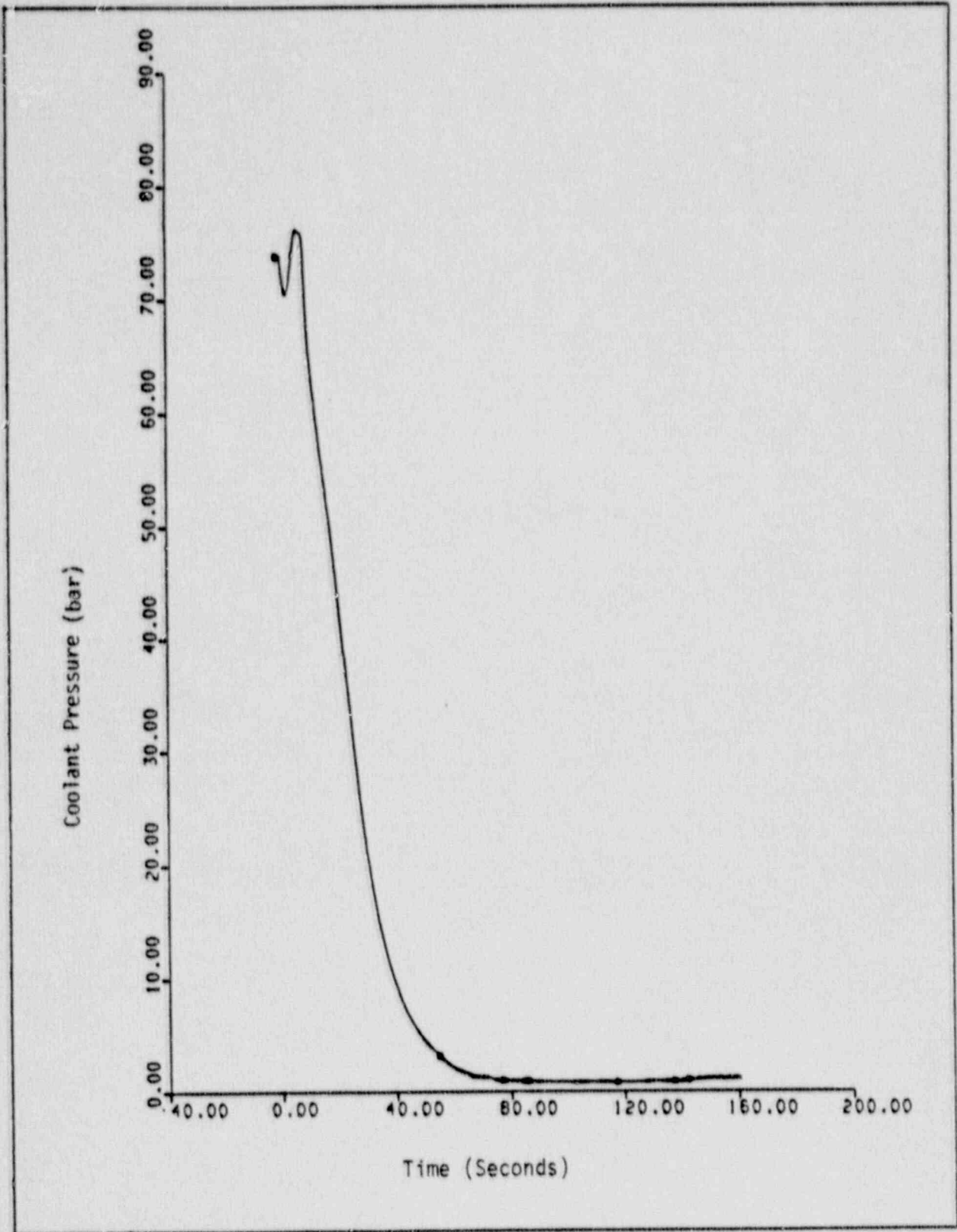
Figure 3.19 - Coolant Pressure at Midplane
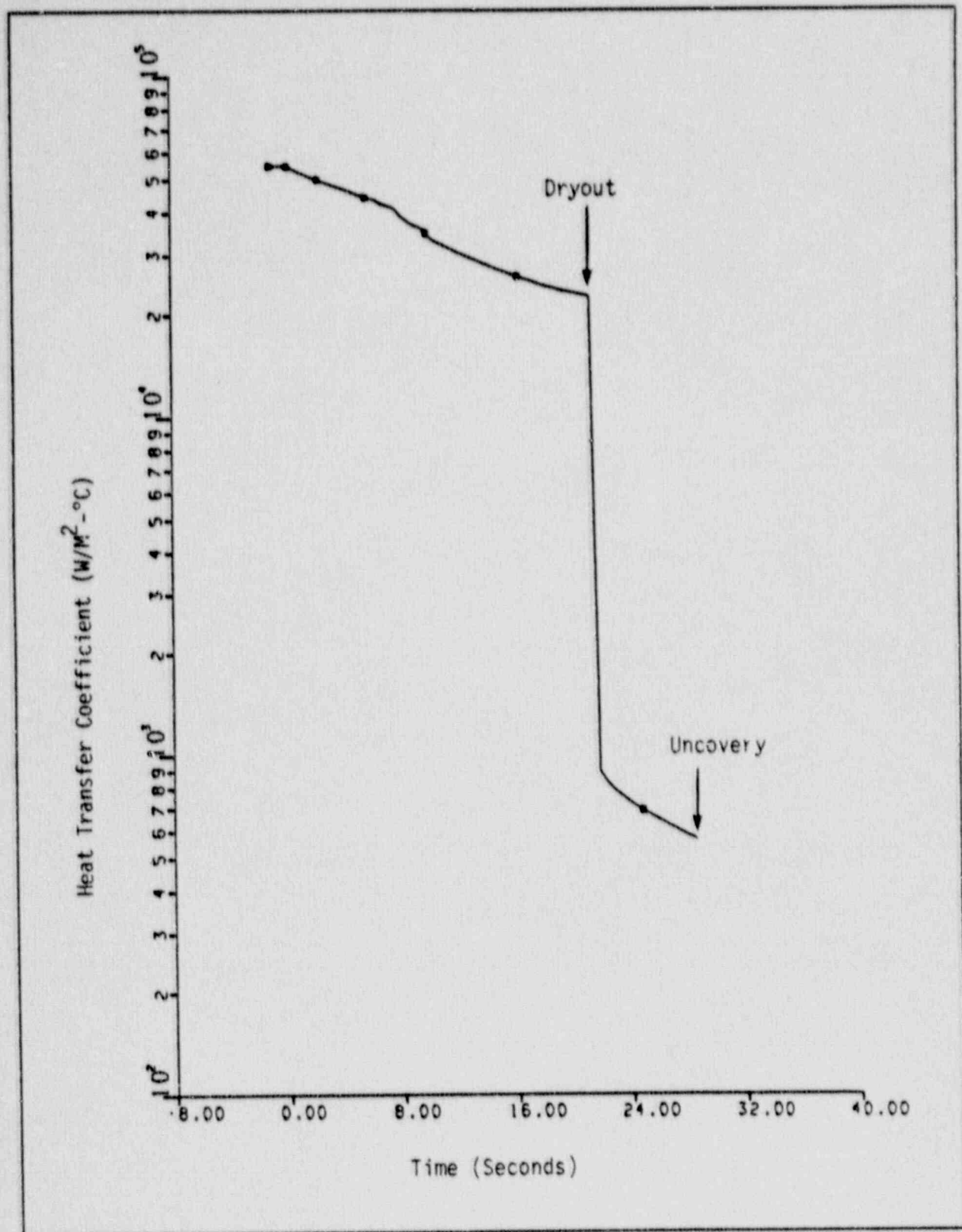
Figure 3.20 - Fuel Rod Heat Transfer Coefficients at Core Midplane
(Prior to Uncovery)

3-30
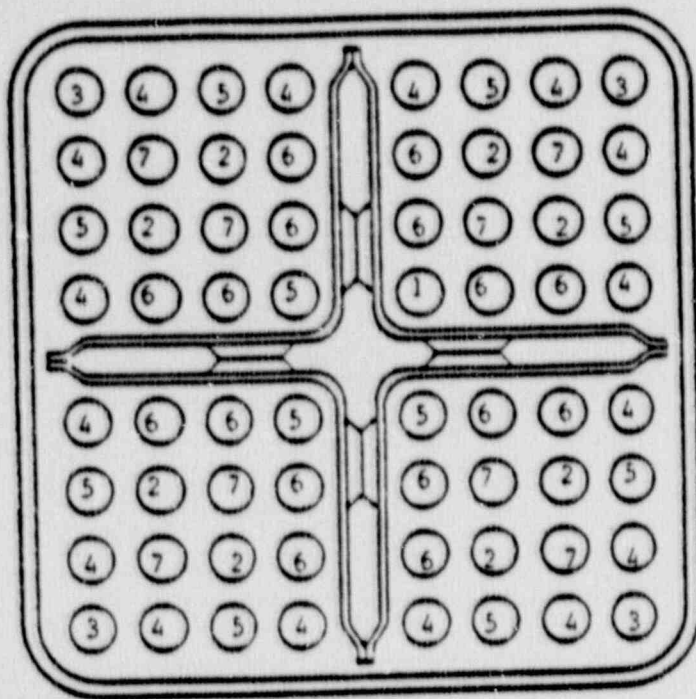
CONTROL ROD GAP
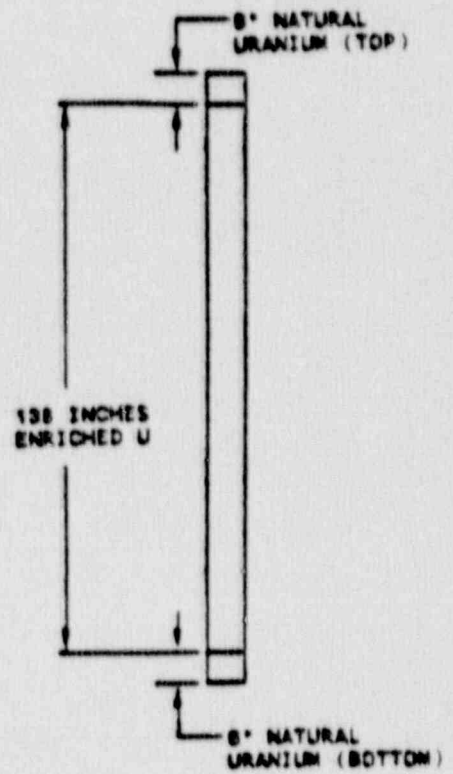
ENRICHMENT TYPE	NO. OF RODS	ENRICHMENT (w/o) U-235	Gd2O3		
		1-5	1	2	3
1	1	3.50	-	-	-
2	8	3.85	6.0	6.0	6.0
3	4	2.40	-	-	-
4	16	3.00	-	-	-
5	11	3.30	-	-	-
6	16	3.85	-	-	-
7	8	4.00	-	-	-

Lattice average U235 enrichment   3.46 w/o
Bundle average U235 enrichment   3.24 w/o

Figure 3.21 - Typical Fuel Design for a BWR/5 -- 24 Months Fuel Cycle

Control Rod Gap

0.934	0.967	1.001	0.982	+	0.984	1.005	0.973	0.941
				+				
0.967	1.028	0.978	1.044	+	1.046	0.983	1.038	0.977
				+				
1.001	0.978	0.982	1.017	+	1.019	0.987	0.988	1.012
				+				
0.982	1.044	1.017	0.973	+	0.975	1.022	1.053	0.992

+++++++++++++++++++++++++++++++++++ + +++++++++++++++++++++++++++++++++++

0.984	1.046	1.019	0.975	+	1.004	1.024	1.055	0.993
				+				
1.005	0.983	0.987	1.022	+	1.024	0.993	0.993	1.016
				+				
0.973	1.038	0.988	1.053	+	1.055	0.993	1.047	0.982
				+				
0.941	0.977	1.012	0.992	+	0.993	1.016	0.982	0.948

Minibundle Analyzed with CHACHA-3C

Figure 3.22 - Assembly Radial Power Distribution at 22 GWD/MTU

Figure 3.23 - Lead Rod Cladding Temperature Transient

4.0 NODALIZATION STUDIES

The vessel, fuel assembly, and fuel rod nodalizations used in the Westinghouse BWR LOCA evaluation model are evaluated in this section.

4.1 GOBLIN Model

The standard GOBLIN nodalization for the Westinghouse BWR LOCA evaluation model is shown in Figure 3.3. The choices of volume boundaries were determined by considering the physical shapes of the reactor vessel and the important phenomena which occur during a LOCA. The rationale for the nodalization being used and sensitivity studies to support this selection are presented in the following sections.
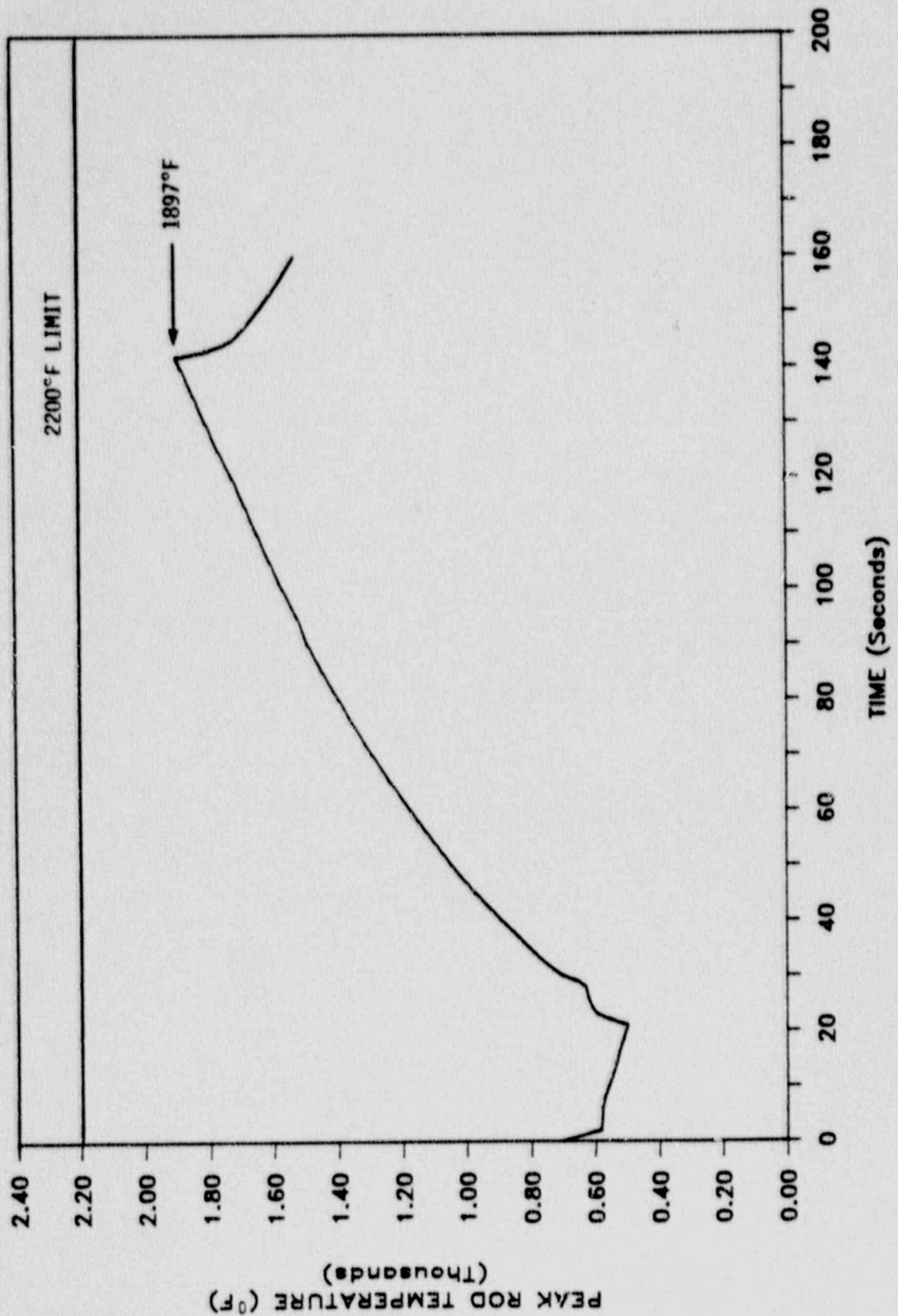
4.1.1 Standard Nodalization

The standard GOBLIN nodalization encompasses the BWR reactor vessel and associated recirculation lines. The steam, feedwater, and ECC system penetrations are treated as time dependent boundary conditions.

As shown in Figure 3.3 the steam dome is represented by a single control volume. During a LOCA transient the steam line is isolated rapidly and the mass inventory decreases. The steam dome is generally a stagnate vapor space and a single control volume is sufficient.

The upper and lower downcomer regions are comprised of six control volumes. Each volume boundary is placed at a discrete area change. Explicit mixture level tracking is calculated throughout the entire downcomer. This means the actual volume boundary nearest to the mixture level is placed at the location of the mixture level. (Reference 1 gives a detailed description of the level tracking model). Because of the large number of downcomer volumes used and level tracking capability the transient response is insensitive to the physical location of the nodes near the jet pump suction and recirculation suction. Therefore no additional noding sensitivity analysis is required for the downcomer region.

The jet pumps are divided into three nodes - the throat, diffuser, and tail section. This jet pump nodalization has been demonstrated to be adequate in predicting the jet pump response during a LOCA (see Reference 1). The same nodalization therefore is used in the evaluation model.

The two recirculation lines are modeled separately and each is modeled with three control volumes. The sensitivity of the transient results to the broken loop noding is addressed below, in Section 4.1.2. The results show that three volumes is sufficient.

The lower plenum is divided into four control volumes. Level tracking is modeled in the lower plenum. With level tracking the actual volume boundary between the liquid and vapor space moves with the mixture level. Hence, the flows between the lower plenum and the jet pump discharge, side entry orifices, and lower support plate all account for the physical elevation of the mixture level.

The reactor channel and watercross are divided into nine and two volumes, respectively. The active fuel region is divided into seven volumes. This detailed discretization is adequate for calculating the average core system response. This is demonstrated in Section 4.2.1 through a comparison with a DRAGON calculation which uses a finer core noding.

The bypass and guide tubes are partitioned into a total of seven control volumes, two of which are in the guide tubes. A sensitivity study of the noding in this region is presented in Section 4.1.3.

Lastly, the upper plenum is divided into four volumes. Level tracking is used in this region. Three volumes model the region above the active core and one volume models the standpipes and steam separators. This is a region where ECC flow is injected, and is considered important in determining the core counter current flow limitation. A sensitivity study to upper plenum nodalization is also presented in Section 4.1.3.

4.1.2 Break Location Noding Sensitivity

A specific requirement of LOCA evaluation models, as stated in 10CFR50 Appendix K, is the demonstration of adequate nodalization near the break location. To demonstrate meeting this requirement, the LOCA blowdown was simulated with three different nodalization schemes. These schemes are shown in Figure 4.1 and designated nominal (6 volumes), coarse (5 volumes), and fine (8 volumes). Figures 4.2 through 4.5 summarize the transient response for the system pressure, vessel side break flow, recirculation line side break flow and total mass inventory, respectively, for the three noding schemes. The fine and nominal schemes give almost identical system responses. With respect to the total inventory loss, the nominal noding scheme loses slightly more inventory.

The coarse noding scheme gives slightly slower system depressurization and less total mass inventory loss than the nominal and fine noding. However, the differences between the coarse and other two nodalization schemes is less than 2 percent.

From the results of this noding sensitivity study it may be concluded that the nominal nodalization of the lower downcomer and recirculation line can adequately calculate the blowdown response.

4.1.3 ECC Location Noding Sensitivity

A second specific requirement of 10CFR50 Appendix K is the demonstration of adequate nodalization at injection locations of the emergency core cooling water. For a BWR/5 (and BWR/6) plant design the ECC system injection locations for the high and low pressure spray are through spargers above the reactor core, and for the low pressure core injection it is in the top of the core bypass region.

Several bypass and upper plenum nodalization schemes and upper plenum level tracking schemes were examined to determine the impact of the nodalization on the resultant system refill and reflood response. The different nodalizations studied are summarized in Table 4.1. The system response is assessed

by comparing the key parameters which impact the resultant peak cladding temperature. These parameters are the time when spray cooling is initiated and the time when the core midplane refloods.

The results of the ECC nodalization study are summarized in Table 4.2. The reference transient is case A which gives a start of spray cooling time of 48 seconds and midplane reflood time of 142 seconds. The sensitivity to the location of the bottom of level tracking can be seen by comparing cases A, B, and D. In all cases the level tracking is deactivated below the spray injection location but above the top of the core. Clearly, the time of spray cooling initiation and time of reflood are not significantly affected by the actual elevation. Other parameters, however, do vary slightly, such as the time at which the guide tubes and lower plenum fill. This is because the timing of the ECC water flashing in the guide tubes and bypass, and the collapsing of voids due to steam condensation varies slightly.

Case C shows the significance of tracking the mixture level in the upper plenum. In case C the level tracking was manually deactivated creating fixed control volume boundaries in the upper plenum. With fixed volumes the ECC spray is assumed to mix homogeneously with the node fluid due to the homogeneous equilibrium model in GOBLIN. This simplified modeling causes a homegeneous mixing of the ECC spray flow with the liquid and vapor phases in the spray injection volume. In actuality the spray flow will mix only with the liquid when the mixture level is significantly above the spray spargers. Also as the mixture level drops a gradually increasing amount of steam condensation occurs. These phenomena are considered only when the level tracking model is used. The unrealistically higher fluid enthalpy in the upper plenum results in a [$]^{a,c}$ later time of midplane reflood. The level tracking model shall be used in the evaluation model. A significant reduction in computational time was achieved in case B, when the bottom of level tracking was raised by 0.1 meter, with a negligible change in transient results. This higher elevation for the bottom of level tracking shall be used in the evaluation model.

The sensitivity to the number of control volumes in the bypass and upper plenum regions was studied by combining the five volumes in the bypass

into three, and the four volumes in the upper plenum into three as shown in Figure 4.6. Comparing the results between case A with the nominal noding and case E with the coarser noding it is seen that the coarser noding allows about a [   ]^{a,c} faster refilling of the guide tubes and bypass. However, the final reflooding of the midplane, a parameter important in determining the peak cladding temperature, remains [   ]^{a,c}.

This nodalization study shows that, aside from eliminating level tracking in the upper plenum completely, the final midplane reflood time and the time when the cladding temperature transient is mitigated are not very sensitive to the nodalization near the ECC injection point. Therefore the reference nodalization scheme of Figure 3.3 with level tracking shall be used in the evaluation model.

4.2 DRAGON Model

The standard DRAGON noding for the Westinghouse BWR LOCA evaluation model is shown in Figure 3.14. The transient fluid conditions (pressure and enthalpy) for the DRAGON boundary nodes are supplied by GOBLIN. Relative power versus time is also taken from the GOBLIN run. DRAGON then calculates the thermal and hydraulic conditions in the fuel assembly throughout the transient.

Normally DRAGON is used to determine the hot assembly behavior throughout the LOCA transient. For the core nodalization study an average power assembly has been simulated. By comparing the DRAGON average power assembly results with the GOBLIN core average results it is possible to determine the impact of the DRAGON and GOBLIN core noding differences (13 versus 7 active channel nodes, 13 versus 2 watercross nodes).

Figures 4.7 through 4.11 show comparisons of the DRAGON and GOBLIN transient results for the key parameters. The mass flow rates through the side entry orifice (Figure 4.7) show no discernible difference until the reflood portion of the transient, when the DRAGON results show more oscillations. The impact of these oscillations is evaluated later. The flow rates from the bottom nozzle region into the active channel, watercross, and leakage holes are compared in Figures 4.8 through 4.10, respectively. The active channel mass

flow rates also match almost exactly until the reflood phase. The watercross mass flow rates show only minor differences throughout the transient, and the leakage mass flow rates are virtually identical. The mass flow rates out of the fuel assembly (i.e., at the upper tie plate) are compared in Figure 4.11. Again, the agreement is excellent.

A comparison of the DRAGON and GOBLIN bundle masses will show the integrated effect of the noding differences. This comparison has been made using DRAGON nodes (1,3) through (1,16) and GOBLIN nodes (4,3) through (4,10) (refer to Figures 3.14 and 3.3), and the results are shown in Figure 4.12. The results are again in very good agreement. Note that the oscillations which were evident in some of the DRAGON mass flow rates during reflood are also evident in the DRAGON bundle mass.

The difference between the DRAGON and GOBLIN results during reflood can be explained with the aid of Figure 4.13. This figure compares the void fractions at the peak power plane from the two runs. After the temperature transient turns around there is a periodic cycling of the DRAGON void fraction between the low flow film boiling regime and the transition to the dispersed flow regime. Physically this corresponds to the feedback from the fuel rod heat transfer to the nodal void fraction. This effect is not seen in the GOBLIN results, due to the larger hydraulic nodes. Since this difference does not occur until the temperature transient turns around, there is no impact on the fuel rod heatup calculation. Section 5.2 discusses the results of a sensitivity study which examines the impact on reflood of changing the void fraction criteria used to define the transition from the dispersed flow regime to the low flow film boiling regime.

As a result of the comparisons presented here it is concluded that the difference between the DRAGON and GOBLIN core noding has a negligible impact on LOCA transient results. The GOBLIN core noding is therefore acceptable for use in calculating the system response. The finer DRAGON noding will be used for the hot assembly analysis.

4.3 CHACHA-3C Model

4.3.1 Rod Noding Sensitivity

The standard CHACHA-3C fuel rod noding for the Westinghouse BWR LOCA evaluation model consists of seven pellet nodes of equal volume and three cladding nodes of equal thickness. The sensitivity of the calculated peak cladding temperature to fuel rod noding has been evaluated by comparing results obtained from the standard case to those obtained with 5 pellet/2 cladding nodes and 10 pellet/4 cladding nodes. In each case the pellet nodes were of equal volume and the cladding nodes were of equal thickness. Transient boundary conditions from the reference DRAGON run (presented in Section 3) were used for this evaluation. A flat pellet radial power distribution was assumed for simplicity.

The results from this sensitivity study are shown in Table 4.3. It can be seen that increasing the number of nodes decreases the peak cladding temperature. The change in PCT resulting from using 10 pellet/4 cladding nodes versus the standard noding is essentially negligible[   ]^{a,c} It is therefore concluded that the use of seven pellet nodes of equal volume and 3 cladding nodes of equal thickness is appropriate for the evaluation model.

4.3.2 Channel Noding Sensitivity

The CHACHA-3C results presented for the reference case are based on a lumped treatment of the channel and watercross. The watercross thickness was used in the channel temperature calculations. Table 4.4 shows a comparison of the results for the reference transient using the watercross and channel thicknesses. Results are also shown from a divided channel calculation. The noding used for the reference and divided channel models are shown in Figure 4.14. From these results it is concluded that peak cladding temperature is relatively insensitive to the channel noding, and that the modeling used for the reference LOCA calculation is conservative.

Spray heat transfer tests performed with a simulated watercross fuel assembly have shown that the channel and watercross rewetting times are substantially overpredicted by the current evaluation model. The evaluation model treatment of channel rewet may be revised in the future to incorporate the results of these experiments.

Table 4.1
ECC LOCATION NODALIZATION SCHEMES

	CASE				
	A	B	C	D	E
Bypass nodes	5	5	5	5	3
Upper plenum nodes	4	4	4	4	3
Upper plenum level tracking	ON	ON	OFF	ON	ON
Bottom of level tracking (meters above top of channel)	0.03	0.13	--	0.0	0.13
Nodalization Figure	3.3	3.3	3.3	3.3	4.6

Table 4.2
ECC LOCATION NODALIZATION RESULTS

CASE

Time (sec)	A	B	C	D	E
HPCS Actuation						a,c
Initiation of Spray Cooling					
LPCI Actuation					
Guide Tubes Full					
Bypass Full					
Lower Plenum Full					
Midplane Reflood					

TABLE 4.3
EFFECT OF ROD NODING ON PCT

No. of Pellet Nodes	No. of Cladding Nodes	Peak Cladding Temperature
5	2	
7*	3*	
10	4	

$$\begin{bmatrix} & \\ & \\ & \end{bmatrix}^{a,c}$$

TABLE 4.4
EFFECT OF CHANNEL NODING ON PCT

No. of Nodes	Thickness (cm)	Peak Cladding Temperature
1*	0.08*	
1	0.14	
2	0.08	
2	0.14	

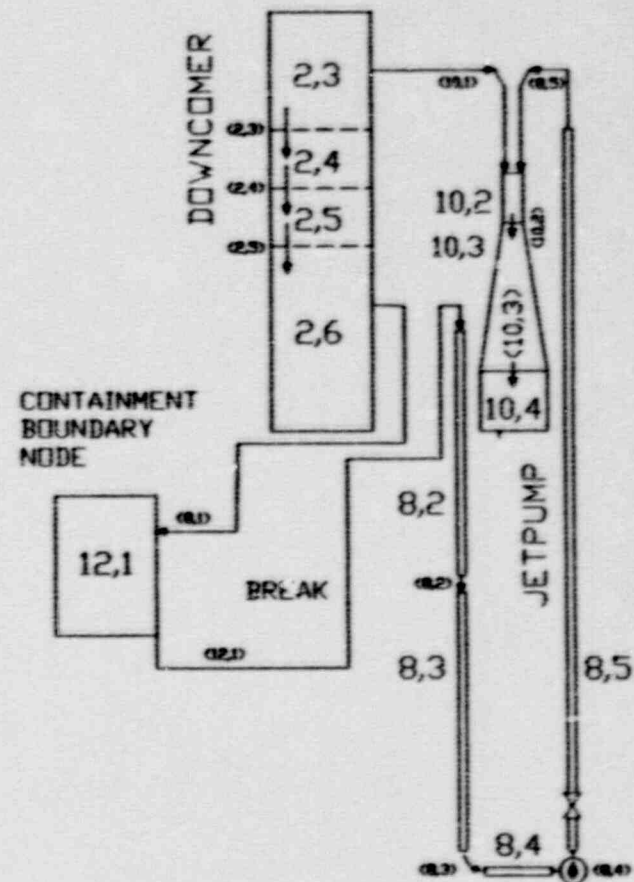$$\begin{bmatrix} & \\ & \\ & \\ & \end{bmatrix}^{a,c}$$

* Noding used in evaluation model
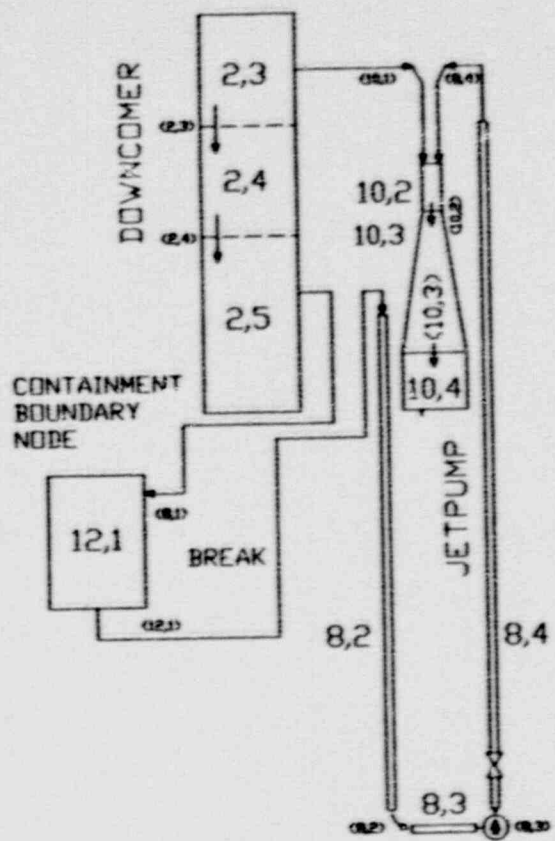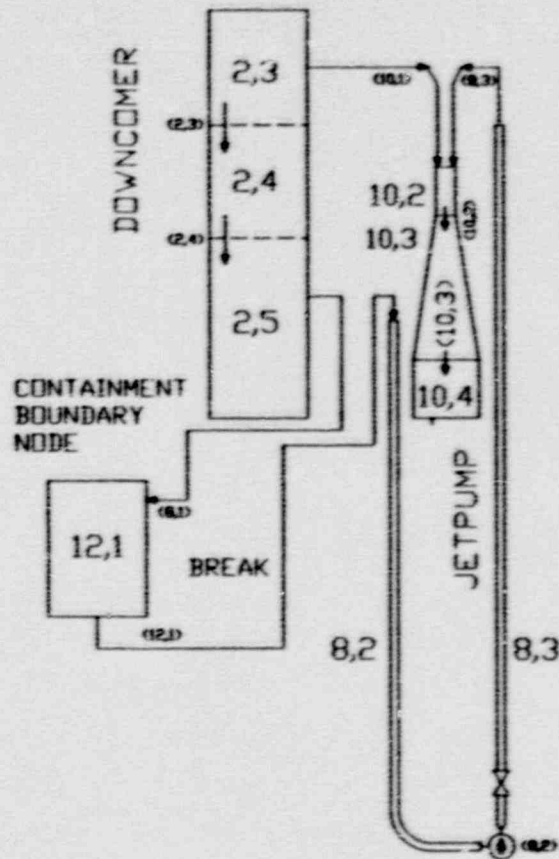
(a) Nominal Noding   (b) Coarse Noding   (c) Fine Noding

(I,J) = FLOWPATH

I,J = FLUID NODE
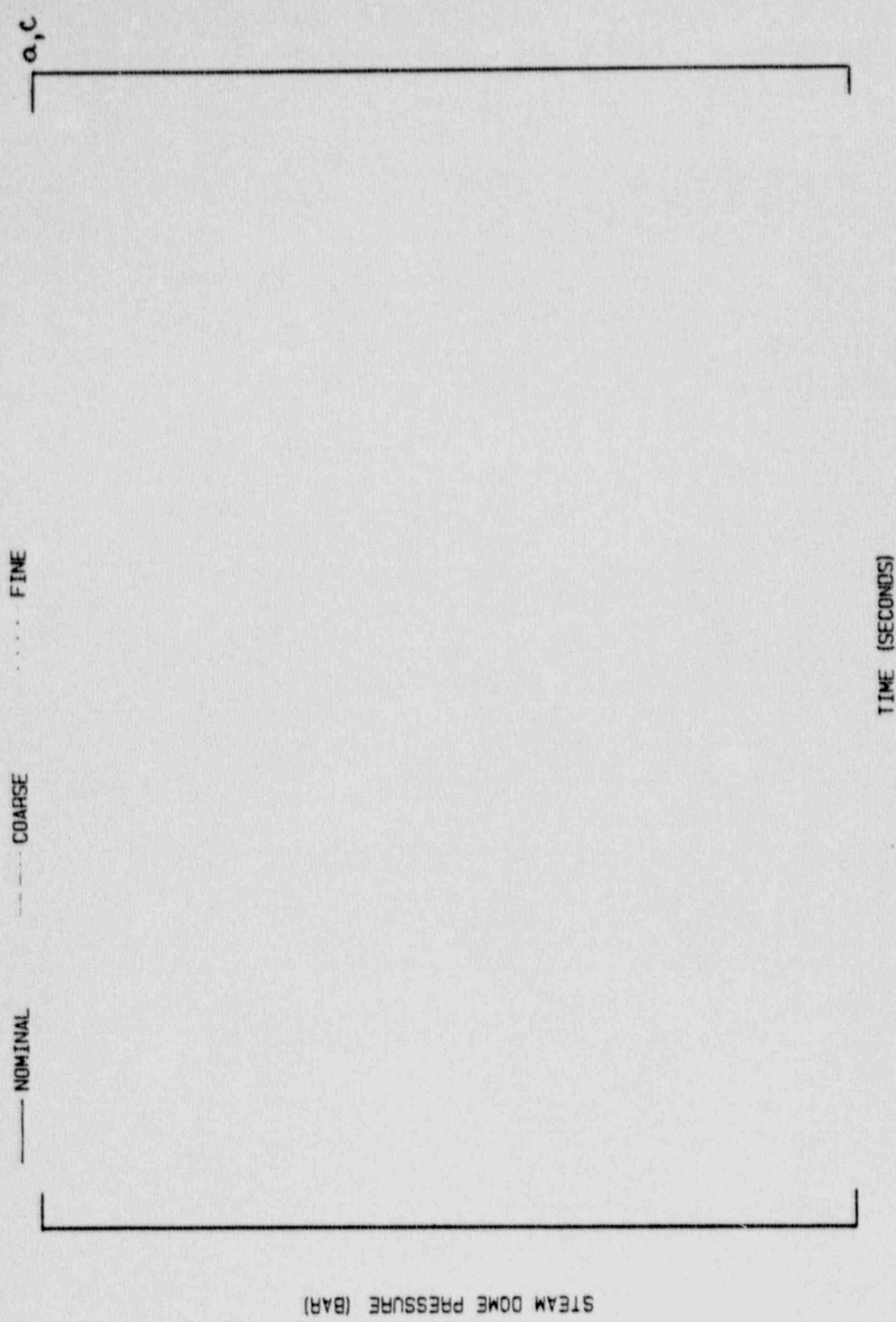
Figure 4.1 - Break Location Nodalization Schemes

a,c

─── NOMINAL   ──── COARSE   ····· FINE

STEAM DOME PRESSURE (BAR)

TIME (SECONDS)

Figure 4.2 - Sensitivity of System Pressure to Break Location Noding

a,c

NOMINAL   ----- COARSE   ...... FINE

VESSEL BREAK FLOW (kg/sec)

TIME (SECONDS)
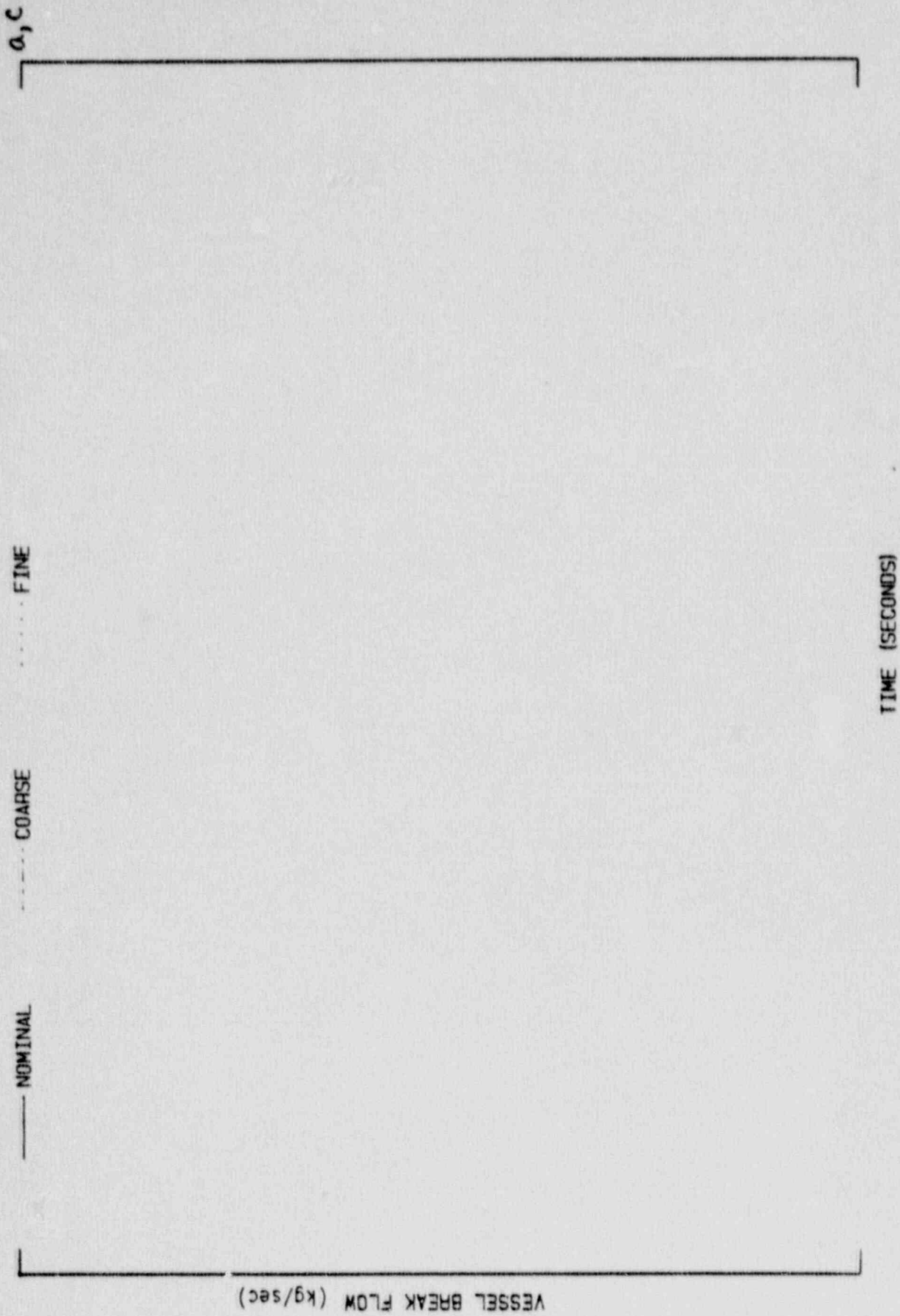
Figure 4.3 - Sensitivity of Vessel Break Flow to Break Location Noding

————— NOMINAL   ——·—— COARSE   ······ FINE   a,c

RECIRCULATION LINE BREAK FLOW (kg/sec)

TIME (SECONDS)
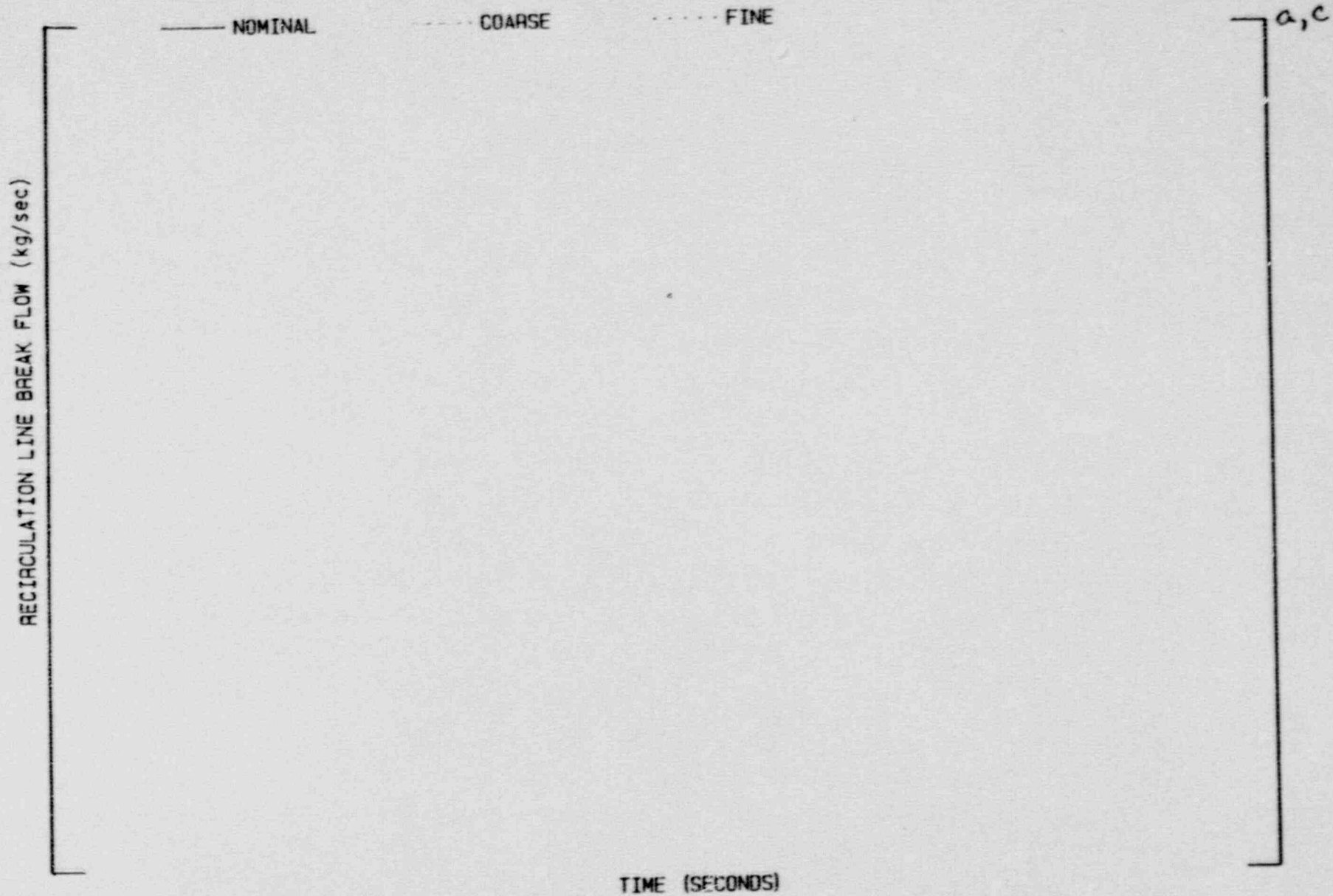
Figure 4.4 - Sensitivity of Recirculation Line Break Flow to Break
Location Noding

NOMINAL   COARSE   FINE   G,C

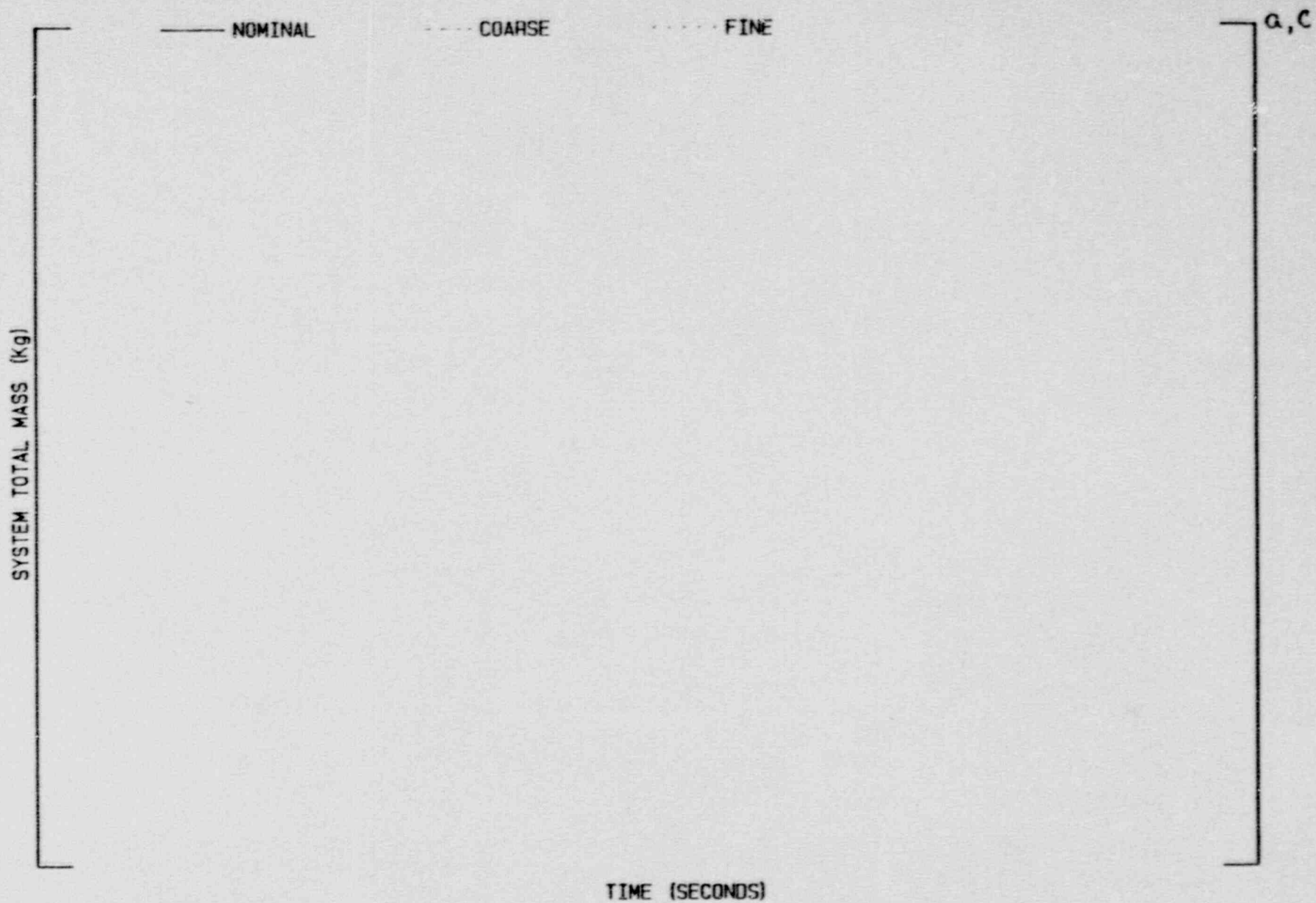SYSTEM TOTAL MASS (Kg)

TIME (SECONDS)

Figure 4.5 - Sensitivity of Total Mass Inventory Loss to Break
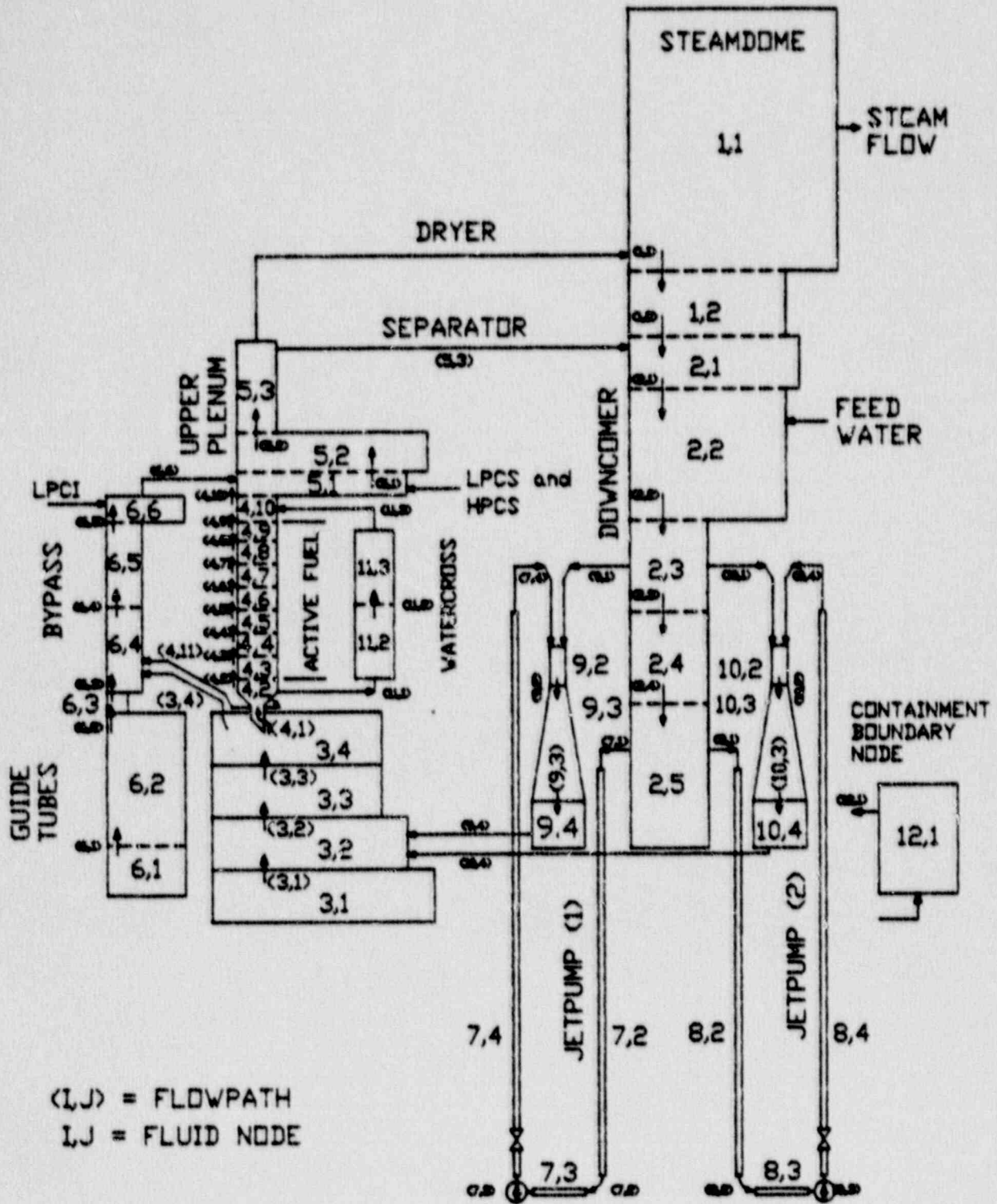Location Noding

Figure 4.6 - Coarse ECC Nodalization

a,c

Figure 4.7 - Comparison of Side Entry Orifice Mass Flow Rates

a,c
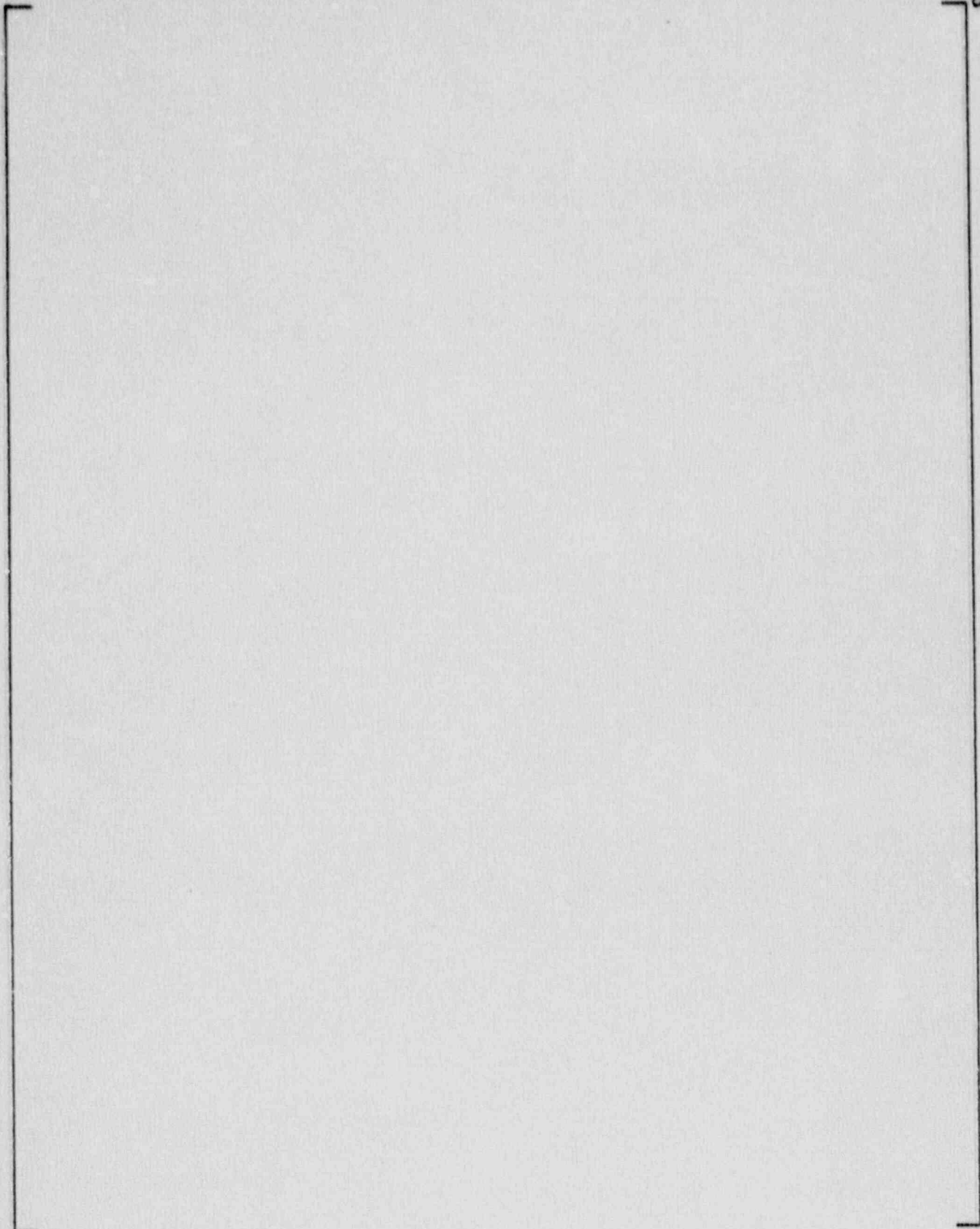
Figure 4.8 - Comparison of Active Channel Inlet Mass Flow Rates
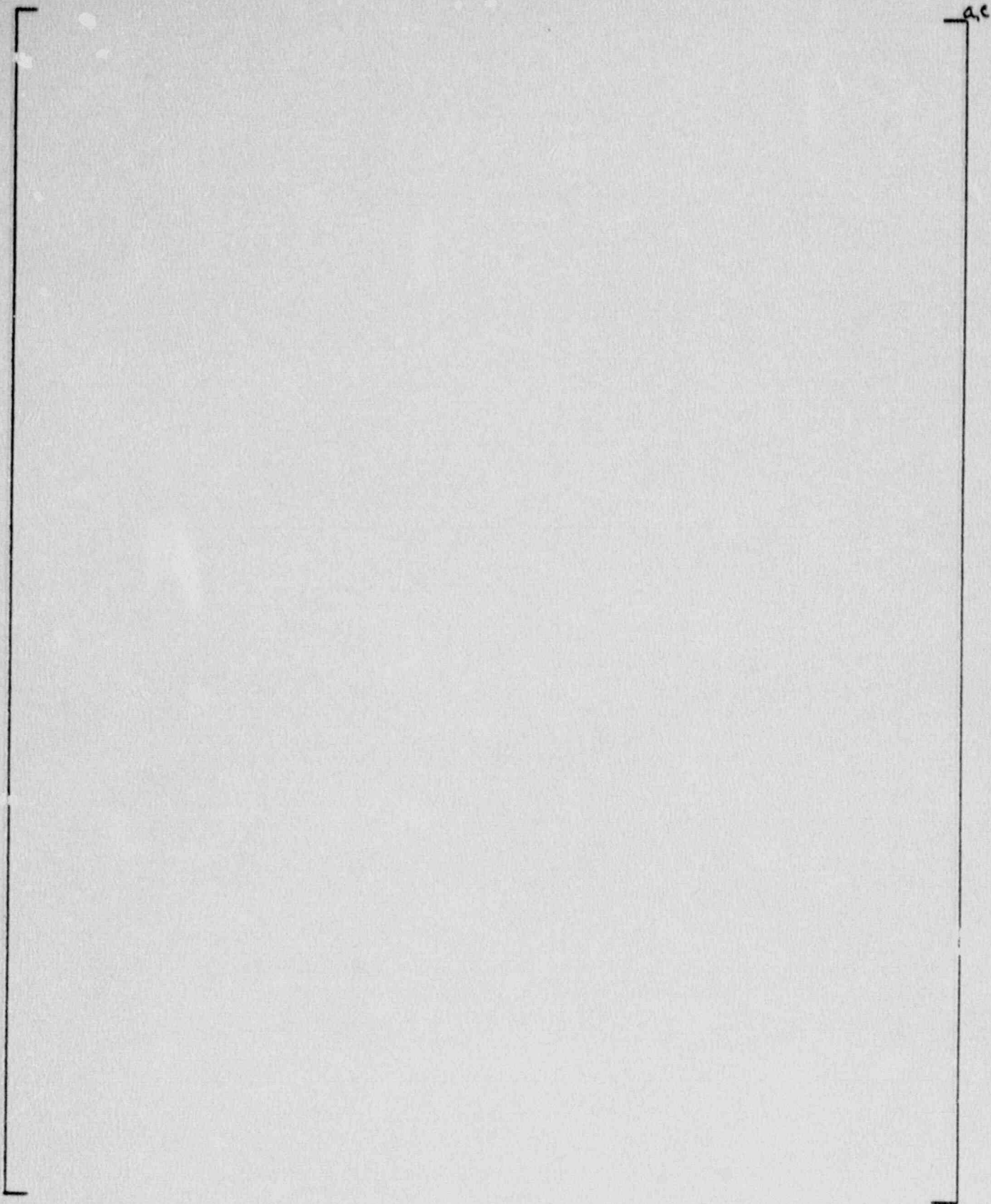
a,c

Figure 4.9 - Comparison of Water Cross Inlet Flow Rates

a,c
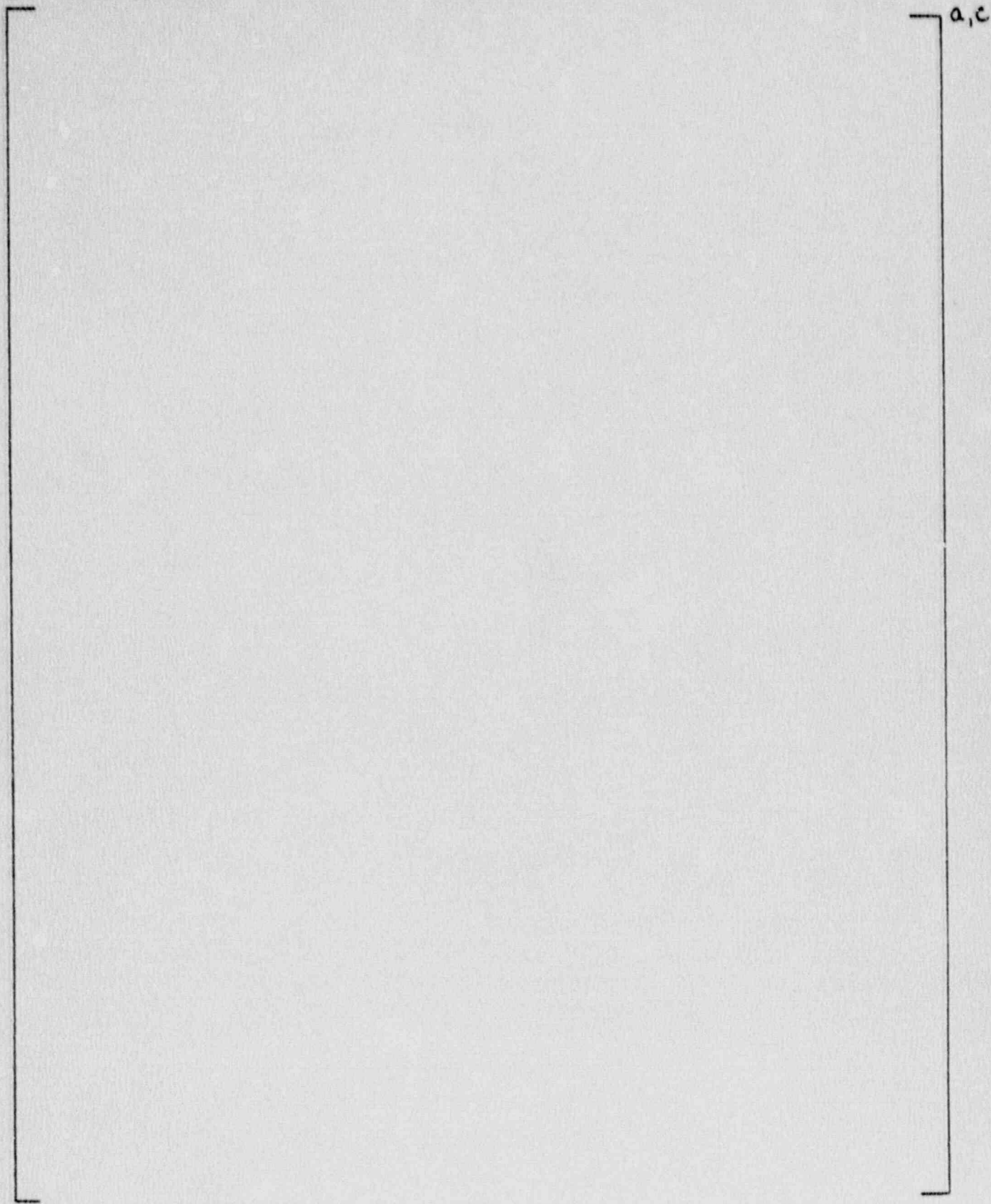
Figure 4.10 - Comparison of Leakage Flow Rates

4-21

a,c

Figure 4.11 - Comparison of Assembly Exit Flow Rates

[   ] a,c
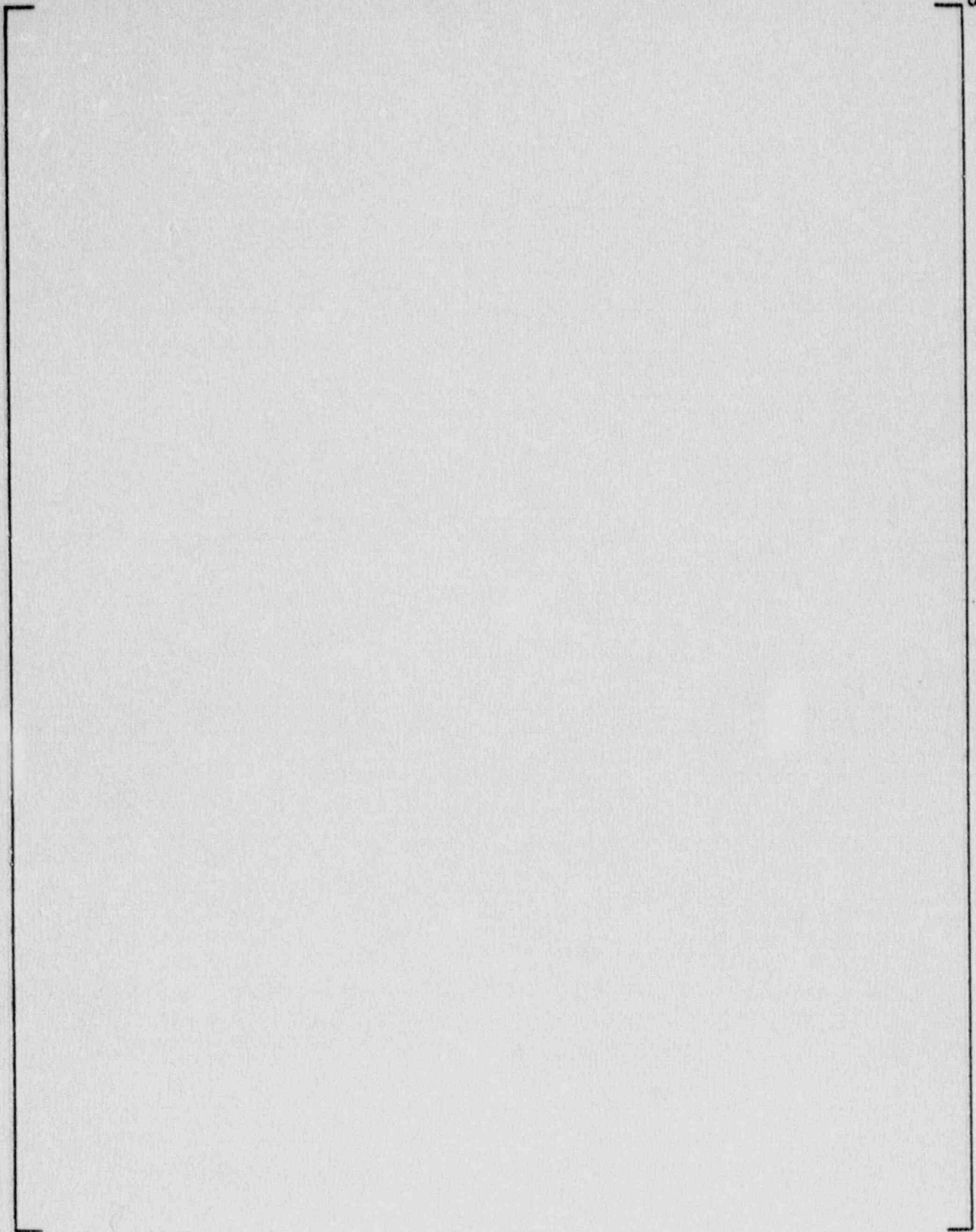
Figure 4.12 - Comparison of Bundle Mass Inventory

a,c
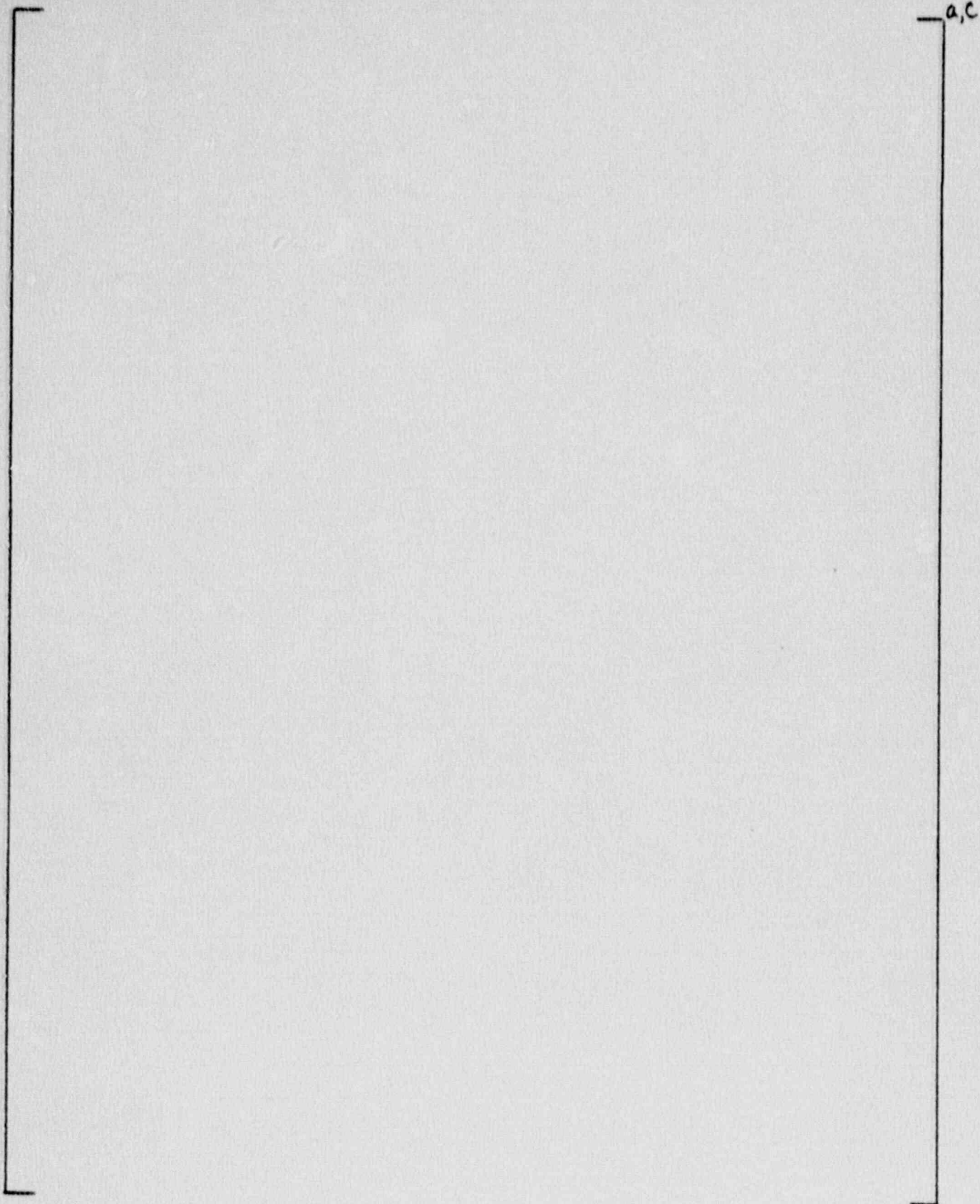
Figure 4.13 - Comparison of Peak Power Node Void Fraction

17

$$\begin{array}{cccc}
① & ⑤ & ⑨ & ⑬ \\
② & ⑥ & ⑩ & ⑭ \\
③ & ⑦ & ⑪ & ⑮ \\
④ & ⑧ & ⑫ & ⑯
\end{array}$$

17   17

17

a. Single Channel Model

17

$$\begin{array}{cccc}
① & ⑤ & ⑨ & ⑬ \\
② & ⑥ & ⑩ & ⑭ \\
③ & ⑦ & ⑪ & ⑮ \\
④ & ⑧ & ⑫ & ⑯
\end{array}$$

17   18

18
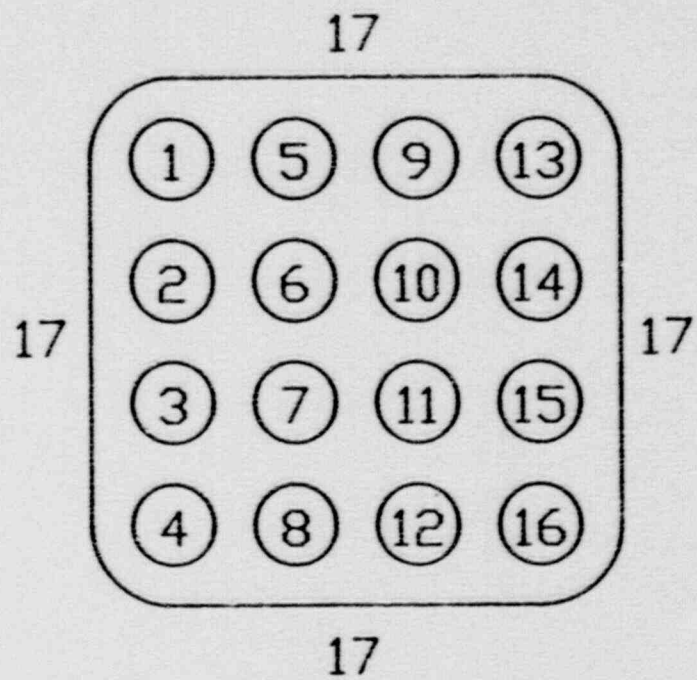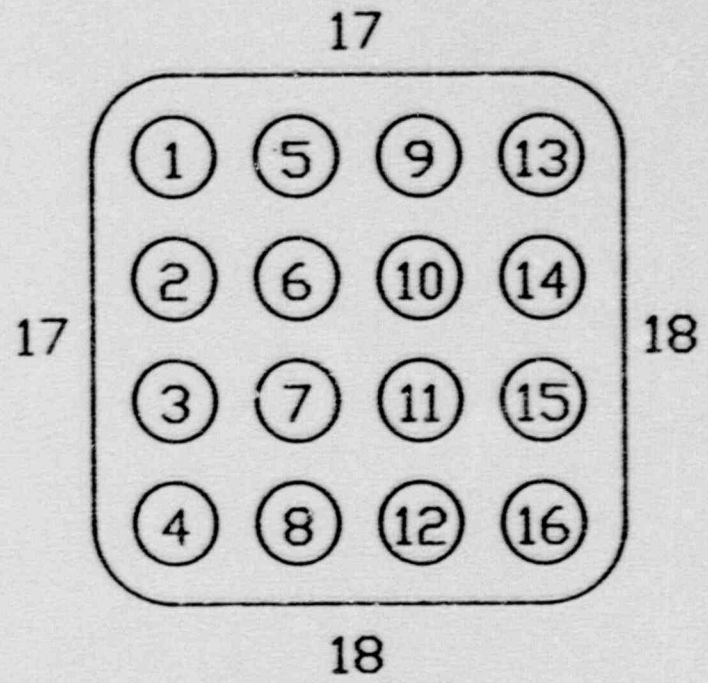
b. Divided Channel Model

Figure 4.14 - Sensitivity of Channel Noding in CHACHA-3C

5.0 ASSESSMENT OF KEY CODE MODELS

This section addresses the applicability of several key code models. First, the GOBLIN and DRAGON models for countercurrent flow limitation and heat transfer during refill/reflood are addressed. Then the CHACHA-3C models for convective heat transfer during spray cooling and channel rewet time are evaluated.

5.1 Countercurrent Flow Limitation

The Westinghouse BWR LOCA evaluation model has a comprehensive Countercurrent Flow Limitation (CCFL) model for determining the rate of liquid drainage into the QUAD+ fuel assembly. The original CCFL correlation was developed by ASEA-ATOM, for 8x8 fuel assemblies. Since its original development, the correlation has been generalized and validated for many geometries. In addition, Westinghouse has independently compared the CCFL model against test data from a prototypical Westinghouse QUAD+ fuel assembly. The test data included countercurrent flow measurements in the bundle with and without watercross flooding, and in the watercross itself. Tests were conducted with water injection by spraying and by spillover at flowrates of 5 and 10 gallons per minute. The test results were compared to the CCFL correlation in GOBLIN/DRAGON. The correlation conservatively calculates at least 25 percent less liquid penetration into the fuel bundle than was observed in the test. Furthermore the evaluation model and the test both show that the most restrictive CCFL occurs at the top spacer grid location in the bundle. Based on these qualification results, no additional CCFL sensitivity studies are deemed necessary.

5.2 Heat Transfer During Reflood

The Westinghouse BWR LOCA evaluation model defines the upper limit of the low flow film boiling regime to be at a void fraction (α) of $\left[\right]^{a,c}$ The modified Bromley correlation is used, as described in Reference 1, for this heat transfer regime. The lower limit of the dispersed flow regime is defined as $\left[\right]^{a,c}$ Above this void fraction heat transfer is by steam cooling only. In the transition between these two regimes the heat transfer coefficient is obtained by $\left[\right]^{a,c}$ between the low flow film boiling and steam cooling correlations.

An evaluation of the impact of this heat transfer regime transition on reflood has been performed. The DRAGON reference transient described in Section 3 was restarted from 110 seconds with the upper limit of the low flow film boiling regime redefined as $\alpha =$ [   ]^{a,c} and the lower limit of the dispersed flow regime redefined as $\alpha =$ [   ]^{a,c} Figure 5.1 shows the resulting void fraction for the peak power node. A comparison with the reference calculation results (Figure 3.17) shows that there is no impact on the void fraction until after the cladding temperature turnaround. Therefore it is concluded that the heat transfer regime transition has no impact on the reflood time which is a key parameter used in the CHACHA-3C heatup calculation.

5.3 Convective Heat Transfer During Spray Cooling

Preliminary convective heat transfer coefficients for the QUAD+ fuel design under spray cooling conditions have been derived from the heat transfer coefficients recommended in 10CFR50 Appendix K for 7x7 fuel (Reference 1). The resulting values are reproduced in Table 5.1. Since the submittal of the Reference 1 report spray heat transfer tests performed with a simulated watercross fuel assembly have shown that these heat transfer coefficients are slightly conservative for the peak power plane of a lead fuel assembly. As an example, in a test which simulated the spray cooling of a watercross fuel assembly with the midplane initially operating at 13.7 kw/ft, the heat transfer coefficients shown in Table 5.2 gave very good agreement between calculated and measured rod midplane temperatures. The CHACHA-3C reference transient of Section 3 was repeated using the more realistic spray cooling heat transfer coefficients in Table 5.2. The results showed a decrease in calculated peak cladding temperature of [   ]^{a,c} The Westinghouse BWR LOCA evaluation model will continue to use the spray cooling heat transfer coefficients from Table 5.1 (derived from Appendix K requirements) to provide additional conservatism in the evaluation methodology.

5.4 Channel and Watercross Rewet

The Westinghouse BWR LOCA evaluation model predicts channel and watercross rewet time by applying the Yamanouchi correlation as recommended in 10CFR50 Appendix K. Spray heat transfer tests performed with a prototypic watercross

fuel assembly have clearly shown that the channel and watercross rewet times are substantially overpredicted by this conservative model. Rewet at the peak power elevation (midplane) was observed to occur [   ]^{a,b,c,g} from the time of spray initiation in these experiments. The reference CHACHA-3C calculation of Section 3 has been repeated with the channel and watercross rewetting [   ]^{a,c} after the start of spray cooling. The results indicated a reduction in peak cladding temperature of [   ]^{a,c} This evaluation shows that there as much as [   ]^{a,c} of conservatism in the evaluation model associated with the use of the Yamanouchi correlation for the limiting break in a BWR/5.

TABLE 5.1
EVALUATION MODEL SPRAY HEAT TRANSFER COEFFICIENTS (CHACHA-3C)

Rod Type	h_{conv} $(\frac{W}{M^2 \, {}^\circ C})$
Inner	
Side	
Corner	
Channel Wall	

$$\begin{bmatrix} & \\ & \\ & \end{bmatrix}^{a,c}$$

TABLE 5.2
SPRAY HEAT TRANSFER COEFFICIENTS FROM SPRAY COOLING TESTS

Rod Type	h_{conv} $(\frac{W}{M^2 \, {}^\circ C})$
Inner	
Side	
Corner	

$$\begin{bmatrix} & \\ & \\ & \end{bmatrix}^{a,b,c,g}$$
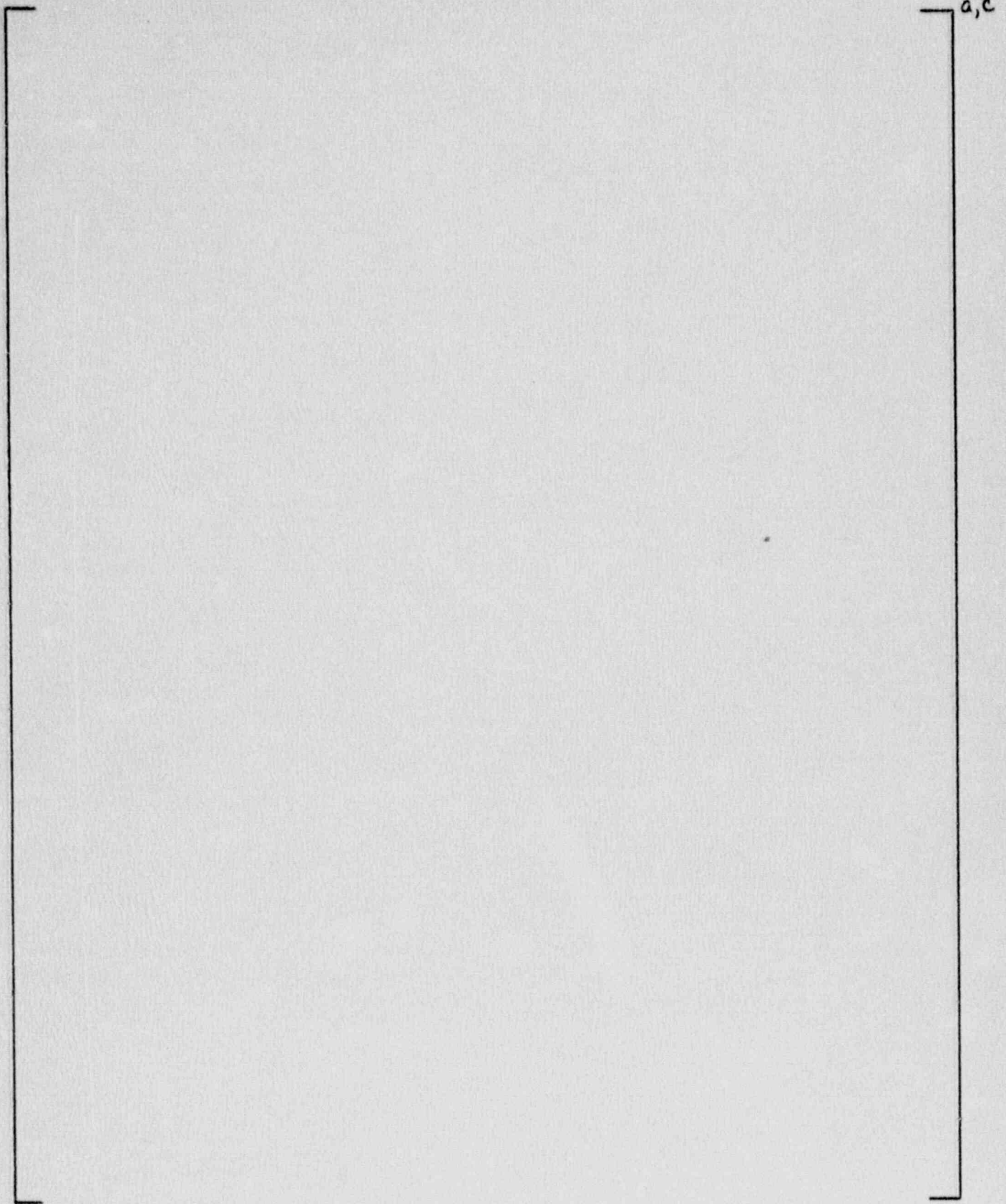
a,c

Figure 5.1 - Impact of Heat Transfer Regime Transition on Reflood

5-5

6.0 PLANT PARAMETERS STUDIES

6.1 Plant Initial Conditions

The plant initial conditions for the LOCA analysis are conservatively chosen to be outside the limits of normal plant operating conditions. This is done to create a safety analysis which bounds current and possible future operating conditions. The initial conditions shall also bound those used in applicable LOCA analysis for other fuel resident in the core.

Table 6.1 lists the key plant initial conditions and the values used for the reference transient described in Section 3. The LOCA system analysis was done at 105 percent of rated steam flow at the plant design pressure. The corresponding reactor power at these conditions is 104.3 percent of rated power. This power level is 2.3 percent higher than the 102 percent of rated power required by 10CFR50 Appendix K to account for calorimetric measurement uncertainties.

From the standpoint of a LOCA analysis, a high initial power is conservative because more initial stored energy is present and has to be removed following the accident. A high initial vessel pressure is conservative because it creates a longer blowdown with more mass inventory loss. The initial reactor power and system pressure determine the initial steam flow. The Westinghouse BWR LOCA evaluation model shall use plant initial conditions that bound the plant technical specification operating limits in the conservative direction. The power level to be used in plant specific analyses shall be at least 102 percent of licensed power as required by 10CFR50 Appendix K.

6.2 Nuclear Peaking Factors

Constraints on nuclear peaking factors in boiling water reactors are applied via the minimum critical power ratio (MCPR), maximum linear heat generation rate (MLHGR) and maximum average planar linear heat generation rate (MAPLHGR) limits. Sensitivity studies have been performed to determine the axial power distribution and bundle relative power appropriate for use in the DRAGON hot assembly analyses. A MLHGR limit of 14.5 kw/ft was assumed for this study.

Axial peaking factors for a BWR/5 can normally be expected to be no higher than 1.5 to 1.6. A bundle relative power of 1.5 (or lower) is a realistic upper limit, due to MCPR constraints. Local peaking factors are very dependent on fuel cycle management strategies, but are normally no higher than 1.3 at beginning of life (BOL). The local peaking factor will decrease with irradiation. Since LOCA is not limiting at BOL, a more reasonable value for consideration here would be in the range of 1.1 to 1.2. Based on these considerations the five cases in Table 6.2 were selected for study. The corresponding axial power shapes studied are shown in Figures 6.1 and 6.2. Boundary conditions from the GOBLIN reference calculation (Section 3) were used in the DRAGON calculations.

The dryout and uncovery times calculated by DRAGON for the peak power planes are shown in Table 6.2. The results were found to be [   ]^{a,c} The cases with a bundle relative power of 1.6 dried out and uncovered [   ]^{a,c} than the cases with a bundle relative power of 1.47. Time to dryout and uncovery was also [   ]^{a,c} as the peak power plane was moved higher in the assembly. Therefore the cases with the 1.5 cosine and 1.5 peaked-to-top axial power shapes were selected for further study with CHACHA-3C.

The CHACHA-3C heatup calculations were performed using the radial power distribution from the reference CHACHA-3C run of Section 3. The planar linear heat generation rate was increased from the DRAGON runs to maintain a MLHGR of 14.5 kw/ft. The calculated peak cladding temperatures are shown in Table 6.2. The results are seen to be [   ]^{a,c}. The peaked-to-top shape was found to give a slightly higher PCT than the cosine shape, due to the earlier dryout and uncovery times. However, the peaked-to-top power distributions shown in Figures 6.1 and 6.2 correspond to operation with the control rods inserted approximately half way into the core. This is inconsistent with plant operation at full power. Due to the relative insensitivity to power distributions shown in Table 6.2, and the inherent tendency of boiling water reactors to operate with slightly peaked-to-bottom power shapes, the 1.5 cosine shape has been selected for use in the DRAGON evaluation model calculations.

6.3 Plant Blowdown Sensitivities

An extensive sensitivity study was conducted to evaluate the impact of various plant parameters on the initial blowdown phase of the design basis LOCA. The key phenomena occurring during this phase of the transient are shown in Figure 6.3, which plots the active bundle (core) inlet flow rate with time. The phenomenon of most importance in determining the resultant peak cladding temperature is the time of midplane dryout (boiling transition). Other phenomena which can influence the time of midplane dryout are the time of jet pump suction uncovery, jet pump fluid saturation and flashing, and lower plenum fluid saturation and flashing. As shown in Figure 6.3 each of these phenomena can be identified by a noticable change in the core inlet flow. The higher the active core inlet flow rate, the later boiling transition (dryout) will occur and consequently the lower the peak cladding temperature will be.

Numerous plant initial conditions and transient actions were varied to determine their impact on the time of midplane dryout. The plant conditions and actions studied include: scram time, time of main steam isolation valve (MSIV) closure, initial water level, pressure form loss coefficients, and feedwater and recirculation pump coastdown rates. Table 6.3 lists the nine sensitivity runs and Figures 6.4 through 6.10 show the results. None of the sensitivities showed a marked change in dryout time.

Figures 6.4 through 6.6 show the impact of the time of reactor scram and MSIV closure on the core inlet flow. The reactor will typically scram in a large break LOCA on a high drywell pressure signal or the first low reactor water level signal. The MSIV will close typically on the third low level signal. In the base case (Figure 6.3) both signals are assumed to occur at one second after initiation of the break. Figure 6.4 shows the impact of a very early reactor scram and initiation of MSIV closure, both occurring at 0.1 second after the break. The earlier occurrence of the various phenomena is [
$\rceil$ a,c
] and the impact on the midplane dryout time is [$\rceil$ a,c]. In actual operation MSIV closure does not occur with reactor scram but later. The impact of delaying initiation of MSIV closure by two seconds is shown in Figure 6.5. The results show that the base case is conservative with respect to the time of dryout. This is because the

delay in MSIV closure depressurizes the vessel faster, causing a later jet pump uncovery, and earlier lower plenum flashing. Both changes help maintain a more steady and gradual drop in the core flow rate after low plenum flashing. Figure 6.6 shows the consequence of an earlier MSIV closure (0.1 second) while maintaining reactor scram at one second. The resultant change in the predicted phenomena is again very small, and similar to the case when both scram and MSIV closure occurred at 0.1 seconds. In the Westinghouse BWR LOCA evaluation model, MSIV closure will be assumed to occur with reactor scram on the first low level signal. The MSIV will close in the minimum time allowed by the plant technical specifications.

The impact of a lower initial downcomer water level on the midplane dryout time is shown in Figure 6.7. The difference in the initial water level between the two cases is equivalent to the elevation between nominal and low alarm water levels. The scram and MSIV closure times were kept the same as in the base case (1.0 second). The impact of a lower initial inventory in the downcomer on blowdown phenomena is $\left[\quad \right]^{a,c}$. The initial water level actually impacts not only the initial downcomer inventory but also time of reactor scram (and MSIV closure). In the Westinghouse BWR LOCA evaluation model the low level alarm elevation will be used as the initial water level.

The base case assumes a rapid flow coastdown of the feedwater flow rate after initiation of the break. The consequence of instantaneously stopping the feedwater flow was studied. The results are shown in Figure 6.8. The loss of subcooled fluid instantaneously, instead of taking a few seconds to coastdown, causes a slightly earlier flashing of the jet pumps and lower plenum. The impact on dryout time is $\left[\quad \right]^{a,c}$. A conservatively fast feedwater flow coastdown rate that bounds available coastdown data is used in the evaluation model.

Almost immediately after initiation of the recirculation line break, the broken leg jet pump flow stops. The intact loop recirculation pump, however, takes approximately 20 seconds to coastdown. The impact of a 35 percent faster coastdown was studied and the result is shown in Figure 6.9. The faster recirculation pump coastdown causes a marginally lower core inlet flow for the first 10 seconds after which lower plenum flashing dominates the core inlet flow. Again, the impact on the time of midplane dryout $\left[\quad \right]^{a,c}$.

The impact of pressure losses on jet pump flashing was also examined. This was accomplished by reducing the suction nozzle form losses. [

$$]^{a,c}$$

Lastly, the contribution of the bypass and watercross draining to the active core inlet flow were examined. This was accomplished by increasing the form losses of the leakage holes and the watercross orifice. Figure 6.10 shows the study results. As can be seen, [$]^{a,c}$ in the inlet core flow occurred.

In summary, the largest change in midplane dryout time as a consequence of any of these sensitivities was [$]^{a,c}$. None of the changes caused the midplane dryout to occur much earlier, such as before lower plenum flashing. The assumptions used in the Westinghouse BWR LOCA evaluation model, outlined above, will ensure a conservative calculation of the plant blowdown, time of midplane dryout and peak cladding temperature.

6.4 Reduced Core Flow Sensitivity

The range of plant operation for a boiling water reactor can be shown on a power-flow map. A sample map is shown in Figure 6.11. Under normal operation, the maximum power level is at 100 percent of rated core flow. Some utilities may license "extended limits of operation" to allow greater plant operating flexibility. One extended limit of concern to LOCA analysis is reduced core flow operation for power levels near or at 100 percent of rated power. In this section the impact on the LOCA analysis of an initial reduced core flow at 100 percent power is examined.

The purpose of this sensitivity is to determine the impact that a reduced core flow (at LOCA full power conditions) has on the MAPLHGR limits based on the LOCA analysis for normal operation. An evaluation of the impact that core inlet flow rate has on the LOCA blowdown, dryout time, vessel depressurization rate, and the time of core reflood is presented. A LOCA was initiated from a steady state plant condition of 105 percent of steam flow and 68 percent of rated flow. Table 6.4 summarizes the reduced flow case initial conditions.

The transient response of hot assembly inlet flow is shown in Figure 6.12. The initial assembly flow decreases dramatically during the first second. The flow is essentially zero by six seconds when jet pump flashing forces fluid up through the core. The assembly inlet flow decreases again until the lower plenum begins flashing at 11 seconds. This momentarily increases the inlet flow to approximately 66 percent of the flow at time zero. Subsequently the flow decreases again and at 24 seconds midplane dryout occurs. The hot assembly inlet flow for the reference case of Section 3 is also shown in Figure 6.12 for comparison. Aside from the reduced magnitude, there is one main difference between the reference case and the reduced flow case. That is the time of lower plenum flashing. A comparison of the timing of the phenomena is also given in Table 6.4.

The lower plenum has a lower initial enthalpy in the reduced flow case. This is a consequence of maintaining the same steam flow for the reduced flow case as for the reference case (same initial conditions). For the coolant to remove the same core power at a lower flow rate, the enthalpy increase across the core at steady state must increase. This increase in enthalpy rise across the core is balanced between an increase in the vapor fraction out of the core and a decrease in the core inlet enthalpy. Hence, the lower plenum enthalpy is lower at steady state during reduced flow operation. Since the lower plenum enthalpy is more subcooled, it takes longer for the system to reach the saturation pressure of the fluid in the lower plenum. The delayed flashing in the lower plenum extends the time of dryout from 21.5 seconds in the reference case to 24 seconds in the reduced flow case.

As shown in Table 6.4, the depressurization rate and the time of core reflood for the reduced flow case compare well with the reference transient in Section 3. The net result is that the reduction in initial core flow delays the time of midplane dryout without delaying the time at which the midplane refloods. For this sample calculation, the Westinghouse BWR LOCA evaluation model would calculate a lower midplane peak cladding temperature for reduced flow plant operation than in the full power and flow operation.

TABLE 6.1
LOCA INITIAL CONDITIONS

Core Thermal Power	3461 MWt
Vessel Steam Output	1891 kg/sec (15.0×10^6 lbm/hr)
Percent of Rated Steam Flow	105%
Vessel Pressure	72.7 bar (1055 psia)
Total Core Flow Rate	13667 kg/sec (108.5 Mlbm/hr)
Percent of Rated Core Flow	100%
Maximum Area of Recirculation Line Break	0.292 m^2 (3.14 ft^2)

TABLE 6.2
POWER DISTRIBUTION SENSITIVITY STUDY RESULTS

Axial Peaking Factor	Location of Axial Peak	Bundle Relative Power	Dryout Time (sec)	Uncovery Time (sec)	CHACHA-3C Peak Cladding Temperature
1.63	1.9m (6.25 ft)*	1.47			-
1.63	2.5m (8.0 ft)	1.47			-
1.5	1.3m (4.5 ft)	1.60			-
1.5	1.9m (6.25 ft)*	1.60	21.5	28.7	1036°C (1897°F)
1.5	2.5m (8.0 ft)	1.60			

a,c

*Cosine

TABLE 6.3
LIST OF BLOWDOWN SENSITIVITY RUNS

Case	Parameter Change	Figure
A	Base Case	6.10
B	Earlier Scram and MSIV Closure	6.11
C	Later MSIV Closure	6.12
D	Earlier MSIV Closure	6.13
E	Lower Initial Water Level	6.14
F	Instantaneous Feedwater Cutoff	6.15
G	35% Faster Pump Coastdown	6.16
H	Lower Jet Pump Suction Losses	-
I	Higher Watercross and Leakage Losses	6.17

TABLE 6.4

COMPARISON OF 100 PERCENT AND REDUCED CORE FLOW CASES

	Reference Case	Reduced Flow Case
Percent of Rated Core Flow	100%	68%
Percent of Rated Power	104.3%	104.3%
Initial Lower Plenum Enthalpy	1239 KJ/Kg	1216 KJ/Kg
Initial Core Exit Enthalpy	1429 KJ/Kg	1484 KJ/Kg
Lower Plenum Flashing	10 sec	11 sec
Midplane Dryout	21.5 sec	24 sec
Initiation of Spray Cooling	48 sec	51 sec
Midplane Reflood	142 sec	143 sec
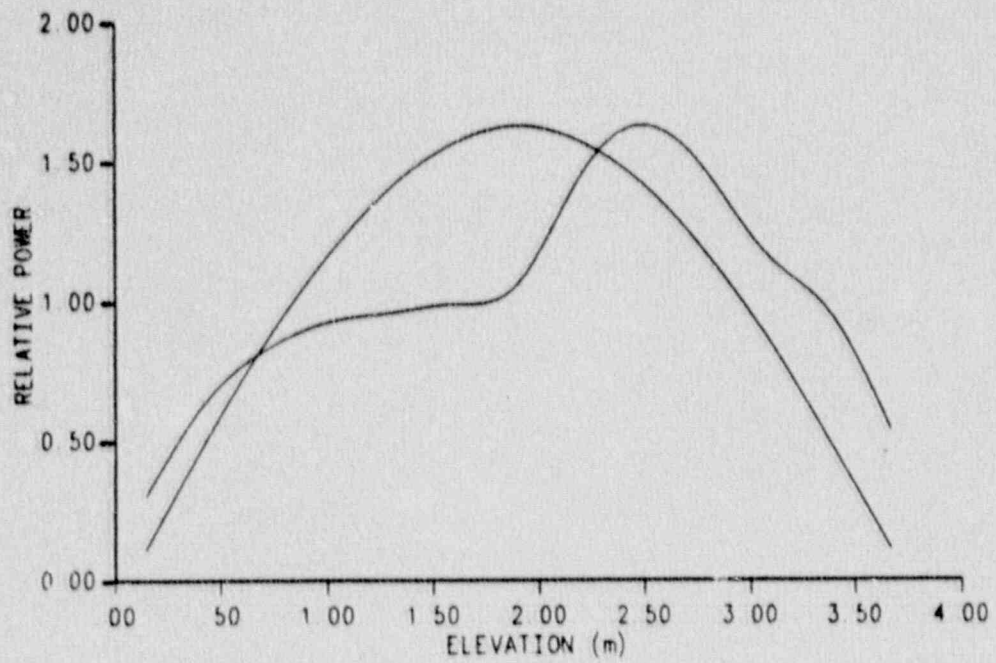
Figure 6.1 - Power Shapes with 1.63 Axial Peaking
Factor
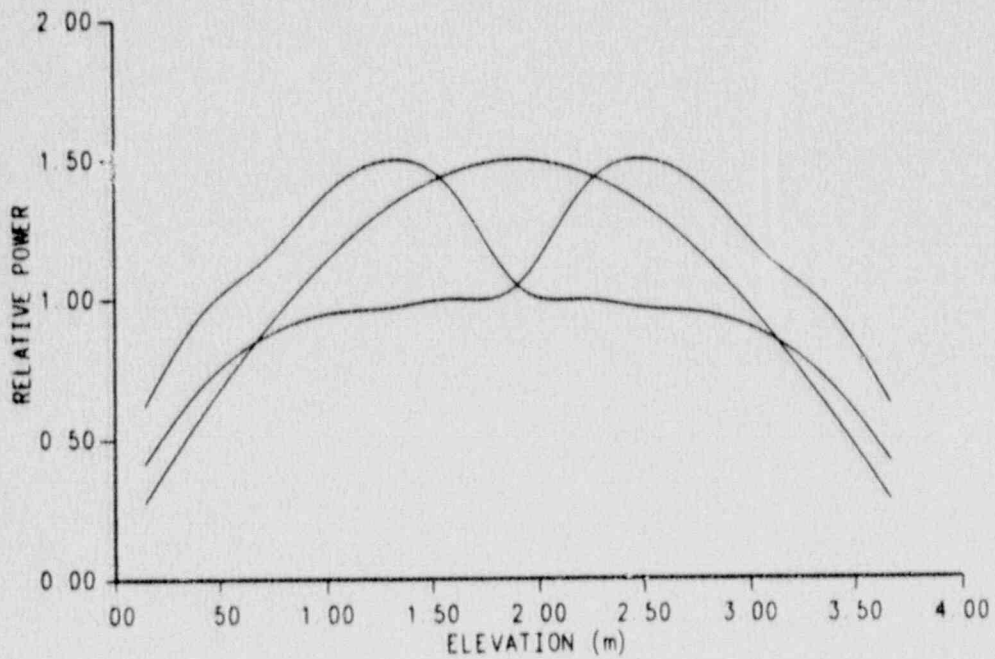
Figure 6.2 - Power Shapes with 1.50 Axial Peaking
Factor
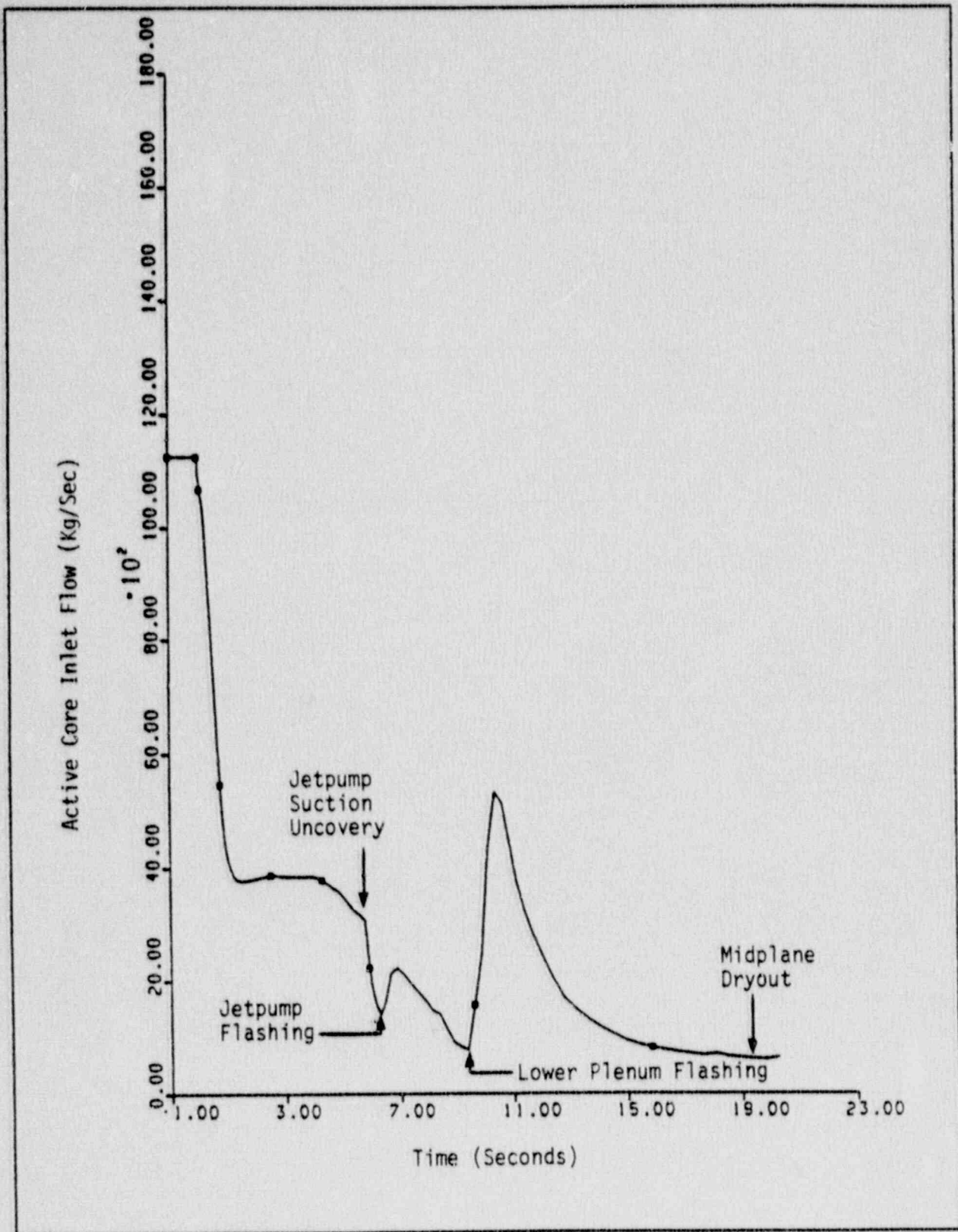
Figure 6.3 - Active Core Inlet Flow During Initial Blowdown

a,c

Figure 6.4 - Blowdown Sensitivity to Early Reactor Scram and MSIV Closure

a,c

a,c

Figure 6.5 - Blowdown Sensitivity to Late MSIV Closure

—a,C
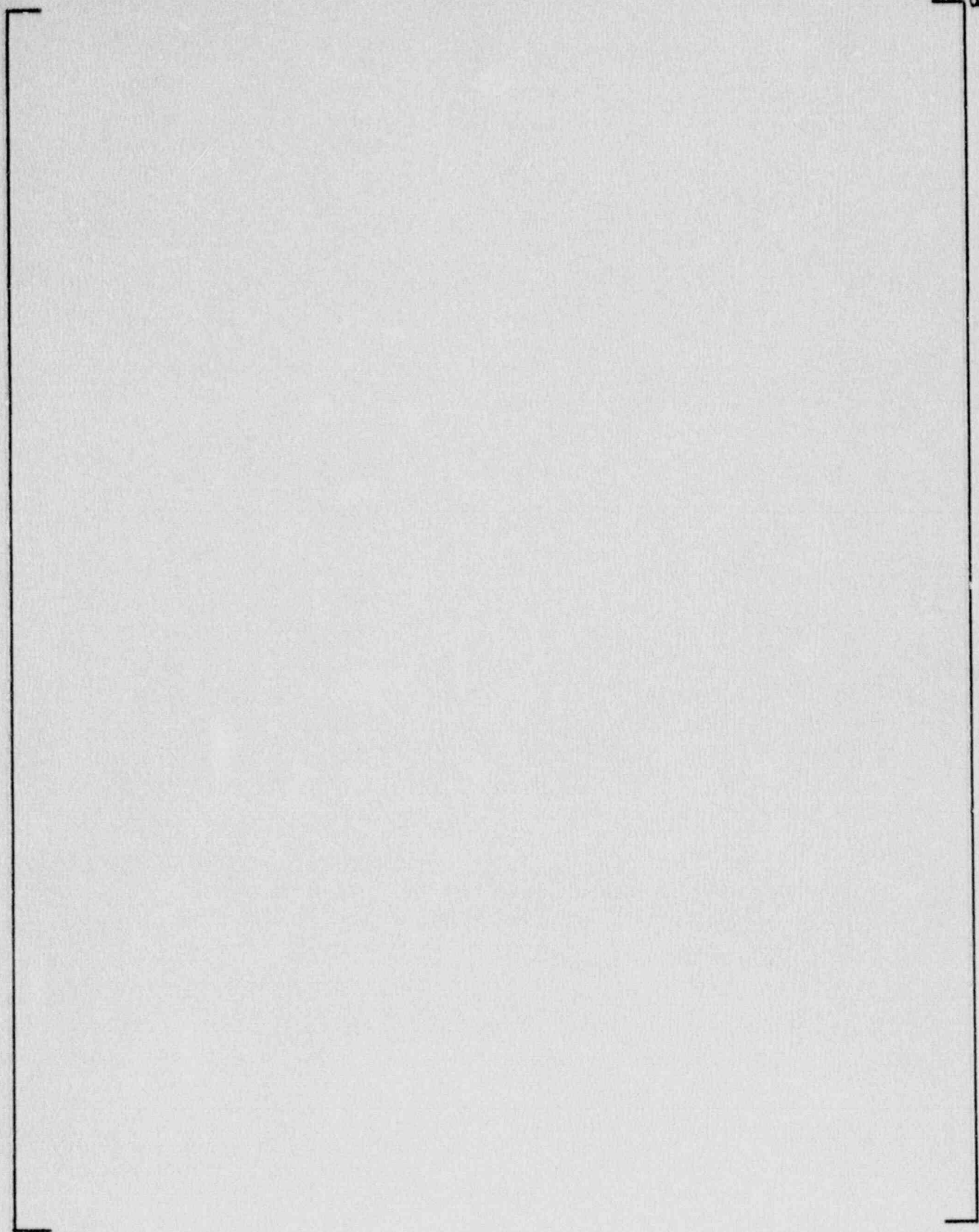
Figure 6.6 - Blowdown Sensitivity to Early MSIV Closure

a,c

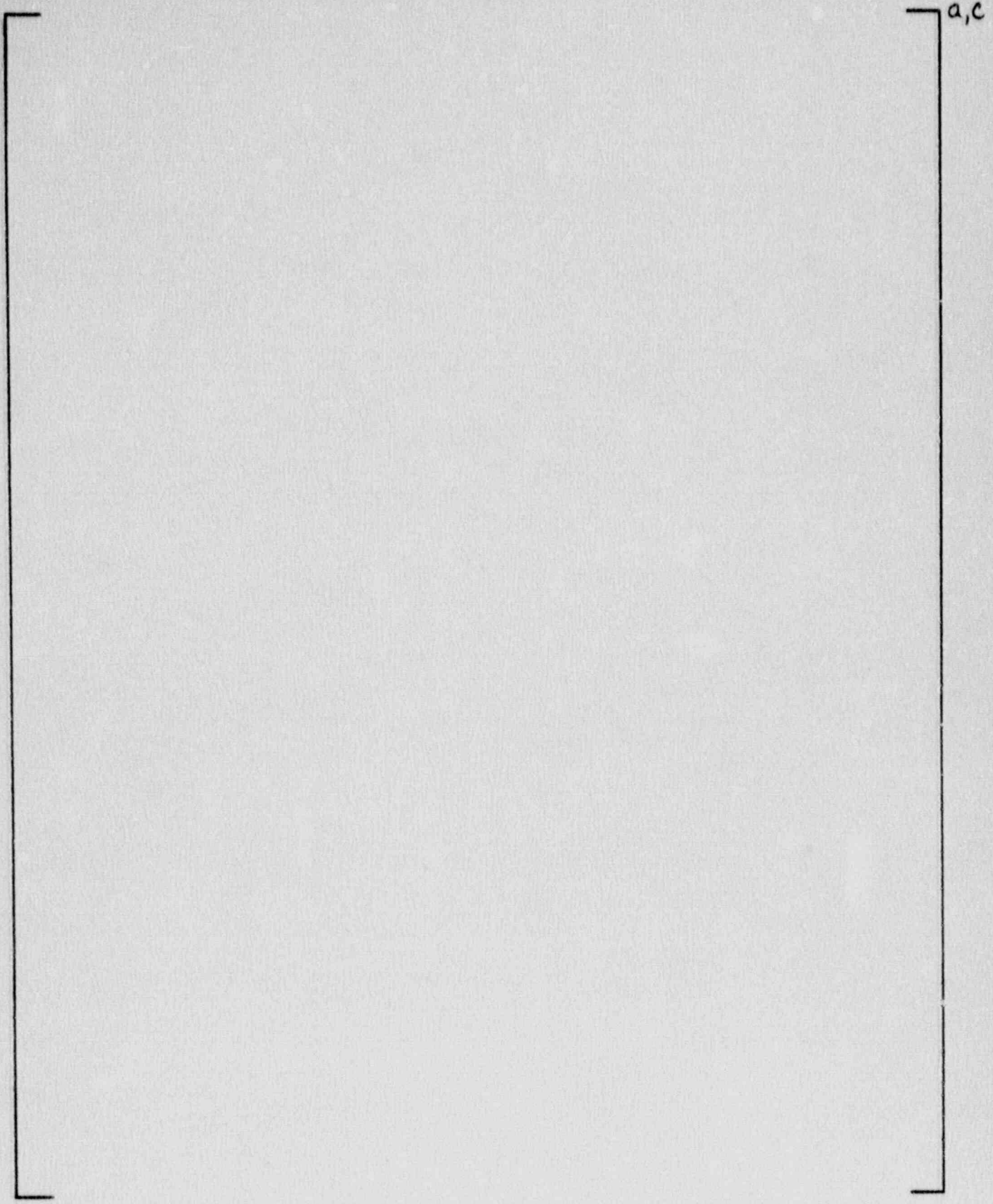Figure 6.7 - Blowdown Sensitivity to Low Initial Water Level

a,c

Figure 6.8 - Blowdown Sensitivity to Instantaneous Feedwater Cutoff

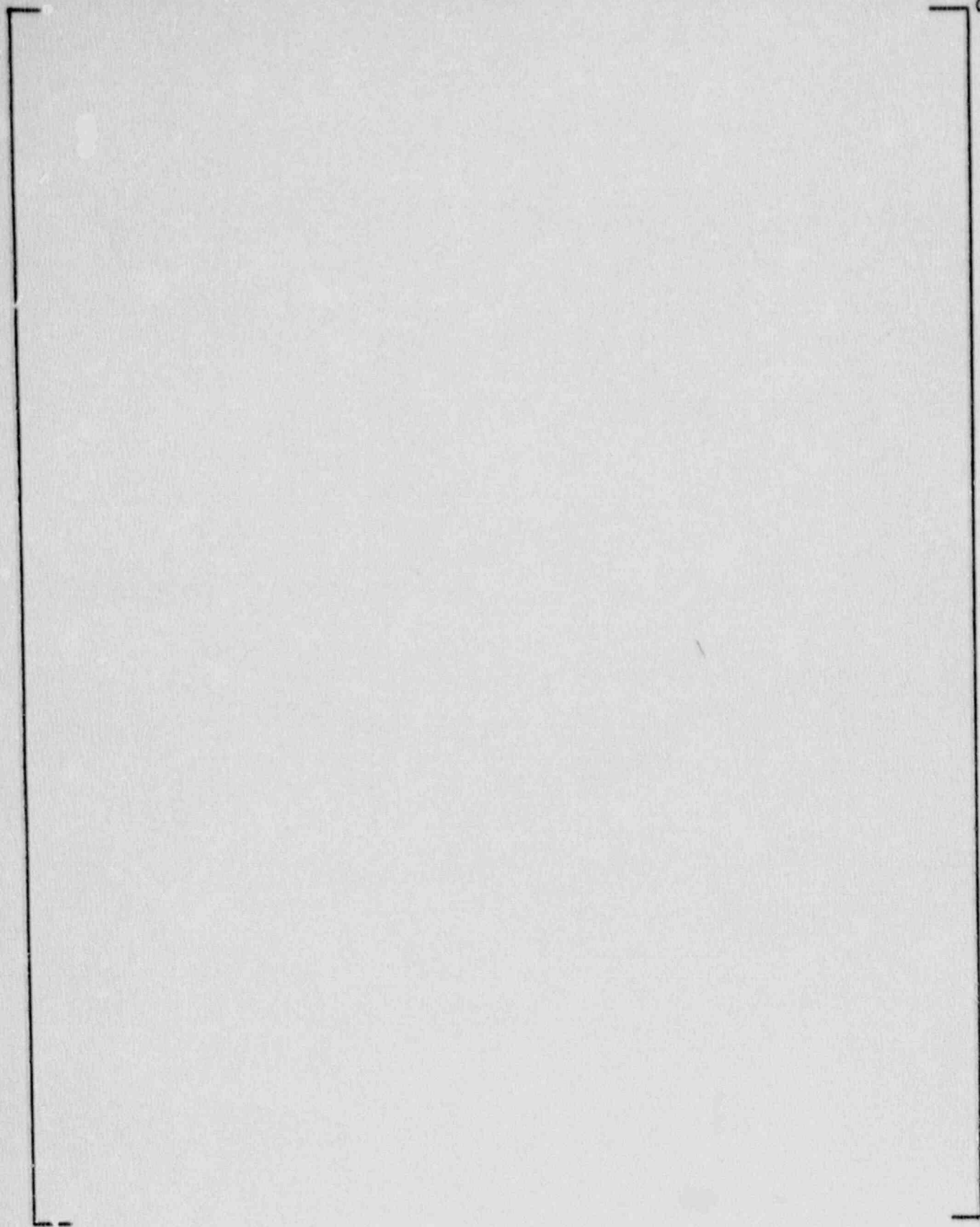a,c

Figure 6.9 - Blowdown Sensitivity to 35 Percent Faster Recirculation
Pump Coastdown

[⌐a,c

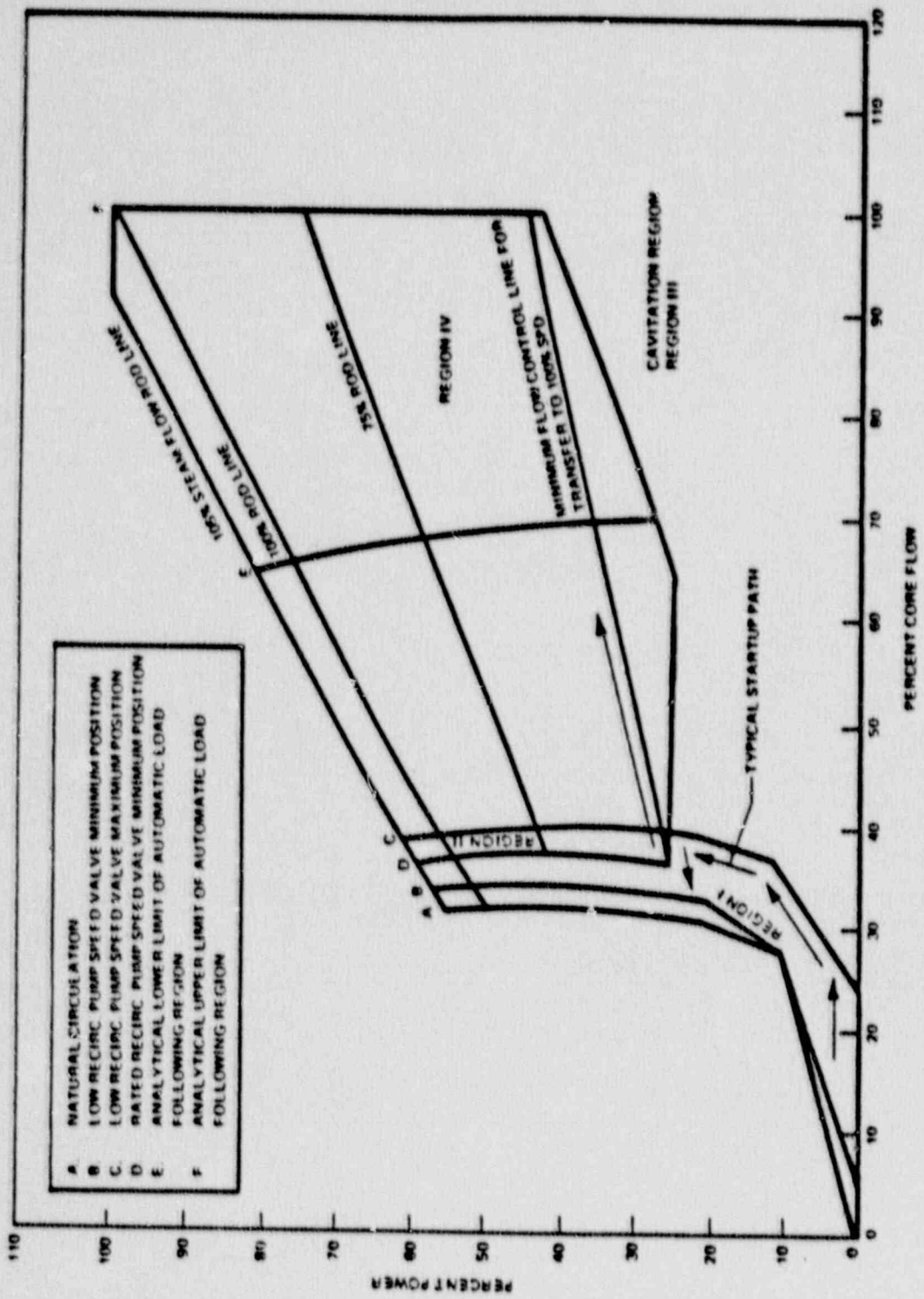

└   ⌐

Figure 6.10 - Blowdown Sensitivity to Bypass and Water Cross Draining
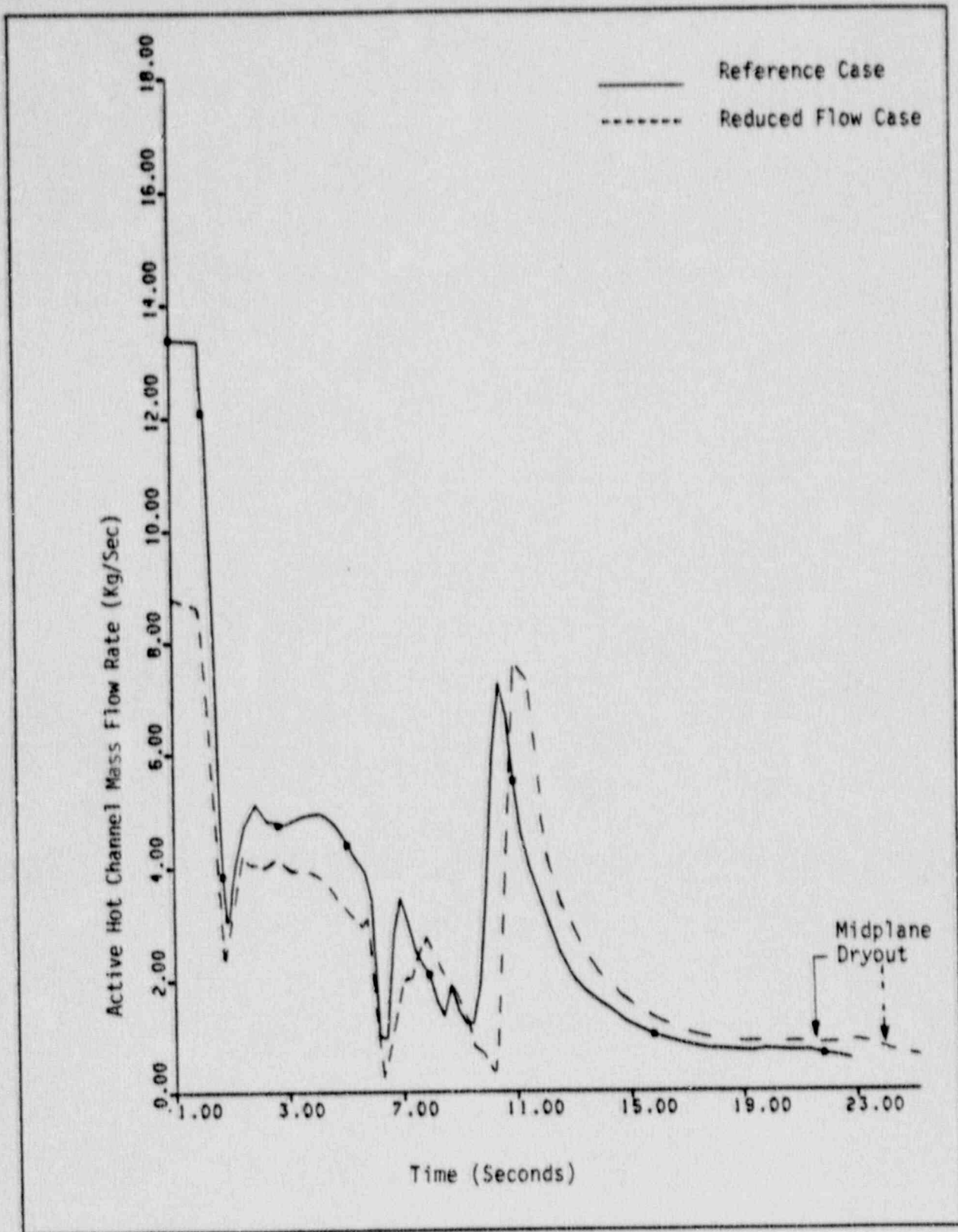   Rate

Figure 6.11 - Typical Power - Flow Operating Map

Figure 6.12 - Comparison of Hot Assembly Inlet Flow Rate - Reduced
Flow Sensitivity

7.0 NUMERICAL STUDIES

This section demonstrates that the GOBLIN/DRAGON and CHACHA-3C computer solutions converge uniquely. Demonstrating convergence of the evaluation model codes is a requirement of 10CFR50 Appendix K. The convergence criteria and time step size used in each code were studied. A single transient was simulated using varying convergence limits and time steps to show that the calculated solution is unique and within acceptable limits of the ideal asymptotic solution.

7.1 GOBLIN/DRAGON Code

The GOBLIN/DRAGON code solves the one-dimensional thermal-hydraulic conservation equations by matrix inversion of the fully implicit finite differenced equations. Following a converged thermal-hydraulic solution, the material conduction solution is iteratively calculated. The only explicit step is surface to fluid heat fluxes in the thermal-hydraulic solution.

Three user-specified convergence criteria are required in this numerical solution scheme:

(1) A thermal-hydraulic criterion (EPS)
(2) A fuel rod temperature criterion (DIFFT), and
(3) A surface heat transfer criterion (DIFFQ).

The convergence criteria used in the evaluation model are EPS $= 10^{-4}$, DIFFT $= 5 \times 10^{-3}$, and DIFFQ $= 10^{-4}$.

Also required in this numerical solution scheme is a transient time step size. The GOBLIN/DRAGON code employs an automatic time step logic to determine the transient time step. A maximum allowable time step size is specified by the user. However, the actual time step used is generally less than the maximum allowable time step. The actual time step size is dictated by the change in thermal-hydraulic conditions and ability to calculate a converged solution. If the transient thermal-hydraulic conditions are changing slowly, the time step size is increased. However, if conditions are

changing rapidly and a converged solution is not obtained in a reasonable number of iterations, the time step size is reduced. The evaluation model shall use maximum allowable time step sizes throughout the transient which minimize the computational recalculations.

The time step size is indirectly linked to the hydraulic convergence criteria. A more restrictive hydraulic criteria will force the required time step size to be reduced. For this reason the sensitivity of time step size and convergence criteria were studied simultaneously.

Table 7.. summarizes the range of convergence criteria and maximum time step sizes examined. The maximum time step was changed between 0.5 and 0.05 seconds and the convergence criteria were changed by three orders of magnitude. For runs with a maximum allowable time step of 0.5 seconds, the actual time step selected by the code was less than 0.5 seconds during certain periods of the transient.

Figure 7.1 shows the change in several key output variables as the time step is reduced. The output variables were compared at the same time in the transient and normalized to the extrapolated limiting value at an infinitesimal time step. The figure shows that the solution monotonically approaches an unique solution as the time step is reduced and the error associated with specifying a large discrete time step is less than 3 percent.

The effect of changing the convergence criteria on the solution is minimal. For small time steps the solution converges well within the convergence limits with one or two iterations. Hence, relaxing the convergence criteria has negligible impact on the simulation results. For example, with a maximum allowable time step of 0.1 seconds the same results were obtained for a two order of magnitude relaxation in the convergence criteria (comparing cases A, E, and F). For larger time steps a two order of magnitude change in convergence criteria results in less than a 0.5 percent change in simulation results (case B, H, and I). Figure 7.2 shows graphically the sensitivity to changes in convergence criteria.

These sensitivity results demonstrate that the automatic time step logic and the convergence criteria used in GOBLIN evaluation model will result in a calculated solution within acceptable limits of the ideal asymptotic solution.

7.2 CHACHA-3C Code

The key convergence criteria used in the CHACHA-3C heat-up code are shown in Table 7.2. The reference CHACHA-3C transient (Section 3) has been repeated with these convergence criteria relaxed by an order of magnitude. The results are found to be identical to the reference case, demonstrating that the CHACHA-3C convergence criteria used in the evaluation model are sufficiently stringent.

The CHACHA-3C time step size is selected by the user. The maximum values to be used in the evaluation model are shown in Table 7.3. (If the convergence criteria cannot be satisfied, the time step size is reduced accordingly.) The reference CHACHA-3C transient has been repeated with all time steps reduced by 80 percent. The results show a change in peak cladding temperature of 1°C. These results verify that the typical time steps sizes shown in Table 7.3 are sufficiently small to ensure an accurate solution to the heatup calculation.

In summary, this time step/convergence criteria study demonstrates convergence of the GOBLIN/DRAGON and CHACHA-3C codes to unique asymptotic solution. The GOBLIN/DRAGON automatic time step logic limits the transient time step to ensure a sufficiently converged solution. Hence the actual time step size used in the evaluation model will be dependent on the transient being simulated. The maximum allowable time step will be adjusted only to help minimize the number of computational recalculations performed during searches for the appropriate transient time step. The GOBLIN/DRAGON convergence criteria used in the evaluation model were shown to optimize the computation time without compromising solution accuracy.

The CHACHA-3C convergence criteria and time step sizes used in the evaluation model are shown to be sufficiently stringent and will result in an accurate solution.

TABLE 7.1

GOBLIN/DRAGON NUMERICAL SENSITIVITY RUNS

Case	Maximum Time Step (sec)	Hydraulics	Convergence Criterion Rod Temperature	Surface HT
A	0.1-0.5*	10^{-4}	5×10^{-3}	10^{-4}
B	0.5	10^{-4}	5×10^{-3}	10^{-4}
C	0.1	10^{-4}	5×10^{-3}	10^{-4}
D	0.05	10^{-4}	5×10^{-3}	10^{-4}
E	0.1	10^{-3}	5×10^{-2}	10^{-3}
F	0.1	10^{-5}	5×10^{-4}	10^{-5}
G	0.2	10^{-4}	5×10^{-3}	10^{-4}
H	0.5	10^{-3}	5×10^{-2}	10^{-3}
I	0.5	10^{-2}	5×10^{-1}	10^{-2}

* The maximum time step was relaxed as the transient progressed.

TABLE 7.2
CHACHA-3C CONVERGENCE CRITERIA

Convergence Criterion	Evaluation Model Value	Relaxed Case Values
Relative Change in Rod Surface Heat Flux	10^{-3}	10^{-2}
Relative Change in Rod Surface Temperature	10^{-4}	10^{-3}
Absolute Change in Nodal Temperature	10^{-2}	10^{-1}
Relative Change in Channel Temperature	10^{-4}	10^{-3}
Peak Cladding Temperature	1036°C	1036°C

TABLE 7.3
TYPICAL CHACHA-3C TIME STEPS

Phase of Transient	Time Step Size (sec) Evaluation Model	Reduced 80%
Blowdown (0-1 sec)	0.1	0.02
(1.5 sec)	0.25	0.05
(after 5 sec)	0.5	0.10
Dryout	0.1	0.02
Dryout to Uncovery	0.5	0.10
Uncovery	0.1	0.02
Uncovery to Reflood	1.0	0.20
Peak Cladding Temperature	1036°C	1037°C

CALCULATIONAL TIME STEP (SECOND)
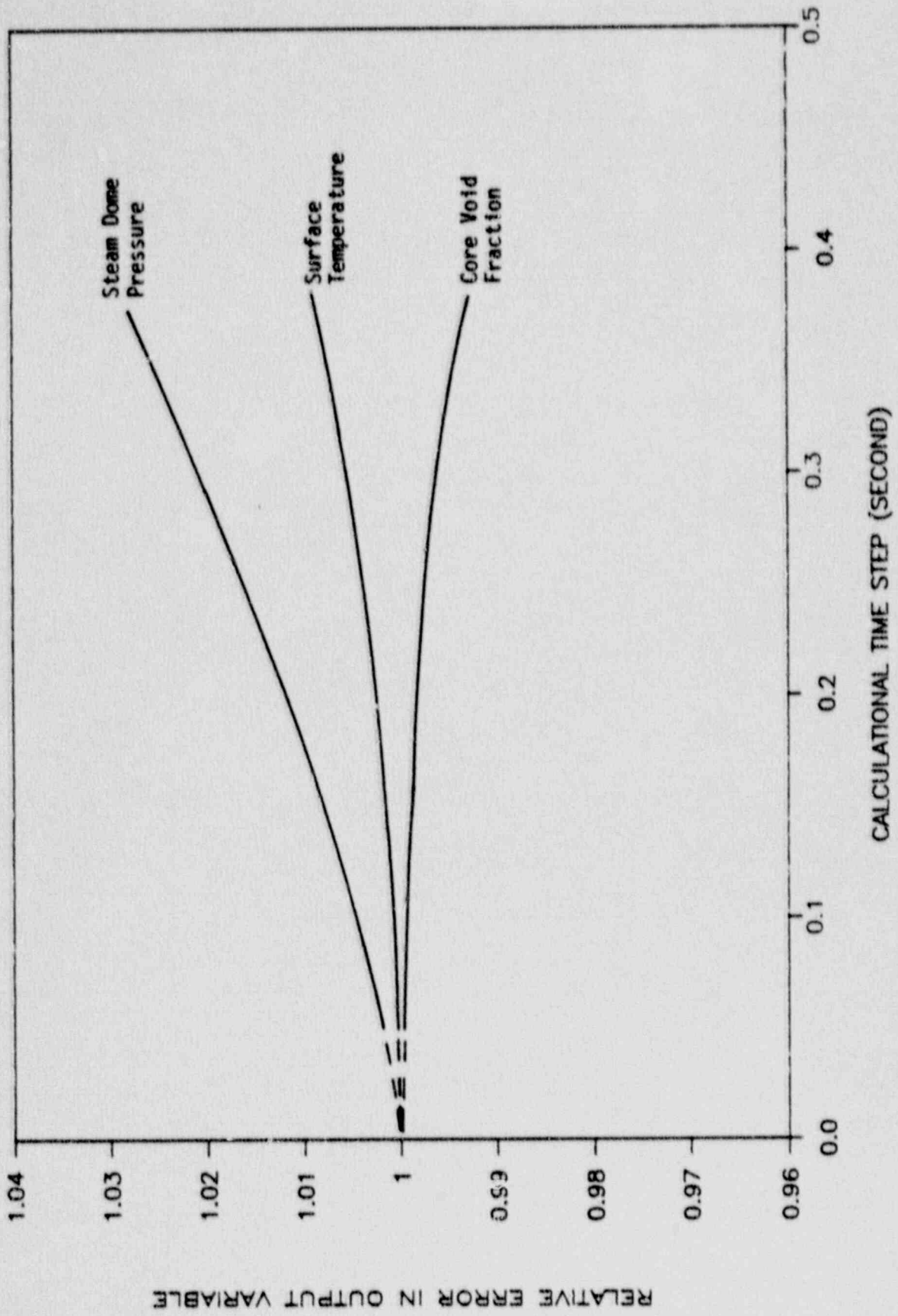
Figure 7.1 - Change in Simulation Results Versus Average Calculational Time Step
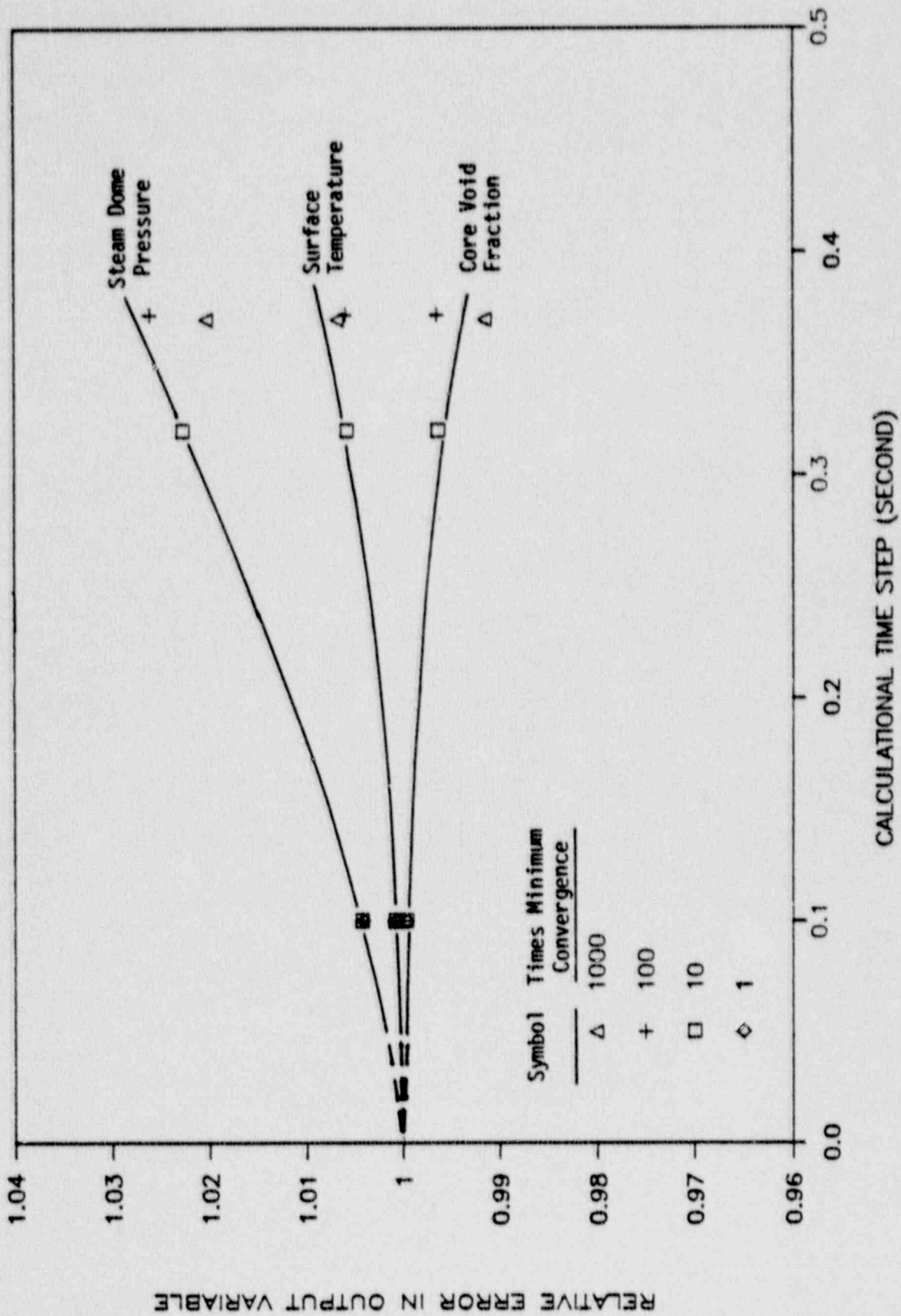
Figure 7.2 - Change in Simulation Results With Relazed Convergency Criteria

8.0 BREAK SPECTRUM

The reactor coolant pressure boundary contains numerous pipes of varying lengths, diameters, and elevations. Thus a postulated LOCA may be initiated by a pipe break of a wide range of sizes and locations. In performing a LOCA analysis 10CFR50 Appendix K requires that the worst possible single failure of the ECC system be assumed. A spectrum of breaks covering the range of pipe breaks and single failures is necessary in the evaluation of a loss of coolant accident. The limiting break is the combination of break size, location, and single failure that yields the highest calculated peak cladding temperature.

8.1 Break Spectrum Methodology

The Westinghouse BWR LOCA evaluation model described in Reference 1 and this report are used to determine the peak cladding temperature for a given postulated break and single equipment failure. The limiting break size, location, and worst single failure is determined by confirming the same break spectrum dependence using the Westinghouse evaluation model as was determined in the original plant ECC system design analysis. If a discrepancy in the limiting break is observed the deviation will be justified by evaluating the differences in analysis methods and conservative assumptions. If warranted, additional break spectrum analyses will be conducted to identify the limiting break. The limiting break is that which yields the highest peak cladding temperature.

To demonstrate this methodology, a break spectrum analysis for a reference BWR/5 plant with a full core of QUAD+ fuel has been performed. The break spectrum considered in the Final Safety Analysis Report (FSAR) for the reference BWR/5 is shown in Figure 8.1.

The limiting break for this plant design is a full double-ended guillotine break of a recirculation suction line with the worst single failure being the loss of the LPCS diesel generator (Division I in Figure 3.2). Other breaks which are near limiting include:

o A full guillotine break in a recirculation suction line with failure of the HPCS system.

o A 0.0084 m^2 (0.09 ft^2) split break in a recirculation suction line with failure of the HPCS system.

o A full spray line break with failure of the LPCS diesel generator (Division I).

Each of these breaks has been analyzed with the Westinghouse BWR LOCA evaluation model to determine whether the break spectrum dependence is the same as in the original plant LOCA analyses. The results are presented below.

8.2 Large Breaks

The Westinghouse BWR LOCA evaluation model has shown that the limiting break for a BWR/5 is the design basis break -- a full double-ended guillotine break of a recirculation suction line with failure of the LPCS system diesel generator (which also fails one LPCI pump.) This break is the reference transient described in detail in Section 3. The resultant peak cladding temperature is 1036°C (1897°F).

To demonstrate that the LPCS diesel generator failure assumption is limiting, another full guillotine break of a recirculation suction line with failure of the HPCS system diesel generator is analysed. Figures 8.2 and 8.3 show plots of the system pressure response and mass inventory, respectively, during the transient. The transient response to this break is similar to the reference transient (comparing with Figure 3.4 and 3.8, respectively). The major difference is a much larger supply of ECC water with the LPCS system now available. The larger capacity LPCS system introduces a larger quantity of

ECC water into the vessel which results in an earlier midplane reflood than the reference case by about 13 seconds. The resultant peak cladding temperature is 976°C (1789°F).

To show that the full guillotine recirculation line break with failure of the LPCS diesel, is the most limiting break size for a BWR/5, three additional large breaks were analysed. They are 80, 60, and 40 percent of the full doubled-end guillotine recirculation pipe break. Figures 8.4, 8.5, and 8.6 show the hot assembly mass inventory for these large breaks, respectively. (The full guillotine break plot is shown in Figure 3.18.) As the break size is reduced the initial rate of inventory loss is slower which delays the time of midplane dryout. Midplane reflood is also delayed by the slower depressurization, and hence, later actuation of the low pressure ECC systems. The net result is a lower peak cladding temperature for the smaller large breaks, as shown in Figure 8.7. In Figure 8.7, the differences between the calculated peak cladding temperature for the actual break minus the limiting break peak cladding temperature are plotted. It is seen from this figure that a full 100 percent guillotine recirculation suction line break is indeed limiting.

8.3 Small Breaks

Two small break LOCAs in the BWR/5 break spectrum (Figure 8.1) are within approximately 500°F of the limiting break. These are the 0.09 ft^2 recirculation suction line break and the 100 percent spray line break. To confirm this small break trend these two small breaks were analysed with the GOBLIN and DRAGON evaluation models.

For the 0.0084 m^2 (0.09 ft^2) recirculation suction line LOCA the worst single failure is the HPCS system. Figure 8.8 shows the reactor system pressure response for this small recirculation line break. The initial pressure response is governed by the relative contributions of the volumetric flow of the break, the response of the pressure regulating system, and the vapor generation from the reactor power. The reactor power changes in the initial phase of the transient from the reactivity change due to voiding in

the core and the subsequent reactor scram. After an initial pressure drop, the vessel pressure stabilizes at the regulating valve setpoint. When the vessel level decreases enough the MSIV are closed. Once the MSIVs close, the system repressurizes to the safety/relief valve setpoint. The valve(s) cycle open and closed several times.

The Automatic Depressurization System (ADS) is activated to increase the effective break area two minutes after the ADS signal level setpoint is reached. The increased break size rapidly reduces the vessel pressure and allows the low pressure ECC systems to be initiated (Figure 8.8).

Eventually, the integrated coolant inventory loss due to the ADS and break flow is sufficient to deplete the inventory in the vessel to the point where the water level falls below the top of the active fuel (see Figure 8.9). As indicated in Figure 8.10 the hot assembly does not go through boiling transition until the active core is uncovered. This is because the decrease in core flow is more gradual than for the large breaks. The recirculation loops remain intact and the core flow is governed by the coastdown of the recirculation pumps. The break flow rate is slow enough so that the core is still covered when the recirculation pumps have fully coasted down.

Once the core uncovers the fuel cladding temperature increases rapidly. As the transient continues the core remains uncovered and cladding heat up continues until the vessel pressure is reduced sufficiently to allow initiation of the low pressure ECC systems. Once low pressure ECC systems are initiated, the contribution of low pressure spray cooling reduces the rise in cladding temperature. Finally the ECC systems replenish the coolant inventory enough to reflood the core and terminate the cladding temperature heat up. The peak cladding temperature for the 0.0084 m^2 (0.09 ft^2) recirculation line break is 575°C (1067°F), substantially below the limiting break peak cladding temperature.

The 100 percent spray line break is a small break of particular significance because the break disables one ECC spray system. When the worst single failure is assumed (failure of the LPCS diesel generator) the remaining ECC

spray system is disabled. The transient response to a full spray line break is similar to the 0.0084 m^2 (0.09 ft^2) small break described above. The major differences are that the larger break area 0.318 m^2 (0.34 ft^2) and the higher elevation of the spray line. As shown in Figure 8.11, these differences cause a more rapid depressurization. The core refill and reflood is provided by the remaining ECC system, the LPCI pumps. Because of the faster depressurization and earlier LPCI actuation a slightly lower peak cladding temperature than the recirculation line small break, 532°C (990°F), was calculated.

8.4 Summary

The results of the Westinghouse BWR LOCA break spectrum analysis for a typical BWR/5 are summarized in Table 8.1. A comparison with the original break spectrum for the reference BWR/5 is shown in Figure 8.12. Note that in the comparison the Westinghouse results are for QUAD+ fuel operating at a maximum linear heat generation rate of 14.5 kW/ft, whereas the original analysis is for General Electric 8x8 fuel at 13.4 kW/ft. The large break calculated peak cladding temperatures show the same relative magnitude and trend as the original results. The small break results are also consistent with the original analysis, except for a somewhat lower peak cladding temperature.

The results presented above demonstrate that the limiting break for QUAD+ fuel operating in the reference BWR/5 plant design is the full double-ended guillotine break of a recirculation suction line with the worst single failure being the loss of the LPCS diesel generator. The peak cladding temperature calculated for the limiting break is well below the acceptance criterion of 2200°F.

TABLE 8.1
BREAK SPECTRUM RESULTS
(QUAD+ FUEL, MLHGR = 14.5 KW/FT)

	Peak Cladding Temperature
100% Recirculation Suction Break With LPCS Diesel Generator Failure	1036°C (1897°F)
100% Recirculation Suction Break With HPCS Diesel Generator Failure	976°C (1789°F)
0.0084 m^2 (0.09 ft^2) Recirculation Suction Break With HPCS Diesel Generator Failure	575°C (1067°F)
100% Spray Line Break With LPCS Diesel Generator Failure	532°C (990°F)
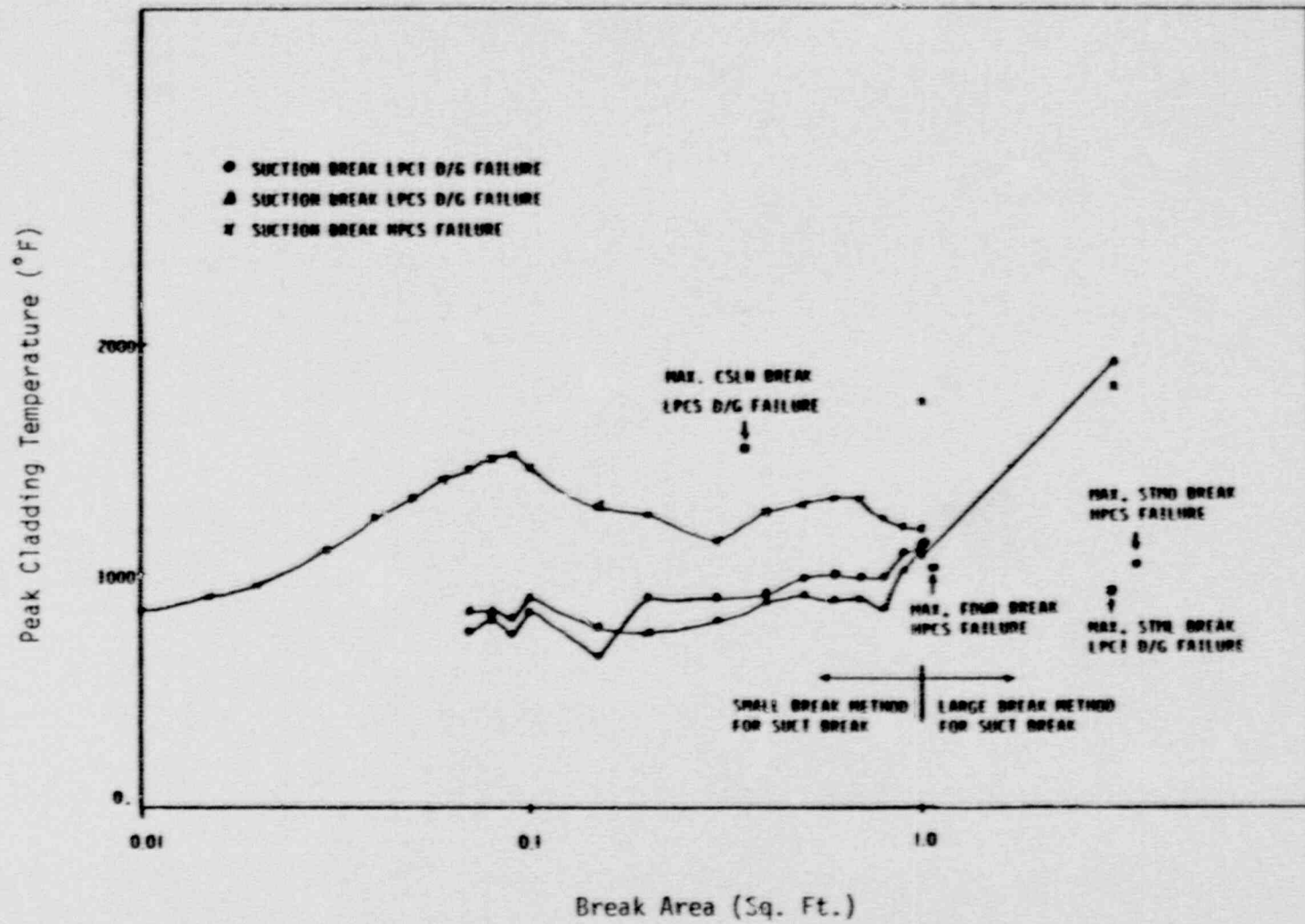
Figure 8.1 - Typical FSAR Break Spectrum for a BWR/5
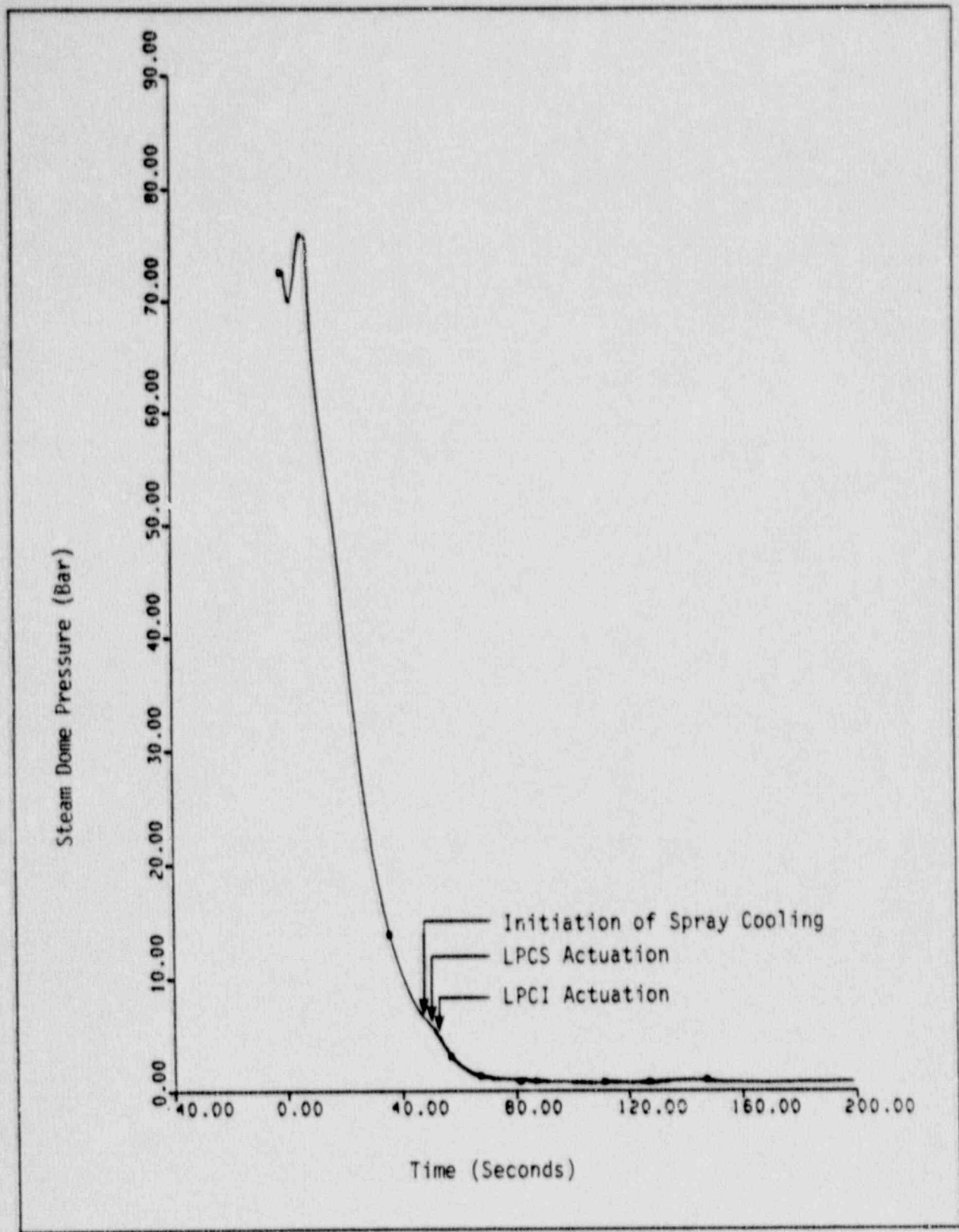
Figure 8.2 - Vessel Steam Dome Pressure for 100 Percent Recirculation
Line Break With HPCS Failure
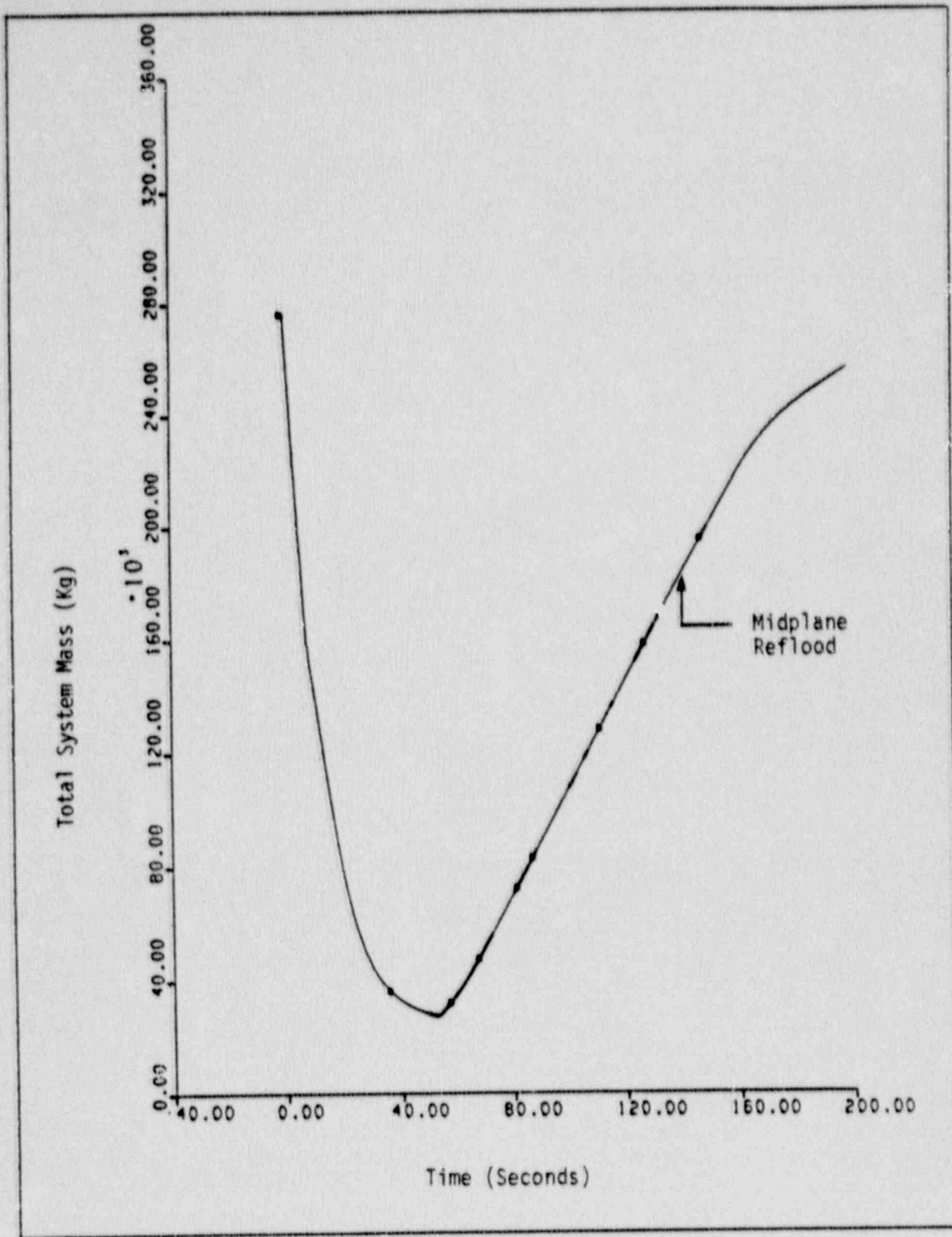
Figure 8.3 - Total Mass Inventory for 100 Percent Recirculation Line
Break With HPCS Failure
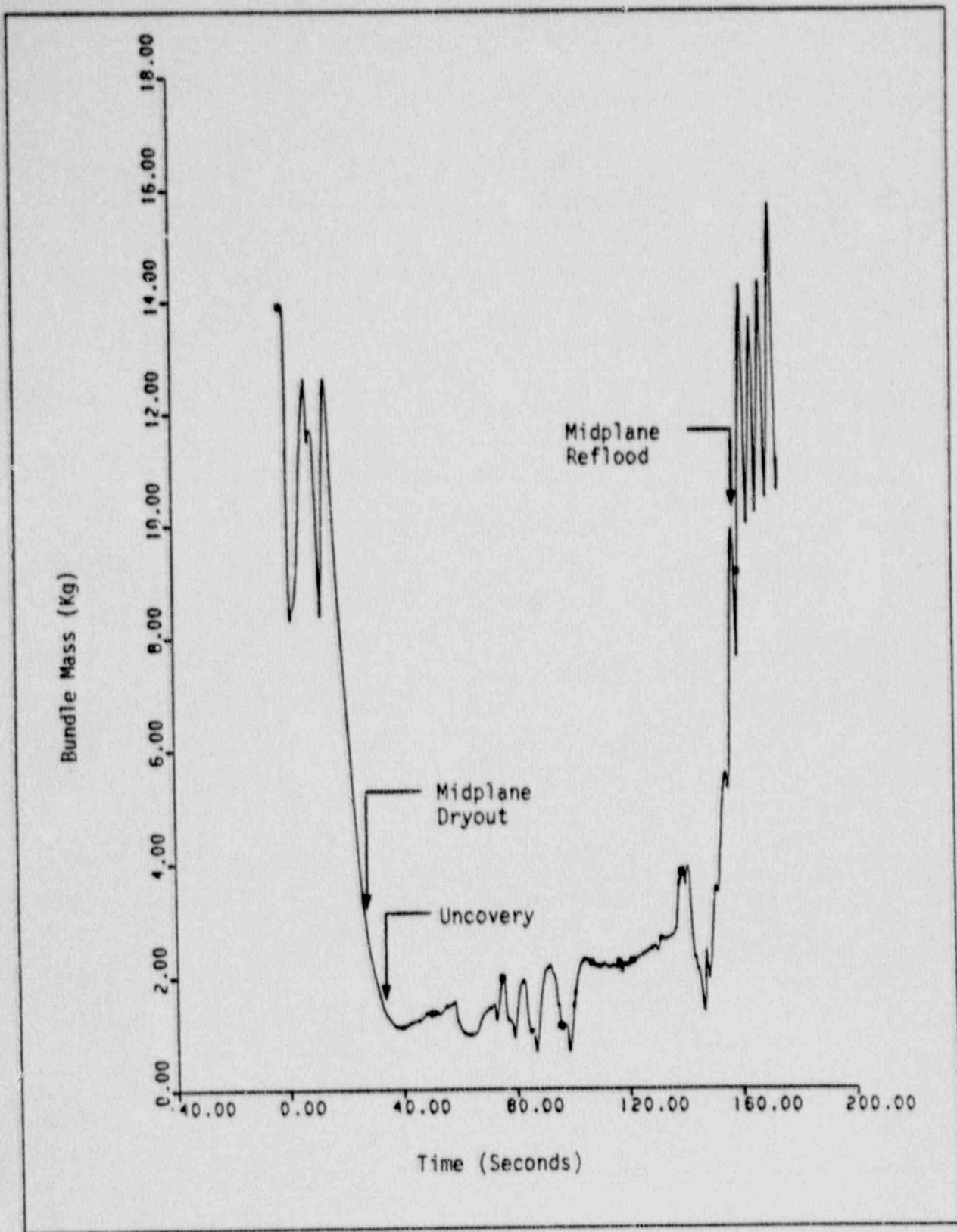
Figure 8.4 - Hot Assembly Mass Inventory for 80 Percent of Full Recirculation Line Break
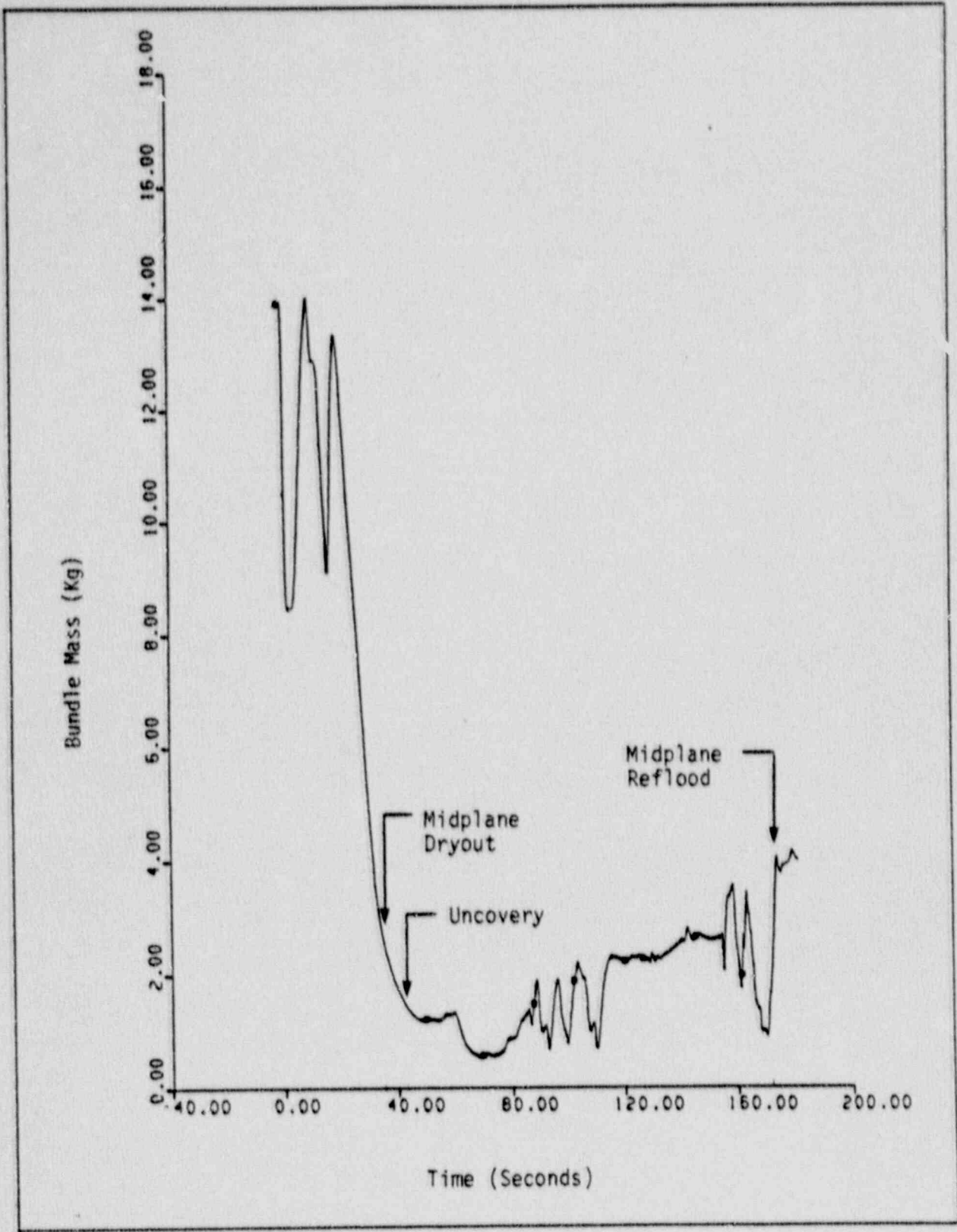
Figure 8.5 - Hot Assembly Mass Inventory for 60 Percent of Full
Recirculation Line Break
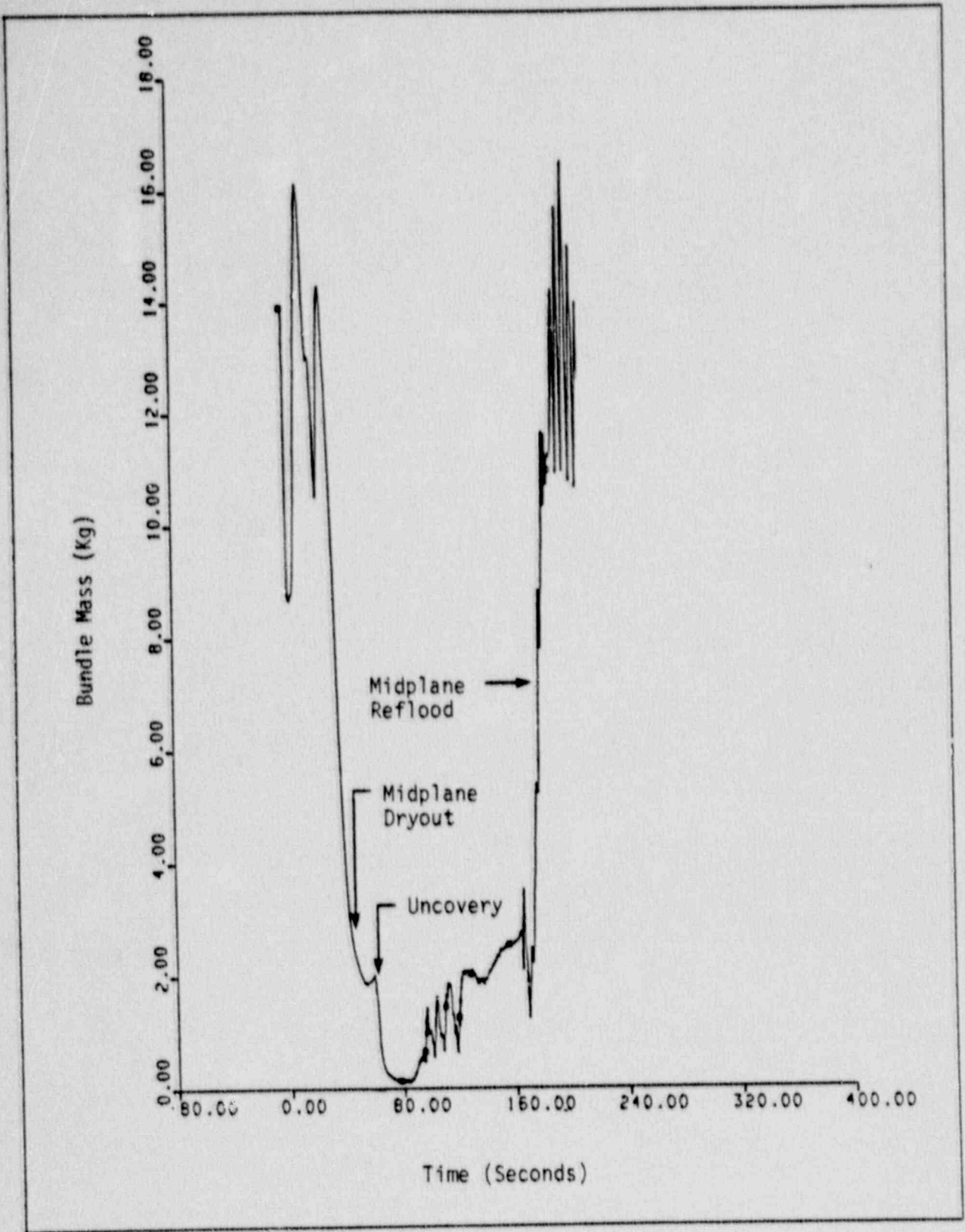
Figure 8.6 - Hot Assembly Mass Inventory for 40 Percent of Full
Recirculation Line Break
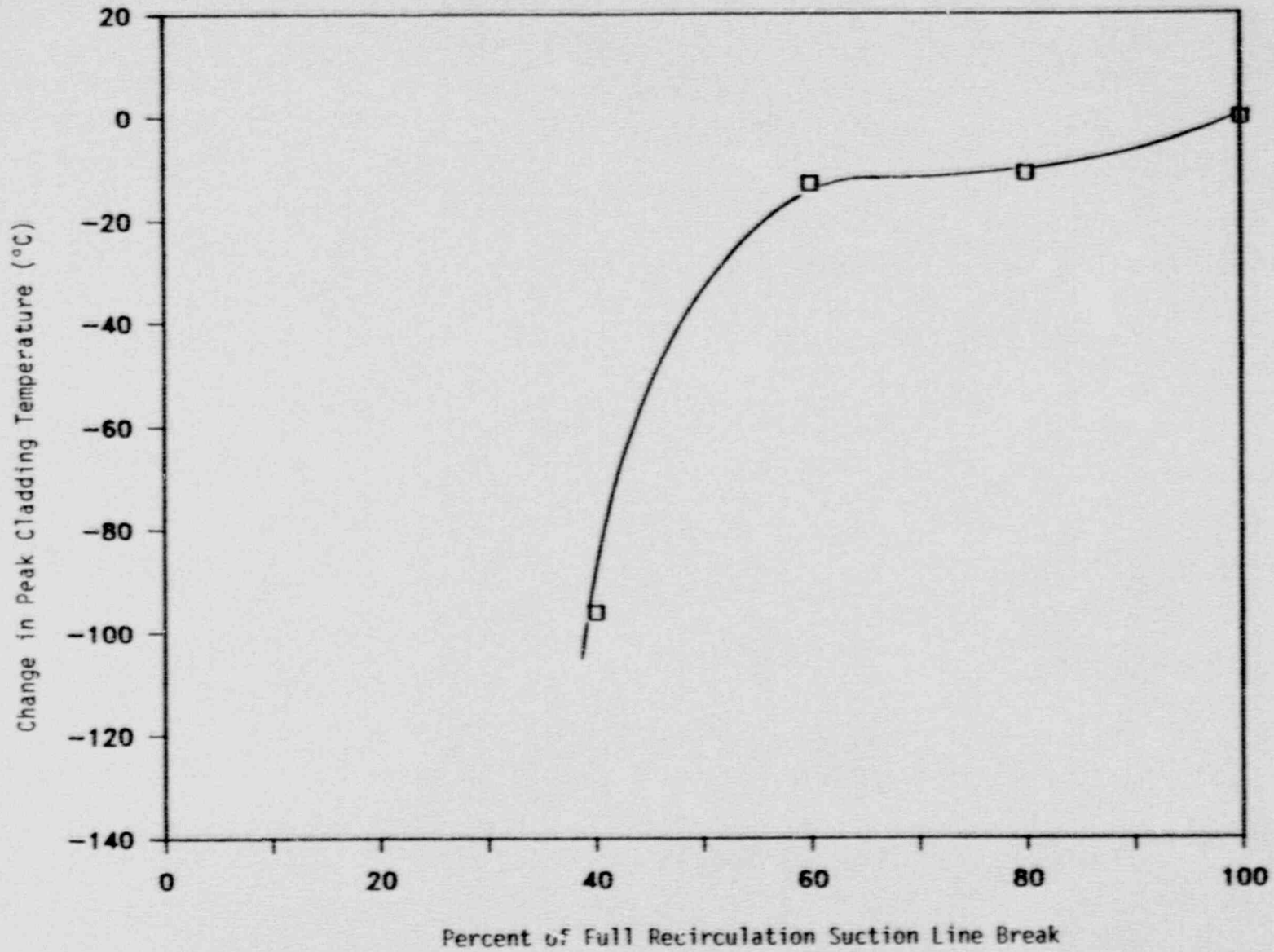
Figure 8.7 - Break Spectrum for Recirculation Suction Line Break with
Failure of the LPCS Diesel Generator
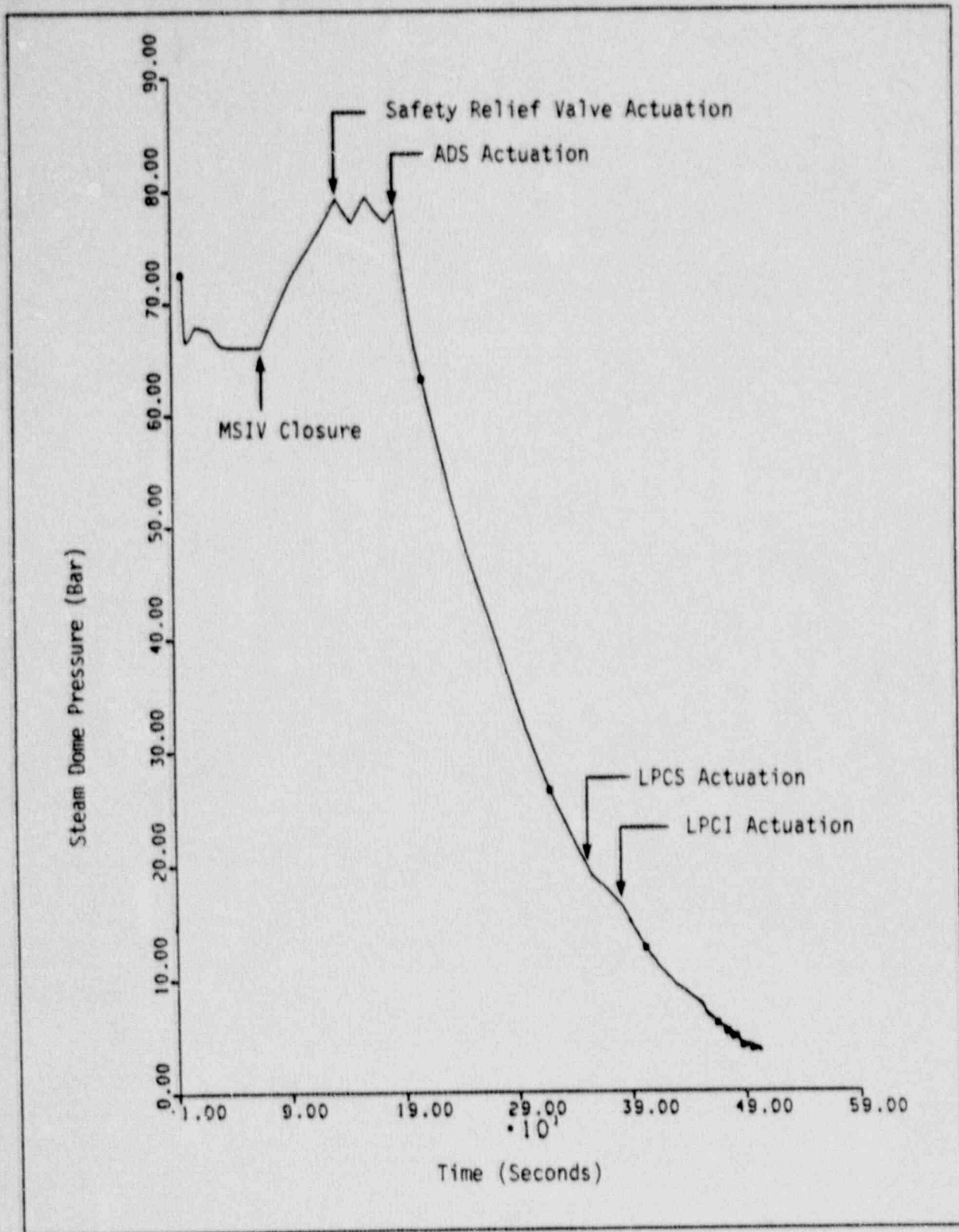
Figure 8.8 - Reactor Steam Dome Pressure for 0.09 ft^2 Recirculation Suction Line Break
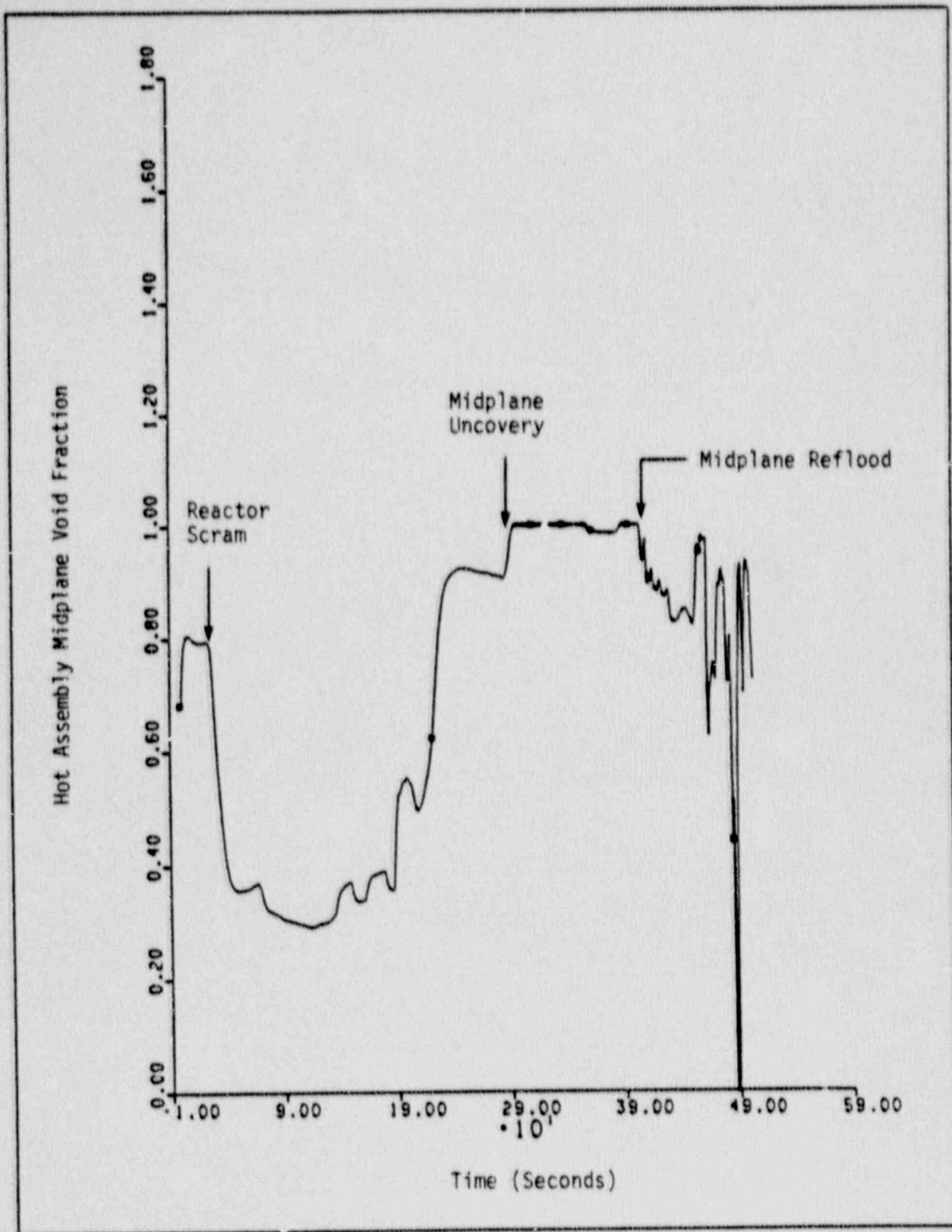
Figure 8.9 - Hot Assembly Midplane Void Fraction for 0.09 ft² Recirculation Suction Line Break
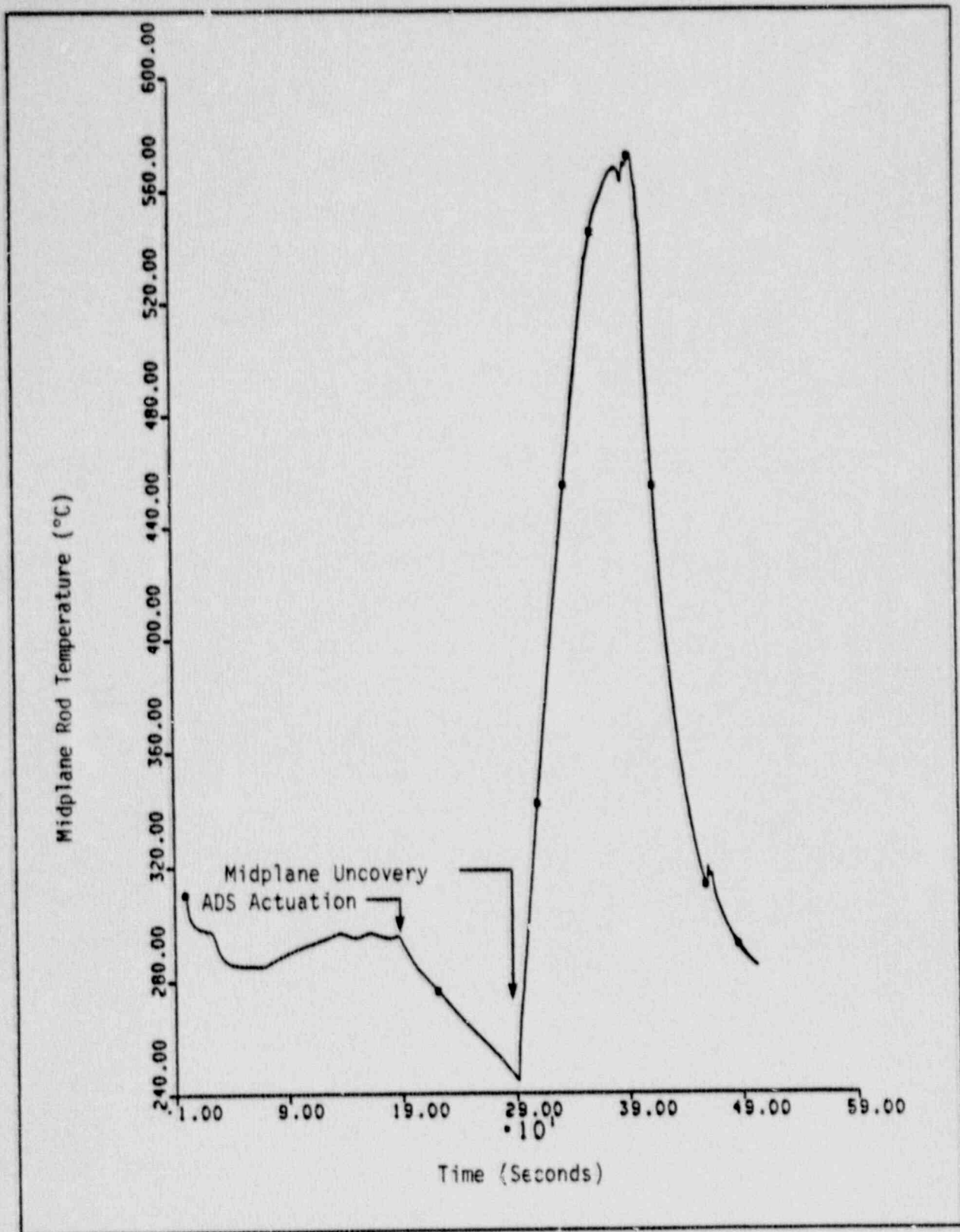
Figure 8.10 - Hot Assembly Midplane Temperature for 0.09 ft^2 Recirculation Suction Line Break
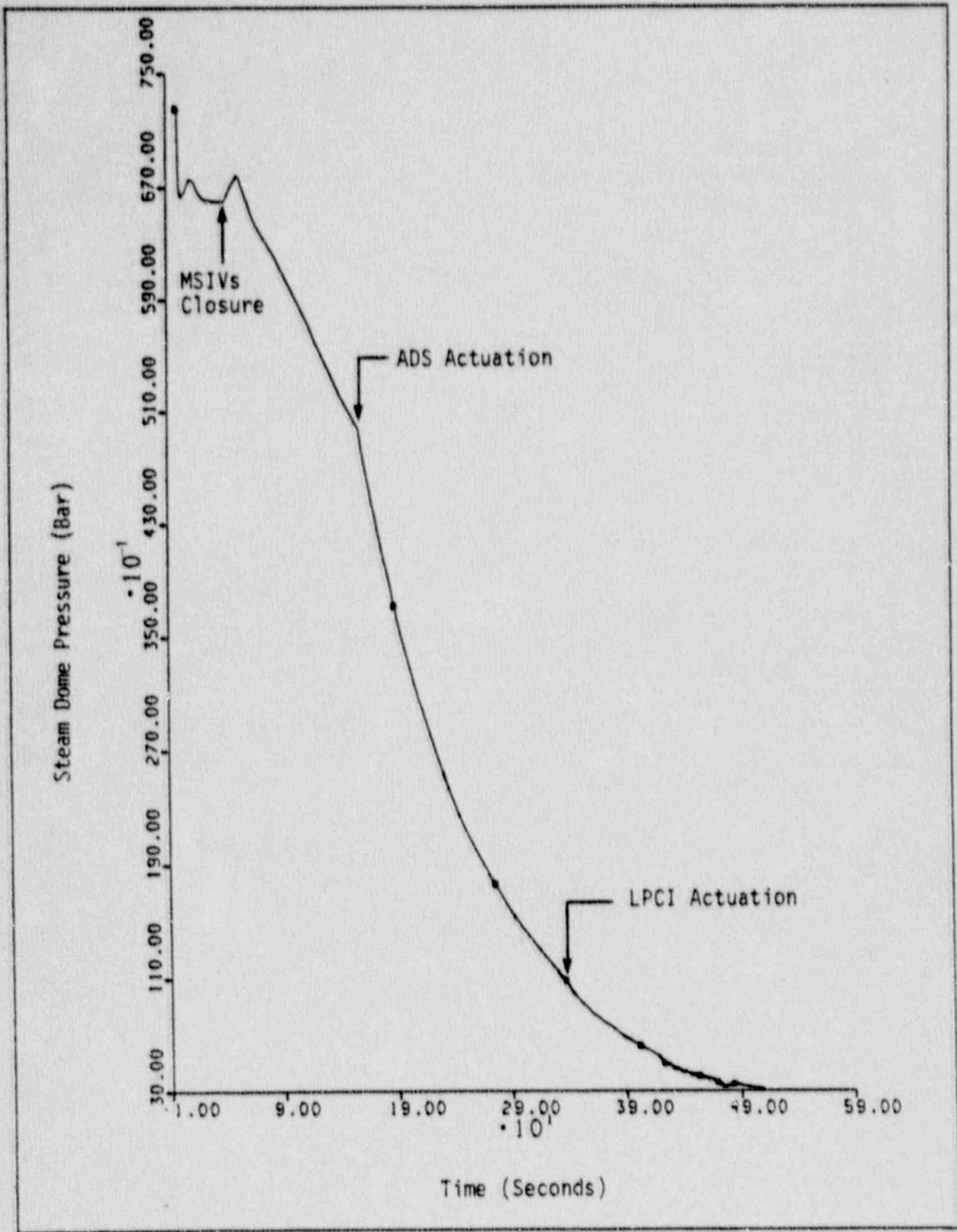
Figure 8.11 - Reactor Steam Dome Pressure for 100 Percent Spray Line Break
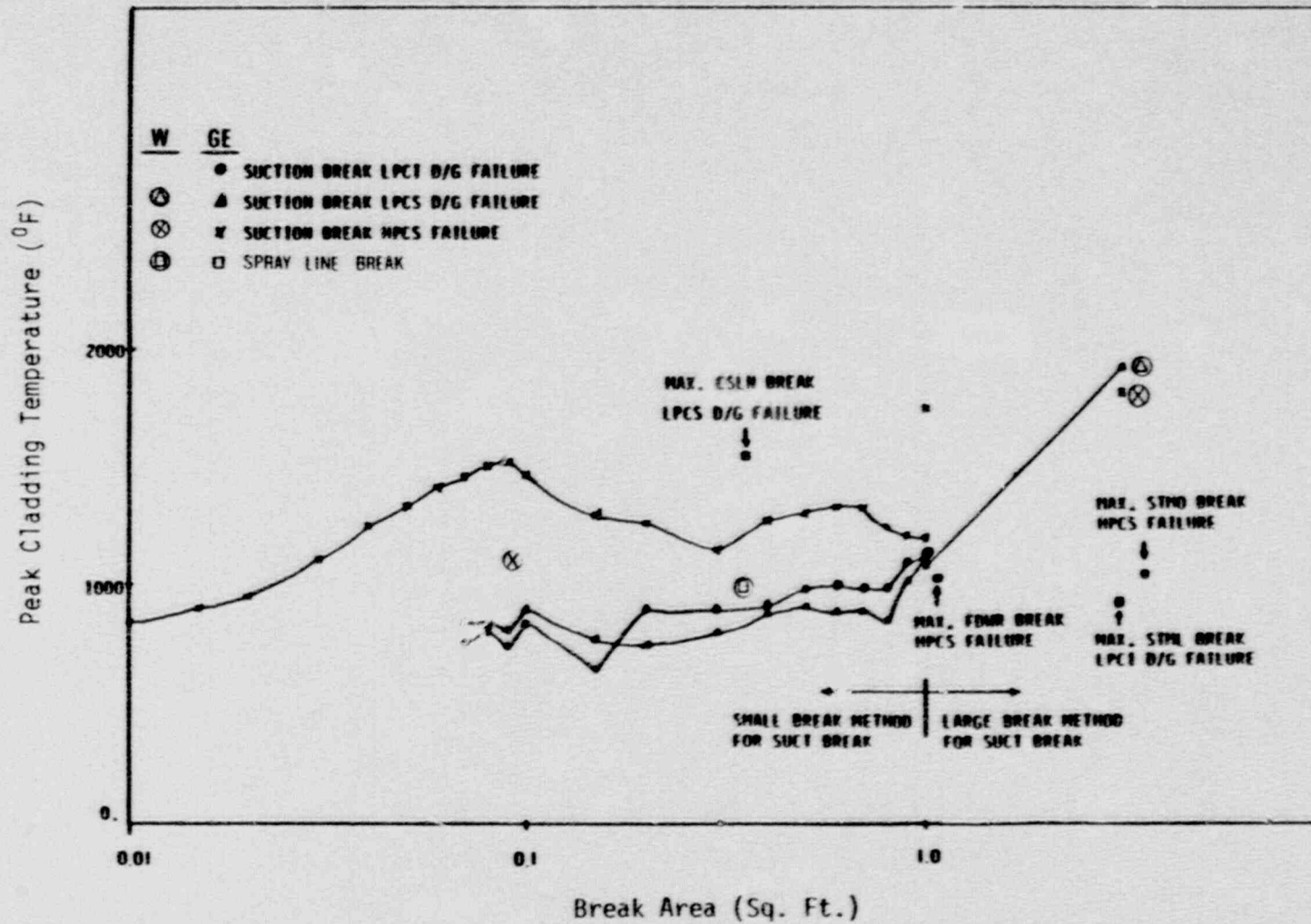
Figure 8.12 - Comparison of Westinghouse BWR LOCA Evaluation Model and
Original FSAR Break Spectrum

9.0 TRANSITION CORE STUDIES

9.1 Methodology Description

When a utility is changing to a new fuel design, the reactor core can have several different fuel designs present. These reload cycles are referred to as mixed, or transition cores. The presence of more than one fuel design requires that two potential LOCA concerns be addressed. These are:

o   Will the presence of a mixed core adversely affect the dryout or reflood time of the various fuel designs?

o   Will one fuel design cause an adverse flow distribution of ECCS water into the other fuel designs?

Individual BWR fuel assemblies are enclosed in fuel channels. The only thermal-hydraulic communication between different fuel assemblies is through the fluid conditions in the upper and lower plenums. If the reactor system response to a LOCA is unchanged for a full core and a mixed core loading, then the individual fuel design MAPLHGR limits will be applicable regardless of the fuel loading.

To determine the effect of the fuel loading, the limiting break from Section 8.2 was analysed using the GOBLIN code, with a full core of General Electric (GE) 8x8 fuel, and again with a mixed core comprised of both Westinghouse QUAD+ and GE 8x8 fuel designs. The key phenomena to be compared are the core inlet flow rate during blowdown, the vessel depressurization rate, and the time of core reflood. The core inlet flow dictates the time of boiling transition and uncovery. The vessel depressurization rate determines the time at which spray flow is initiated. Finally, the reflood time determines the time at which the fuel rod heat-up is terminated.

If the mixed core analysis shows an adverse impact on one of the key phenomena, the change in the peak cladding temperature and cladding oxidation will be assessed at the current MAPLHGR limits for the fuel type. If the

design acceptance criteria are exceeded, the MAPLHGR limits shall be reduced during transition cores to ensure compliance with the acceptance criteria.

A parallel channel mixed core system analyses is performed to demonstrate that the important thermal-hydraulic response characteristics (described above) of each fuel design are similar, and that one fuel design does not adversely impact the flow of ECC water into the other fuel designs.

9.2 Full Core Analysis

The LOCA system response for a full core of 8x8 and a full core of QUAD+ fuel were compared using the Westinghouse BWR evaluation model. The limiting break, as determined in Section 8, was used for the comparison; specifically, a full double-ended guillotine break of a recirculation suction line with the assumed failure of the LPCS diesel generator (Division I in Figure 3.2).

The GOBLIN nodalization for a full core of 8x8 fuel is shown in Figure 9.1. There are three major noding differences for the 8x8 fuel. These are:

o   GE fuel assemblies have one more spacer grid than QUAD+, hence an additional core node is included.

o   GE fuel assemblies do not have a watercross, so the watercross nodes are eliminated.

o   GE fuel assemblies have an additional leakage path between the region above the lower tieplate and the bypass region. This additional flow path was explicitly modelled.

As stated in the previous section, the key phenomena to examine in this analysis are the core inlet flow rate during initial blowdown, vessel depressurization, and time of midplane reflood. The active core inlet flow transient is shown in Figure 9.2. This figure can be compared with that for a full core of QUAD+ shown in Figure 3.6. Note that the general phenomena are similar. The QUAD+ active core flow is slightly higher before lower plenum

flashing due to the draining of the watercross. The timing of key phenomena for the full core analyses for QUAD+ and 8x8 fuel are shown in Table 9.1 The midplane dryout times are almost the same. The vessel depressurization rate is virtually identical, as shown by the ECC actuation time and the initiation of spray cooling. Finally, the two LOCA simulations reflood the midplane within 7 seconds of each other. The presence of the watercross in QUAD+ helps refill the lower plenum slightly faster for the analysis with a full core of QUAD+.

From this full core comparison, the two fuel designs have very similar LOCA system responses. This is expected since the QUAD+ and 8x8 fuel are designed to have the same pressure drop in steady state operation.

9.3 Mixed Core Analysis

A mixed core LOCA system response analysis was also done to demonstrate that each fuel design does not have an adverse effect on the other fuel design.

A GOBLIN calculation was made with one-third 8x8 fuel and two-thirds QUAD+ fuel. The GOBLIN nodalization is shown in Figure 9.3. The limiting break calculation was repeated. The timing of the initial blowdown phenomena, depressurization and core reflood are shown in Table 9.1. The results follow very closely that for a full core of QUAD+ fuel.

The active core inlet flow for each fuel type in the mixed core analysis is shown in Figures 9.4 and 9.5. Both curves are very similar to the full core analysis results for QUAD + fuel (Figure 3.6).

The calculated flow rates at the top of a QUAD+ and an 8x8 fuel assembly are shown in Figures 9.6 and 9.7, respectively. Both assemblies receive comparable flow rates. One fuel design clearly does not adversely impact (starve) the other assembly from getting ECC water during spray cooling and reflood.

Finally, the potential for uneven flow distribution of ECCS water into the fuel assemblies has been studied by LOCA refill-reflood experiments summarized in Reference 3. These experiments showed that water pooling exists above the core for all BWR designs with internal jet pumps. This insures an even distribution of ECC spray water between all fuel assemblies. Furthermore, the QUAD+ upper assembly and bail handle are designed similar to the 8x8 fuel design to minimize perturbations in the core spray distribution.

9.4 Summary

The calculated LOCA system responses for a full core of QUAD+ fuel, 8x8 fuel, and a mixed core of one-third 8x8 and two-third QUAD+ fuel show very minor changes in the timing of the key phenomena. The presence of QUAD+ fuel in a mixed core actually causes a slightly faster system reflood time than a full core of 8x8 fuel. Hence it is concluded that the introduction of QUAD+ fuel in a transition core with 8x8 fuel will not adversely impact the fuel type specific LOCA MAPLHGR limits determined based on a full core of the respective fuel type.

TABLE 9.1
MIXED CORE ANALYSIS RESULTS

Times (sec)	Full Core QUAD+	Full Core 8x8	Mixed Core QUAD+	Mixed Core 8x8
Jet Pump Uncovery	5.9	6.8	5.9	
Jet Pump Flashing	6.4	6.8	6.4	
Lower Plenum Flashing	9.7	9.0	9.7	
Midplane Dryout*	22.4	23	22.4	22.0
HPCS Actuation	27	27	27	
Initiation of Spray Cooling	48	46	48	
LPCI Actuation	53	53	53	
Core Midplane Reflood*	142	149	143	143

* Average fuel bundle
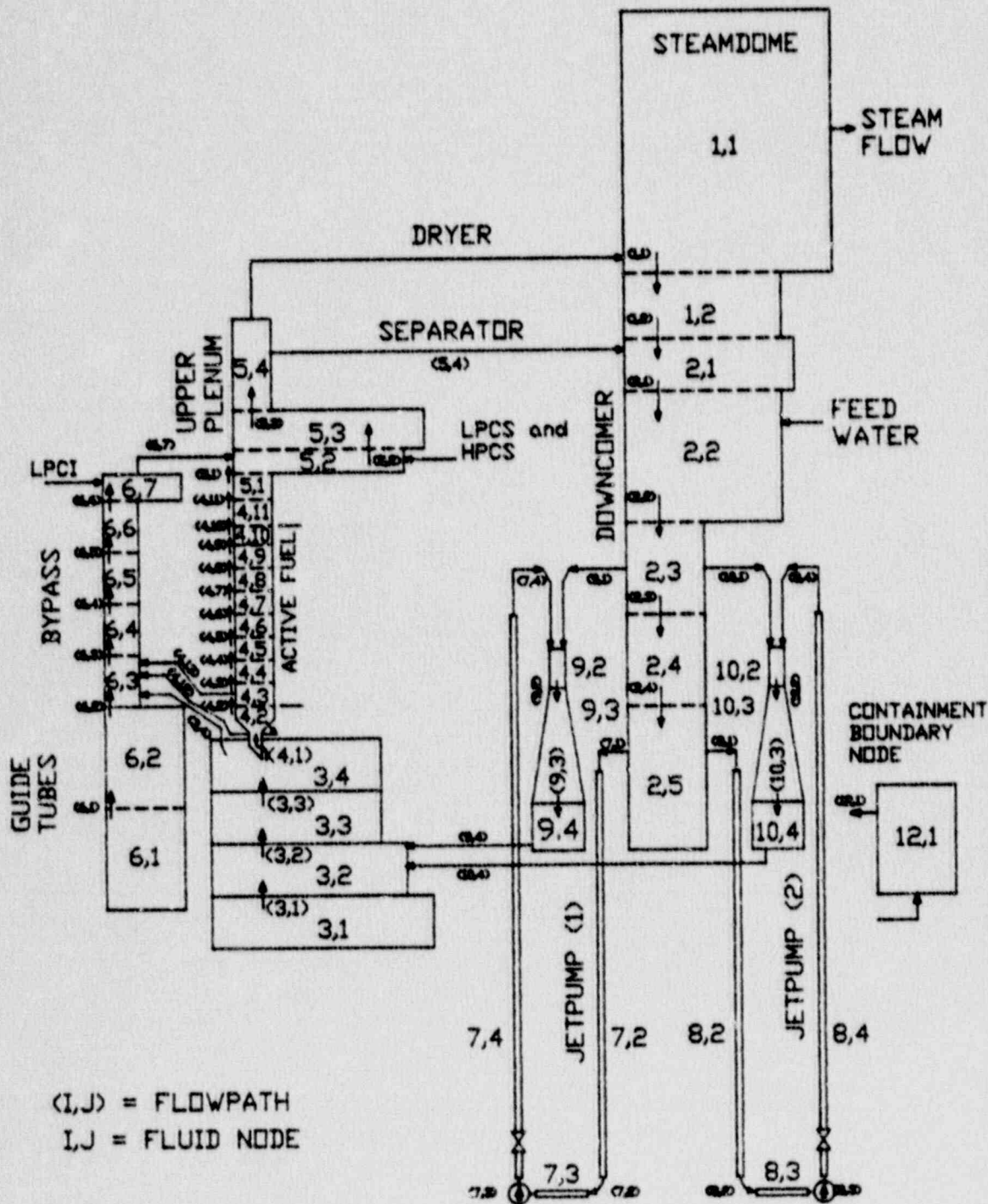
Figure 9.1 - GOBLIN Nodalization for Full Core of GE 8x8 Fuel
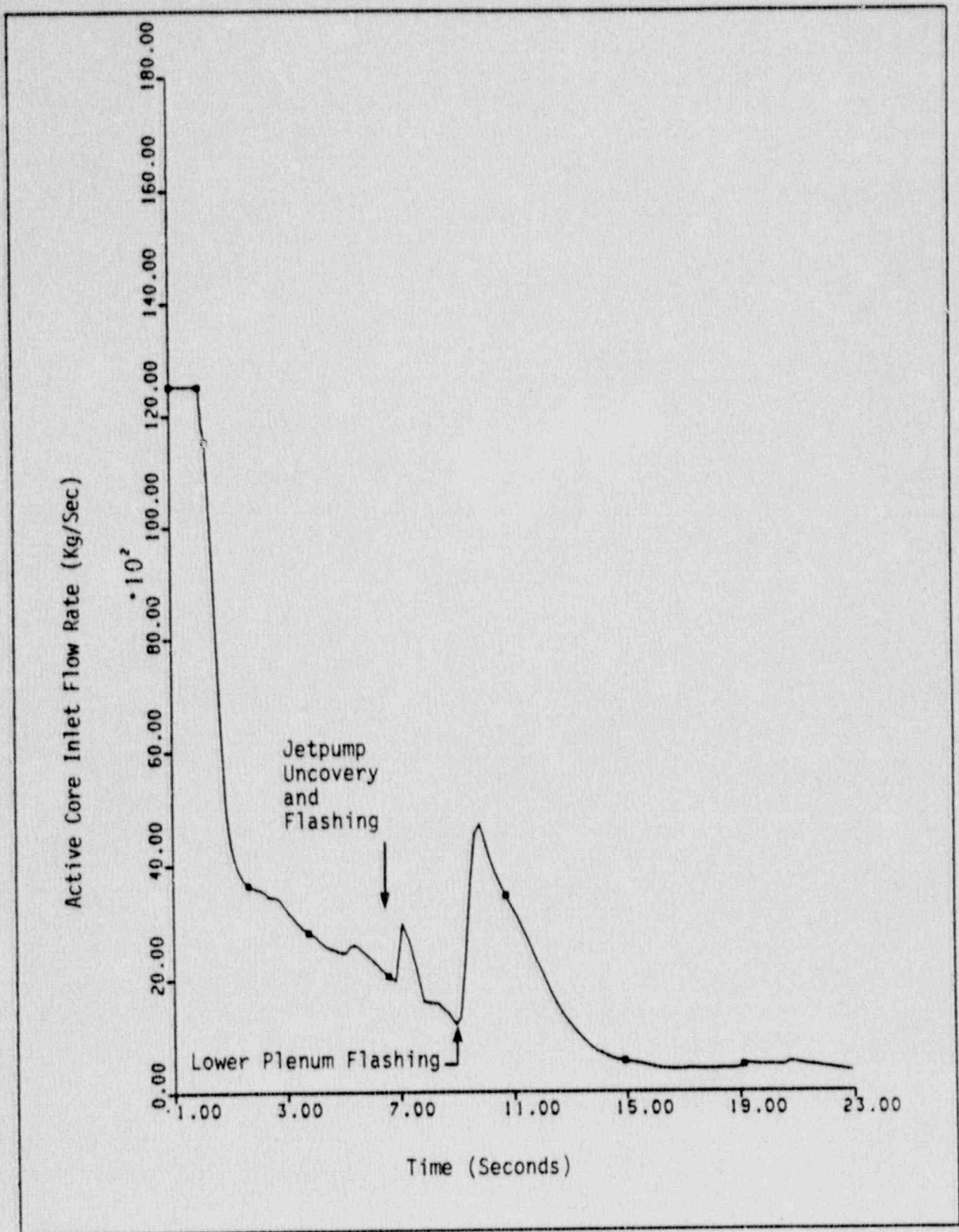
Figure 9.2 - Active Core Inlet Flow for Full Core of 8x8 Fuel
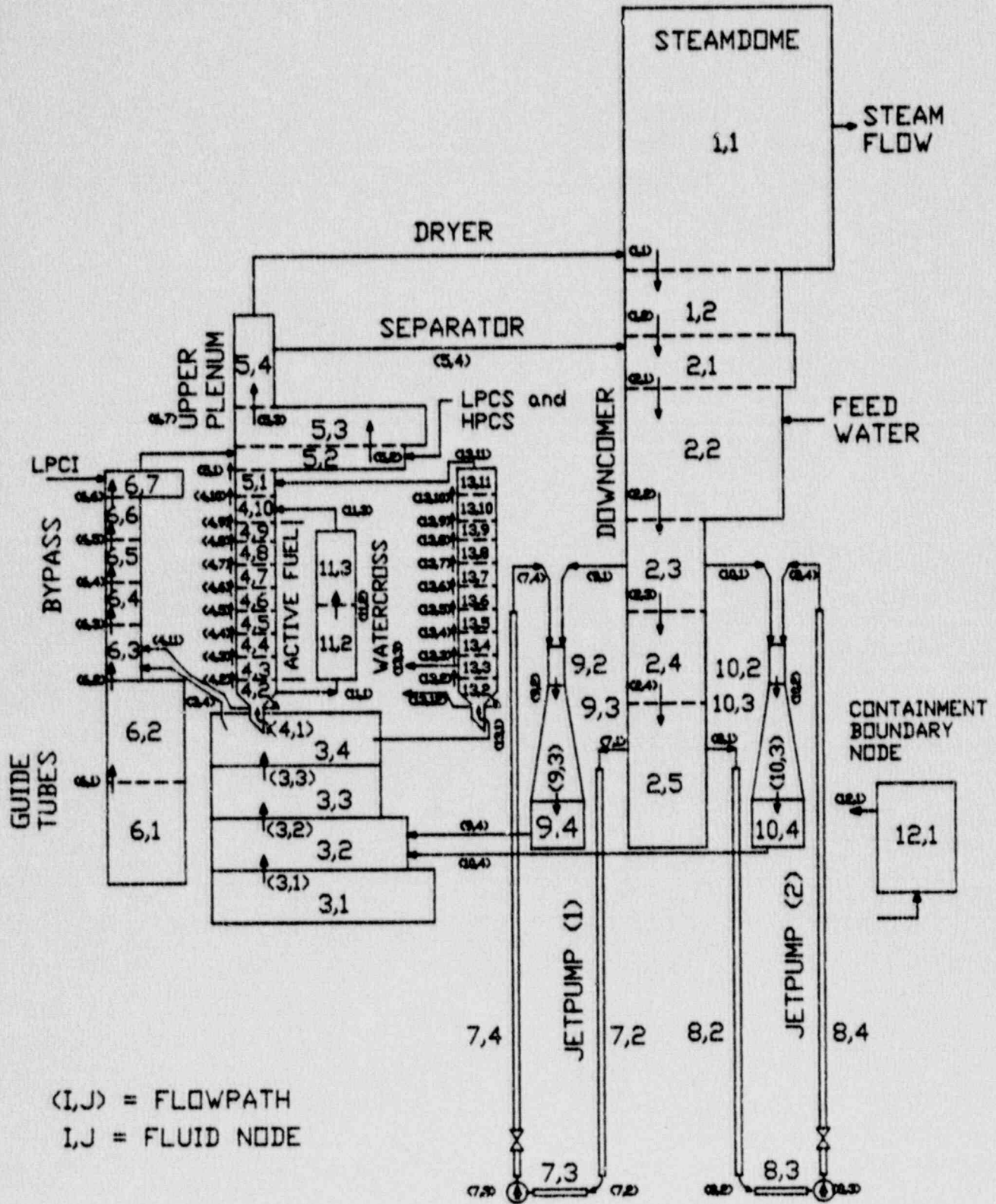
Figure 9.3 - GOBLIN Nodalization for a Mixed Core of GE 8x8 and
    W QUAD+ Fuel
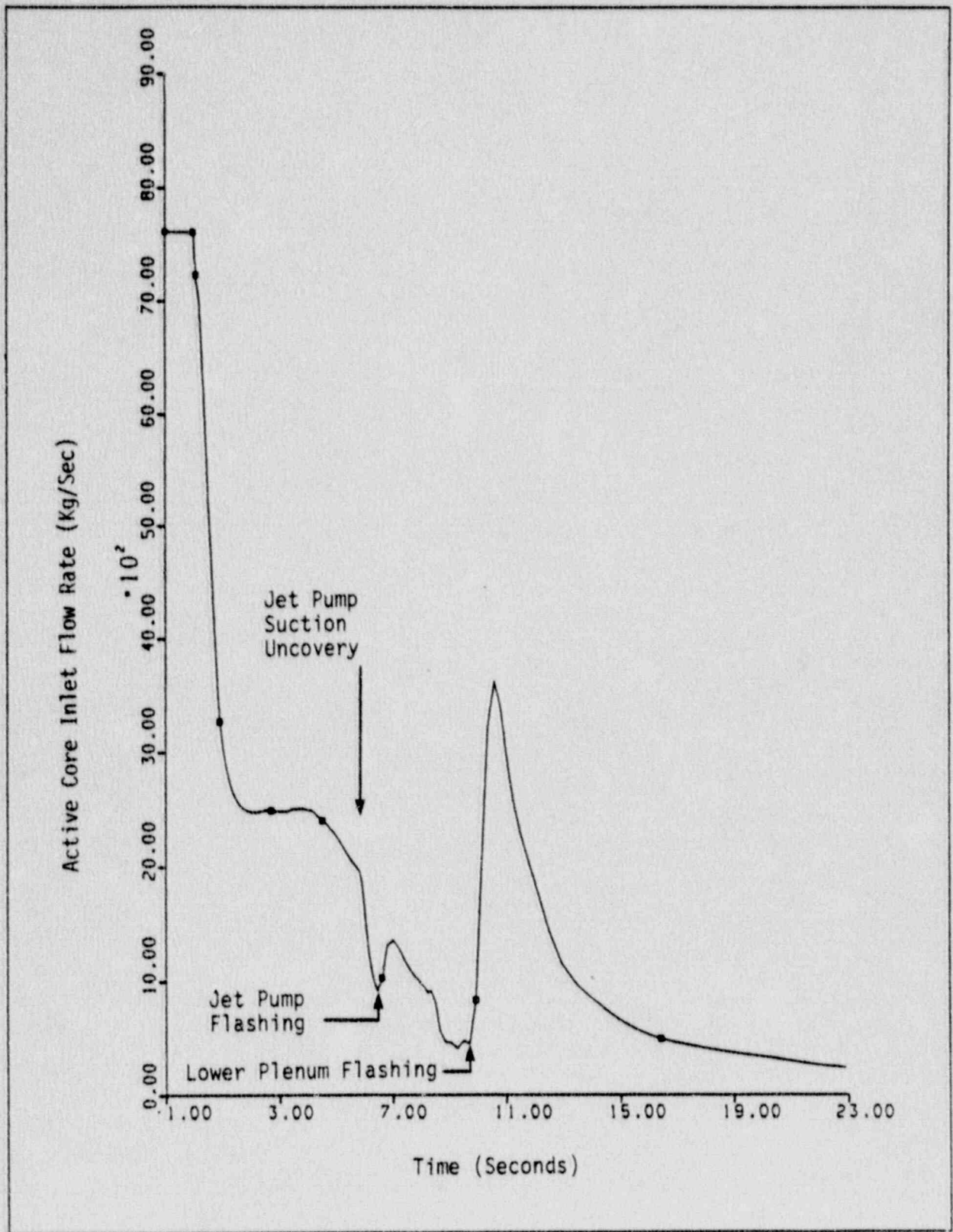
Figure 9.4 - Active Core Inlet Flow Rate of QUAD+ Fuel in Mixed Core
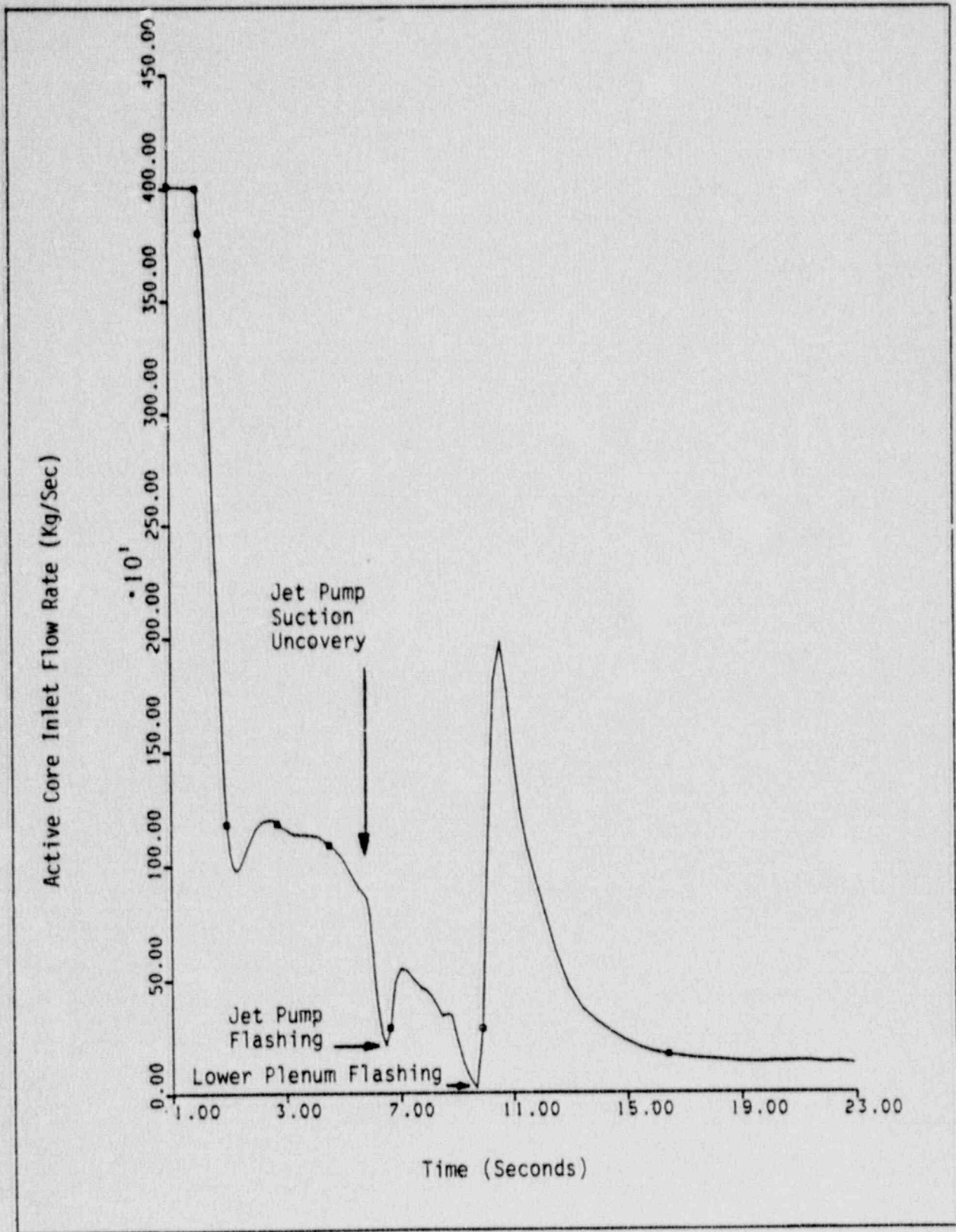
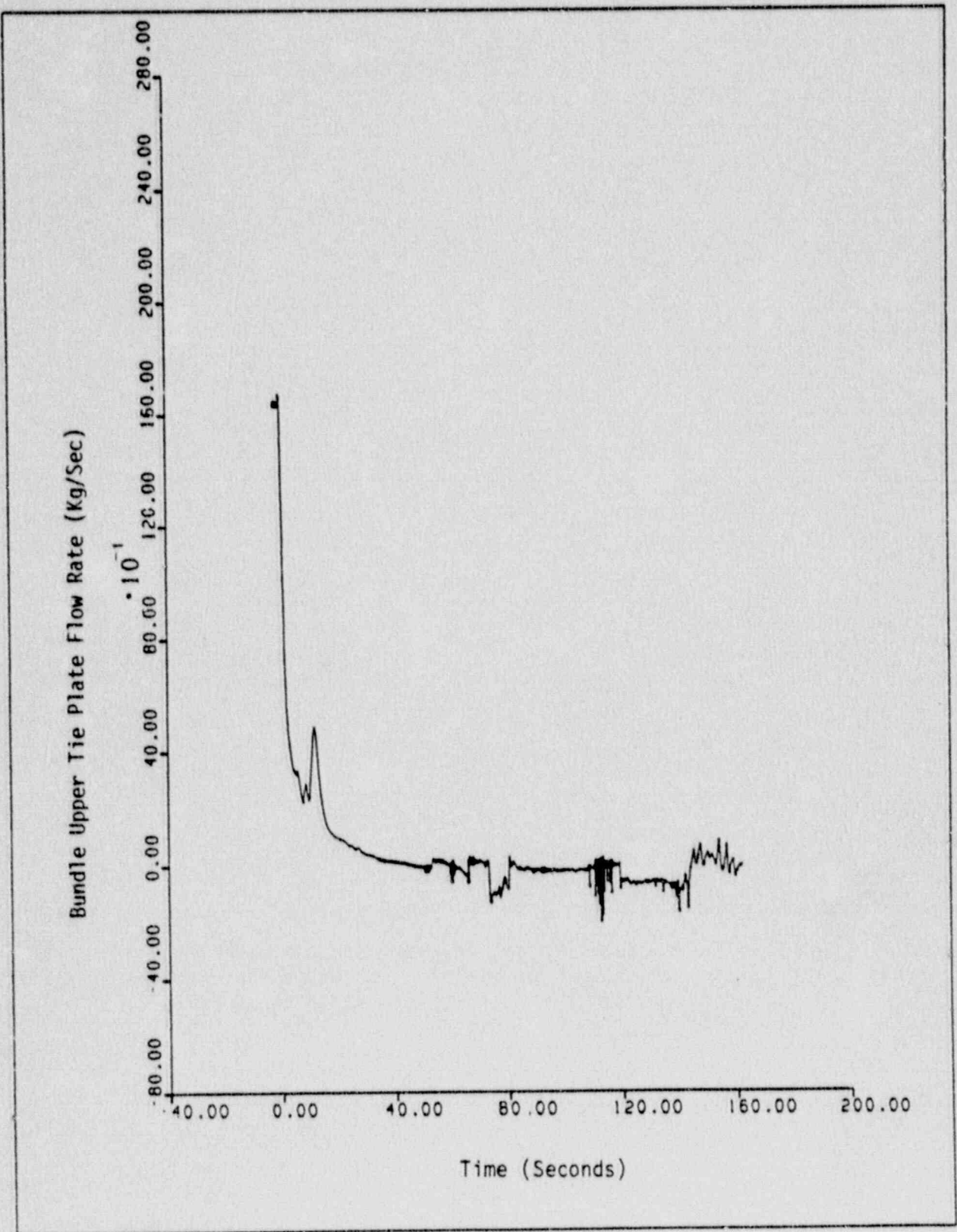Figure 9.5 - Active Core Inlet Flow for 8x8 Fuel in Mixed Core

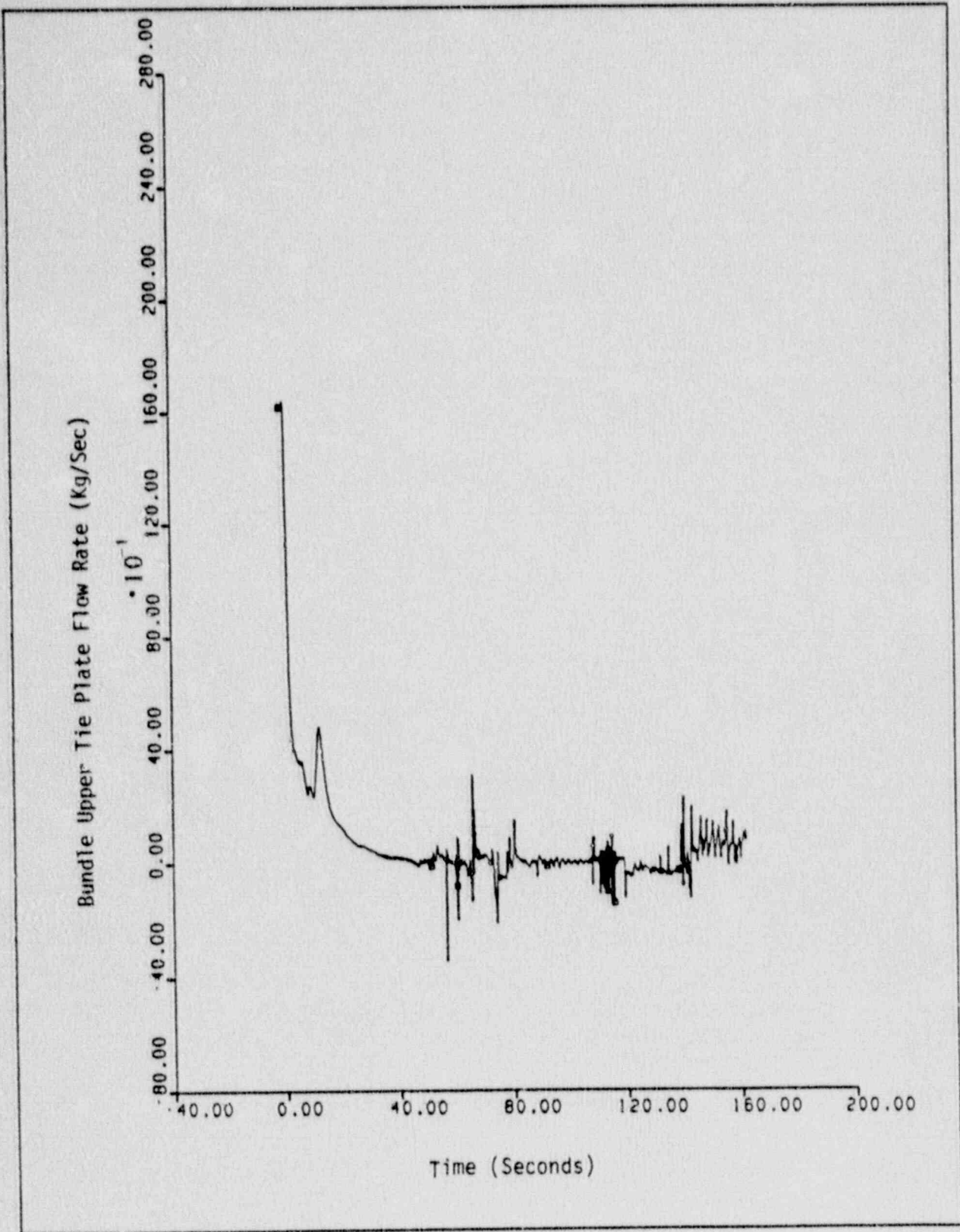Figure 9.6 - Bundle Upper Tie Plate Flow Rate for QUAD+ Fuel in Mixed Core

Figure 9.7 - Bundle Upper Tie Plate Flow Rate for 8x8 Fuel in Mixed Core

10.0 SUMMARY AND CONCLUSION

The Westinghouse approach to performing LOCA sensitivity studies and defining the Appendix K evaluation methodology for boiling water reactors is based on a systematic assessment of the impact of LOCA modelling on calculational results. The Appendix K evaluation model for BWR/5 plant designs has been defined and justified using this methodology. A BWR/5 break spectrum calculation performed with this model has shown the limiting break to be a full double-ended guillotine break of a recirculation suction pipe with the assumed failure of the diesel generator which powers the LPCS system and one LPCI pump. Assuming QUAD+ fuel operating at a MLHGR limit of 14.5 kW/ft, the calculated peak cladding temperature for this break is 1036°C (1897°F), well below the acceptance criterion of 2200°F.

The Westinghouse method for assessing the LOCA impact of using multiple fuel designs in a reload core has also been described. A sample calculation has been performed for a BWR/5 using this mixed core methodology. The results showed no detrimental effect of the mixed core configuration.

Reference 1 and this report together provide the documentation, qualification and justification of the Westinghouse BWR LOCA evaluation model and demonstrates its compliance with Appendix K requirements. The method for application of this fuel reload calculations in compliance with the 10CFR50.46 acceptance criteria is described in Section 5.6 of Reference 4. Taken together, these three reports provide the documentation necessary to obtain approval for use of the Westinghouse BWR LOCA evaluation model in BWR reload licensing applications.

11. References

1. "Westinghouse Boiling Water Reactor Emergency Core Cooling System Evaluation Model: Code Description and Qualification," WCAP-11284 (Proprietary) September 1986.

2. Code of Federal Regulations 10 Part 50, Federal Register, 1974.

3. G. Dix, "BWR Loss of Coolant Technology Review," International Topical Meeting on Nuclear Reactor Thermal-Hydraulics (ANS), Santa Barbara, CA, USA, Jan. 11, 1983.

4. "Westinghouse Reference Safety Report for BWR Fuel," WCAP-11500 (Proprietory) June 1987.

Addendum to

Westinghouse Boiling Water Reactor Emergency
Core Cooling System Evaluation Model:
Code Sensitivity

The following are responses to twelve questions pertaining to the review Westinghouse Topical Reports WCAP-11284 and WCAP-11427. The topical reports are refer to here in as:

Ref. 1: Westinghouse Boiling Water Reactor Emergency Core Cooling System
        Evaluation Model: Code Description and Qualification, WCAP-11284,
        September 30, 1986, and
Ref. 2: Westinghouse Boiling Water Reactor Emergency Core Cooling System
        Evaluation Model: Code Sensitivity, WCAP-11427, June 30, 1987

Question 1

Page 4-27, Ref. 1. The use of a lower surface emissivity would result in a higher peak clad temperature in the DBA when radiation heat transfer becomes significant. Discuss the conservatism of the input values of 0.67 [dry surface] and 0.96 [wet surface], taking into consideration the oxide layer buildup.

Response

Dry surface emissivity - The dry surface value of 0.67 is conservative, based on comparisons with the model described in Reference (1-1) below. This model, based on data reported in References (1-2) through (1-4), gives

$$\varepsilon = 0.325 + 0.1246 \times 10^6 d \text{ for } d < 3.88 \times 10^{-6} m$$

$$\varepsilon = 0.808642 - 50.0d \qquad \text{for } d \geq 3.88 \times 10^{-6} m$$

where d is the oxide layer thickness in meters. The best-estimate for the standard error of the model prediction is quoted as ± 0.1.

CHACHA-3C uses the best-estimate oxide thickness correlation described in Appendix A of Reference (1-5) to obtain the initial cladding oxide thickness for each rod being analyzed. Expressed as a function of local burnup, this correlation gives:

$$\Delta r_{oxide} = \left[\qquad\qquad\qquad \right]^{a,c}$$

where the oxide thickness is in μm and the local burnup, BU, is in GWD/MTU. Examination of the above equations shows that incorporating the Reference (1-1) emissivity correlation in CHACHA-3C would give emissivities in excess of 0.67 for all local burnups greater than[   ]^{a,c} For burnups below[   ]^{a,c} an oxide layer quickly builds up due to zirc-water reaction. Use of the Reference (1-1) correlation for these cases would show that the emissivity would increase rapidly and exceed 0.67 by the time the clad temperatures reach the level at which radiation heat transfer becomes significant. A review of CHACHA-3C analyses performed at low burnups shows that use of the Reference (1-1) correlation would result in emissivities in excess of 0.67 by the time the cladding temperature reaches 1700°F.

The dry surface value of 0.67 is also conservative relative to the correlation given in Equation 4.8-16 of Ref. 1. This correlation, based on Reference (1-6), gives

$$\varepsilon = \left[\hspace{8cm} \right]^{a,c}$$

where T is the Zircaloy temperature in °R. Use of this correlation gives emissivities in excess of 0.67 for Zircaloy temperatures above[   ]^{a,c}.

Wet surface emissivity - The wet surface value of 0.95 is consistent with Table D-3 of Reference (1-7), which quotes emissivities of 0.95 - 0.97 for water films.

References

(1-1)   "MATPRO Version 11: A Handbook of Materials Properties for Use in the Analysis of Light Water Reactor Fuel Rod Behavior," NUREG/CR-0497, 1979.

(1-2)   E. F. Juenke and L. H. Sjodahl, "Physical and Mechanical Properties: Emittance Measurements," GEMP-1008, pp. 239-242, 1968.

(1-3)   E. V. Murphy and F. Havelock, "Emissivity of Zirconium Alloys in Air in the Temperature Range 100-400°C," Journal of Nuclear Materials, Vol. 60, pp. 167-176.

(1-4)   T. B. Burgoyne and A. Garlick, OECD-CSNI Meeting on the Behavior of Water Reactor Fuel Elements Under Accident Conditions, Spinad, Norway, September 13-16, 1976.

(1-5)   "Westinghouse Reference Safety Report for BWR Fuel," WCAP-11500 (Proprietary), August 1987.

(1-6)   J. F. White, et al., Eighth Annual Report, "AEC Fuels and Materials Development Program," GEMP-1012, Pt. II, 1969.

(1-7)   J. A. Adams and D. F. Rogers, "Computer Aided Heat Transfer Analysis," McGraw-Hill, 1973.

Question 2

Page 5-6, Ref. 1. What is the assumed fraction of the locally generated gamma energy that is deposited in the fuel and cladding? This fraction needs to be justified if not unity.

Response

The Westinghouse LOCA evaluation model assumes that the total gamma energy deposition fraction outside of the fuel rod is 2% of the total power generation. Evaluations have been performed which show this energy is partitioned as follows:

Active Channel Steam Fraction	Channel/ Watercross	Active Channel Coolant	Outer Water Gaps	Coolant in Watercross
0.40	0.8%	0.6%	0.4%	0.2%
0.70	0.9%	0.4%	0.5%	0.2%
1.00	1.1%	0.1%	0.6%	0.2%

This table is applicable for unrodded conditions. Control rod insertion would reduce each of these values.

The evaluation model fuel rod heatup calculations (CHACHA-3C) assume 96% of the total power generation occurs in the pellets until 0.1 second after the break. After that time, 98% of the total power generation is assumed to occur in the pellets. This modelling is based on the conservative assumption that the neutron moderation energy (initially taken as 2%) goes to zero within 0.1 seconds. The CHACHA-3C calculation also assumes gamma energy deposition of 1.5% of the total power generation occurs within the channel/watercross structure throughout the transient, which bounds the above values for all steam fractions.

Two CHACHA-3C sensitivity studies were performed to investigate the impact of the energy deposition fractions on PCT. In the first, the increase in pellet power generation from 96% to 98% of the total generation was delayed until 1 second after the break. This corresponds to the time at which the fission power has decreased to approximately half of the initial fission power, and is a more realistic approximation of the pellet power generation behavior. The power generation in the channel/watercross was also reduced to 1.1%, consistent with the maximum value under rodded or unrodded conditions. These changes reduced PCT by [ ]^{a,c}, which is considered to be a negligible change.

The second sensitivity study reduced the reference case pellet power generation by 1% and added this power generation to the cladding. The result was a decrease in PCT of [ ]^{a,c}. This result demonstrates that it is more conservative to model the fuel rod power generation as occurring entirely in the pellet, rather than partitioning the energy to the pellet and cladding to account for gamma energy deposition in the cladding.

Based on the above discussion it is concluded that the treatment of energy deposition fractions in the evaluation model is slightly conservative. The sensitivity of PCT to the gamma energy deposition treatment is seen to be small.

Question 3

Page 3-7, Ref. 2. Provide additional discussion of the determination of the maximum oxidation fraction of 0.031 in the CHACHA-3C reference transient calculation. What percent of fuel rods is assumed to be perforated in the DBA analysis? Discuss the effect of water blockage from perforated rods on PCT.

Response

The Westinghouse LOCA evaluation model uses the maximum circumferential strain versus hoop stress relation shown on page 7-161 of Reference (3-1) to calculate the maximum oxidation fraction. This relation gives a maximum circumferential strain of 0.39 for cladding hoop stresses below 1500 psi and a maximum circumferential strain of 0.31 for hoop stresses in excess of 1500 psi. For the reference transient in Ref. 2, the cladding hoop stress exceeds 1500 psi (1.03×10^7 Pa). (See Figure 7-5 in the response to Question 7). The initial cold cladding thickness is 29 mils. The strained cladding thickness for use in the maximum oxidation thickness is therefore

$$29 \text{ mils}/1.31 = 22.1 \text{ mils}$$

The final oxide thicknesses for the reference transient are 0.47 mils for the outer surface and 0.27 mils for the inner surface. The maximum oxidation fraction is then

$$\frac{0.47 \text{ mils} + 0.27 \text{ mils}}{22.1 \text{ mils}} = 0.033$$

All of the fuel rods in the hot minibundle were calculated to perforate in the DBA analysis presented in Ref. 2. This analysis used an average planar burnup of 22 GWD/MTU. At this burnup the rod internal pressures are sufficiently high that the final cladding strains are 0.15 for inner rods and 0.105 for outer rods (See Figure 4-8 of Ref. 1). The resulting blockage fraction is calculated as follows:

$$\text{Nominal flow area} = 3.877 \text{ in}^2 \text{ per minibundle}$$

Nominal clad outer radius = 0.2288 in

$$\text{Blocked flow area} = 4\pi (1.15 \times 0.2288 \text{ in})^2 + 12\pi (1.105 \times 0.2288 \text{ in})^2$$
$$- 16\pi (0.2288 \text{ in})^2 = 0.648 \text{ in}^2$$

Blockage fraction = 0.648/3.877 = 0.17

The maximum blockage fraction may be calculated assuming fresh fuel with all rods perforated. (Low burnup calculations have shown that not all rods perforate in the hot mini-bundle. However, this assumption is made to quantify the maximum possible blockage.) With fresh fuel the final cladding strains are 0.23 for inner rods and 0.16 for outer rods. The resulting blockage fraction would be 0.26.

Several investigators have examined the impact of flow blockage on heat transfer under conditions representative of a BWR LOCA. In BWR-FLECHT test Zr-2, a full-scale simulated 7 x 7 fuel bundle was used to determine the effect of rod swelling, rod burst and the resulting flow area blockage on PCT under top spray cooling conditions (Reference (3-2)). The results indicated that "the effectiveness of the BWR ECCS core spray will not be significantly impaired by even very substantial flow area reduction at the worst elevation" (p. III-13 of Reference (3-1)). General Electric estimated the total bundle blockage fraction in that test to be 0.29 to 0.33 (p. I-86 of Reference (3-1)), with local blockages of up to 50 percent. With a nominal test bundle flow area of 15.6 in.^{2}, this corresponds to an effective flow area of 11.1 in.^{2} or less. This bounds the minimum effective flow area of a QUAD+ assembly, which is $4(1-0.26)(3.877 \text{ in}^2) = 11.5 \text{ in.}^2$ assuming a fresh assembly with all rods burst.

General Electric also has evaluated the impact of flow blockage on BWR LOCA heat transfer during bottom flooding (p. III-14 of Reference (3-1)). Their conclusion was that "the effectiveness of the bottom-flooding mode of ECCS cooling will not be significantly affected by flow area reductions

considerably larger than these expected in an actual LOCA. These investigations have indicated that the bundle-wide flow area reduction would need to be in excess of approximately 90 percent before the bottom-flooding method would be impaired."

Kraftwerk Union has investigated the impact of up to 70 percent flow blockage on heat transfer under spray cooling conditions. The results of these tests indicated a slight reduction in PCT relative to a nominal (no blockage) experiment (Reference (3-3)).

Based on the experiments and evaluations described above, it is concluded that no flow blockage penalty is required for QUAD+ LOCA analyses in which rod bursts are calculated to occur.

References

(3-1)   "General Electric Company Analytical Model for Loss-of-Coolant Analysis in Accordance with 10CFR50 Appendix K. Volumes I-III," NEDO-20566, January 1976.

(3-2)   J. D. Dunlon and J. E. Leonard, "Thermal Response and Cladding Performance of an Internally Pressurized, Zircaloy-Clad, Simulated BWR Fuel Bundle Cooled by Spray Under Loss-of-Coolant Conditions," GEAP-13112, April 1971.

(3-3)   H. Schweickert, "Final Report - Emergency Cooling Program, Low Pressure Tests. Blocked Cooling Channels with BWR Configuration (Translation)," Project BMFT-RS-194, Kraftwerk Union Reaktortechnik, October 1978.

Question 4

Pages 6-2 and 6-8, Ref. 2. Provide the following information related to the determination of the limiting power shape for use in the DBA analysis:

a. Identify the physical location of the dryout and uncovery times in Table 6.2.

Response

The dryout and uncovery times in Table 6.2 of Ref. 2 correspond to the peak power elevation. This elevation is presented in the table under the heading "Location of Axial Peak".

b. Discuss why Case 2 is not included in the PCT calculation; Case 2 dries out and uncovers sooner than Case 4.

Response

Cases 2 and 5 both used peaked-to-top power shapes. The peak power elevation was found to dry out and uncover slightly earlier in Case 5 than in Case 2. Since both cases had the same initial stored energy at the peak power elevation (axial peaking factor times bundle relative power equals constant), this implies that he Case 5 PCT would bound the Case 2 PCT. Therefore, only Case 5 was evaluated with CHACHA-3C.

c. Provide bases for selecting the axial peaking factor/bundle relative power ratios of 1.63/1.47 and 1.50/1.60. Were any other combinations considered?

Response

During steady state operation, axial peaking factors for a BWR/5 can normally be expected to be no higher than 1.5 to 1.6. A bundle relative power of 1.40 is also a realistic upper limit. Axial and radial power distributions for typical QUAD+ 24-month cycle BWR/5 transition and equilibrium cycle cores are

presented in Section 3.5.2 of Reference (4-1). These distributions confirm that the peaking factors used in the LOCA power distribution study can be considered as reasonable upper bound values.

Note that it is necessary to use large axial peaking factors and bundle relative powers to achieve the 14.5 kw/ft MLHGR assumed in the LOCA analysis. Comparisons of Case 1 versus Case 4, and Case 2 versus Case 5, show that the cases with the higher bundle relative power are slightly more limiting (earlier dryout and uncovery). These cases used a bundle relative power of 1.60, which clearly bounds the values reported in Section 3.5.2 of Reference (4-1). Therefore it is concluded that the axial peaking factor/bundle relative power combination of 1.50/1.60 is more limiting than the other bounding relative power combination and combinations which would actually occur during operation of a BWR/5.

d. Five cases were studied for various axial peaking factor/bundle power combinations. Discuss why the case of 1.63/1.47 with peaked-to-bottom power is left out of the sensitivity study.

Response

Comparisons of the five cases shown in Table 6.2 of Ref. 2 support the following conclusions:

-   Dryout and uncovery times are delayed as the peak plane is moved downward in the bundle (Case 1 versus Case 2, and Case 3 versus Case 4 versus Case 5).

-   Given the same location of the peak power plane, the axial peaking factor/bundle relative power combination of 1.63/1.47 is less limiting (later dryout and uncovery) than the 1.50/1.60 combination (Case 1 versus Case 4, and Case 2 versus Case 5).

From these conclusions it is apparent that the case of 1.63/1.47 with peaked-to-bottom power would be less limiting than the five cases in Table 6.2. Therefore this case was not analyzed.

e. Complete the PCT data tabulation in Table 6.2 to support the statement, "The results are seen to be relatively insensitive to the power distribution."

Response

CHACHA-3C analyses of Cases 1 and 3 have been performed to augment the information provided in Table 6.2 of Ref. 2. Using a reflood time of 142 sec, the Case 1 PCT was [   ].^{a,c} A PCT of [   ] was calculated for Case 3, using a reflood time of [   ] sec. These results confirm that, for the small changes in dryout, uncovery and reflood time observed in the power distribution sensitivity study, the impact on PCT is relatively small.

Peaked-to-top power shapes in a BWR are indicative of some degree of control rod insertion. Under these conditions, the peak LHGR is typically well below the 14.5 kw/ft MLHGR assumed in the LOCA analysis. Figures 3-28 through 3-41 of Reference (4-1) show typical QUAD+ axial power shapes throughout 24-month transition and equilibrium cycles. The corresponding peak LHGR are shown in Figures 3-42 and 3-43. For cases with peaked-to-top power shapes the corresponding peak LHGR are seen to be on the order of 11 to 12 kw/ft. Since limiting MLHGR and MAPLHGR are not consistent with peaked-to-top power distributions, these shapes (including Cases 2 and 5) were removed from final consideration as the design basis shape. Therefore, a PCT calculation has not been performed for Case 2.

f. The statement that "the inherent tendency of BWRs operating with slightly peak-to-bottom power shapes" does not justify the use of the 1.5 cosine shape. Provide results from analyses with more peak-to-bottom power shapes.

Response

As previously discussed, peaked-to-bottom shapes are less limiting than cosine shapes with the same axial peaking factor because the peak power plane dries out and uncovers later, and reloads earlier. This effect was quantified in

response to item (e) above, and was shown to be a[   ]^{a,c} benefit for Case 3 versus Case 4. The discussion in response to item (c) explains why the axial peaking factor bundle relative power combination of 1.50/1.60 can be considered bounding for BWR/5. Therefore, it is concluded that analyses of additional peaked-to-bottom power shapes is not required.

Reference

(4-1)   "Westinghouse Reference Safety Report for BWR Fuel," WCAP-11500 (Proprietary), August 1987.

Question 5

Page 9-3, Ref. 2. Justify that the use of results from analyzing a 1/3-core 8 x 8 and a 2/3-core QUAD+ fuel is adequate to represent generic mixed-core characteristics.

Response

The QUAD+ fuel assembly is designed to be hydraulically compatible with the resident fuel assemblies in the core (e.g., GE 8 x 8R fuel). An in depth description of the fuel hydraulic compatibility is given in Section 4.2.2 of Reference (5-1). The QUAD+ fuel assembly total pressure drop across the assembly is the same as that of the GE 8 x 8R assembly during normal operation. However, the component pressure drops do differ. The grid spacers for the QUAD+ fuel were designed to be less restrictive than the 8 x 8R spacers. In order to improve stability margin and reduce CCFL concerns, the QUAD+ upper tie plate was designed to be less restrictive than the 8 x 8R, and the lower tie plate was designed to be more restrictive (for the same flow conditions). Due to these design differences, the question arises whether the presence of the QUAD+ fuel in a mixed core would adversely alter the blowdown response, ECCS cooling, or the reflood time of the 8 x 8R fuel. To address these concerns, a mixed core analysis was performed using a core configuration of 2/3 QUAD+ fuel and 1/3 GE 8 x 8R fuel. The purpose was to evaluate the impact of a mixed core on the fuel assembly response for the reference transient of Ref. 2.

The attached figures present a comparison of the mixed core response to the full core response for each fuel type. Figure 5-1 shows the normalized total core differential pressure during the blowdown for the mixed core and both full core analyses. The core responses compare very well. Figure 5-2 shows the side entry orifice flow (per assembly) for each analysis which also compare very well. These figures demonstrate that the blowdown response is essentially the same for the three transients.

The normalized component differential pressures along the fuel assembly are shown in Figures 5-3 through 5-6. Figure 5-3 shows the pressure difference

across the side entry orifice for the different fuels. As expected, they agree well. The pressure drop across the lower tie plate is shown in Figure 5-4. The magnitude of the responses are different due to the different tie plate designs, but the same trend is followed for each fuel design. Figure 5-5 presents the pressure drop across the heated length of the assembly. Again the trends are the same, although the QUAD+ grid spacers are less restrictive than the 8 x 8R spacers. Figure 5-6 presents the upper tie plate response for the three transients. The less restrictive upper tie plate for the QUAD+ design is prominent at 10 seconds when lower plenum flashing begins. These figures show that although the individual component pressure drops may vary between fuels, the transient trends are essentially the same.

Figure 5-7 shows a comparison of the void distribution throughout the fuel assemblies at 20 seconds into the transient. Twenty seconds is just prior to midplane dryout, when the mass distribution in the bundle is important. It can be seen that since the transients are very similar, the mixed core does not significantly alter the individual assembly mass distributions. Because the mass distribution does not vary considerably, the dryout times for each transient are comparable, as seen in Table 9.1 of Ref. 2.

The midplane reflood portion of the transient is presented in Figure 5-8. Figure 5-8 shows the normalized total core differential pressure for the three transients from 130 to 150 seconds. The midplane reflood times for each case are indicated in the figure. These times compare well due to the similarity in the system mass distributions for each case. It can be seen that the driving force for reflooding the core is essentially the same for each transient.

The QUAD+ fuel is designed to be hydraulically compatible with the GE 8 x 8R, hence the LOCA system responses for a full core of either fuel type are very similar. Also, the system responses for one mixed core configuration has been shown to very closely follow the full core system responses for each respective fuel. It may be concluded any other mix of QUAD+ and 8 x 8R fuel would yield comparable results. Therefore, the MAPLHGR limits based on a full core analysis are directly applicable to mixed core configurations, since the mixed core configuration has no detrimental effect on the LOCA analysis.

It can be concluded from the above information that the core differential pressure response is relatively independent of local assembly differences. Highly localized effects would not alter the core average response. One example of a local effect is rod perforation. Varied degrees of localized rod perforations would have no impact on the global results for a mixed core.

Reference

(5-1)   "Westinghouse Reference Safety Report for BWR fuel," WCAP-11500, August 1987.
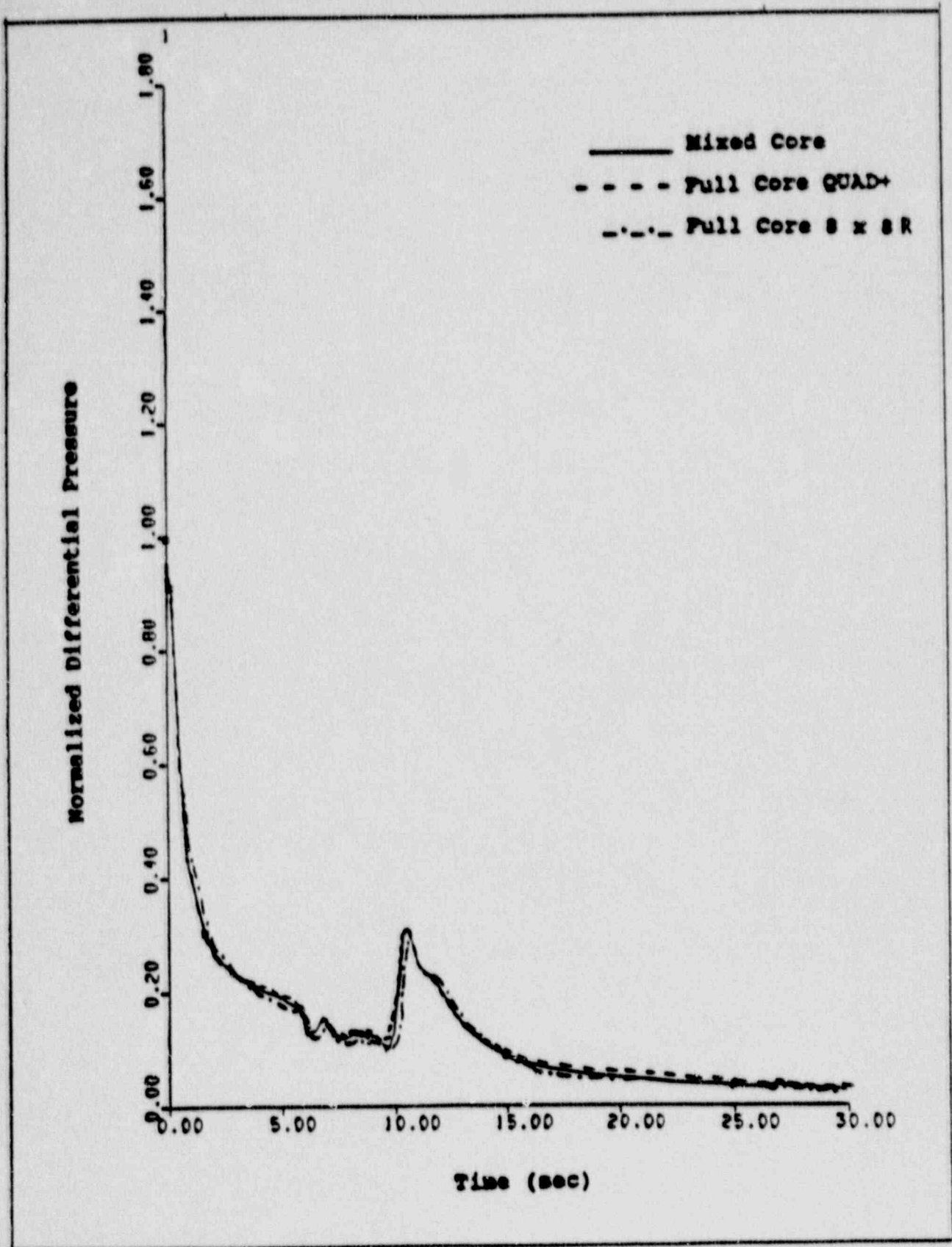
Figure 5-1 Normalized Assembly Differential Pressure vs Time

18
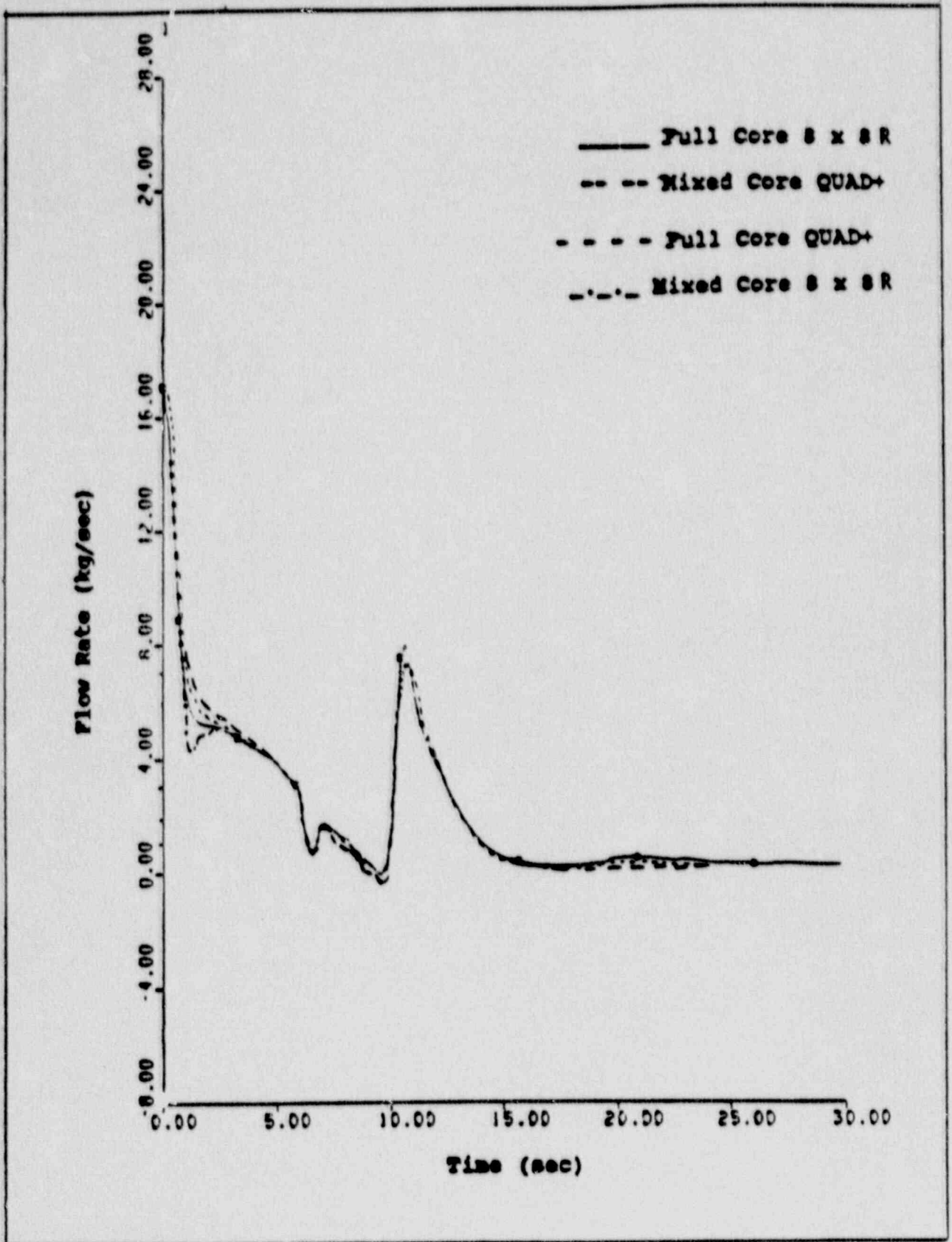
Figure 5-2 Side Entry Orfice Flow Per Assembly vs Time

19
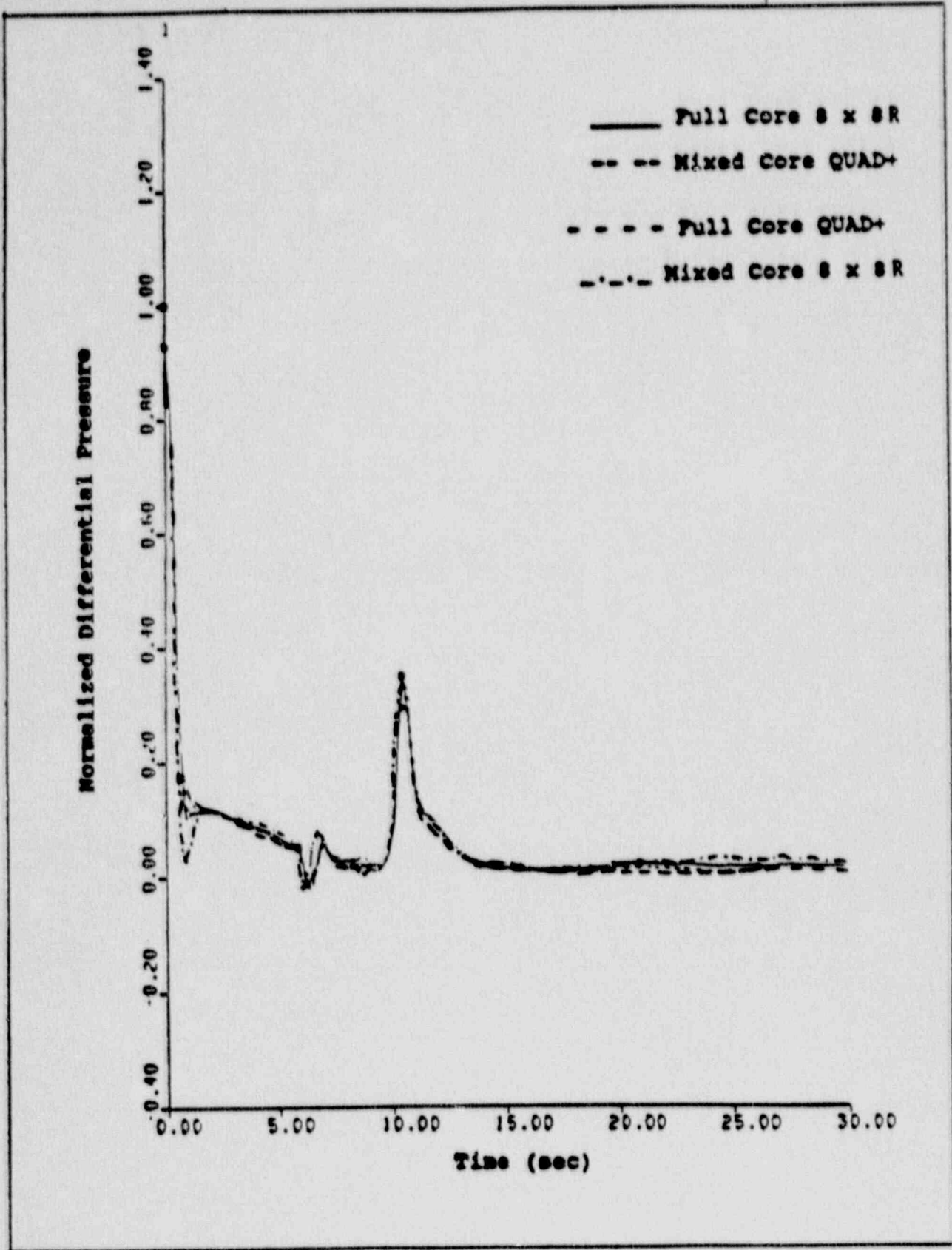
Figure 5-3   Normalized Side Entry Orifice Differential Pressure vs Time
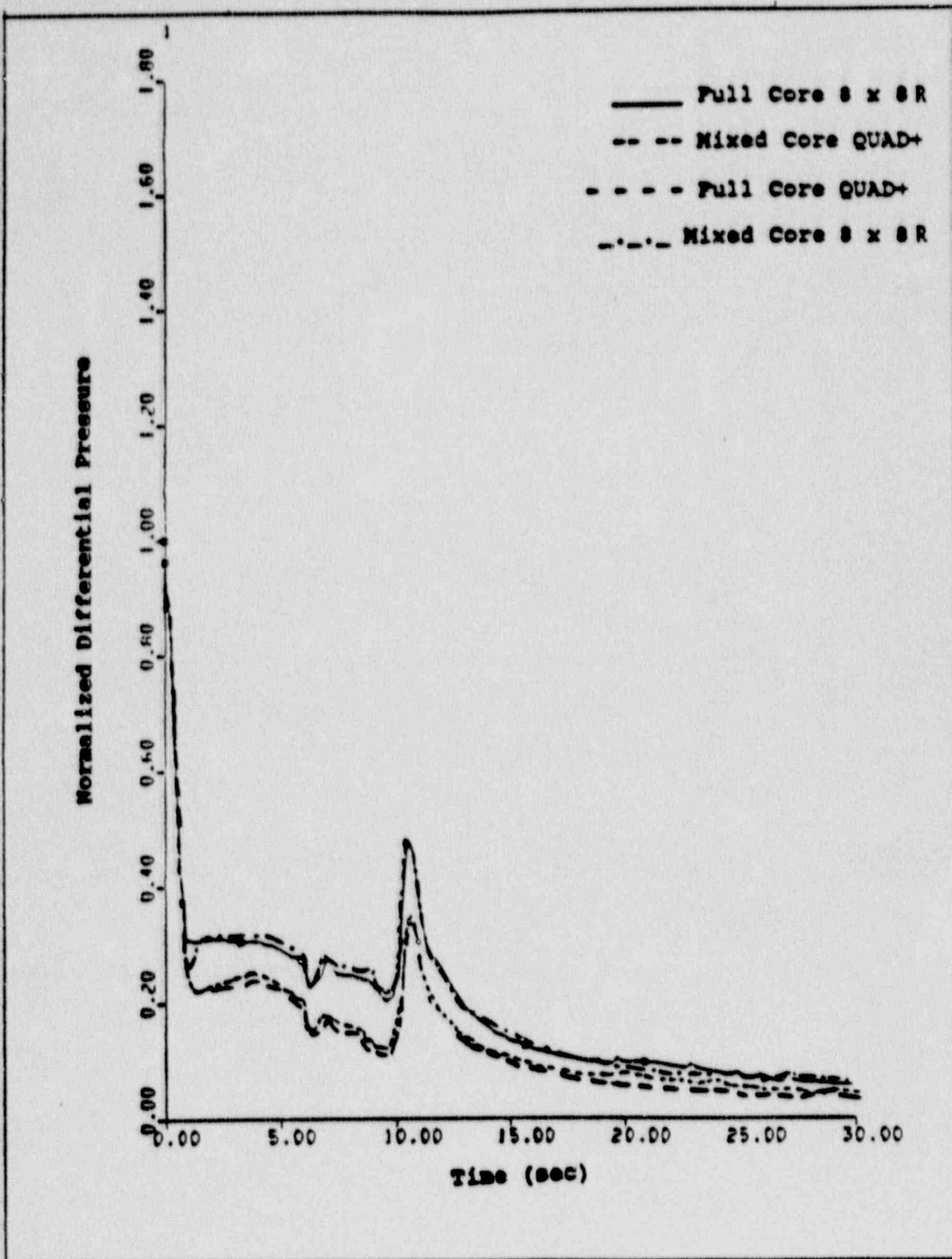
Figure 5-4 Normalized Lower Tie Plate Differential Pressure vs Time
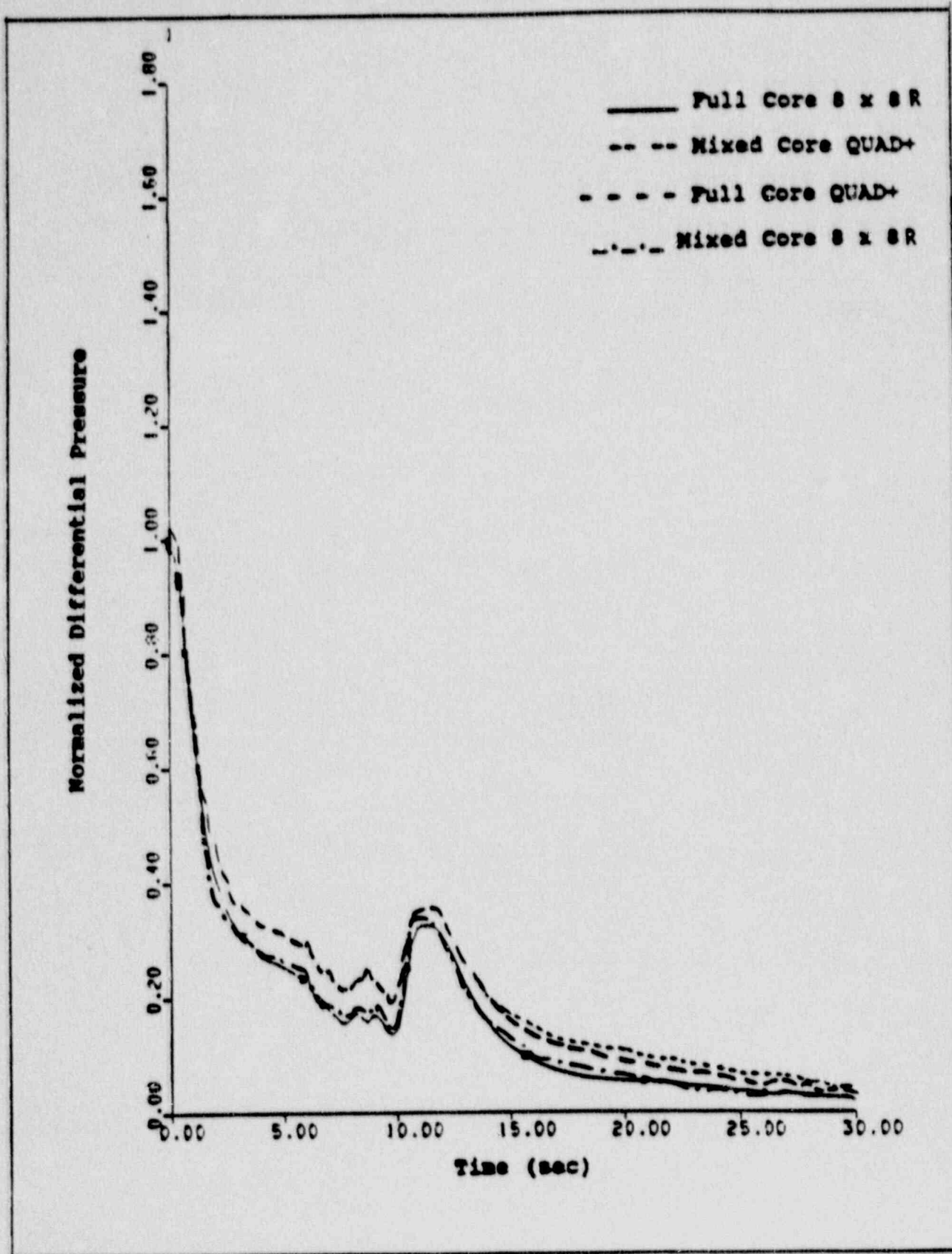
Figure 5-5 Normalized Heated Length Differential Pressure vs Time
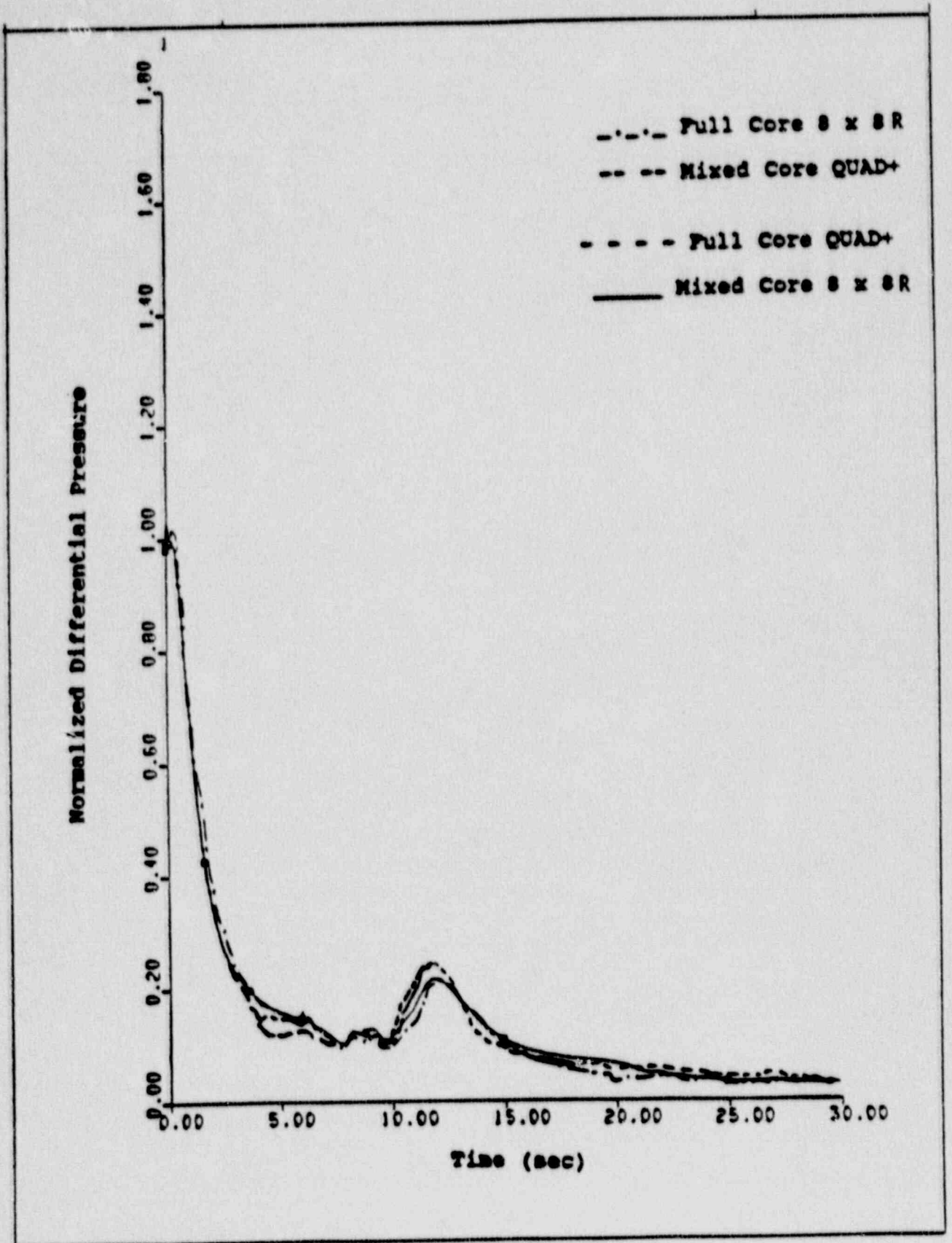
Figure 5-6 Normalized Upper Tie Plate Differential Pressure vs Time
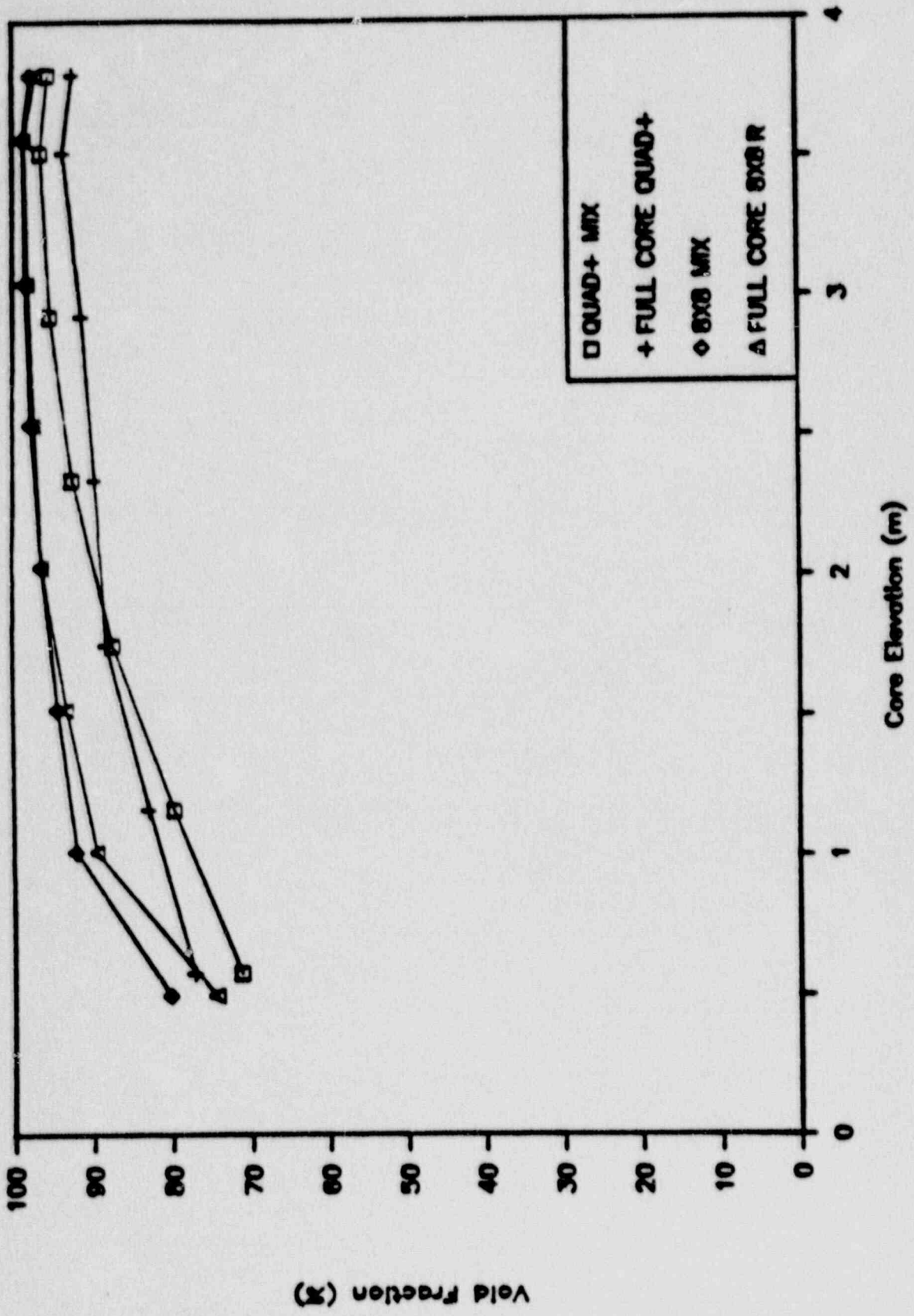
Figure 5-7   Core Void Fraction at 20 Seconds vs Core Elevation

24
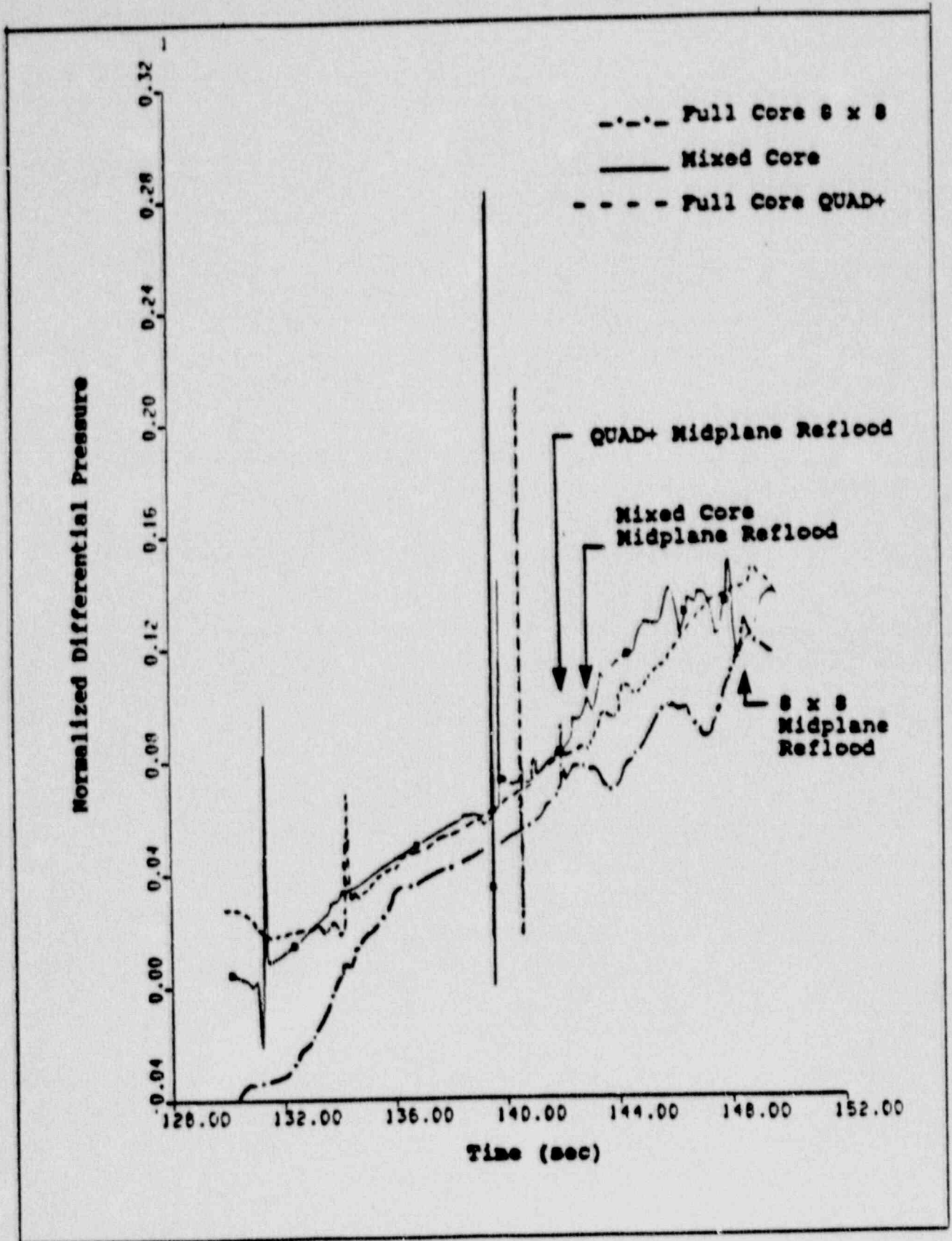
Figure 5-8 Normalized Assembly Differential Pressure vs Time

Question 6

Sec. 4-8, Ref. 1. Discuss the effect of radiation heat transfer on the PCT when rods start to perforate and the core geometry starts to change, including the possibility of the rod bowing.

Response

Upon the calculated perforation of the first rod, the gray body factors used in the radiation heat transfer calculation are modified to reflect the strained bundle geometry. For conservatism, the modified gray body factors are calculated assuming all rods are at their final strained dimensions.

Two CHACHA-3C sensitivity studies were performed to evaluate the impact of the strained bundle geometry on the radiation heat transfer for the reference transient. The first case used gray body factors corresponding to the nominal (no strain) geometry for the entire transient. The second case used gray body factors after the first perforation which corresponded to all rods strained such that the rod-to-rod gap is reduced to 1% of the nominal value. For the QUAD+ geometry, with a cladding outer diameter of 0.4576 inch and a rod pitch of 0.609 inch, this corresponds to a final strain of 0.33 for all rods.

Based on comparisons of the reference transient and the parametric runs described above, the effect of the strained bundle geometry on radiation heat transfer and PCT may be summarized as follows:

Outer rods - The temperatures of the 12 peripheral rods in a QUAD+ minibundle decrease as strain increases. This result is due to the increase in radiation heat transfer from the outer rods to the channel as the effective heat transfer area of the rods increases.

Inner rods - The temperatures of the 4 central rods in a QUAD+ minibundle increase as the strain increases. This result is due to the decrease in radiation heat transfer from the inner rods to the channel as the strained

outer rods "block" more and more of the radiation view factor. The increase in radiation heat transfer from the inner to outer rods does not completely compensate for this effect, since the outer rods are still significantly hotter than the channel wall.

For the reference transient, the no strain gray body factors resulted in a PCT of [   ]^{a,c}. The gray body factors corresponding to all rods strained to 99% gap closure resulted in a PCT of 1039°C. These differences would be more pronounced if the channel had rewetted prior to reflood, or if the reference transient had resulted in higher PCT.

The QUAD+ fuel assembly is designed to resist bowing of fuel rods, as described in Section 4.4.1 of Reference (6-1). Even allowing for the possibility of some degree of rod bow, the impact on PCT would clearly be bounded by the second case described above, which used gray body factors corresponding to all rod-to-rod gaps gaps reduced to 1% of the nominal gap.

References

(6-1)   "Westinghouse Reference Safety Report for BWR Fuel," WCAP-11500 (Proprietary), August 1987.

Question 7

Page 3-7, Ref. 2. In order to demonstrate a proper integration of material and hydraulic models, provide the major steps to arrive at the result of peak cladding burst at 98 seconds.

Response

The cladding heatup for the hot rod for 0 to 100 seconds of the reference case is shown in Figure 7-1. The core midplane coolant pressure transient is shown in Figure 7-2. The rod internal pressure is shown in Figure 7-3. A comparison of Figures 7-2 and 7-3 shows that the rod internal pressure exceeds the coolant pressure after 30 seconds. This is reflected in the cladding stress, shown in Figure 7-4. This figure also shows the allowable cladding stress versus time, and the intersection of the actual and allowable stress curves at 98 seconds. The swelling of the cladding prior to burst is shown in Figure 7-5. The rapid swelling from 73 to 98 seconds is due to the plastic deformation of the cladding.
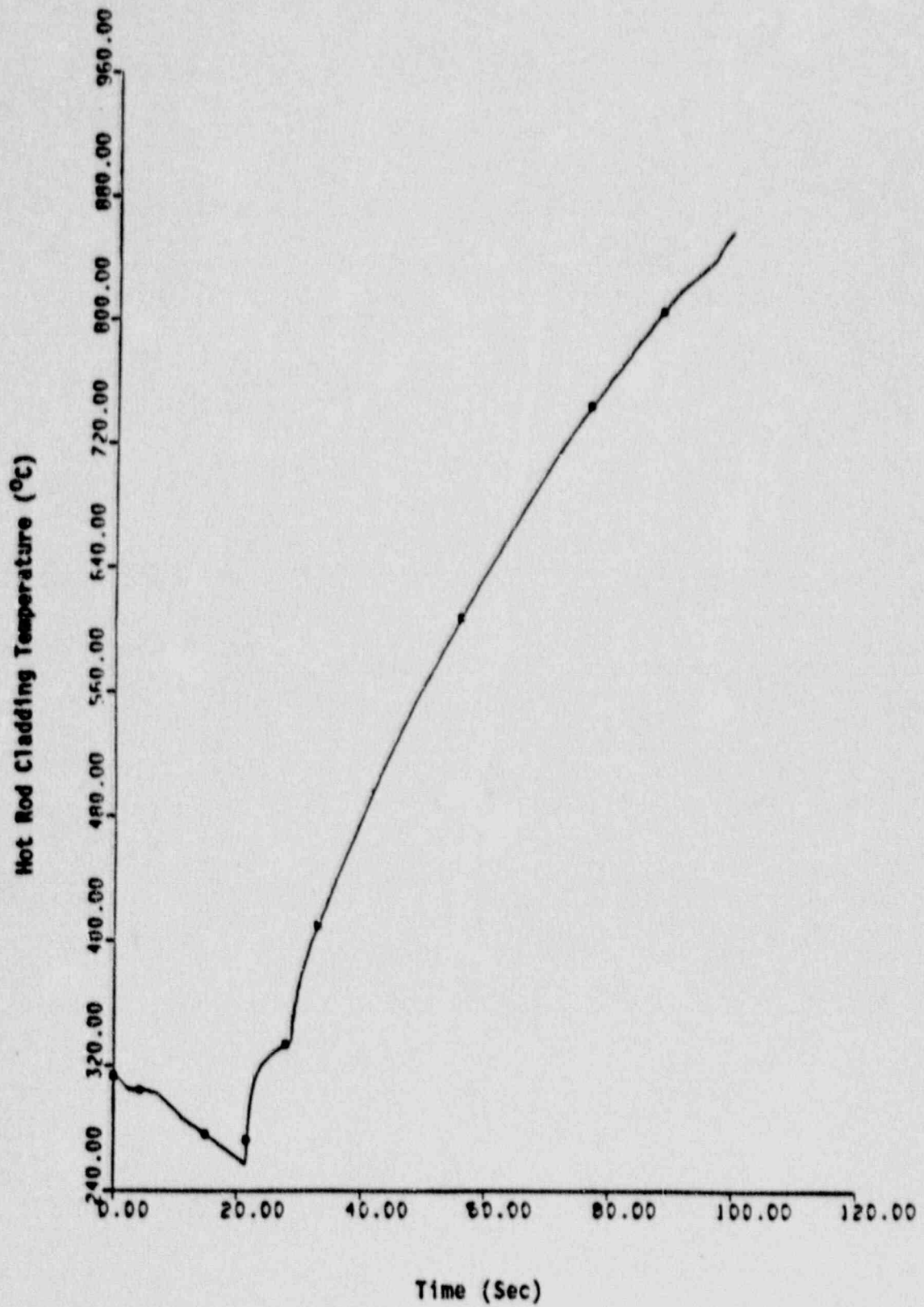
Figure 7-1 Hot Rod Cladding Temperature for Reference Transient
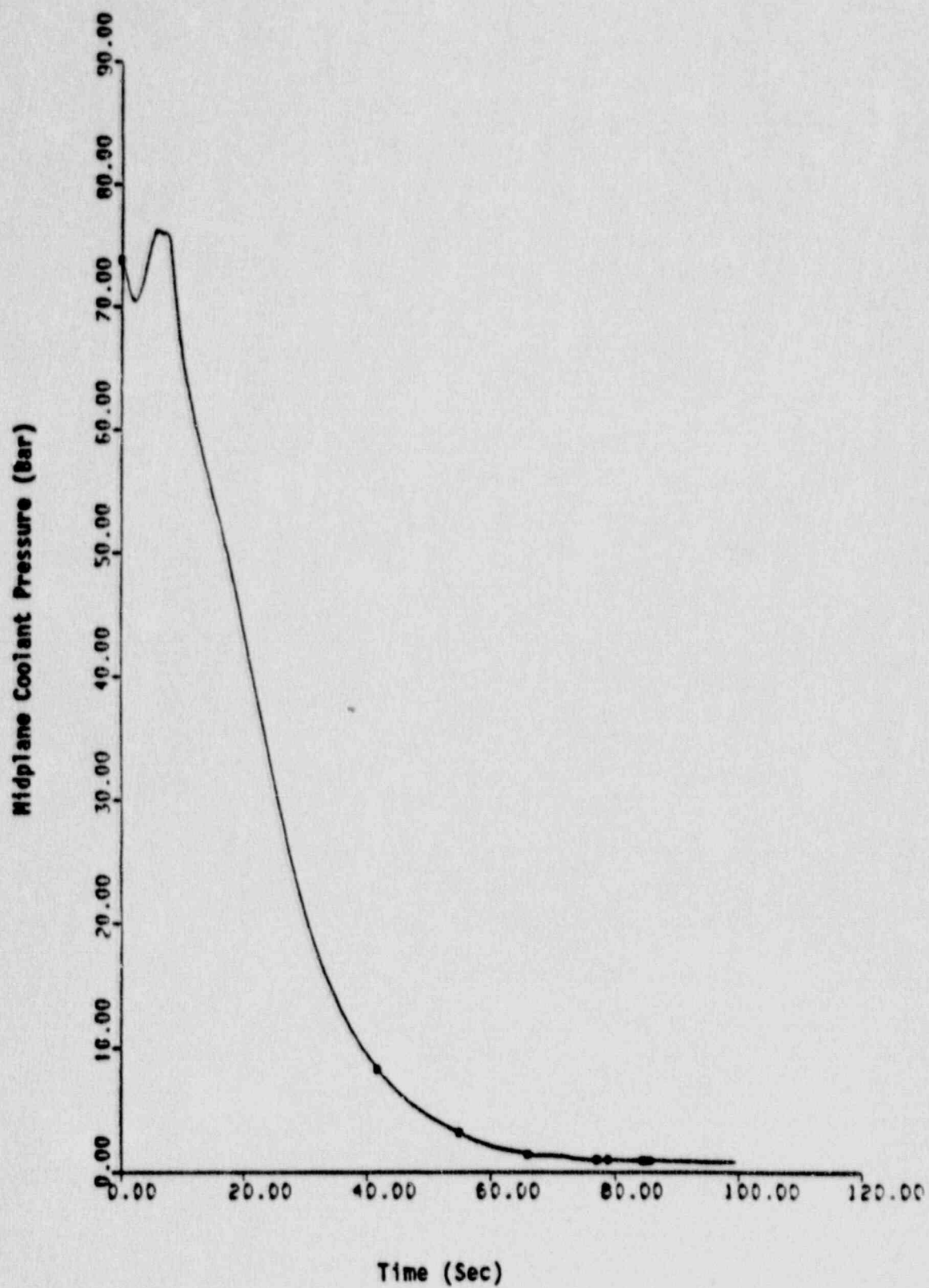
Figure 7-2 Midplane Coolant Pressure for Reference Transient

30

Hot Rod Internal Pressure $(\times 10^{-4}$ Pa)

Time (Sec)

a,c
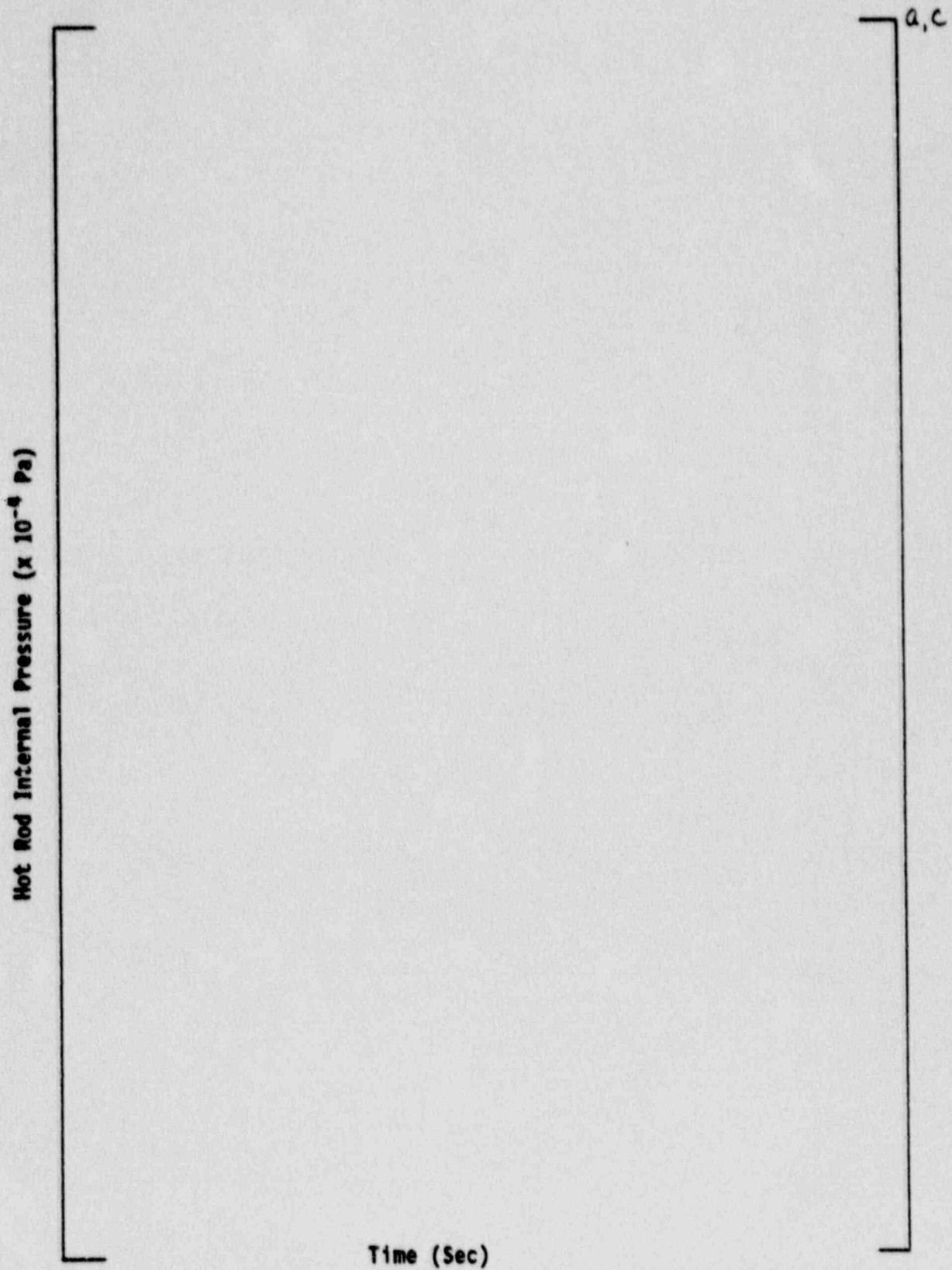
Figure 7-3 Hot Rod Internal Pressure for Reference Transient
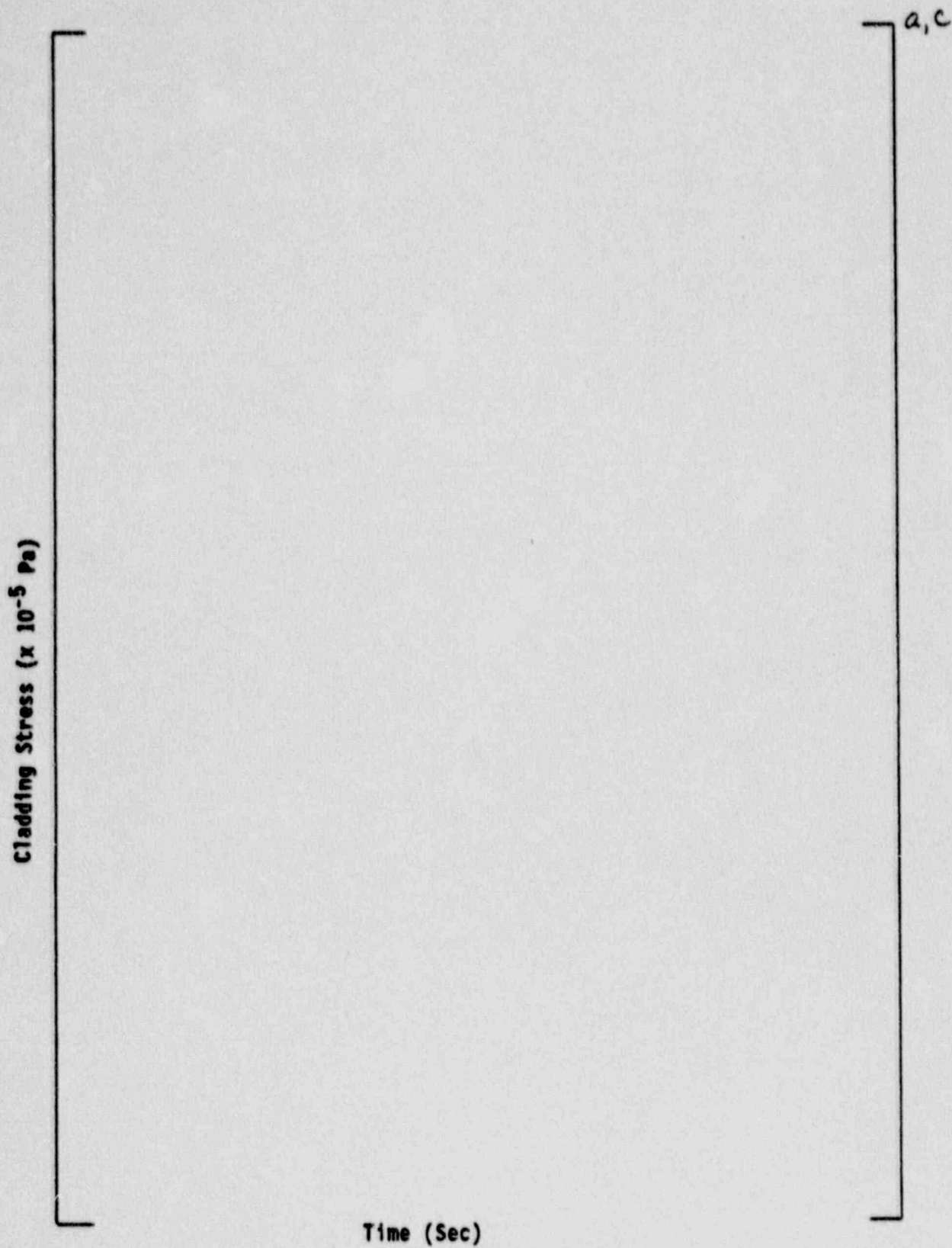
Figure 7-4   Hot Rod Cladding Stress for Reference Transient

32

a,c

Cladding Strain

Time (Sec)
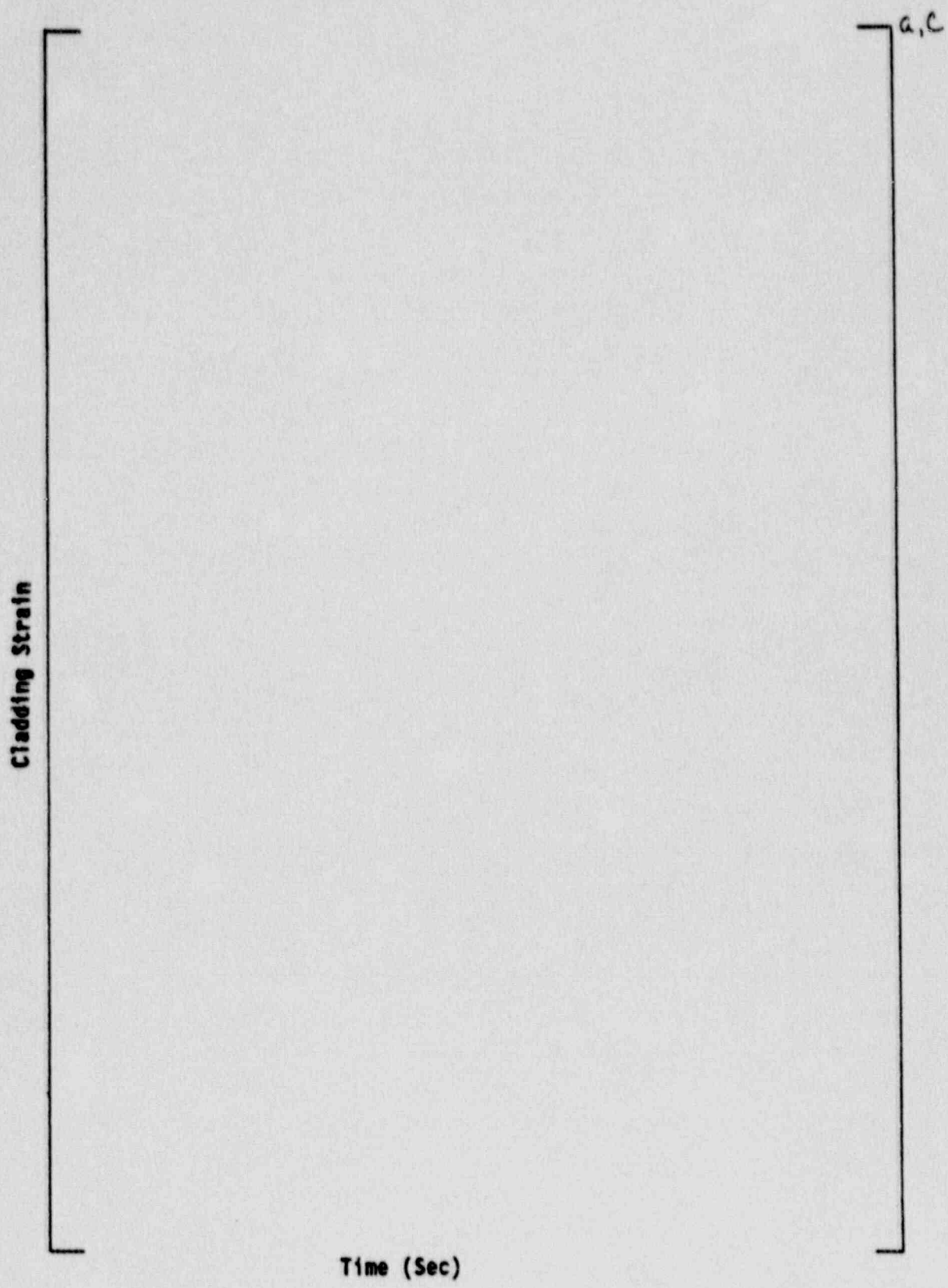
Figure 7-5 Hot Rod Cladding Strain for Reference Transient

33

Question 8

Page 3-22, Ref. 1; Pages 5-1, 5-2, Ref. 2. Values of K_1 and K_u determine the liquid phase and gas phase fluxes in the CCFL correlation. Justify that the use of K_1 and K_u that best fit the A-A 8 x 8 bundle geometry would also be appropriate for the QUAD+ geometry. Describe the experimental geometry and provide results that are used to justify the statement "The correlation conservatively calculates a 25 percent less liquid penetration into the fuel bundle than was observed in the test." In particular, data for liquid draining rate and gas upflow rate are needed.

Response

The countercurrent flow limitation (CCFL) correlation used in GOBLIN/DRAGON contains two correlating coefficients K_1 and K_u. These coefficients were originally determined based on formulations and data by Bailey and Eriksson (Reference (8-1) and (8-2) below).

A CCFL experiment was conducted using prototypical QUAD+ hardware to demonstrate the appropriateness of the GOBLIN/DRAGON CCFL correlation for QUAD+ fuel. A description of the test and summary of the results are presented below.

Nitrogen/water tests were performed on a full-scale model of the upper half of the BWR QUAD+ fuel assembly to determine the countercurrent flow limiting (CCFL) charactersitics of the rod bundle top spacer and upper tie plate. A schematic of the test facility is shown in Figure 8-1. The atmospheric tests were carried out for 5 and 10 gpm spray water injection rates and a range of gas flow rates to obtain data covering the CCFL performance of the fuel assembly from the onset of CCFL to flooding.

The tests were repeated with several different gas/water injection techniques. Tests were run without gas flow up the watercross and with sufficient gas flow to create flooding at the watercross exit. Tests also were run with two different methods of introducing the injected water. A

spillover method was used where the water entered the bundle by spilling over the channel lip. The other method used a shower head to spray the injected water above the bundle.

Figure 8-2 shows the liquid drain rate as a function of gas flow for the 5 and 10 gpm tests with and without gas flow in the watercross. The spillover method was used in the collection of these data. The influence of the watercross flooding is negligible. At low gas flows the water drain rate reaches a plateau due to the limited injection flow rate, not due to CCFL.

Figure 8-3 shows a comparison of the two water injection methods. The shower head water introduction method produced slightly more restrictive CCFL, than the spillover method. This is attributed to the smaller drops created in the shower head. These two methods examine the two limiting water injection configurations. An actual reactor situation would be expected to be some combined condition.

All the data presented above was compared to the CCFL correlation in GOBLIN/DRAGON. The general form of the correlation is

where
$$K_g^{1/2} + K_\ell^{1/2} = K_u^{1/2}$$

$$K_g = \rho_g^{1/2} \; j_g / (\sigma g g_c (\rho_\ell - \rho_g))^{1/4}$$

$$K_\ell = \rho_\ell^{1/2} \; j_\ell / (\sigma g g_c (\rho_\ell - \rho_g))^{1/4}$$

and j_ℓ is positive downward.

Evaluating the GOBLIN/DRAGON correlation for the conditions and geometry of the CCFL test gives Ku =[   ]^{a,c}. A comparison of the GOBLIN/DRAGON correlation with the data is shown in Figure 8-4. The correlation is more restrictive over the range of liquid flows, $K_\ell^{1/2}$, where the facility water flow rate was not limiting ($K_\ell^{1/2}<0.4$). In a typical LOCA analysis calculation $K_\ell^{1/2}$ is much less than 0.4 (less than 0.05). Hence in

a LOCA analysis calculation a more restricted upper bundle CCFL is conservative because it limits the amount of injection water available for cooling the bundle and draining into the lower plenum for refilling the vessel.

In summary, the Westinghouse CCFL tests conducted for the QUAD+ fuel geometry demonstrates that the CCFL correlation in GOBLIN/DRAGON is conservative. The correlation is 25 percent more restrictive in the liquid drain flow rate than observed in the test for typical LOCA analysis conditions (see Figure 8-4)).

References

(8-1)   Bailey, R. V., et al, "Transport of Gases Through Liquid-Gas Mixtures," Paper presented at the AICHE New Orlean Meeting, 1956.

(8-2)   Eriksson, S. O., et al, "Experiment Med Motriktade Ångflöden I strilkyliningskretsen, GÖTA, Studsvik, AEA-15, 1977.

Upper
Plenum

Test Fuel
Assembly

Lower
Plenum
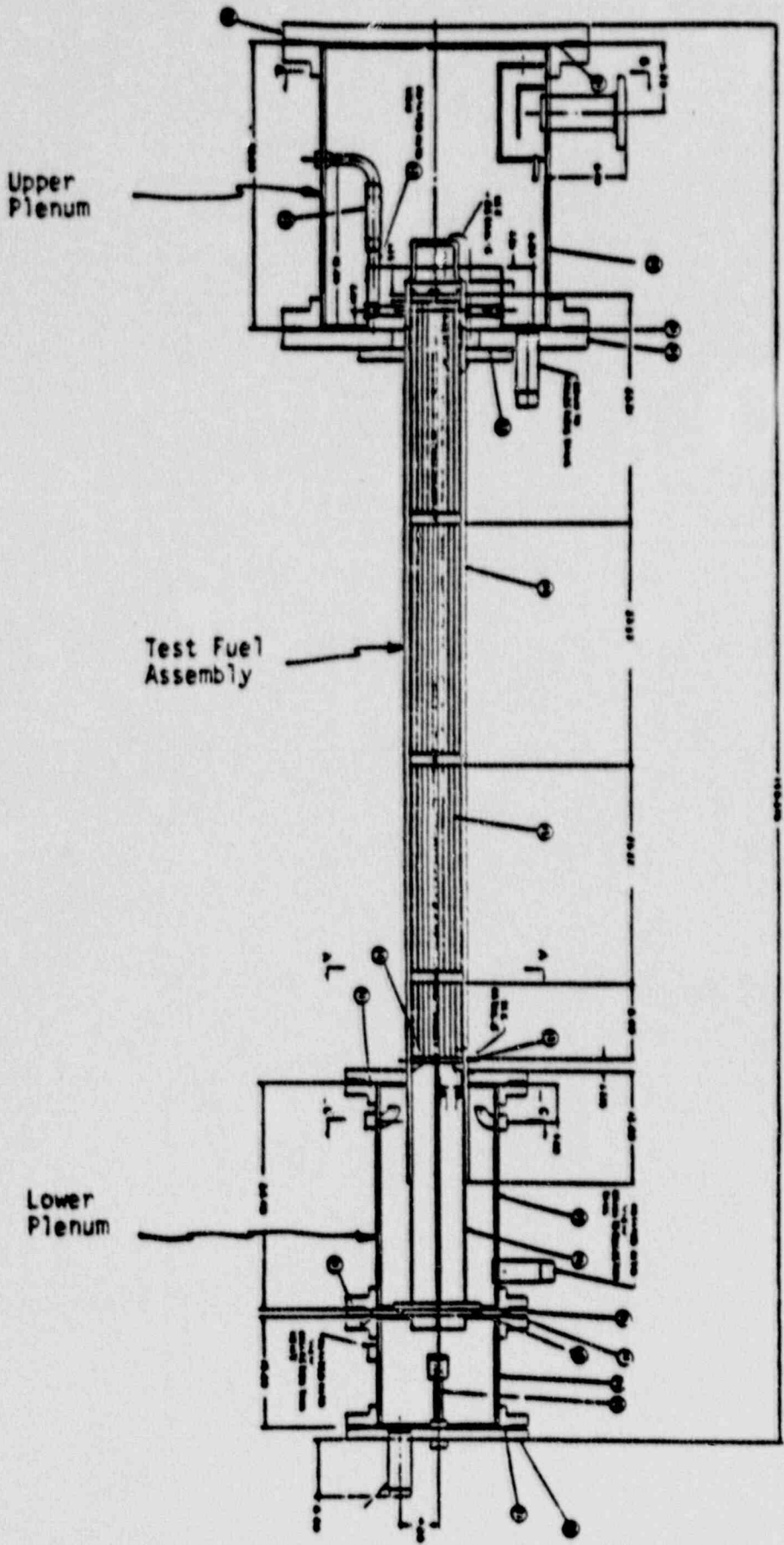
Figure 8-1 QUAD+ Counter Current Flow Test Facility

Figure 8-2 Spillover Water Injection

BWR QUAD+ ROD BUNDLE CCFL DATA
WATER INJECTION TO FUEL ASSEMBLY: 5 GPM AND 10 GPM
WATER CROSS; NITROGEN FLOW: 0.0 AND FLOODING

a,b,c

NITROGEN FLOW IN ROD BUNDLES (LBM/SEC)
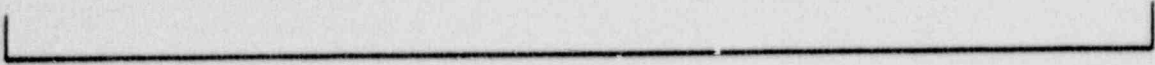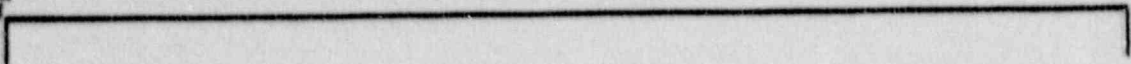
WATER FLOW IN ROD BUNDLES (LBM/SEC)

38

Figure 8-3 Shower Head Water Injection

BWR QUAD+ ROD BUNDLE CCFL DATA
WATER INJECTION TO FUEL ASSEMBLY: 5 GPM AND 10 GPM
WATER CROSS NITROGEN FLOW: 0.0 AND FLOODING

a,b,c

NITROGEN UPFLOW IN ROD BUNDLES (LBM/SEC)

WATER DOWNFLOW IN ROD BUNDLES (LBM/SEC)

Figure 8-4 Data Correlation Comparison

BWR QUAD+ ROD BUNDLE CCFL DATA
WATER INJECTION TO FUEL ASSEMBLY: 5 GPM AND 10 GPM
WATER CROSS NITROGEN FLOW: 0.0 AND FLOODING
WATER INJECTION METHOD: SPILLOVER AND SHOWER HEAD

a,b,c

KL**0.5

KG**0.5

40
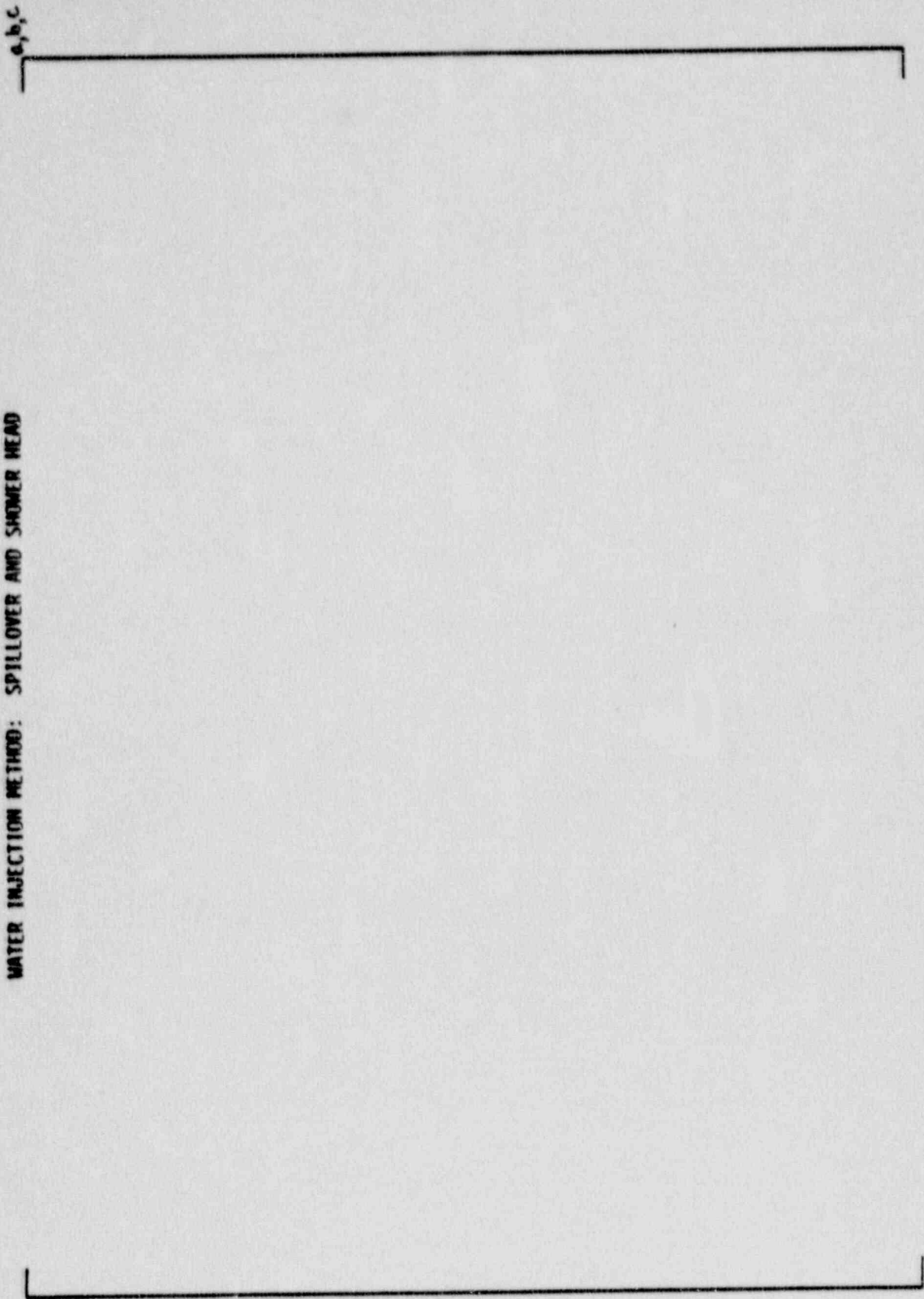
Question 9

Page 3-36, Ref. 1. Reference 1 characterizes the modified Bernoulli equation as providing a conservative prediction of subcooled break flow. Identify the reference to the modified Bernoulli equation which discusses the conservatism. In the Westinghouse model, what guidance is provided to a user for critical flow checks so that the consistency of solutions is ensured?

Response

The modified Bernoulli equation is conservative for the prediction of the maximum subcooled break flow rate (calculated using equation 3.3-57 of Ref. 1) because friction is neglected. The flow resistance coefficient (ξ) from the stagnation point to the exit is set equal to zero in the Westinghouse LOCA evaluation model.

The GOBLIN critical flow check compares the flow rate determined by the solution of the momentum equation and the flow rate determined from the applicable critical flow model. Critical flow is used when the flow rate calculated by the momentum equation is greater than the critical flow rate for that flowpath.

For recirculation line breaks, the Westinghouse evaluation model methodology uses critical flow checks at three locations. Each critical flow check is in the broken recirculation line at the location of greatest physical restriction or largest pressure drop (i.e., the locations where choked flow is expected to occur). Two of the locations are at each side of the break point and the third is at the jet pump drive nozzle.

The critical flow check is used at two locations where a two-phase level may uncover the flowpath. These locations are the drive nozzle of the broken jet pump and the vessel side of the guillotine break in the recirculation line. The two-phase level is the downcomer level, which drops rapidly during the initial blowdown. The description of the two-phase level includes the position or height and the quality of the fluid in the appropriate regions.

When the two-phase level uncovers a flowpath, the level is traced within the height of the flow path. As the level moves, the conditions above the level are mixed with the conditions below the level to accurately model the quality of the fluid at the break location.

Question 10

Page 3-63, Ref. 1. Identify the new correlation to replace or modify the A-A correlation for the critical heat flux in order to reflect the QUAD+ fuel design.

Response

Steady-state and transient CHF tests have been conducted by Westinghouse using a simulated QUAD+ minibundle. The resulting test data were used to develop and verify the WB-1 correlation, which uses the critical quality-boiling length formulation. The correlation description and comparisons with steady-state and transient test data are reported in Reference (10-1). The WB-1 correlation has been incorporated into GOBLIN/DRAGON and replaces the AA-74 correlation for use in QUAD+ fuel analysis. (Note that when fluid conditions

are outside of the range of the WB-1 correlation Equation 3.5-34 is replaced with $q''_{crit} = q''_{pc}$.)

Reference

(10-1) "QUAD+ BWR Critical Power Correlation Development Report," WCAP-11287 (Proprietary), September 1986.

Question 11

Page 6-77, 6-84, 6-92 and Sec. 6.2.4, Ref. 1. GOBLIN significantly overestimates early bundle flow rate (0 to 2 s) for all the cases presented (Figs. 6-33, 6-40, and 6-48,) which is a nonconservative result. Rod temperature test results for TLTA test 6423 indicate early rod dryout in the upper regions of the core (Ref: US Nuclear Regulatory Commission report NUREG/CR-3633, EGG-2294, Vol. 4, p. 65). The GOBLIN analysis might miss this early dryout because of an excessive core flow rate. The TLTA test results mentioned above are not available in the Westinghouse report. It is essential that rod temperature analysis results be supplied so that the effect of overestimated bundle flow rate can be assessed.

Response

Part of the qualification of the GOBLIN/DRAGON code presented in Ref. 1 consisted of simulations of two integral tests conducted in the two-loop test apparatus (TLTA) (Ref. 1). The tests (Reference (11-1)) simulated were an average power bundle with nominal emergency core cooling (case 6425 run 2) and a high power bundle with degraded emergency core cooling (case 6423 run 3). The more severe transient, case 6423 run 3, was repeated with several refinements included to reaffirm the initial integral qualification assessment and provide additional detail regarding the simulation.

TLTA case 6423, run 3 is an integral simulation of a full guillotine break of the recirculation line in a jet pump boiling water reactor. The test models a single, full length 8 x 8 fuel assembly at a peak power of 6.46 MW. The high and low pressure core spray systems were degraded from their nominal flow rates and emergency core cooling fluid temperature was increased from nominal to 200°F.

The primary difference between the simulation of case 6423 run 3 presented here and that documented in Ref. 1 is in the initial and boundary conditions. An effort was made to much more closely match the test initial and boundary conditions to confirm that observed deviations in the original simulation were a consequence of these initial condition differences. Table 11-1 summarizes the test, original simulation, and revised simulation initial conditions. The significant changes are better matches of initial downcomer mass inventory and lower plenum enthalpy. The downcomer mass affects the initial depressurization through break uncovery timing and the lower plenum enthalpy affects the timing of lower plenum flashing.

One key boundary condition is the steamline flow rate. Modelling of the steam line valve closure was also modified to better match the measured steam line flow (See Figure 11-1). This change noticeably improved the early pressure transient as will be seen in the results presented below.

The GOBLIN simulation of TLTA case 6423 run 3 excluded several Appendix K evaluation model requirements in order to properly evaluate the code. The Appendix K requirements excluded from the system simulation are:

o   Rewetting of the fuel rods was allowed

o   The best estimate homogeneous equilibrium critical flow model with subcooled flow multipliers based on TLTA orifice critical flow data, was used, replacing the Appendix K required Moody model.

o   The actual test power history was used whereas Appendix K requires the ANS 1971 decay heat curve plus 20 percent conservatism.

A comparison of the GOBLIN system simulation with test measurements is presented first. Then an additional heatup calculation is presented, which includes some Appendix K conservatism, to demonstrate the conservative margin inherent in the LOCA evaluation model.

The GOBLIN simulation system pressure response is shown in Figure 11-2. The simulation agrees very well with the measured pressure. The initial depressurization is due to the subcooled break flow. The pressure recovery from about 4 to 7 seconds is a consequence of the rapid steamline valve closure (See Figure 11-1). At 7 seconds the downcomer level uncovers the jet pump allowing vapor to flow out the drive line side of the break and causing a return of the system depressurization. The jet pump uncovery is shown in the downcomer level plot of Figure 11-3 and is apparent in Figure 11-4 where the intact jet pump performance is severely degraded after 7 seconds. A more rapid depressurization occurs at about 10 seconds once the downcomer is empty and vapor also flows out the recirculation line suction side of the break. The remainder of the depressurization follows the test data very closely with a slightly lower final pressure.

The bundle inlet flow for the initial phase of the transient is shown in Figure 11-5. The general agreement with data is good. The initial drop in bundle flow is a little sharper in the test. This is a reflection of the initial flow reversal in the broken jet pump (Figure 11-6) which is attributed to the initial, rapid nonequilibrium break flow out the broken jet pump drive line. The GOBLIN equilibrium code does not fully capture this small nonequilibrium effect. The start of lower plenum flashing also is visible in Figure 11-5 in the rise in bundle inlet flow at about 15 seconds.

The total vessel mass inventory is shown in Figure 11-7. The good agreement of the total mass inventory and system pressure responses confirms the accurate calculation of the break flow throughout the transient. (Accurate direct measurements of the break flow in the test were not available).

A comparison of the mass inventory distribution throughout the transient are shown in Figures 11-8 and 11-9. The agreement in the trends and timing of event is quite good. The downcomer mass inventory agreement is excellent. The bypass and guide tube also agree well when considering the offset in the initial and final all liquid states. The larger initial guide tube mass and smaller bypass mass is attributed to the deviation in the definition of the boundary between the guide tubes and bypass for the simulation versus the test.

The upper plenum, bundle, and lower plenum mass distributions also have good agreement with the data. (Please note that level tracking in the GOBLIN simulation continuously redefined the control volumes in the upper plenum/separator region, therefore, comparison of the upper plenum mass over the exact same region of measured in the test was not possible). In summary, GOBLIN does an excellent job of predicting the mass inventory distribution through the vessel during the LOCA transient.

Comparisons of the test rod thermocouple measurements at various elevations with the GOBLIN predictions are shown in Figures 11-10, 11-11, and 11-12. The GOBLIN simulation gives a good prediction of the average rod temperature response throughout the bundle. Note that the simulation provides average hydraulic and rod conditions, hence, all the local thermocouple variations are not predicted. The simulation generally does an excellent job of predicting the rod dryout, heatup, and rewet. The blowdown dryout occurring high in the bundle is calculated to be later in time and more pronounced. This is a consequence of the later and longer drop in calculated bundle inlet flow discussed earlier and shown in Figure 11-5. The lower temperatures following rewet at the lower bundle elevations are a result of the lower predicted system pressure reducing the fluid saturation temperature.

The test simulation comparison presented here shows the ability of GOBLIN to calculate the average thermal-hydraulic response during a LOCA transient. To demonstrate that substantial conservative margin above the peak TLTA measured temperature is inherent in LOCA evaluation model, the Appendix K required rod heat transfer was introduced in a hot plane heatup calculation of the TLTA simulation. The prescribed rod heat transfer coefficients as a function of time are shown in Figure 11-13. The Appendix K requirements are no rewetting of the rods, zero heat transfer following uncovery and prescribed heat transfer during spray cooling and after reflood. The resultant rod temperature transient is shown in Figure 11-14. Clearly, the conservatism from the above stated Appendix K requirements introduces a large peak cladding temperature margin above the rod temperature measurements for the TLTA simulation. Additional PCT margin is inherent in the evaluation model due to other conservative assumptions excluded from this simulation (e.g., break flow model and decay heat curve).

Figures 11-15 through 11-21 are replotted results of the original TLTA case
6423 run 3 simulation reported in Ref. 1. These figures supersede the
original Figures 6-40 through 6-46 of Ref. 1 and shall be incorporated in the
final (approved) version of the topical report.

Reference

(11-1) W. J. Letzing et.al., BWR Blowdown Emergency Core Cooling Program
        Preliminary Facility Report for the BD/ECC-1A Test Phase, GEAP-23592,
        December 1977.

TABLE 11-1
COMPARISON OF TLTA 6423 RUN 3 INITIAL CONDITIONS

	Test	GOBLIN Original	Revised
Bundle Power (MW)	6.46	6.46	6.46
Steam Dome Pressure (psia)	1037 ± 5	1016	1031
Lower Plenum Enthalpy (Btu/lbm)	518 ± 5	451	518
Feedwater Enthalpy (Btu/lbm)	41 ± 2	41	41
Feedwater Flow (lbm/sec)	1.0 ± 0.3	1.0	1.2
Jet Pump 1 Flow (lbm/sec)	17 ± 2	20	18.5
Jet Pump 2 Flow (lbm/sec)	19 ± 2	20	19.0
Bundle Inlet Flow (lbm/sec)	33 ± 5	37	34
Downcomer Mass (lbm)	310	460	312
Initial Water Level (inch elev.)	123 ± 6	122	122
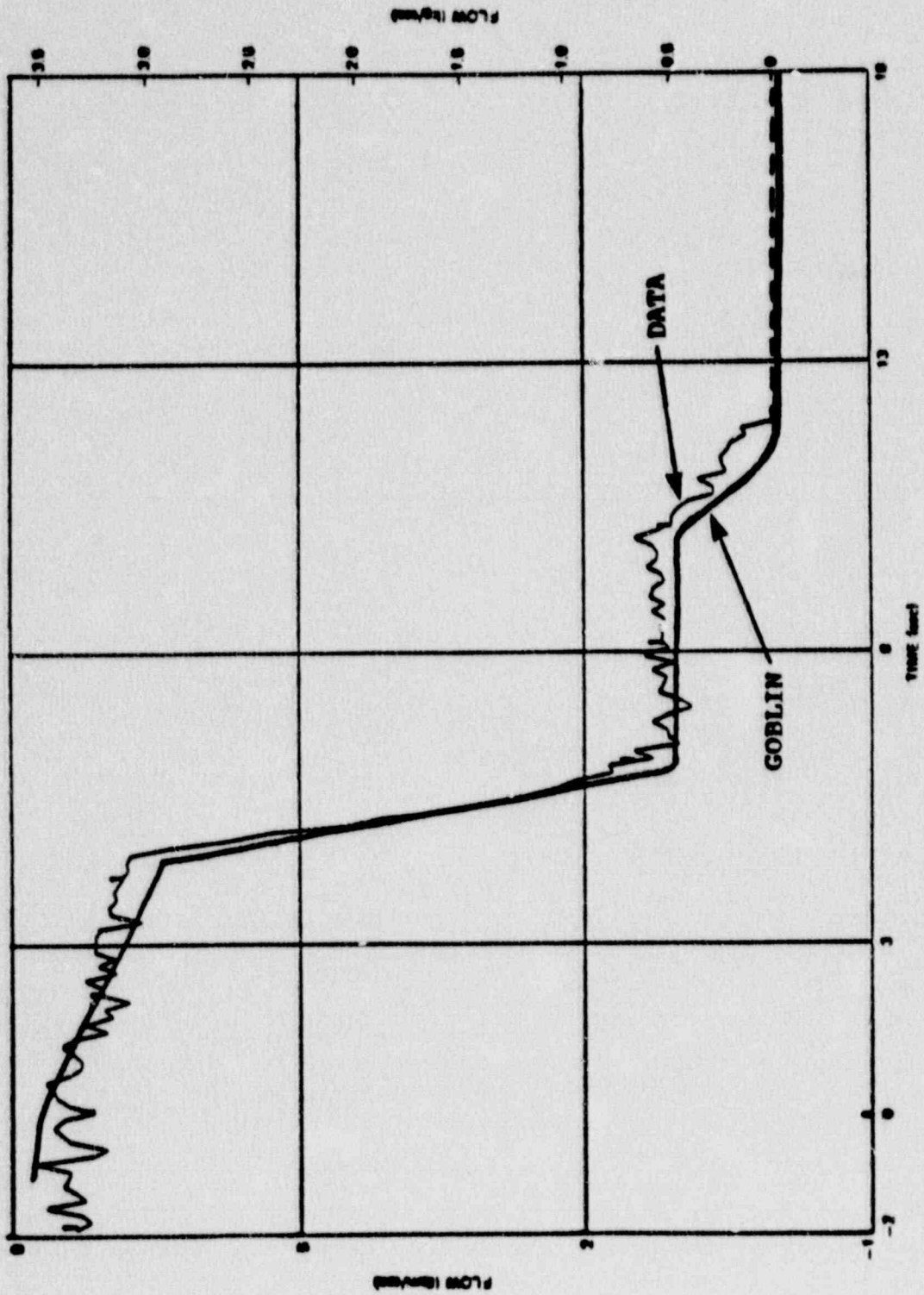
Figure 11-1 TLTA 6423/3 Steamline Mass Flow Rate Boundary Condition
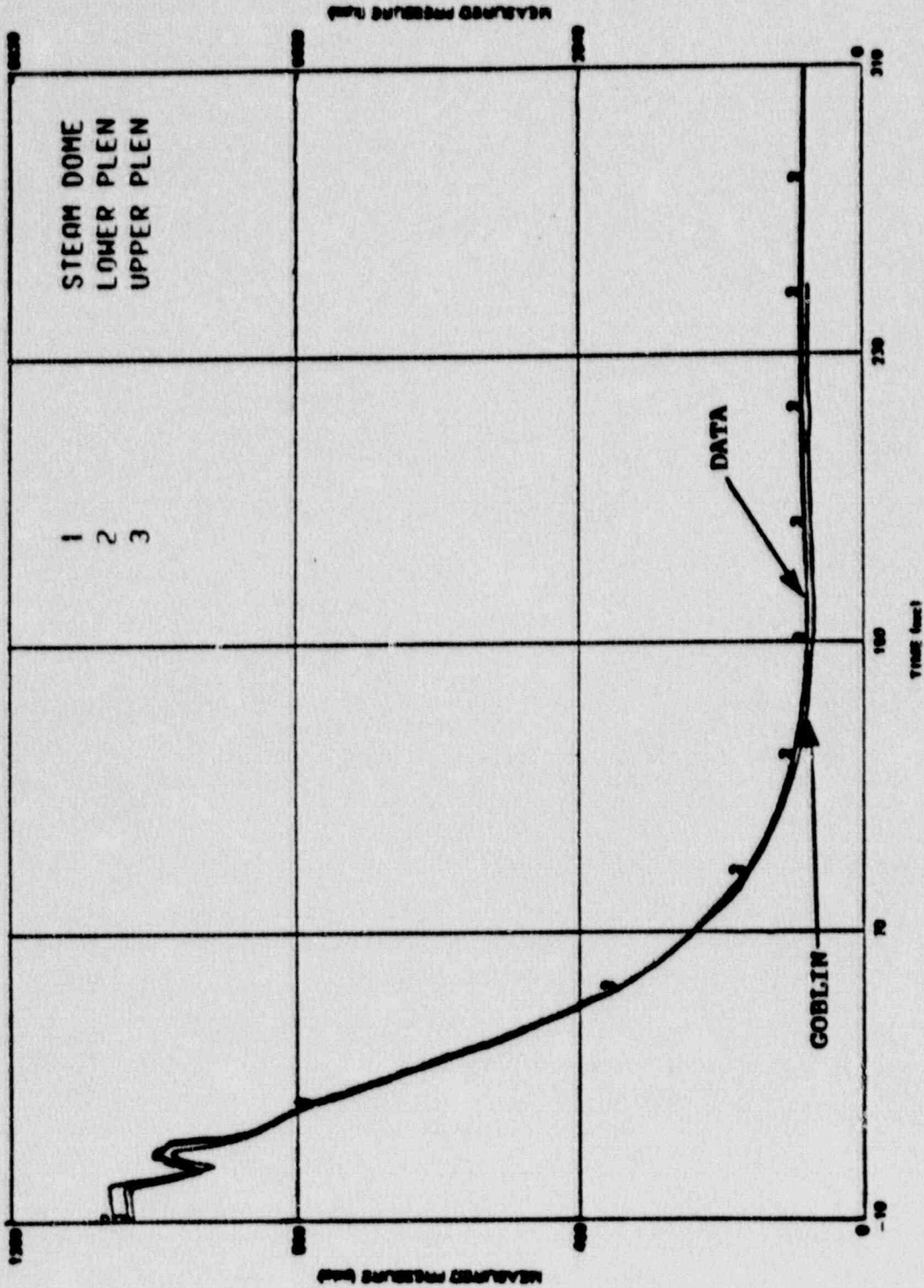
Figure 11-2 TLTA 6423/3 System Pressure Response
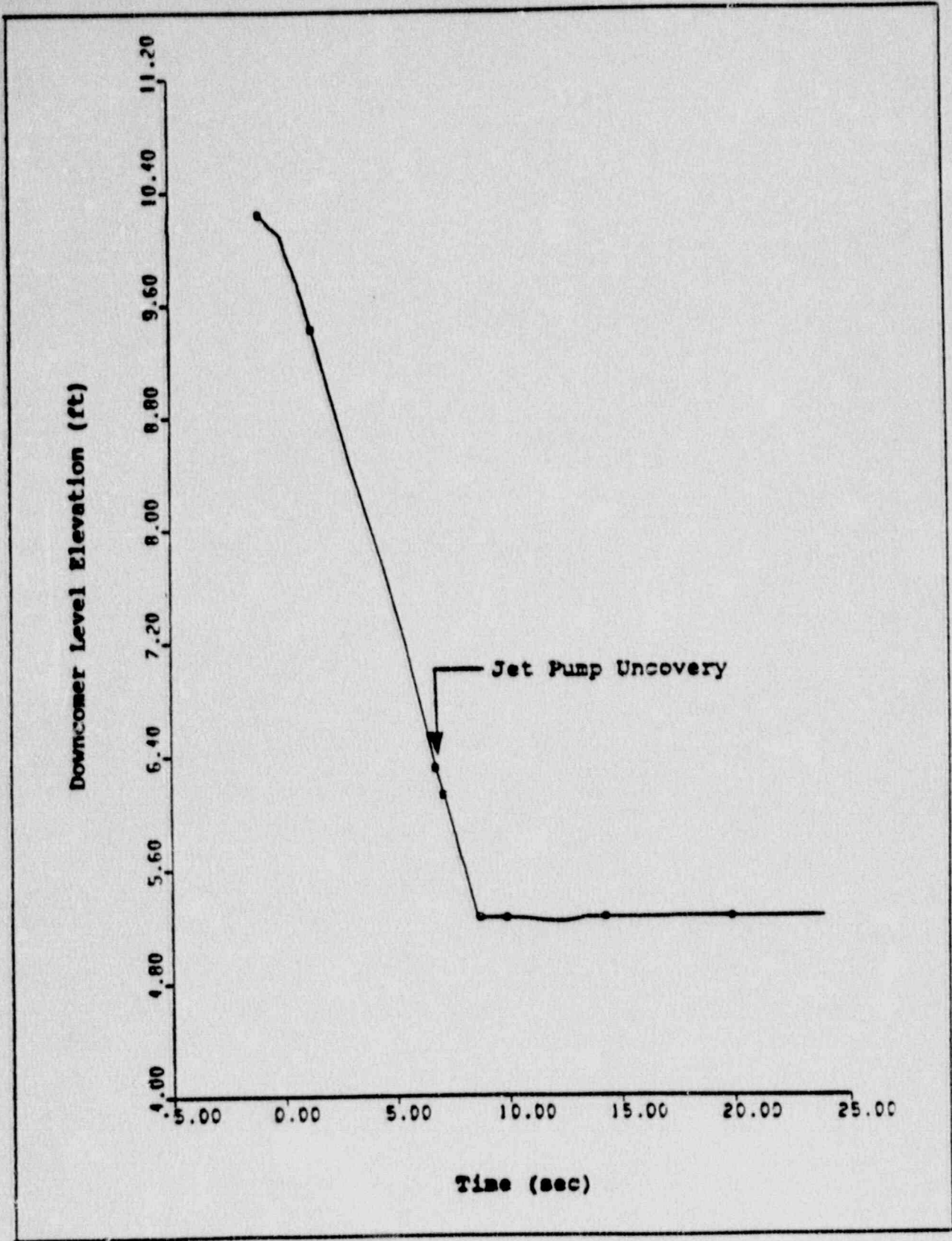
Figure 11-3 TLTA 6423/3 Downcomer Level Transient Response

52
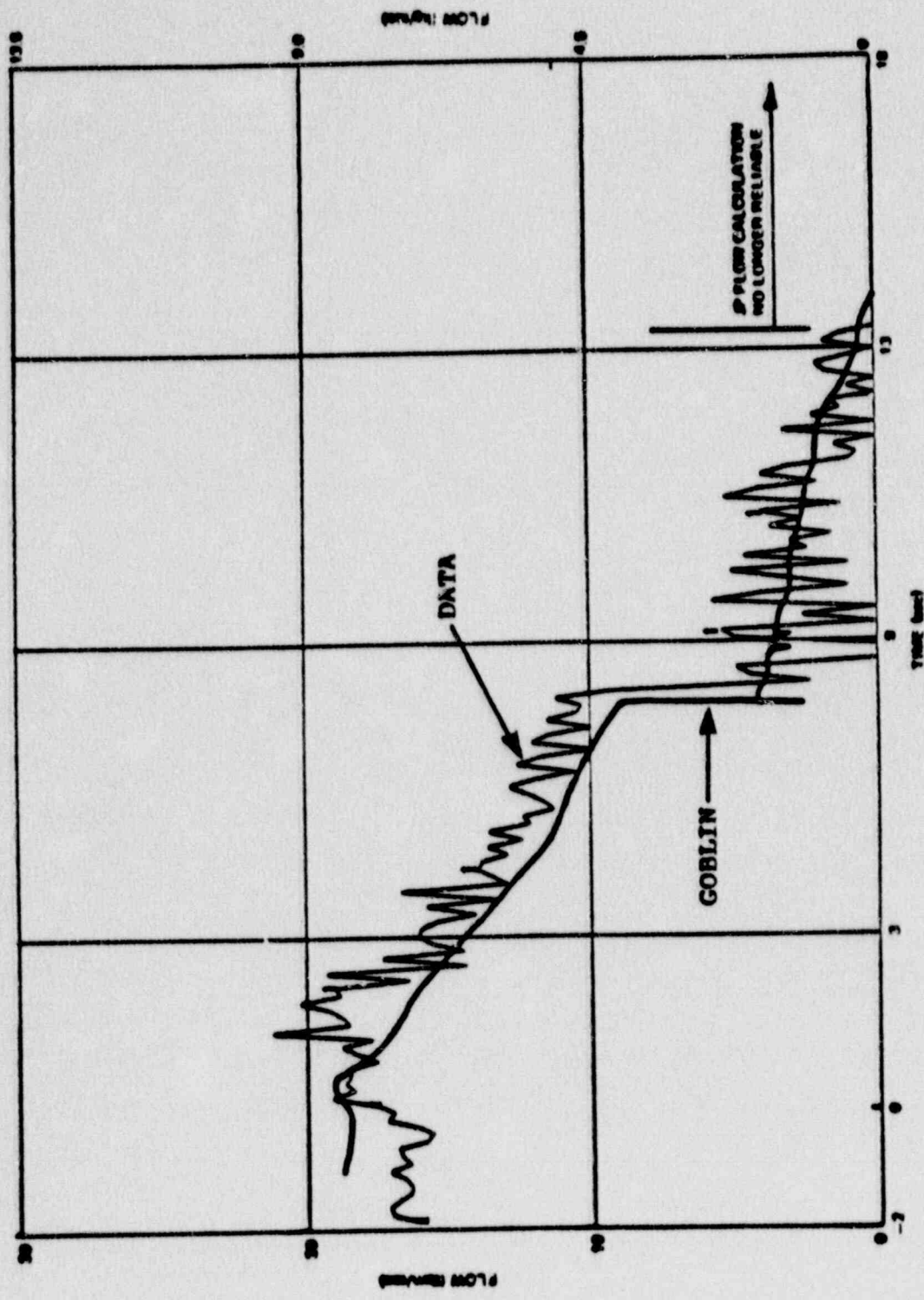
Figure 11-4 TLTA 6423/3 Intact Loop Jet Pump Mass Flow Rate
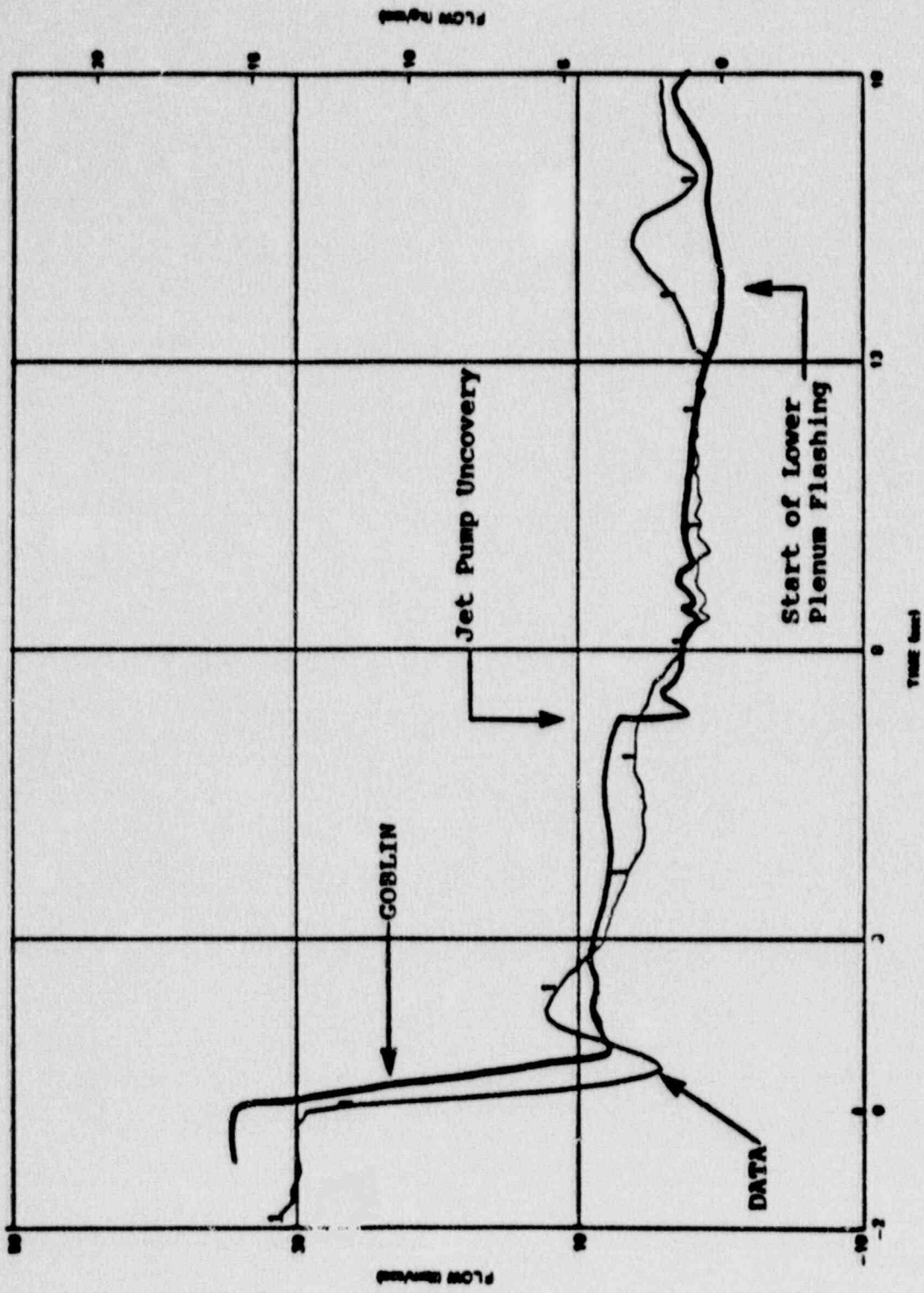
Figure 11-5 TLTA 6423/3 Bundle Inlet Mass Flow Rate
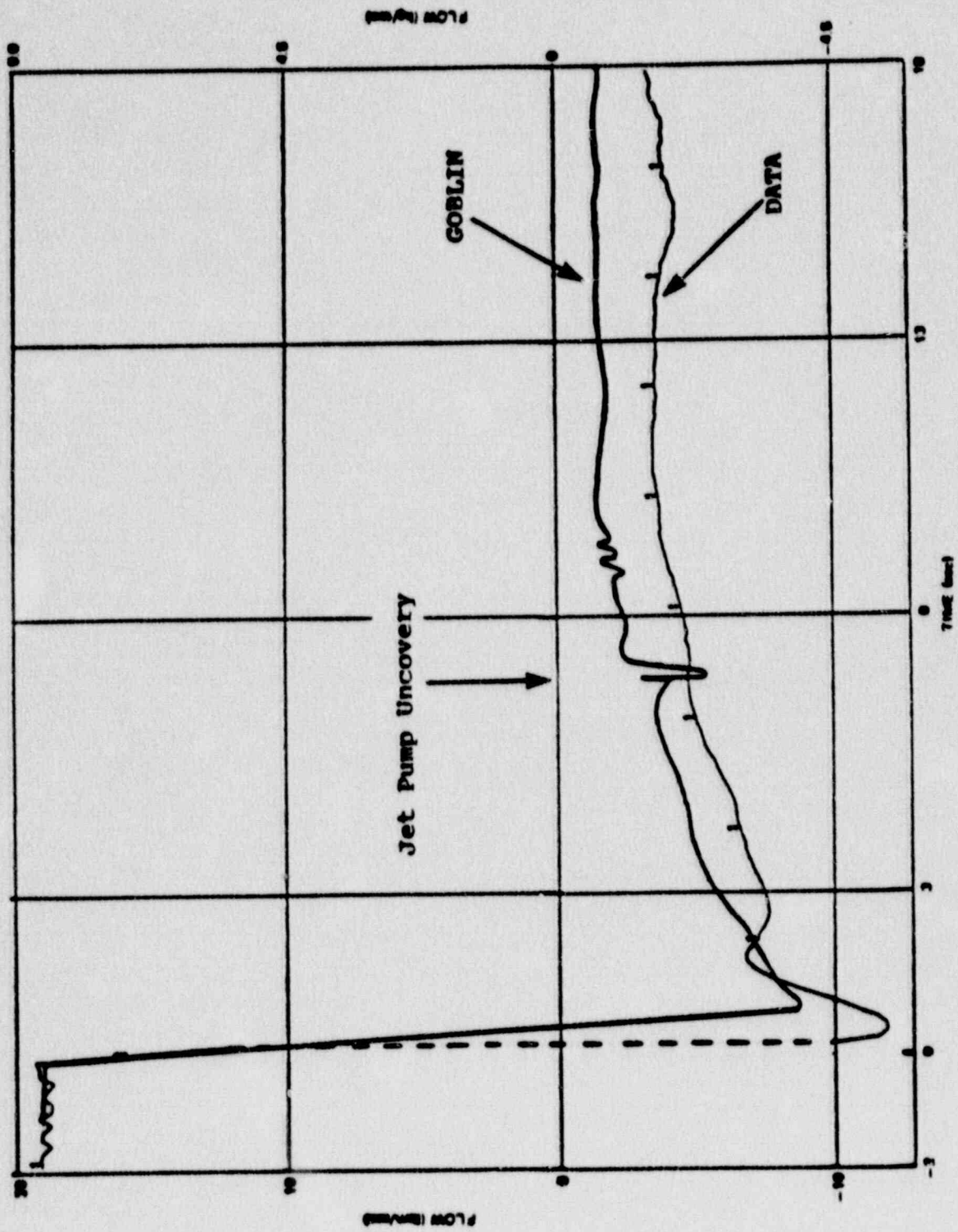
Figure 11-6 TLTA 6423/3 Broken Loop Jet Pump Mass Flow Rate

55
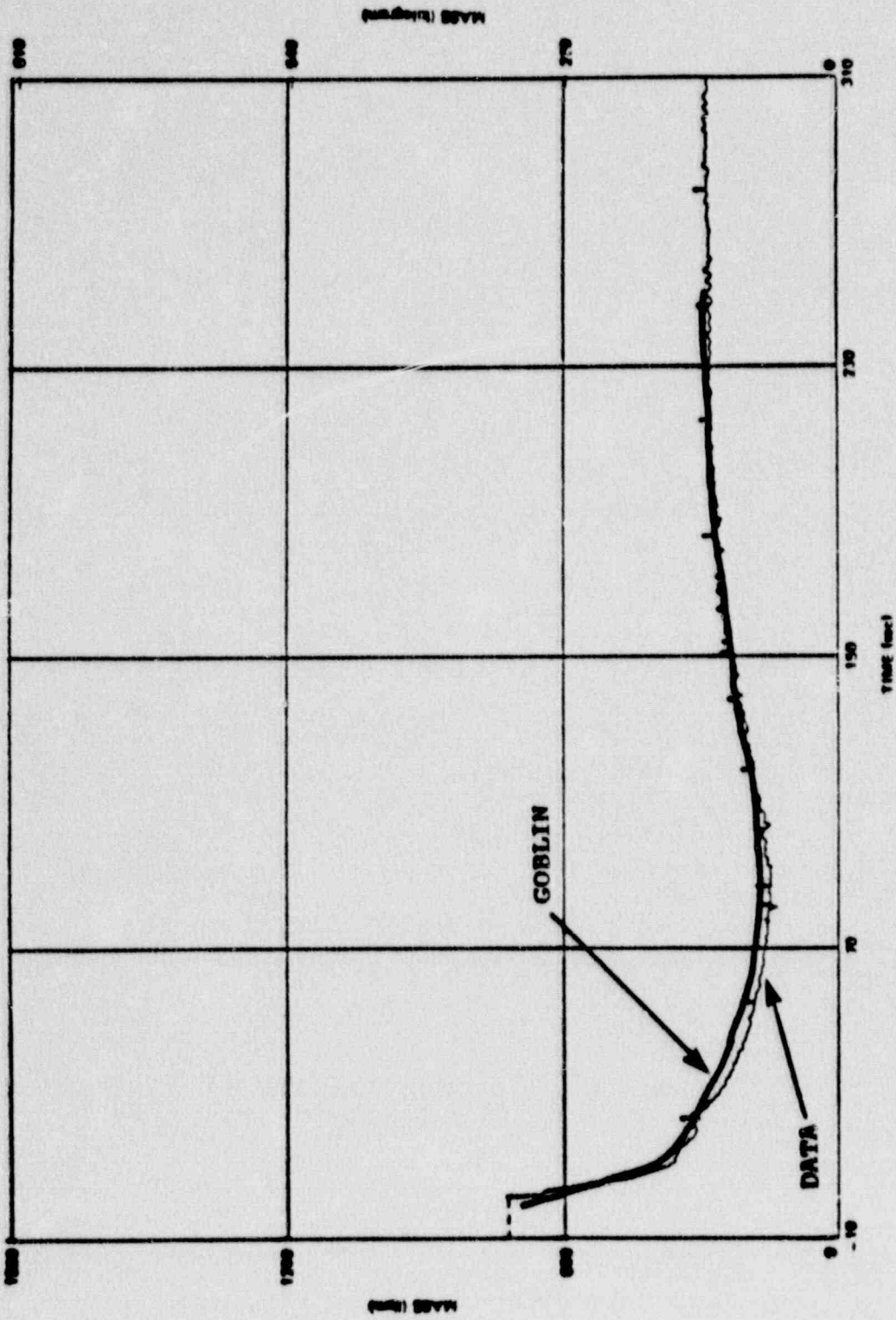
Figure 11-7 TLTA 6423/3 Total Vessel Fluid Mass Inventory

56
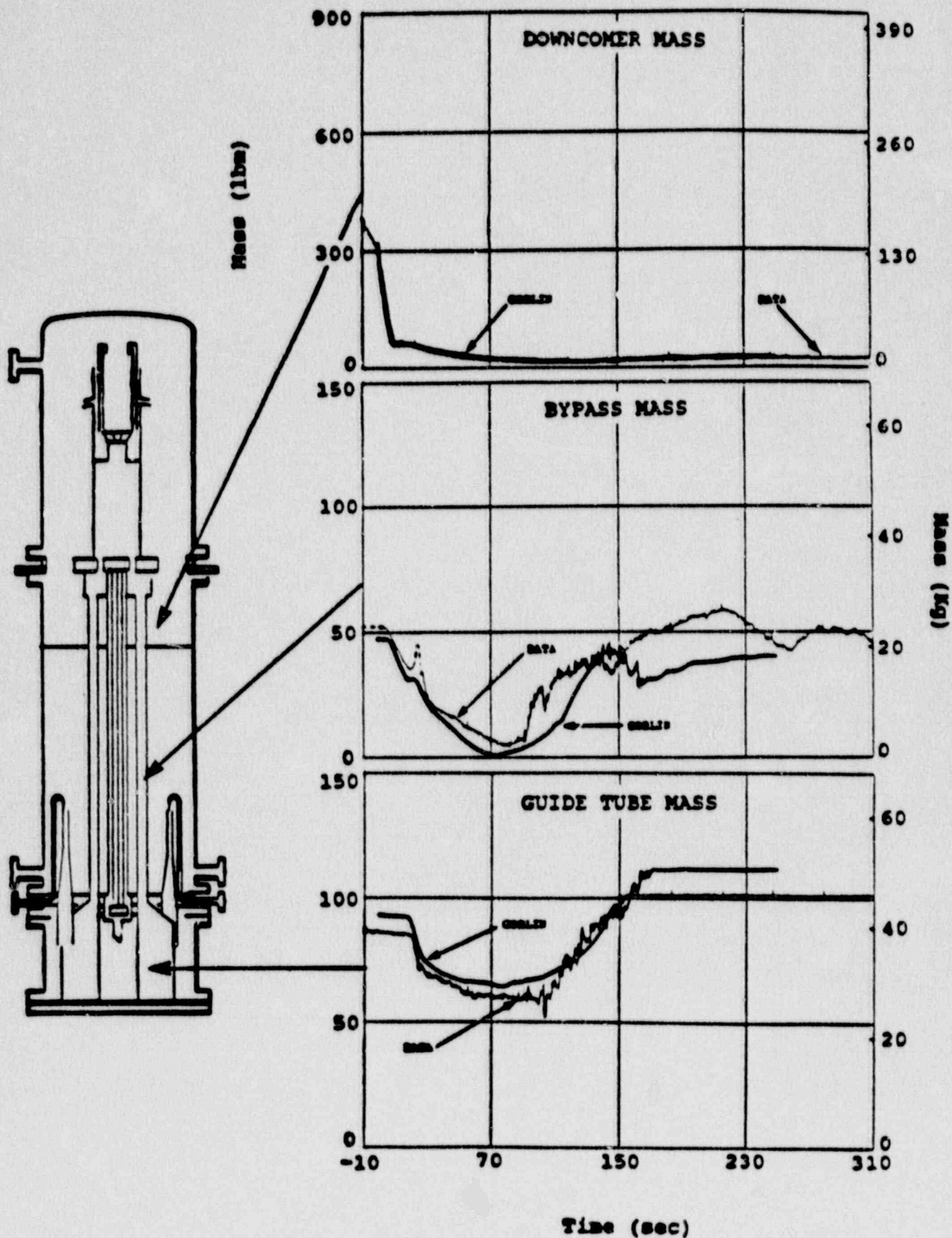
Figure 11-8 TLTA Run 6423/3 Mass Inventory Distribution
(Downcomer Bypass, and Guide Tubes)

57
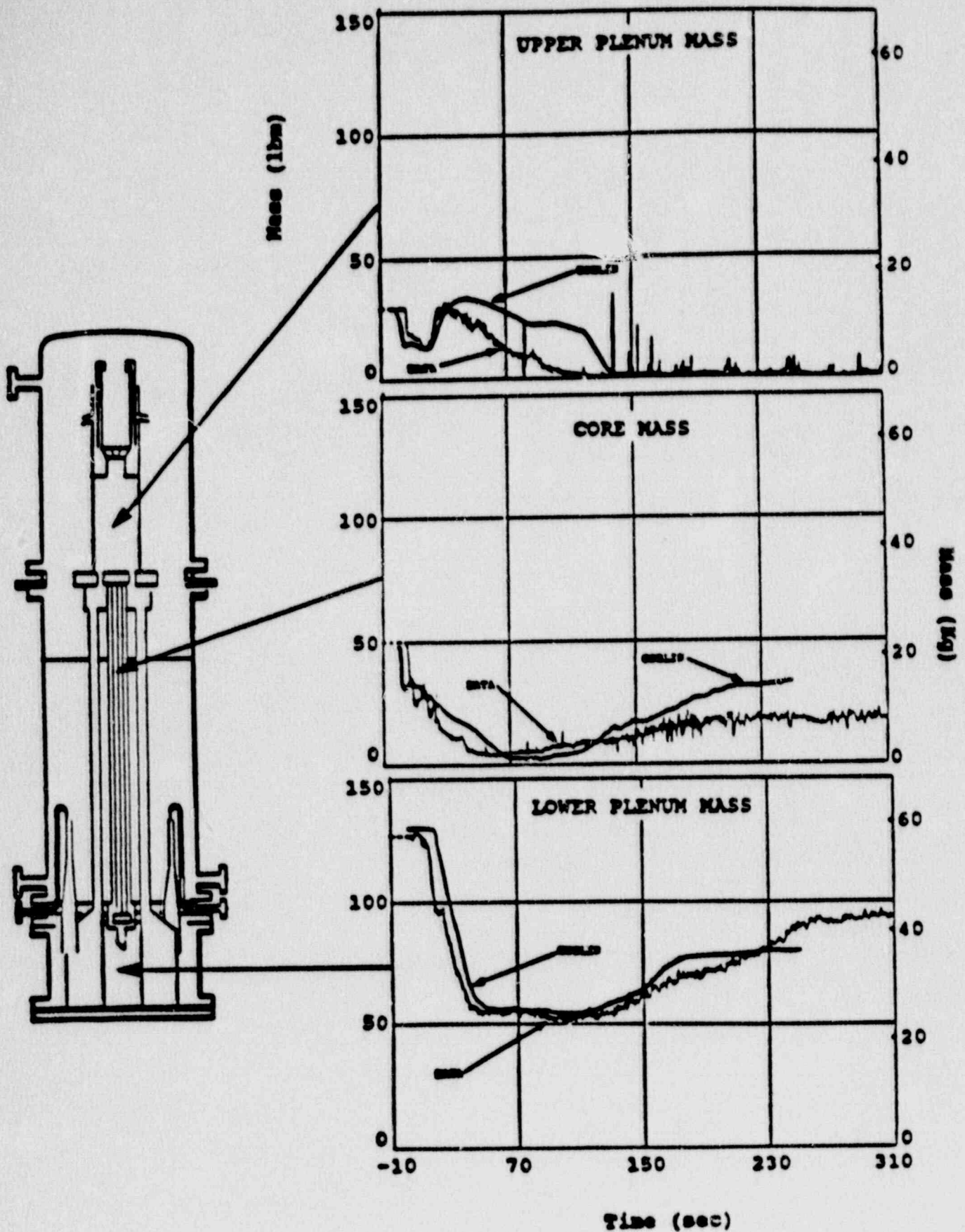
Figure 11-9 TLTA Run 6423/3 Mass Inventory Distribution
(Upper Plenum, Core, and Lower Plenum)
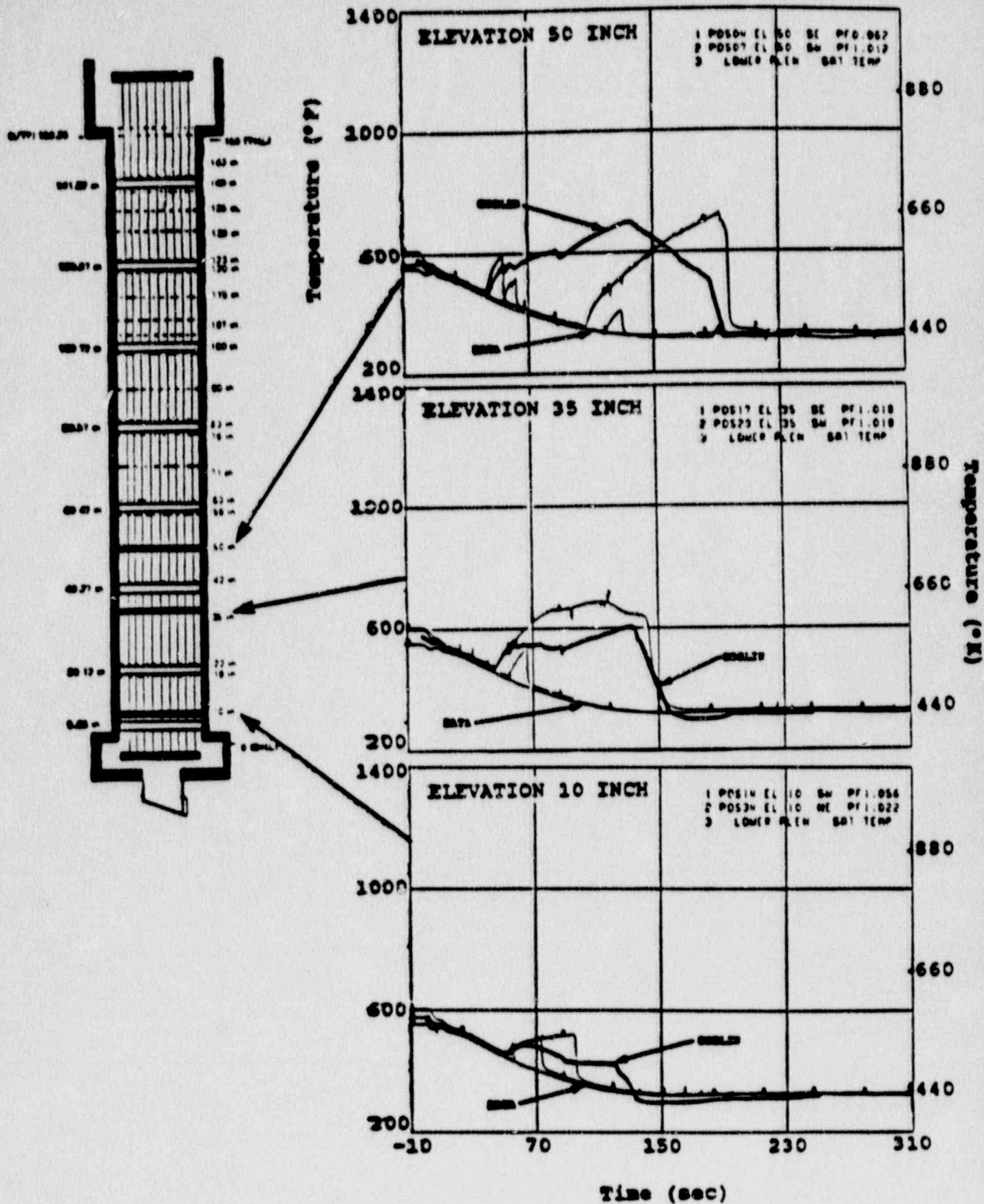
Figure 11-10 TLTA 6423/3 Lower Elevations Rod Temperature Response
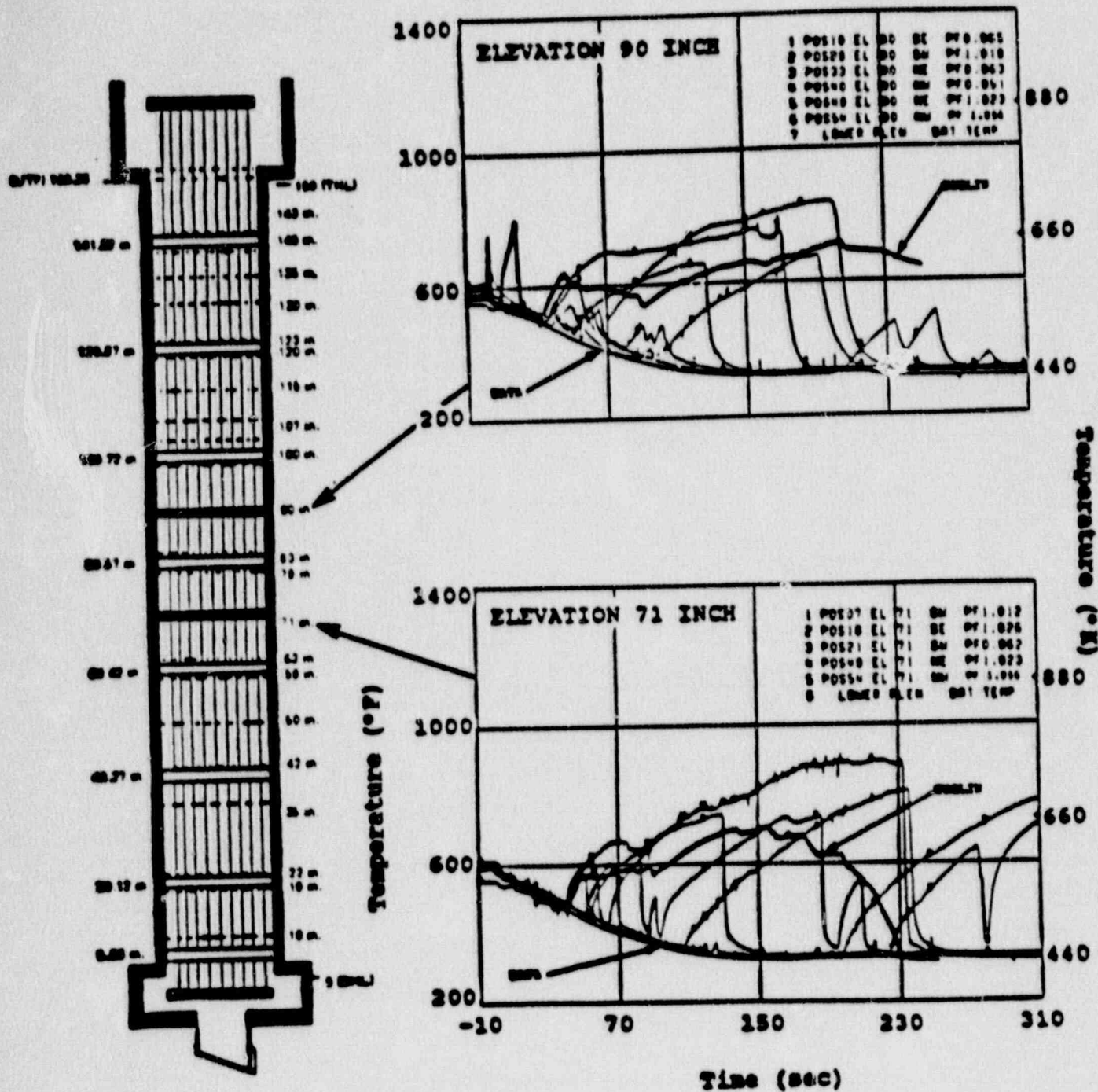
Figure 11-11   TLTA 6423/3 Middle Elevations Rod Temperature Response
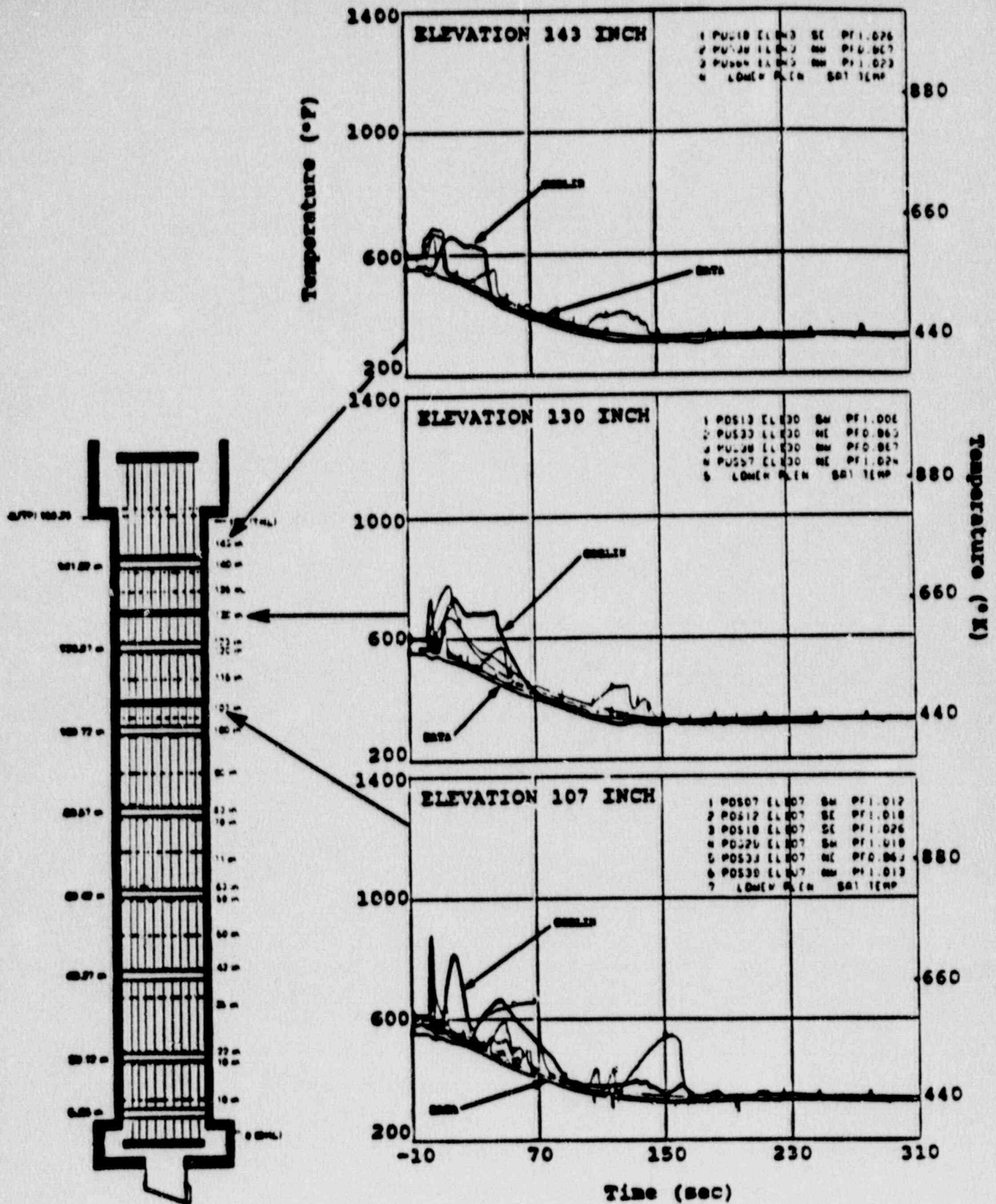
Figure 11-12 TLTA 6423/3 Top Elevations Rod Temperature Response

61

—a,c

Figure 11-13 Conservative Hot Plane Calculation Prescribed Rod
Surface Heat Transfer Coefficients

62
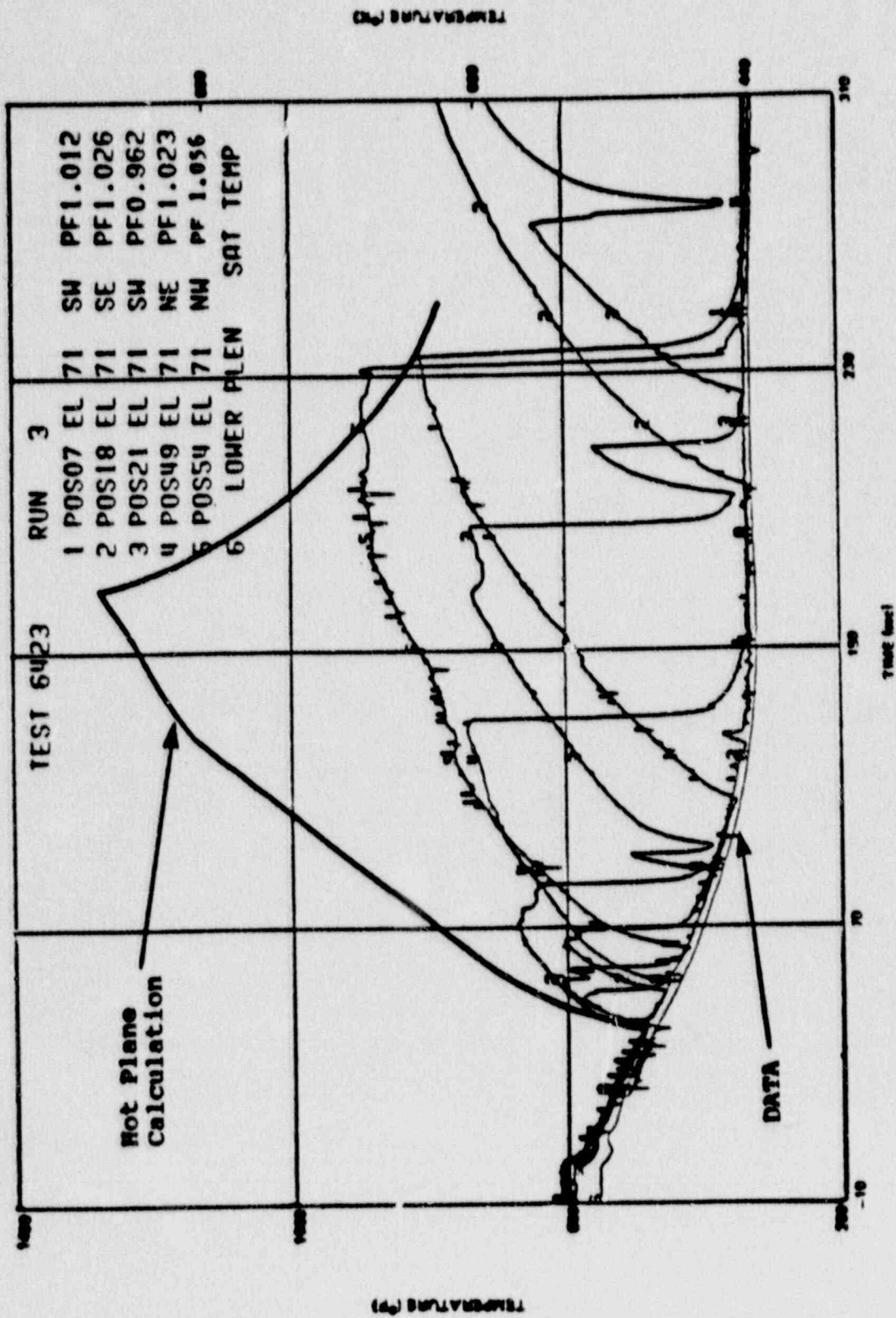
Figure 11-14 Conservative Hot Plane Calculation Peak Cladding
Temperature Comparison
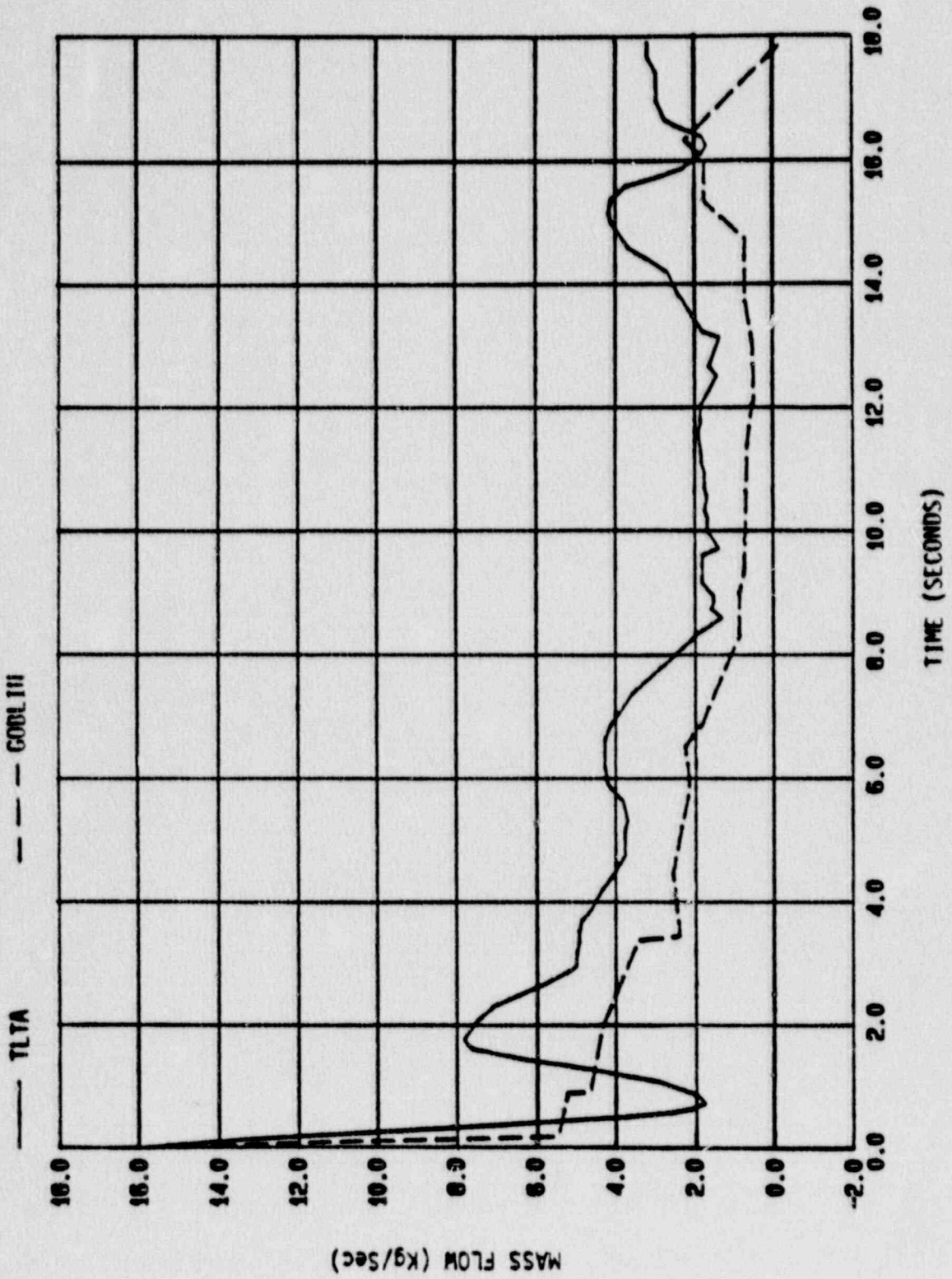
Figure 11-15 Bundle Flowrate for TLTA5A Test 6423/3

64
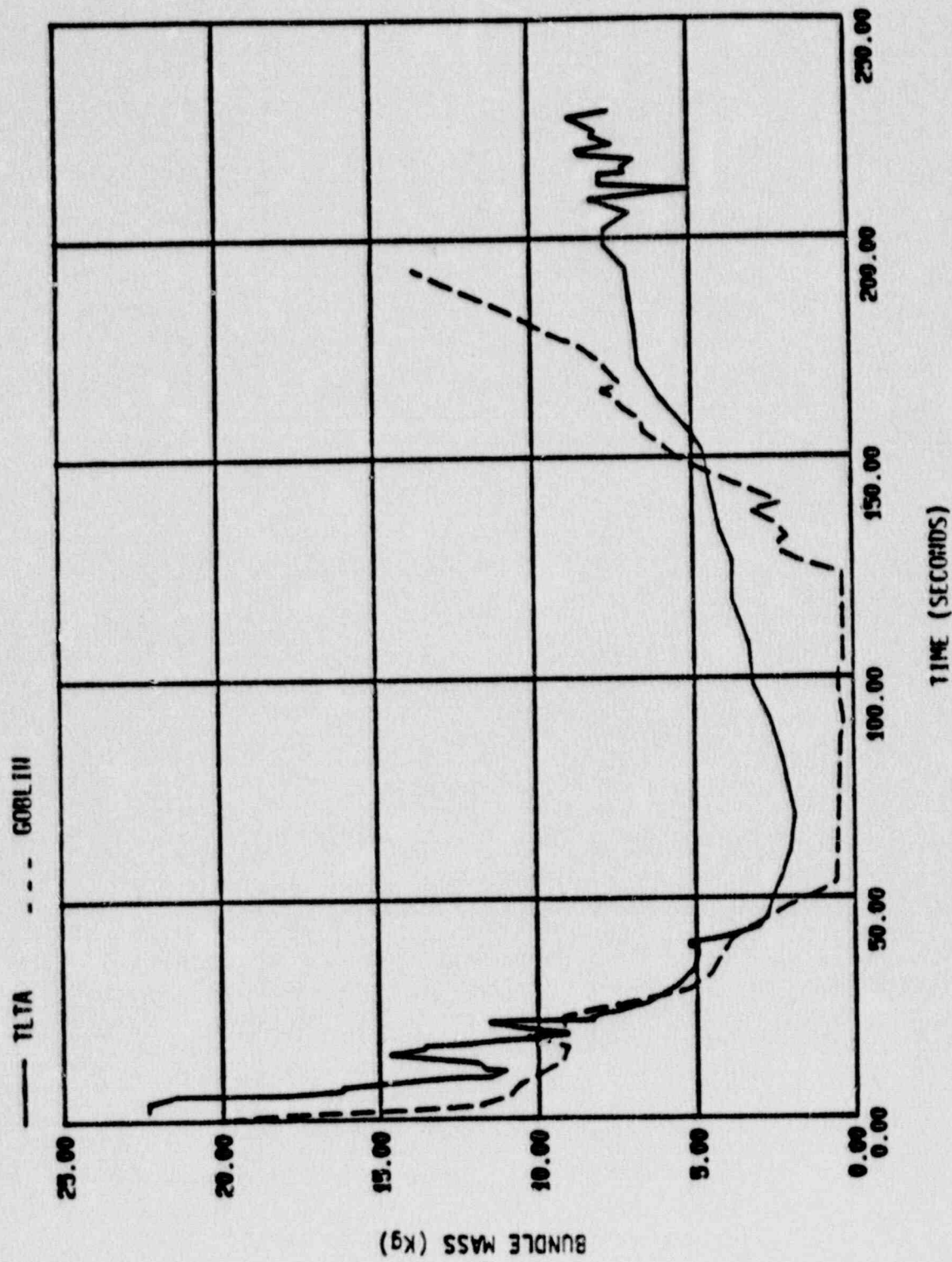
Figure 11-16 Bundle Mass for TLTA5A Test 6423/3
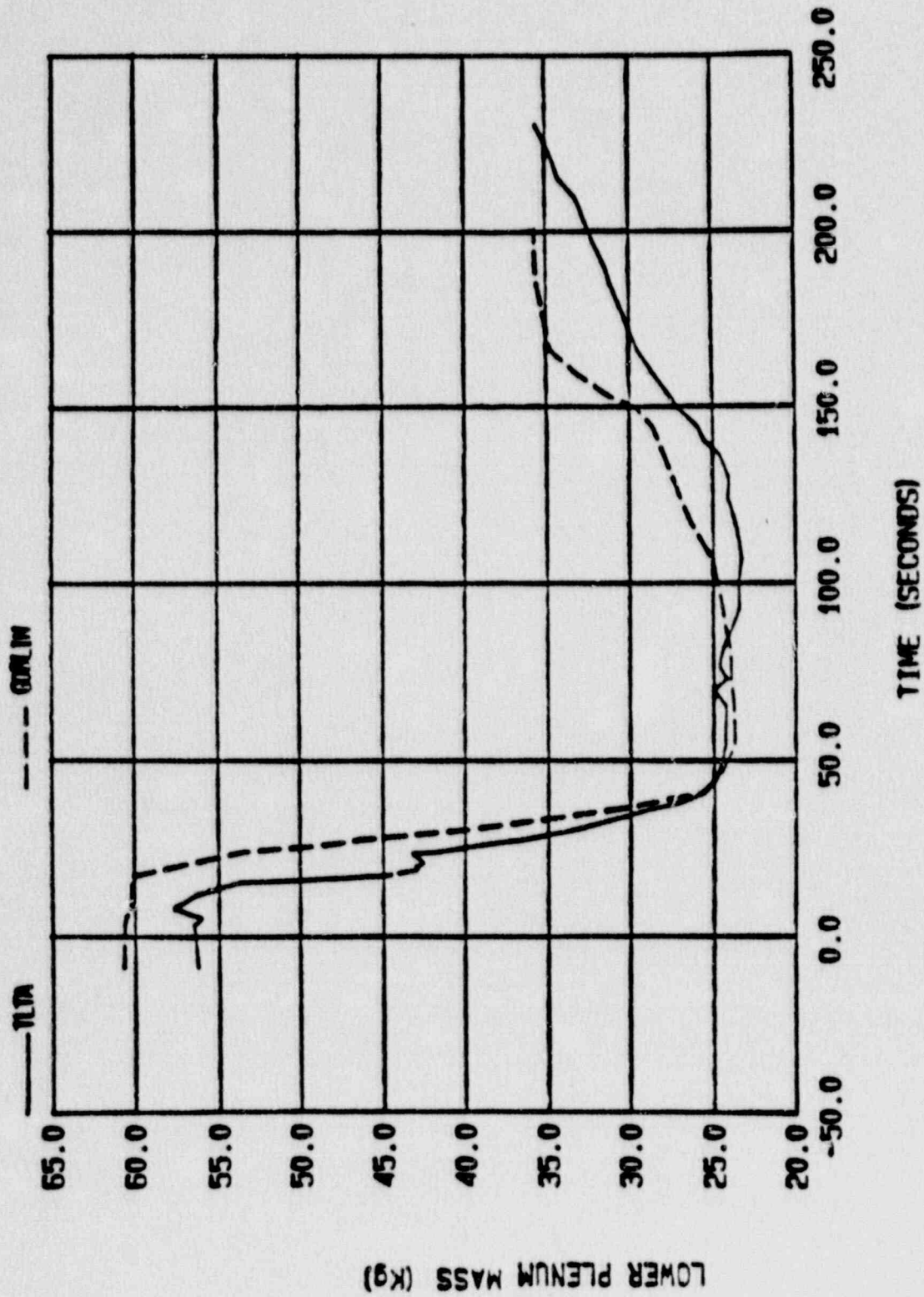
Figure 11-17 Lower Plenum Mass for TLTA5A Test 6423/3
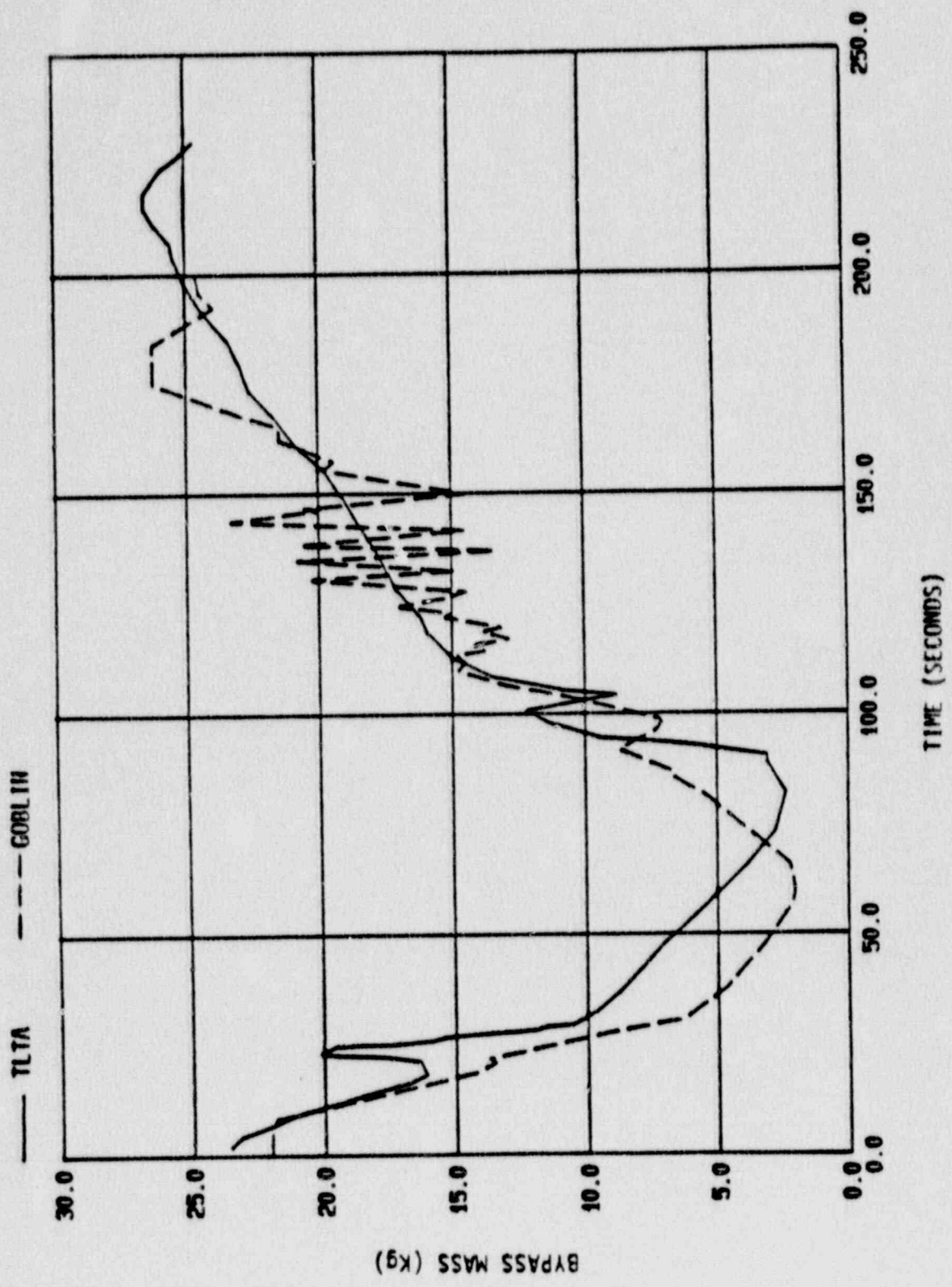
Figure 11-18 Bypass Mass for TLTA5A Test 6423/3

67
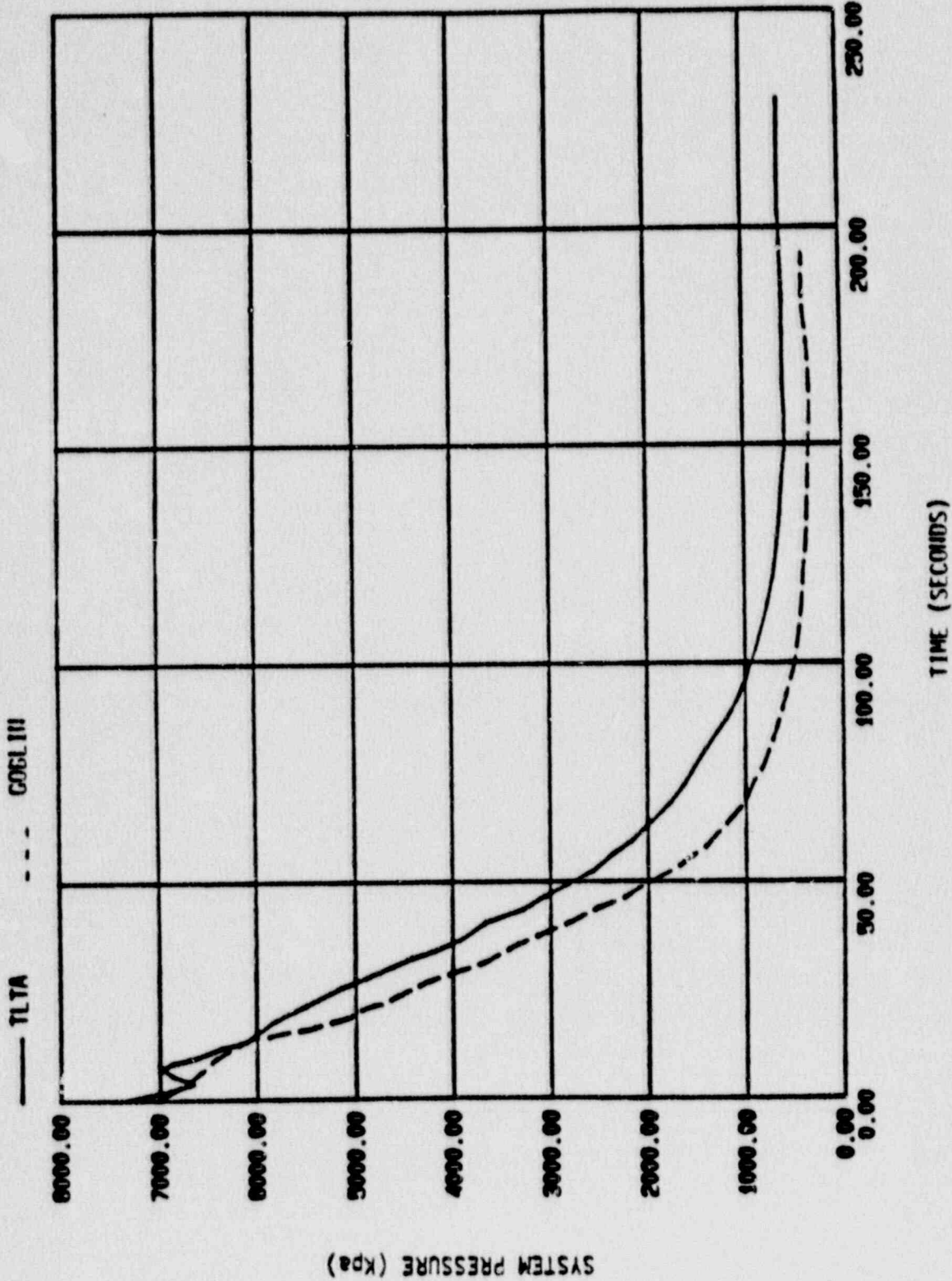
Figure 11-19 System Pressure for TLTA5A Test 6423/3
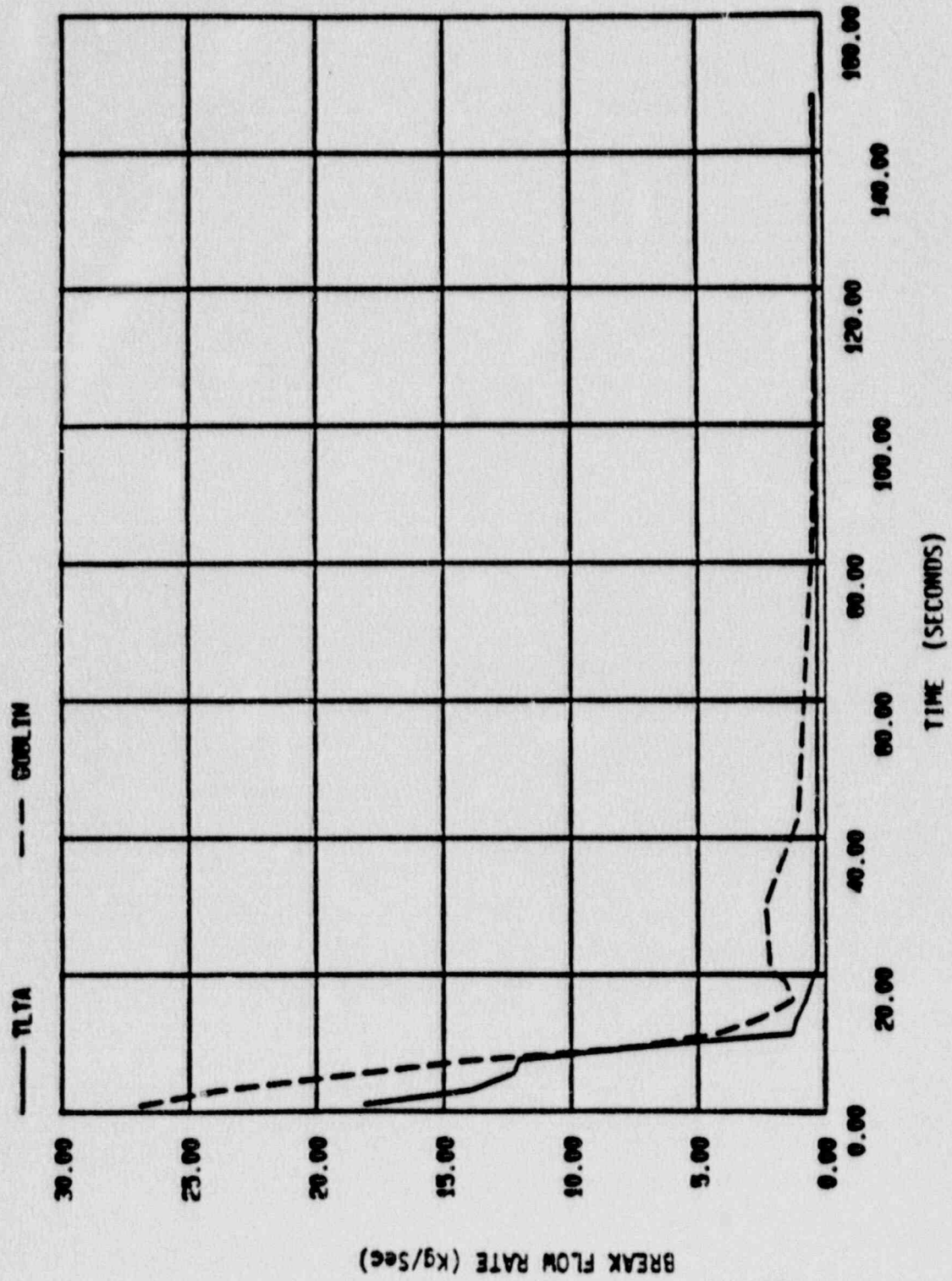
Figure 11-20 Break Flow for TLTA5A Test 6423/3
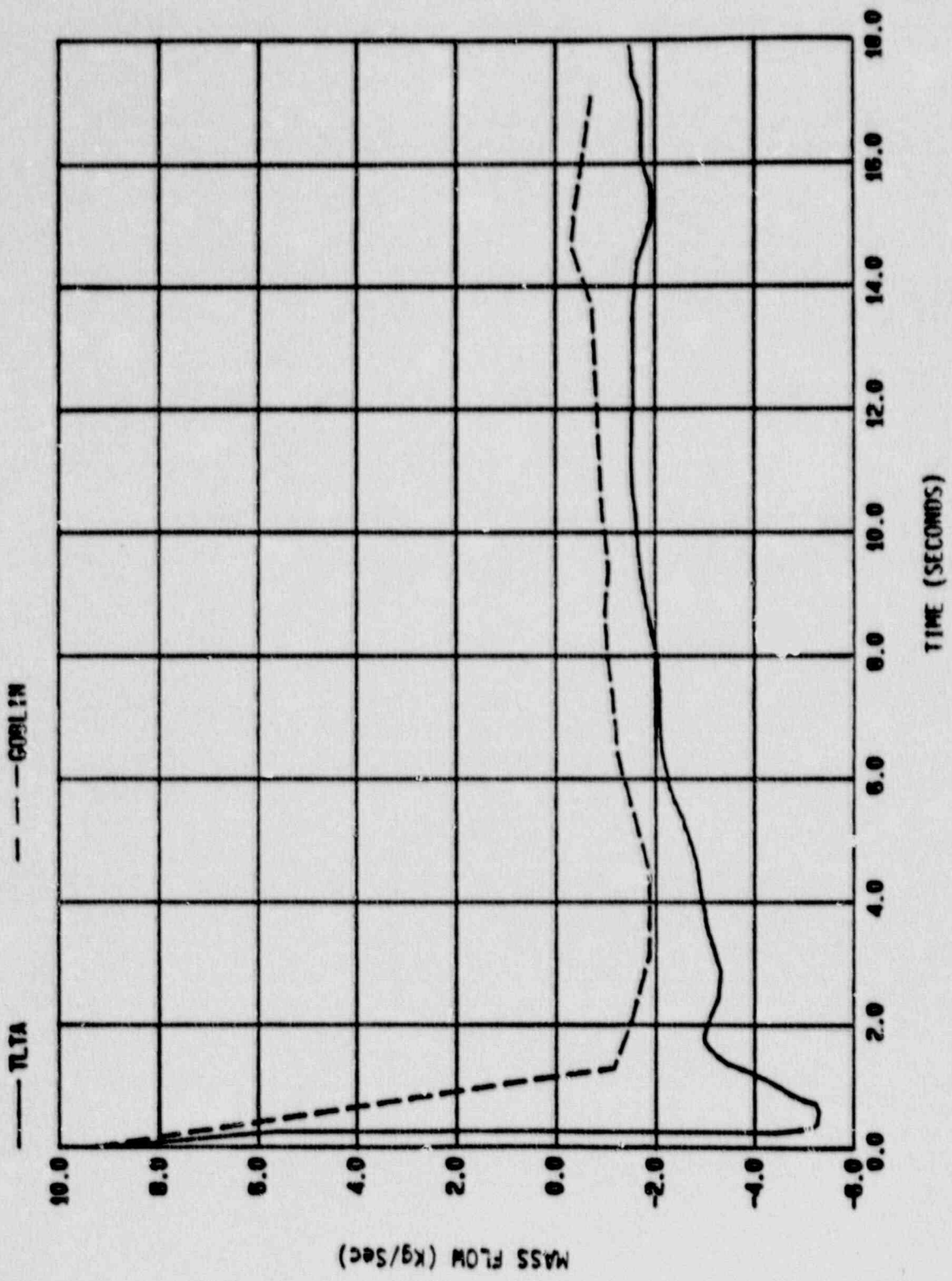
Figure 11-21 Broken Jet Pump Flow Rate for TLTA5A Test 6423/3

70

Question 12

Pages 6-94, 6-98 and Sec. 6.2.3, Ref. 1. The rod temperature results are missing in the Westinghouse analysis of TLTA test 6425. In effect, these analyses have been presented in the form of separate-effects tests to demonstrate the correct response of the fuel rods. Based on Figs. 6-50 and 6-54, it appears that the code has no conservative margin in terms of PCT. In fact, the code predicts a cooldown from 40 s to 70 s in Fig. 6-50, and the data indicate a heatup. The observed differences need to be explained. Fig. 6-54 does not indicate which test rod the computational rod was simulating or what the differences are between the curves for the measured data. The rod locations for the measurement curves and which rod(s) were being simulated with the computational rod need to be identified.

Response

The TLTA integral qualification simulation results of case 6425 run presented in Ref. 1 are repeated here. Table 12-1 shows the initial conditions for the test and simulation. Figures 12-1 through 12-7 are replotted comparisons of the transient hydraulic response. These figures supersede Figures 6-33 through 6-39 of Ref. 1. Figure 12-8 shows the corresponding rod temperature response.

The calculated rod temperature response compare reasonably well with the test data. The deviations in the simulation are a result of the variation in the initial conditions as demonstrated in the addition simulation of case 6423 run 3 presented in the response to Question 11.

Figure 6-50 of Ref. 1 shows the comparison of the rod temperature response for the TLTA case 6007 run 26. The GOBLIN/DRAGON simulation predicts a early dryout at the midplane after the initial drop in bundle flow rate. This is a consequence of the slightly sharper predicted depressurization following the jet pumps uncovery (as shown in Figure 6-47 of Ref. 1). The rod heatup is terminated by the subsequent lower plenum flashing. Because of the

conservatively low calculated minimum stable film boiling temperature, the rod heat transfer did not return to nucleate boiling resulting in sustained higher rod temperatures than is the test.

At approximately 40 seconds the lower plenum drains enough to allow steam venting out the jet pumps, resulting in a rapid draining of the bundle and upper plenum coolant through the side entry orifice and subsequent rod dryout. The GOBLIN/DRAGON simulation had a prolonged draining period due to overpredicted mass inventory in the upper plenum and bundle at 40 seconds. The overpredicted upper plenum mass inventory in the simulation is attributed to an overpredicted initial mass and to the prolonged dryout in the bundle from 10 to 50 seconds.

Additional TLTA qualification simulations presented in Ref. 1 and in response to Question 11 demonstrate that the rod temperature deviation is unique to this simulation.

Figure 6-54 of Ref. 1 shows a comparison of the predicted and measured midplane rod temperatures for FIX II test 3061. Attached is Figure 12-9, a copy of Figure 6-54 with the rod numbers of the five thermocouples indicated. The midplane is at a distance of 71.5 inches from the bottom of the heated length. This elevation corresponds to node 14 in the GOBLIN simulation. The GOBLIN simulation modelled a single rod at the average planar power. This average rod temperature is compared to the rod temperature measurements at the same elevation.

The rod temperature comparisons presented here reaffirm the ability of the GOBLIN/DRAGON code to predict the average rod temperature response. The conservative margin in PCT of the Westinghouse LOCA evaluation model due to the 10CFR50 Appendix K requirements was not included in this simulation. (See the response to Question 11 for a discussion of the PCT conservatism resulting from the Appendix K requirements.)

The revised figures of Ref. 1 presented in this response will be incorporated into the final (approved) version of the topical report.

TABLE 12-1
COMPARISON OF TLTA 6425 RUN 2 INITIAL CONDITIONS

	TLTA	GOBLIN
Bundle Power (Mw)	5.05 ± 0.03	505
Steam dome pressure (psia)	1044 ± 5	1031
Lower plenum enthalpy (Btu/lbm)	528 ± 5	508
Feedwater enthalpy (Btu/lbm)	41 ± 2	41
Feedwater flow (lbm/sec)	1.4 ± 0.3	1.1
Jet Pump 1 flow (lbm/sec)	22 ± 2	20
Jet Pump 2 flow (lbm/sec)	20 ± 2	21
Bundle inlet flow (lbm/sec)	39 ± 5	41
Downcomer Mass (lbm)	310	558
Initial Water level (inch elev.)	123 ± 6	122
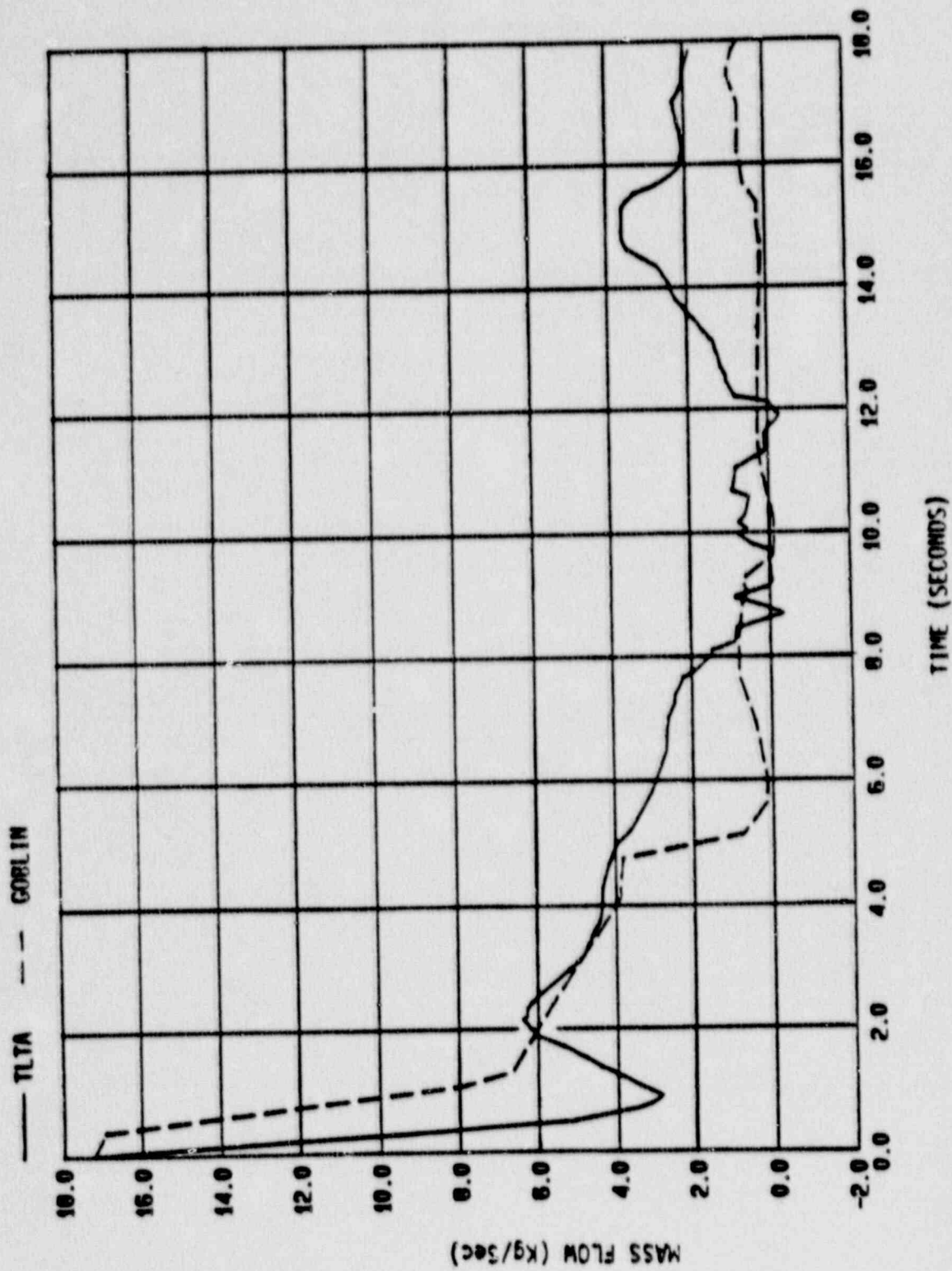
Figure 12-1 Bundle Flow Rate for TLTA5A Test 6245/2

74
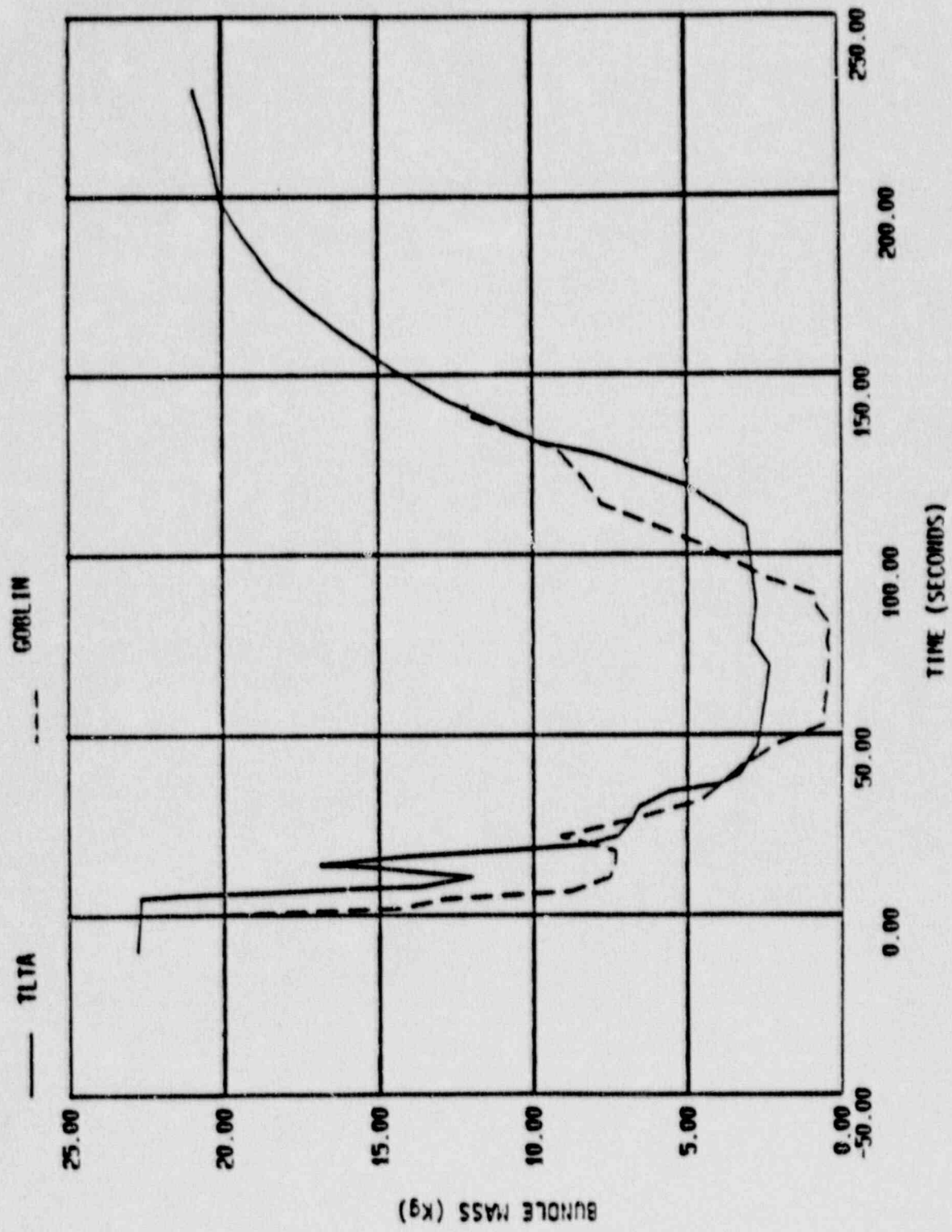
Figure 12-2 Bundle Mass for TLTA5A Test 6425/2

75
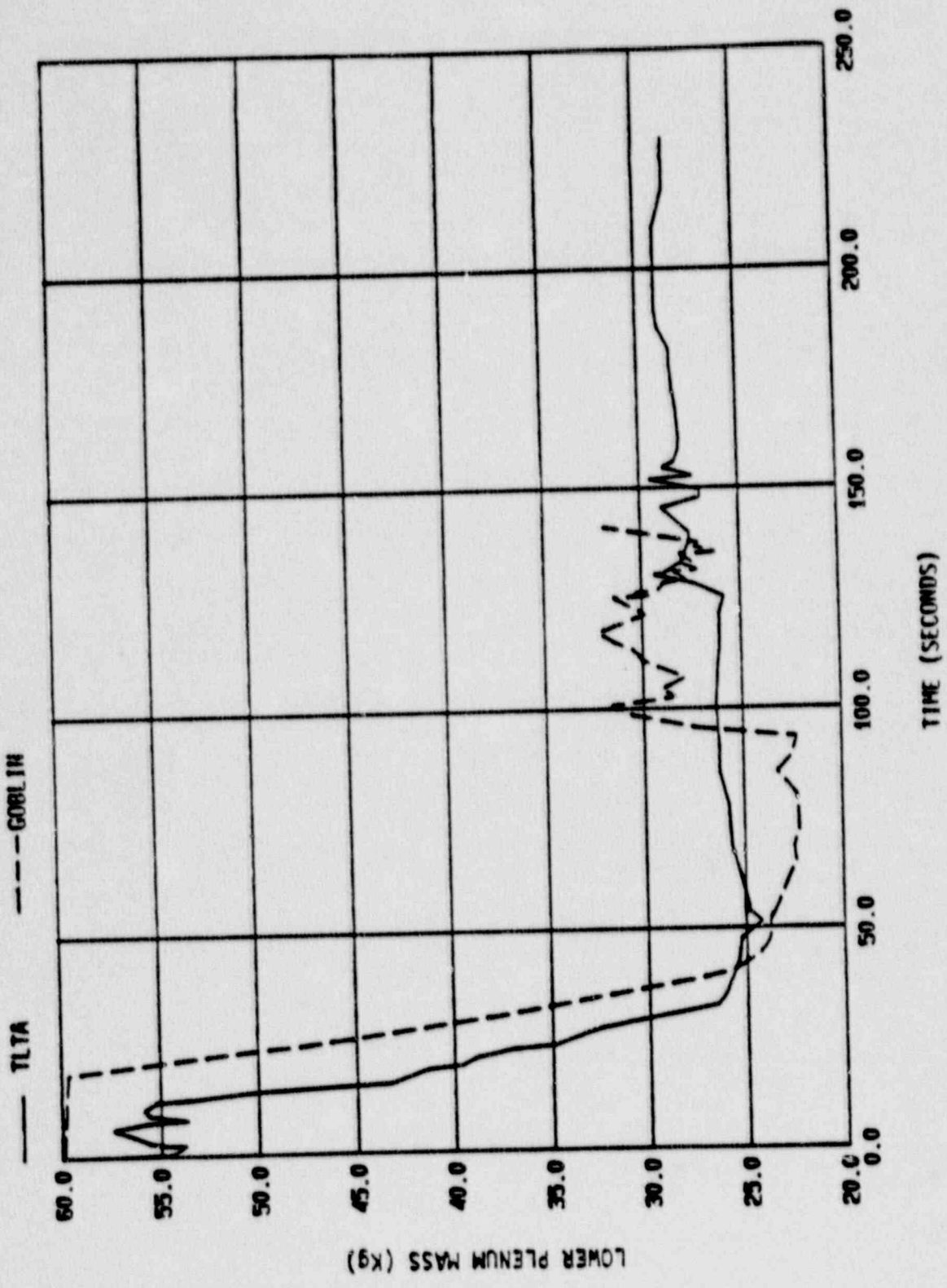
Figure 12-3 Lower Plenum Mass for TLTA5A Test 6425/2

76
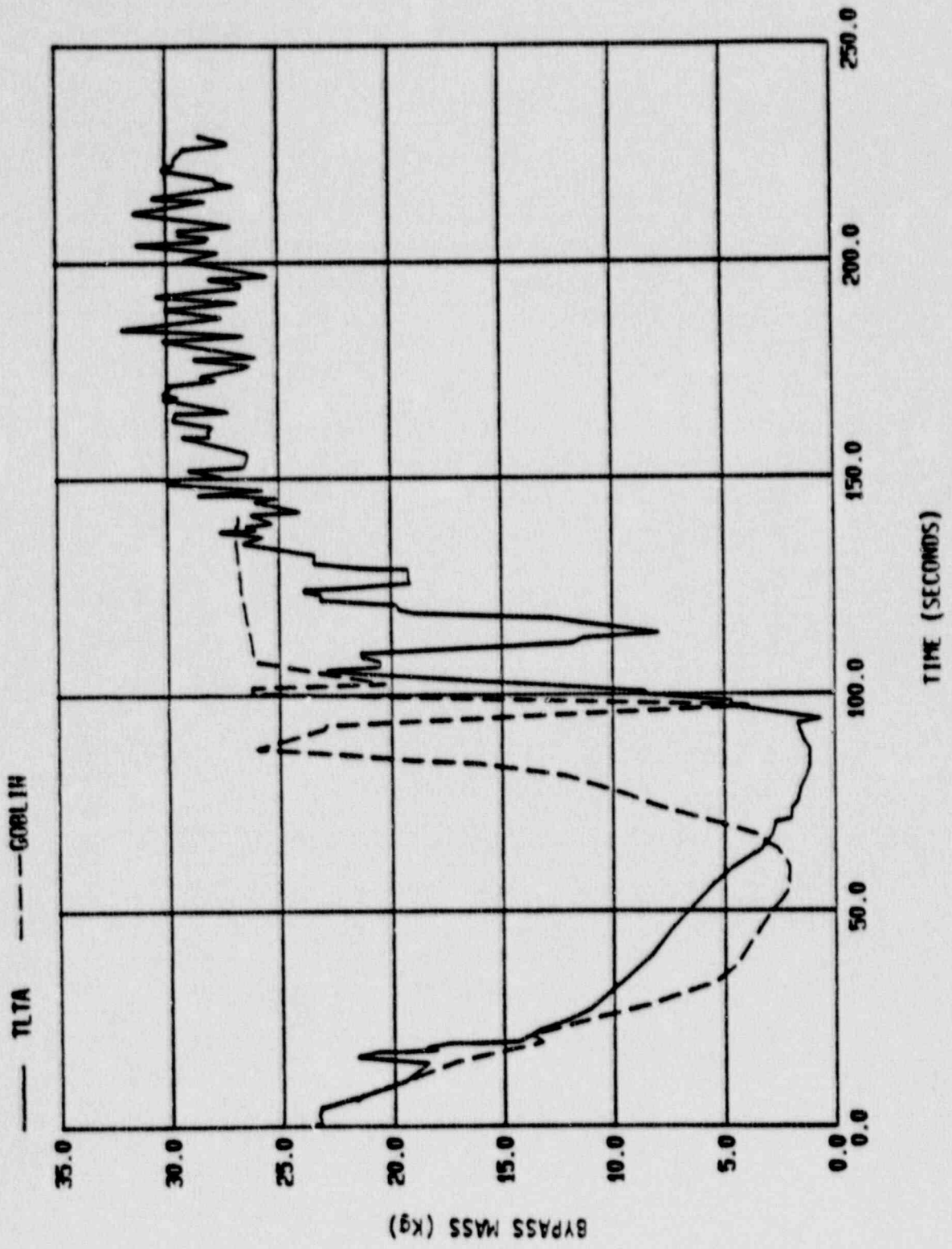
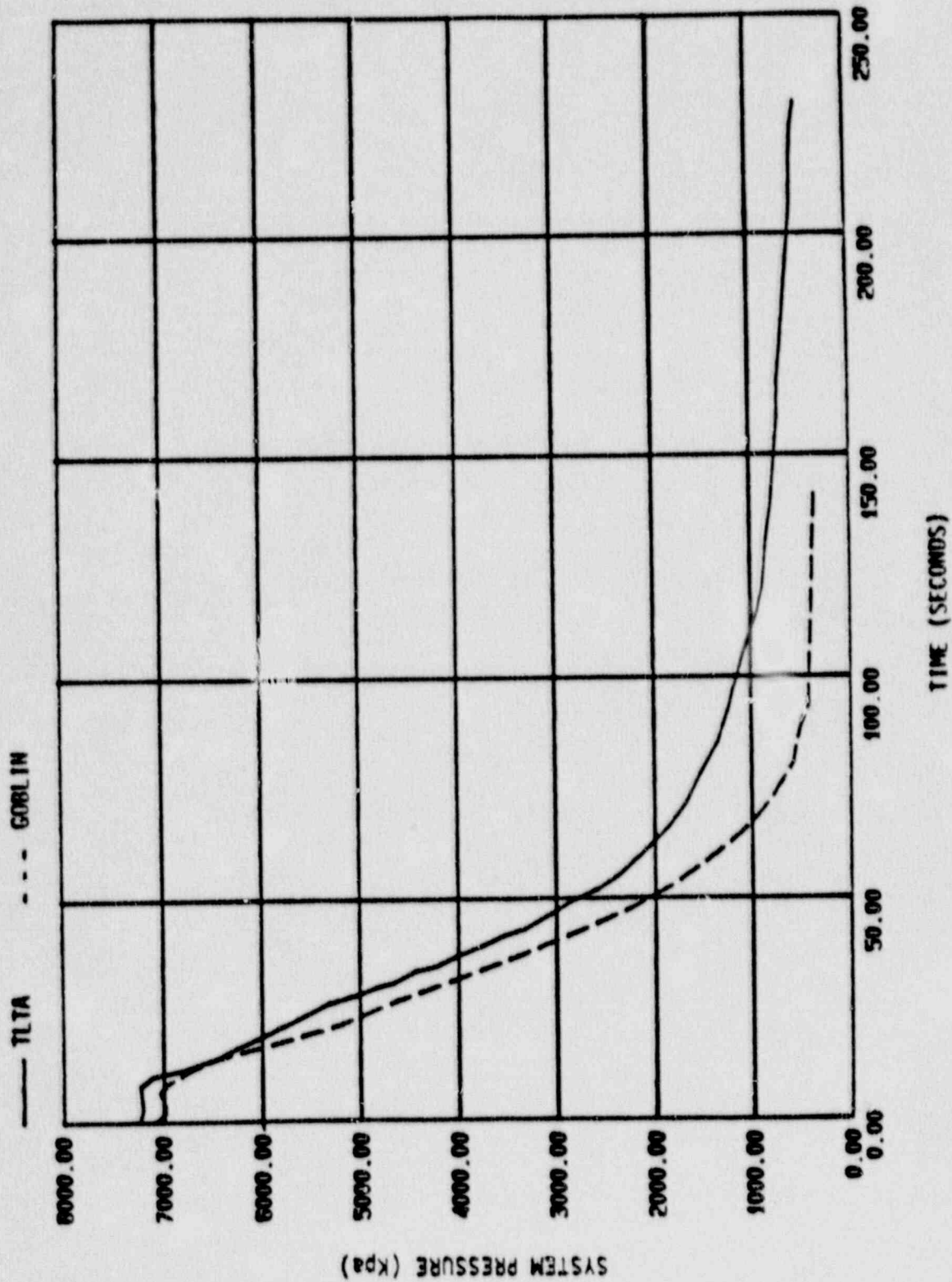Figure 12-4 Bypass Mass for TLTA5A Test 6425/2

77

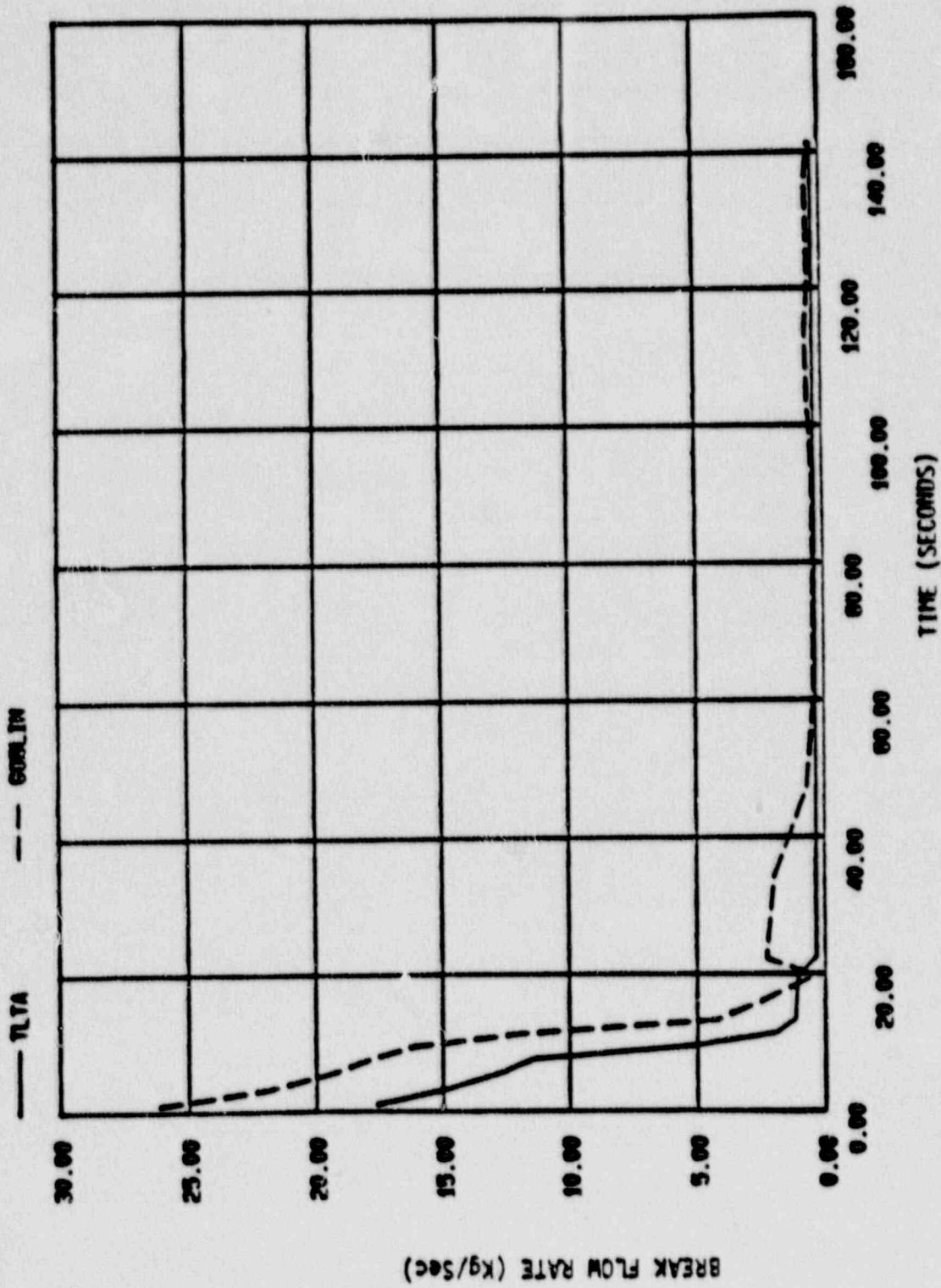Figure 12-5 System Pressure for TLTA5A Test 6425/2
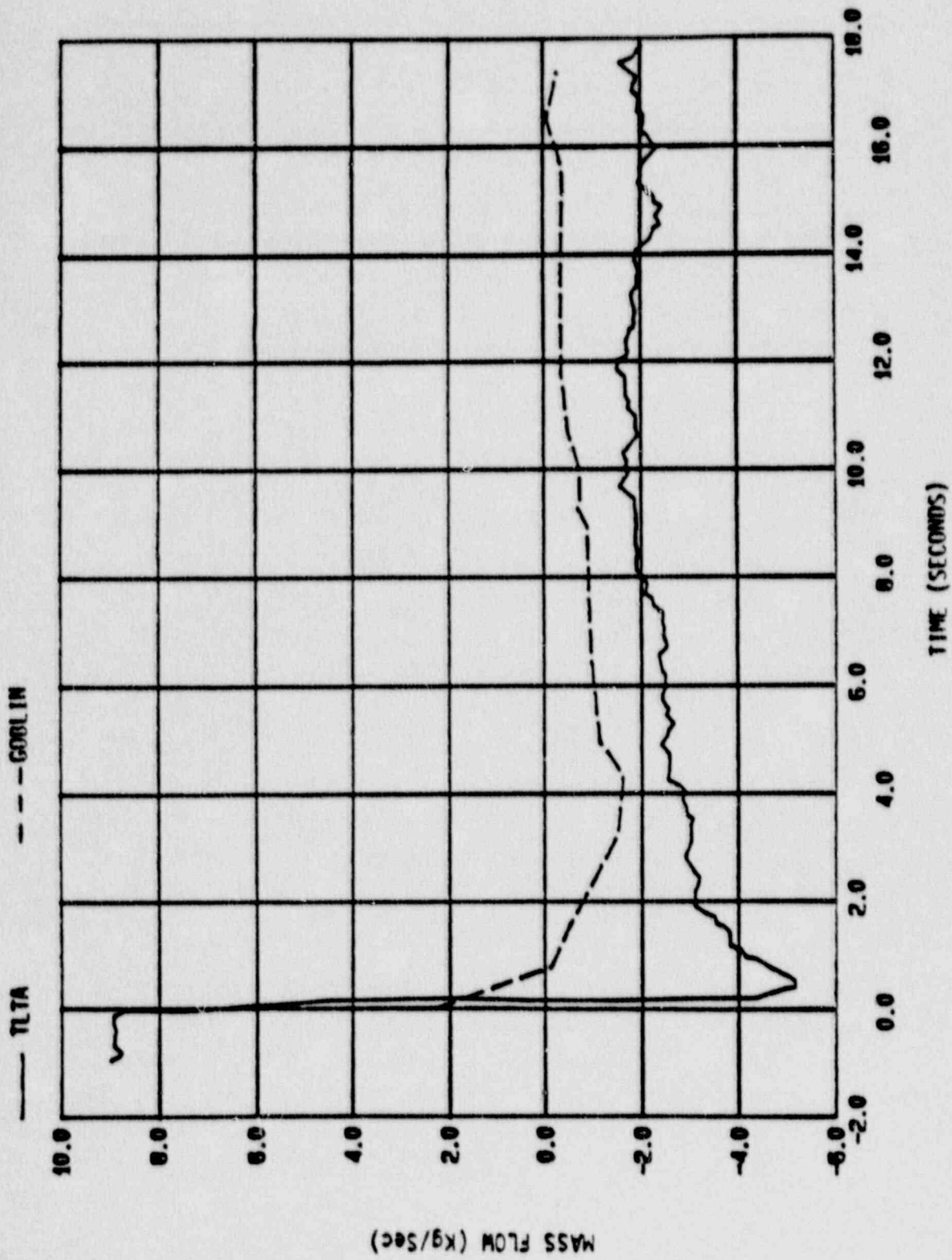
Figure 12-6 Break Flow for TLTA5A Test 6425/2

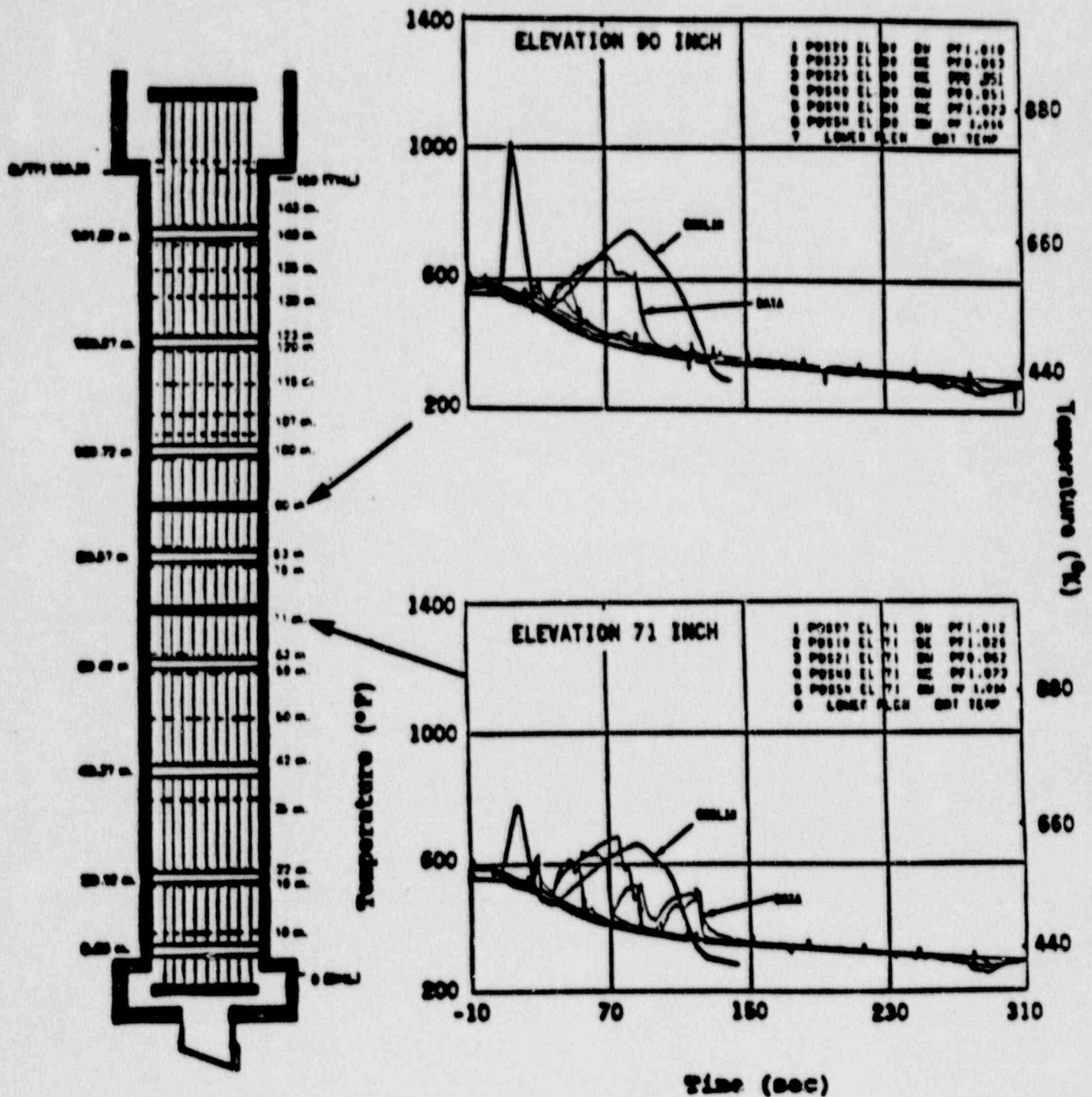Figure 12-7 Broken Jet Pump Flow Rate for TLTA5A Test 6425/2

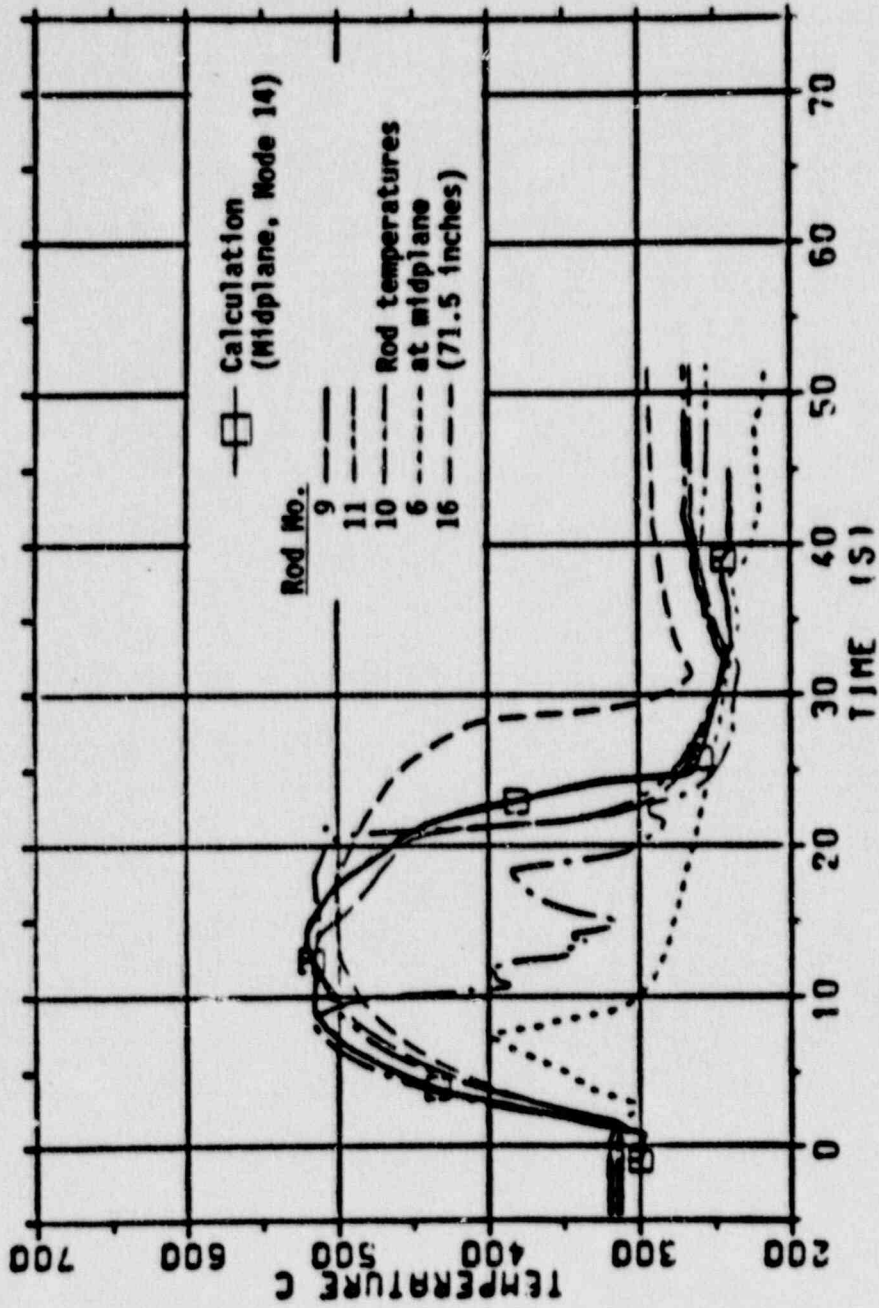Figure 12-8 TLTA 6425/2 Rod Temperature Response

Figure 12-9 Midplane Rod Temperature for FIX-II Test 3061.
100% Break at 2.51 kw